



# Gels d'acide hyaluronique contenant des liposomes pour la libération prolongée d'un corticoïde dans l'oreille interne

Naila El Kechai

## ► To cite this version:

Naila El Kechai. Gels d'acide hyaluronique contenant des liposomes pour la libération prolongée d'un corticoïde dans l'oreille interne. Pharmacie galénique. Université Paris Saclay (COmUE), 2015. Français. NNT : 2015SACLS155 . tel-01653079

**HAL Id: tel-01653079**

<https://theses.hal.science/tel-01653079>

Submitted on 1 Dec 2017

**HAL** is a multi-disciplinary open access archive for the deposit and dissemination of scientific research documents, whether they are published or not. The documents may come from teaching and research institutions in France or abroad, or from public or private research centers.

L'archive ouverte pluridisciplinaire **HAL**, est destinée au dépôt et à la diffusion de documents scientifiques de niveau recherche, publiés ou non, émanant des établissements d'enseignement et de recherche français ou étrangers, des laboratoires publics ou privés.

**UNIVERSITÉ PARIS-SACLAY  
UNIVERSITÉ PARIS-SUD**

**ÉCOLE DOCTORALE :**  
**INNOVATION THÉRAPEUTIQUE, DU FONDAMENTAL À L'APPLIQUÉ**  
Pôle : Pharmacotechnie et physicochimie pharmaceutique

**Discipline :**  
Pharmacotechnie et biopharmacie

**THÈSE DE DOCTORAT**

Soutenue le 30 novembre 2015

Par

**M<sup>me</sup> Naila EL KECHAI**

**Gels d'acide hyaluronique contenant des liposomes  
pour la libération prolongée d'un corticoïde dans  
l'oreille interne**

**Devant un jury composé de :**

M. Dominique HOURDET	Professeur (Université Pierre et Marie Curie)	Rapporteur
M. Juergen SIEPMANN	Professeur (Université Lille 2 droit et santé)	Rapporteur
M. Elias FATTAL	Professeur (Université Paris-Sud)	Examinateur
M <sup>me</sup> Evelyne FERRARY	Docteur (UMR-S 1159 Inserm)	Examinateur
M. Alexandre GIL	Docteur (SANOFI)	Examinateur
M <sup>me</sup> Florence AGNELY	Professeur (Université Paris-Sud)	Directeur de thèse
M <sup>me</sup> Amélie BOCHOT	Professeur (Université Paris-Sud)	Directeur de thèse

*A mes très cher parents, Djafar et Samia*

*A mon cher époux, Yacine*

*J'adresse mes remerciements les plus sincères,*

*Au Professeur **Elias Fattal** pour m'avoir accueillie à l'Institut Galien Paris-Sud et au sein de son équipe. Merci pour tes encouragements et tes conseils tout au long de ma thèse et enfin, merci de me faire l'honneur d'être membre du jury.*

*Au Professeur **Juergen Siepmann** et au Professeur **Dominique Hourdet** pour avoir accepté d'être les rapporteurs scientifiques de ce travail. Je les prie de bien vouloir trouver ici mes plus vifs remerciements pour l'honneur qu'ils me font en acceptant d'examiner ce travail.*

*Au Docteur **Alexandre Gil**, Directeur du département Drug Delivery et Préformulation chez Sanofi, pour l'intérêt qu'il a bien voulu porter à ce travail en acceptant de faire partie du jury.*

*Au Docteur **Evelyne Ferrary**, qui a beaucoup contribué dans ce travail. Merci pour vos conseils avisés et pour votre disponibilité. Enfin, merci de me faire l'honneur d'être présidente du jury.*

*A mes deux directrices de thèse :*

*Le Professeur **Florence Agnely** et le Professeur **Amélie Bochot** pour la confiance qu'elles m'ont accordée en me confiant ce projet et pour toutes les heures qu'elles ont consacrées à diriger cette recherche. Merci de m'avoir fait profiter de votre savoir-faire et de votre expertise chacune dans son domaine. J'ai particulièrement apprécié nos discussions fructueuses, vos conseils toujours avisés et vos critiques pertinentes qui ont fait de ce travail ce qu'il est. J'aimerais également vous remercier pour votre grande disponibilité et votre respect sans faille des délais serrés de relecture des documents que je vous ai adressés.*

*A ma co-équipière dans ce travail, le Docteur **Elisabeth Mamelle**. Je te remercie pour ton implication dans ce projet, ton efficacité, ta persévérance et ton éternel optimisme.*

*Au Docteur **Yann Nguyen** pour m'avoir formée sur les tests ABR. Je te remercie également pour nos nombreuses discussions scientifiques qui ont permis de faire avancer le projet.*

*Au Docteur **Nicolas Huang** pour m'avoir initiée et formée à la rhéologie. Merci pour ton enseignement ludique, ta bonne humeur et tes conseils tout au long de ma thèse.*

*Au Docteur Jean-Marc Edeline et à Victor Adenis qui m'ont accueillie chaleureusement au Centre de Neurosciences Paris-Sud et qui m'ont apporté une aide précieuse lors de l'évaluation thérapeutique sur le modèle de traumatisme sonore.*

*Au Docteur Sandrine Geiger et au Docteur Ingrid Cañero-Infante qui ont mis au point et réalisé les expériences d'AFM au SPMS, Ecole Centrale Paris.*

*Au Docteur Claire Gueutin pour m'avoir formée et aidée à mettre au point la méthode de dosage par HPLC.*

*A Stéphanie Nicolaï et Audrey Solgadi au SAMM, UMS IPSIT, et au Professeur Pierre Chaminade pour leur aide précieuse lors de la longue épreuve qui a été la mise au point de la méthode de dosage par LC-MS.*

*A Valérie Nicolas de la plate-forme d'imagerie cellulaire, UMS IPSIT, grâce à qui les analyses de microscopie confocale et de vidéomicroscopie ont pu être menées à bien.*

*A Valérie Domergue de la plateforme AnimEx, UMS IPSIT, qui nous a permis de réaliser les expériences *in vivo* au sein de son animalerie et qui a été d'une aide précieuse lors de la rédaction du protocole pour le comité éthique.*

*Aux stagiaires qui ont contribué dans ce travail : Giovanni Tonelli, Erica Leite-Delinquines et Arianna Fallacara.*

*Au Docteur Nicolas Tsapis, co-responsable de l'équipe 5. Je te remercie pour ton implication dans la vie du laboratoire qui facilite grandement le travail des doctorants et post-doctorants. Merci pour ta bonne humeur et tes conseils tout au long de ma thèse.*

*Au Docteur Ghoulène Mekhloufi et à Sarah Villebrun pour leur gentillesse et leurs encouragements.*

*A toute l'équipe d'enseignement galénique et en particulier à Claire et Anne-Marie.*

*A tous les membres de l'équipe 5 et ceux de l'équipe 3 mais aussi aux autres équipes de l'Institut Galien Paris-Sud. J'ai une pensée particulière pour ceux et celles avec qui j'ai partagé un bureau, un déjeuner, une soirée, une discussion scientifique....(ou pas) : Thais, Christian, Donato, Guillaume, Marion, Félix, Gopan, Love, Agnès, Samantha, Claire, Mathilde, Tanguy, Sophie, Walhan, Adam, Rosana, Guillaume.*

*A celles qui ont fait de ces trois années une expérience unique : Nadège, Nadia, Dunja, Giovanna, Patricia, Ludivine, Anaelle. Merci tout simplement d'avoir été là, de m'avoir toujours soutenue, encouragée, consolée, aidée et bien plus encore...*

*Je remercie mon frère Yaniss, mon oncle Karim et ma tante Karima pour leur affection et leur soutien inconditionnel.*

*Je remercie du plus profond de mon cœur mes très chers parents qui ont tout fait pour moi. Papa, maman, merci d'avoir toujours cru en moi, de m'avoir encouragée et soutenue dans tout ce que j'ai pu entreprendre et d'avoir tout mis en œuvre pour que je puisse réussir. Vous êtes les piliers fondateurs de ce que je suis et de ce que je fais.*

*Enfin, je remercie Yacine, mon époux. Il est difficile de trouver les mots pour exprimer ma reconnaissance envers toi. Tu m'as tout de suite encouragée à me lancer dans cette aventure et tu l'a ensuite vécu avec moi au quotidien. Merci pour tout !*

# Sommaire

**ABRÉVIATIONS.....**.....5

**INTRODUCTION GÉNÉRALE.....**.....7

## TRAVAUX ANTÉRIEURS

Introduction-résumé.....13

**Publication 1: Recent advances in local drug delivery to the inner ear.....15**

1. Introduction.....	17
2. The ear.....	18
2.1. Anatomical and physiological issues.....	18
2.2. Inner ear fluids.....	20
2.3. Ear barriers.....	21
2.3.1. Blood-perilymph barrier.....	21
2.3.2. Tympanic membrane.....	21
2.3.3. Round and oval windows.....	22
3. Main inner ear diseases and therapies.....	23
4. Local drug delivery to the inner ear.....	24
4.1. Intratympanic administration.....	27
4.1.1. Transtympanic injection of solutions.....	28
4.1.2. Medical drug delivery devices.....	28
4.1.3. Injectable drug delivery systems.....	33
4.2. Intracochlear administration .....	47
4.2.1. Intracochlear injection.....	47
4.2.2. Cochlear implant coating.....	48
4.2.3. Microfluidic reciprocating reservoir.....	49
4.3. Combination of local drug delivery systems.....	49
4.4. Current hurdles to overcome.....	50
5. Conclusions.....	52
References.....	53

## TRAVAUX EXPÉRIMENTAUX

*Première partie : Etude physicochimique*

Introduction.....67

**Chapitre I : Propriétés rhéologiques et seringabilité de gels d'acide hyaluronique**

**contenant des liposomes pour l'injection par voie locale.....69**

Introduction - résumé.....69

<b>Publication 2: Effect of liposomes on rheological and syringeability properties of hyaluronic acid hydrogels intended for local injection of drugs.....</b>	71
Abstract.....	72
1. Introduction.....	73
2. Materials and methods.....	74
3. Results.....	79
4. Discussion.....	88
5. Conclusions.....	93
References.....	94
Etude complémentaire : Influence des dimensions de l'aiguille et de la viscosité des gels sur les propriétés de seringabilité.....	98
References.....	102
<b>Chapitre II: Mélanges d'acide hyaluronique et de liposomes en milieu aqueux : stabilité, microstructure et mobilité des liposomes.....</b>	103
Introduction - résumé.....	103
<b>Projet de publication: Mixtures of hyaluronic acid and liposomes in aqueous media: phase behavior, microstructure and mobility of liposomes.....</b>	105
Abstract.....	106
1. Introduction.....	107
2. Materials and methods.....	109
3. Results and discussion.....	114
4. Conclusions.....	130
References.....	131
<i>Deuxième partie : Evaluation in vivo du gel de liposomes encapsulant un corticoïde</i>	
Introduction.....	135
<b>Chapitre III : Libération prolongée d'un corticoïde dans l'oreille interne à partir d'un gel de liposomes administré localement dans l'oreille moyenne.....</b>	139
Introduction - résumé.....	139
<b>Projet de publication: Hyaluronic acid liposomal gel sustains the delivery of a corticoid to the inner ear.....</b>	141
Abstract.....	142
1. Introduction.....	143
2. Materials and methods.....	144
3. Results and discussion.....	151
4. Conclusions.....	163
References.....	164
<b>Chapitre IV : Efficacité thérapeutique de gels d'acide hyaluronique contenant un corticoïde sur un modèle de traumatisme sonore chez le cobaye.....</b>	169
Introduction - résumé .....	169

<b>Therapeutic efficacy of a corticoid loaded into hyaluronic acid gels after noise-induced hearing loss in guinea pigs.....</b>	171
Abstract.....	172
1. Introduction.....	173
2. Materials and methods.....	174
3. Results and discussion.....	177
4. Conclusions.....	183
References.....	184
<b>Chapitre V : Etude de l'efficacité thérapeutique du gel de liposomes contenant un corticoïde pour la préservation de l'audition résiduelle durant l'implantation cochléaire manuelle ou robot-assistée.....</b>	187
Introduction - résumé .....	187
<b>Projet de publication: Enhanced hearing preservation in an animal model of cochlear implantation with motorized insertion and dexamethasone loaded liposomes dispersed within a hyaluronic acid gel.....</b>	189
Abstract.....	190
1. Introduction.....	191
2. Materials and methods.....	192
3. Results and discussion.....	196
4. Conclusions.....	201
References.....	202
<b>DISCUSSION GÉNÉRALE.....</b>	205
<b>CONCLUSION ET PERSPECTIVES.....</b>	229

---

ABR	auditory brainstem response
AFM	atomic force microscopy
AIED	autoimmune inner ear disease
BDNF	brain-derived neurotrophic factor
BPLB	blood-perilymph barrier
BSA	bovine serum albumine
Chol	cholesterol
CI	cochlear implantation
CMV	cytomegalovirus
Dex	dexamethasone
DexP	dexamethasone phosphate
DSPE-PEG2000	1,2-distearoyl-sn-glycero-3-phosphoethanolamine-N-[methoxy-poly-(ethyleneglycol)-2000]
DSPE-PEG5000	1,2-distearoyl-sn-glycero-3-phosphoethanolamine-N-[methoxy-poly-(ethyleneglycol)-5000]
EPC	egg phosphatidylcholine
FITC	fluorescein isothiocyanate
GMO	glycerol monooleate
HA	hyaluronic acid
HBPL	hyperbranched poly-L-lysine
HGF	hepatocyte growth factor
IGF-1	insulin-like growth factor-1
JNK	c-Jun n-terminal kinase
LC-MS	liquid chromatography coupled to mass spectroscopy
Lip	liposome
LNC	lipid nanocapsule
MIT	motorized insertion tool
MSD	mean square displacement
NIHL	noise-induced hearing loss
PE	phosphatidylethanolamine
PEG	polyethylene glycol
PG	L- $\alpha$ -phosphatidylglycerol
PK	pharmacokinetic
PLGA	poly(lactic-co-glycolic acid)
Rh	rhodamine
RW	round window
SA	stearylamine
SNHL	sensorineural hearing loss
SPION	superparamagnetic iron oxide nanoparticle
SPT	single particle tracking
TTI	transtympanic injection

# **Introduction générale**

La perte auditive, les acouphènes et les troubles de l'équilibre sont des maladies de l'oreille interne très répandues avec un impact significatif sur la qualité de la vie des personnes atteintes (Lasak et al., 2014, Ayoob and Borenstein, 2015). La perte auditive, également appelée surdité, est un handicap sensoriel fréquent encore insuffisamment corrigé (Lasak et al., 2014). Actuellement, les surdités de perception invalidantes socialement se traitent par la pose de prothèses auditives conventionnelles ou par la mise en place d'implants cochléaires (Bouccara et al., 2012, Nguyen et al., 2015). D'autres thérapies curatives moins invasives sont en cours de développement pour tenter de traiter les surdités potentiellement réversibles (Swan et al., 2008, Staecker and Rodgers, 2013, Ayoob and Borenstein, 2015).

Actuellement, en otologie, des méthodes d'administration des médicaments par voie locale se développent en alternative aux traitements par voie générale (Swan et al., 2008). En effet, l'administration par voie orale ou parentérale est peu efficace et responsable de nombreux effets indésirables du fait des fortes doses nécessaires pour obtenir un effet thérapeutique au niveau de l'oreille interne. Cela est principalement lié à l'anatomie complexe de l'oreille et notamment à la présence d'une barrière hémato-périlymphatique qui isole l'oreille interne de la circulation sanguine (Juhn and Rybak, 1981, Juhn et al., 2001). Parmi ces méthodes d'administration locale, l'injection transtympanique est couramment utilisée en clinique. Cette méthode peu invasive consiste à injecter le médicament directement dans l'oreille moyenne, à travers le tympan, à l'aide d'une aiguille fine et longue. La substance active doit alors diffuser à travers les barrières de l'oreille moyenne pour atteindre les cellules cibles au niveau de l'oreille interne. Comparée à l'administration systémique (*i.e.* injection intraveineuse), l'administration transtympanique permet d'obtenir une concentration plus importante en substance active dans l'oreille interne (Zhou et al., 2009).

A ce jour, il n'y a pas de formulations spécifiquement développées pour la voie transtympanique sur le marché. Pour cette raison, des solutions/suspensions injectables (liquides) sont utilisées hors AMM (Autorisation de Mise sur le Marché) dans la pratique clinique (McCall et al., 2010). Ces solutions/suspensions présentent l'inconvénient d'être éliminées très rapidement en s'écoulant par la trompe d'Eustache, ce qui nécessite des injections répétées (Alles et al., 2006, Herraiz et al., 2010). Des formulations spécifiques pour la voie transtympanique doivent ainsi être développées et devront répondre au cahier des charges suivant pour tenir compte des contraintes de cette voie d'administration : être facilement injectables, présenter une immobilisation rapide et un temps de résidence prolongé au niveau de l'oreille moyenne pour limiter les pertes par la trompe d'Eustache, assurer une libération prolongée de la substance active pour limiter le nombre d'injections et améliorer

ainsi le confort du patient, permettre à la substance active d'atteindre une concentration thérapeutique dans l'oreille interne et enfin, être bien tolérées.

Dans ce travail, nous proposons de concevoir de caractériser et d'évaluer une formulation adaptée à cette voie d'administration constituée de **liposomes** dispersés au sein d'un gel **d'acide hyaluronique (HA)**. L'acide hyaluronique est un polymère naturellement présent dans l'organisme. Biocompatible et biodégradable, il devrait assurer un temps de résidence prolongé dans l'oreille moyenne grâce à ses propriétés mucoadhésives et viscoélastiques (Masuda et al., 2001, Girish and Kemparaju, 2007). Les liposomes sont, pour leur part, des nanovecteurs sphériques constitués de bicouches phospholipidiques. Ils sont biocompatibles et biodégradables et devraient agir comme un réservoir pour la substance active encapsulée afin d'assurer une libération prolongée de celle-ci (Wang et al., 2012). Le système « gel de liposomes » a été développé précédemment au sein de l'Institut Galien Paris-Sud pour l'injection intra-vitréenne en ophtalmologie. Ce travail a fait l'objet de la thèse de Laure Lajavardi (Lajavardi, 2008). Il a été démontré que les liposomes contenant du Vasoactive Intestinal Peptide au sein du gel d'acide hyaluronique permettaient d'obtenir une forme à libération prolongée du peptide intact après injection intra-oculaire, ce qui a conduit à un effet thérapeutique sur l'inflammation chez le rat (Lajavardi et al., 2009). De plus, une étude rhéologique préliminaire a mis en évidence des interactions entre les liposomes recouverts de chaînes de polyéthylène glycol (liposomes PEGylés) et l'HA qui se sont traduites par une augmentation de la viscosité et de l'élasticité du gel de manière dépendante de la concentration en lipides. Il paraissait intéressant d'étendre l'utilisation du système « gel de liposomes », qui s'est montré très prometteur, à d'autres applications telles que l'injection transtympanique en identifiant les paramètres clés de formulation pour les adapter ensuite aux contraintes d'administration.

Ainsi, l'objectif général de ce travail de thèse consiste, d'une part, à caractériser d'un point de vue physicochimique et de façon approfondie les propriétés du gel d'acide hyaluronique contenant différentes formulations de liposomes afin d'en faire une plateforme de formulation pour différentes voies locales. En outre, pour la voie transtympanique, le but est d'évaluer *in vivo*, après administration locale dans l'oreille moyenne, l'intérêt du gel de liposomes encapsulant un corticoïde en ce qui concerne, d'une part, les aspects biopharmaceutiques, et d'autre part, son potentiel thérapeutique pour le traitement des surdités réversibles.

Ce manuscrit s'articule en deux grandes sections :

La section **travaux antérieurs** réalise une synthèse bibliographique des aspects anatomiques, physiologiques et biopharmaceutiques concernant l'oreille moyenne et interne. Elle décrit notamment les difficultés liées au traitement des pathologies de l'oreille interne ainsi que les avancées dans ce domaine en termes de traitements et de stratégies d'administration (voies et formes galéniques).

La seconde section du manuscrit, qui concerne les **travaux expérimentaux**, est rédigée sous forme d'un recueil de publications et chapitres. Cette section est divisée en deux parties :

La **première partie** porte sur l'étude physicochimique et comprend deux chapitres :

- Le **chapitre I** s'intéresse à l'effet des liposomes (composition, concentration, taille) sur les propriétés rhéologiques et de seringabilité des gels d'acide hyaluronique.
- Le **chapitre II** présente, d'une part, une caractérisation approfondie de la compatibilité du système gel de liposomes ainsi que de sa microstructure et, d'autre part, une étude de la mobilité des liposomes au sein du gel d'HA à l'échelle macro- et microscopique.

La **deuxième partie** est consacrée à l'évaluation *in vivo* du gel de liposomes contenant un corticoïde (la dexamethasone phosphate, DexP) chez le cobaye Hartley albinos. Cette partie comprend trois chapitres :

- Le **chapitre III** porte sur l'encapsulation de la DexP dans les liposomes PEGylés, l'évaluation de l'innocuité du gel de liposomes sur la fonction auditive des cobayes ainsi que l'étude de la biodistribution des différents constituants de la formulation (HA, liposomes et DexP) après injection dans l'oreille moyenne.
- Les **chapitre IV et V** sont dédiés à l'évaluation de l'effet thérapeutique de la formulation sur un modèle de traumatisme sonore (Chapitre IV) et sur un modèle d'implantation cochléaire (Chapitre V).

Une discussion générale résume l'intérêt et les potentialités du gel de liposomes pour la voie transtympanique mais aussi pour des applications dans d'autres voies d'administration locales. Cette discussion revient sur les points clé de ce travail en considérant l'ensemble des principaux résultats et en s'appuyant sur les données de la littérature.

Enfin, une conclusion générale fait le point sur les avancées apportées par ce travail et sur les perspectives envisagées pour compléter et approfondir la compréhension des résultats obtenus au cours de cette de thèse.

Ce travail a été réalisé au sein de l’Institut Galien Paris-Sud, UMR CNRS 8612, à la faculté de pharmacie de l’Université Paris-Sud (Université Paris-Saclay) en collaboration entre deux équipes : l’équipe 3 « Physique pharmaceutique » et l’équipe 5 « Ingénierie particulaire et cellulaire à visée thérapeutique » sous la co-direction du Professeur Florence Agnely et du Professeur Amélie Bochot. Une grande partie de ce travail a été effectuée en collaboration avec l’équipe du Docteur Evelyne Ferrary, UMR-S 1159 Inserm, « Chirurgie mini-invasive robotisée » (Hôpital Bichât et Hôpital de la Pitié-Salpêtrière).

## Références

- Alles, M.J., der Gaag, M.A., Stokroos, R.J., 2006. Intratympanic steroid therapy for inner ear diseases, a review of the literature. *Eur Arch Otorhinolaryngol.* 263, 791-797.
- Ayoob, A.M., Borenstein, J.T., 2015. The role of intracochlear drug delivery devices in the management of inner ear disease. *Expert Opin Drug Deliv.* 12, 465-479.
- Bouccara, D., Mosnier, I., Bernardeschi, D., Ferrary, E., Sterkers, O., 2012. Cochlear implant in adults. *Rev Med Interne.* 33, 143-149.
- Girish, K.S., Kemparaju, K., 2007. The magic glue hyaluronan and its eraser hyaluronidase: a biological overview. *Life Sci.* 80, 1921-1943.
- Herraiz, C., Miguel Aparicio, J., Plaza, G., 2010. Intratympanic drug delivery for the treatment of inner ear diseases. *Acta Otorrinolaringol Esp.* 61, 225-232.
- Juhn, S.K., Hunter, B.A., Odland, R.M., 2001. Blood-labyrinth barrier and fluid dynamics of the inner ear. *Int Tinnitus J.* 7, 72-83.
- Juhn, S.K., Rybak, L.P., 1981. Labyrinthine barriers and cochlear homeostasis. *Acta Otolaryngol.* 91, 529-534.
- Lajavardi, L. (2008). Nouvelle stratégie thérapeutique des uvéites par l'administration intraoculaire d'un peptide immunomodulateur, le vasoactive intestinal peptide, dans des liposomes, Paris 11.
- Lajavardi, L., Camelo, S., Agnely, F., Luo, W., Goldenberg, B., Naud, M.-C., Behar-Cohen, F., de Kozak, Y., Bochot, A., 2009. New formulation of vasoactive intestinal peptide using liposomes in hyaluronic acid gel for uveitis. *Journal of Controlled Release.* 139, 22-30.
- Lasak, J.M., Allen, P., McVay, T., Lewis, D., 2014. Hearing Loss: Diagnosis and Management. *Primary Care: Clinics in Office Practice.* 41, 19-31.
- Masuda, A., Ushida, K., Koshino, H., Yamashita, K., Kluge, T., 2001. Novel Distance Dependence of Diffusion Constants in Hyaluronan Aqueous Solution Resulting from Its Characteristic Nano-Microstructure. *Journal of the American Chemical Society.* 123, 11468-11471.
- McCall, A.A., Swan, E.E., Borenstein, J.T., Sewell, W.F., Kujawa, S.G., McKenna, M.J., 2010. Drug delivery for treatment of inner ear disease: current state of knowledge. *Ear Hear.* 31, 156-165.
- Nguyen, Y., Bernardeschi, D., Kazmitcheff, G., Miroir, M., Vauchel, T., Ferrary, E., Sterkers, O., 2015. Effect of embedded dexamethasone in cochlear implant array on insertion forces in an artificial model of scala tympani. *Otol Neurotol.* 36, 354-358.
- Staecker, H., Rodgers, B., 2013. Developments in delivery of medications for inner ear disease. *Expert Opin Drug Deliv.* 10, 639-650.
- Swan, E.E., Mescher, M.J., Sewell, W.F., Tao, S.L., Borenstein, J.T., 2008. Inner ear drug delivery for auditory applications. *Adv Drug Deliv Rev.* 60, 1583-1599.
- Wang, A.Z., Langer, R., Farokhzad, O.C., 2012. Nanoparticle delivery of cancer drugs. *Annu Rev Med.* 63, 185-198.
- Zhou, C.H., Sun, J.J., Gong, S.S., Gao, G., 2009. Comparison of the antioxidants lipoic acid pharmacokinetics in inner ear between intravenous and intratympanic administration in guinea pigs. *Zhonghua Er Bi Yan Hou Tou Jing Wai Ke Za Zhi.* 44, 1034-1037.

## **Travaux antérieurs**

## Introduction – résumé

L'objectif de cette partie bibliographique est d'aborder, d'un point de vue pharmaceutique, les difficultés liées au traitement des pathologies de l'oreille interne ainsi que les avancées dans ce domaine en termes de traitements et de stratégies d'administration (voies et formes galéniques). Dans un premier temps, l'anatomie générale de l'oreille ainsi que sa physiologie seront présentées avec une attention particulière portée à l'oreille moyenne et interne. Les aspects biopharmaceutiques seront développés afin de mieux comprendre les défis liés à la mise à disposition de molécules thérapeutiques dans l'oreille interne. Ensuite, les principales pathologies ainsi que les substances actives fréquemment utilisées en otologie seront brièvement abordées. Enfin, les différentes stratégies d'administration seront plus particulièrement détaillées.

L'efficacité des traitements des pathologies de l'oreille interne dépend principalement de leur capacité à atteindre des concentrations thérapeutiques en substances actives au niveau des fluides et des tissus de l'oreille interne. Actuellement, en otologie, les traitements par voie locale se développent en alternative aux traitements par voie systémique (*i.e.* injection intraveineuse) responsables de nombreux effets indésirables du fait des fortes doses nécessaires pour obtenir un effet thérapeutique au niveau des cibles cellulaires situées dans l'oreille interne. Cela est principalement lié à la présence d'une barrière hémato-périlymphatique. Ainsi, plusieurs méthodes d'administration locales telles que l'administration intratympanique (aussi appelée transtympanique) ou l'administration intracochléaire se sont développées. L'administration intratympanique consiste à administrer le médicament directement dans l'oreille moyenne. Elle est peu invasive mais nécessite la diffusion de la molécule à travers les barrières localisées entre l'oreille moyenne et interne, à savoir, la fenêtre ovale et surtout la fenêtre ronde. L'administration intracochléaire est beaucoup plus invasive mais offre un accès direct à l'oreille interne. Au cours des dix dernières années, une large gamme de systèmes a été évaluée en otologie en recherche pré-clinique et clinique. Dans cette revue de la littérature, nous faisons une synthèse critique des différentes stratégies qui ont été explorées avec une attention particulière pour les études *in vivo*. Seront ainsi présentés les hydrogels et les systèmes nanoparticulaires au sens large pour l'administration intratympanique, ou encore l'enrobage d'implants cochléaires par des polymères contenant la substance active et les dispositifs médicaux pour l'administration intracochleaire. Enfin, nous avons souhaité faire ressortir les systèmes les plus prometteurs pour des applications cliniques futures ainsi que les obstacles et verrous technologiques qui restent à surmonter.

Cette revue a été publiée dans ***International Journal of Pharmaceutics*** :

El Kechai, N., Agnely, F., Mamelle, E., Nguyen, Y., Ferrary, E., Bochot, A.\***, 2015**. Volume 494, 83-101.

## **Publication 1**

### **Recent advances in local drug delivery to the inner ear**

*Naila EL KECHAI<sup>a</sup>, Florence AGNELY<sup>a</sup>, Elisabeth MAMELLE<sup>b,c</sup>, Yann NGUYEN<sup>b,c</sup>,  
Evelyne FERRARY<sup>b,c</sup>, Amélie BOCHOT \*<sup>a</sup>*

<sup>a</sup> *Université Paris-Sud, Faculté de pharmacie, Institut Galien Paris-Sud, CNRS UMR 8612, 5 Rue J-B Clément, 92290 Châtenay-Malabry, France.*

<sup>b</sup> *UMR-S 1159 Inserm / Université Pierre et Marie Curie – Sorbonne Universités “Minimally Invasive Robot-based Hearing Rehabilitation”, 16 rue Henri Huchard, 75018 Paris, France.*

<sup>c</sup> *AP-HP, Pitié-Salpêtrière Hospital, Otolaryngology Department, Unit of Otology, Auditory Implants and Skull Base Surgery, Paris, France*

#### **\* Corresponding Author**

Pr. Amélie BOCHOT: +33 1 46 83 55 79; amelie.bochot@u-psud.fr

## Abstract

Inner ear diseases are not adequately treated by systemic drug administration mainly because of the blood-perilymph barrier that reduces exchanges between plasma and inner ear fluids. Local drug delivery methods including intratympanic and intracochlear administrations are currently developed to treat inner ear disorders more efficiently. Intratympanic administration is minimally invasive but relies on diffusion through middle ear barriers for drug entry into the cochlea, whereas intracochlear administration offers direct access to the cochlea but is rather invasive. A wide range of drug delivery systems or devices were evaluated in research and clinic over the last decade for inner ear applications. In this review, different strategies including medical devices, hydrogels and nanoparticulate systems for intratympanic administration, and cochlear implant coating or advanced medical devices for intracochlear administration were explored with special attention to *in vivo* studies. This review highlights the promising systems for future clinical applications as well as the current hurdles that remain to be overcome for efficient inner ear therapy.

## Keywords

Cochlea, hydrogels, intracochlear administration, intratympanic administration, medical drug delivery devices, nanoparticulate systems.

## Abbreviations

AIED, autoimmune inner ear disease; BDNF, Brain-derived neurotrophic factor; BPLB, blood-perilymph barrier; BSA, bovine serum albumine; CMAP, Na-carboxymethyl- $\beta$ -cyclodextrins modified activated polyamidoamine; CMV, cytomegalovirus; FITC, fluorescein isothiocyanate; GMO, glycerol monooleate; HA, hyaluronic acid; HBPL, hyperbranched poly-L-lysine; HGF, hepatocyte growth factor; IGF-1, insulin-like growth factor-1; JNK, c-Jun n-terminal kinase; LNC, lipid nanocapsule; NIHL, noise-induced hearing loss; PEG-PCL, poly(ethyleneglycol)-*b*-poly( $\epsilon$ -caprolactone); PHEA, poly(2-hydroxyethyl aspartamide); PK, pharmacokinetic; PLGA, poly(lactic-co-glycolic acid); RW, round window; SNHL, sensorineural hearing loss; SPION, superparamagnetic iron oxide nanoparticle; TTI, transtympanic injection.

## 1. Introduction

Despite the high incidence of inner ear diseases (Ayoob and Borenstein, 2015), there are currently no dedicated medicines available on the market. Indeed, the inner ear is one of the most challenging target organs for drug delivery. Conventional routes of administration such as oral or parenteral routes are largely ineffective principally because of the blood-perilymph barrier (BPLB) that isolates the inner ear from the blood (Saito et al., 2001). Therefore, local rather than systemic drug delivery is being developed to treat inner ear diseases (Salt and Plontke, 2005, Swan et al., 2008, McCall et al., 2010, Pararas et al., 2012, Staeker and Rodgers, 2013). Besides, advances in molecular biology showed that the regeneration of neural and possibly sensory cells in the inner ear is a way for the treatment of hearing loss and other inner ear diseases (Holley, 2005). This highlights the need for suitable and precisely controlled local drug delivery systems for inner ear therapy.

There are currently two main approaches for local drug delivery to the inner ear: intratympanic administration (drugs are introduced into the middle ear) and intracochlear administration (drugs are introduced directly into the inner ear). Both techniques allow to maximize drug concentration in the inner ear while minimizing systemic exposure (Wang et al., 2009, Pararas et al., 2012, Honeder et al., 2014). A suitable drug delivery system for intratympanic administration should be minimally invasive and easily injectable. It should achieve a prolonged residence time in the middle ear, a therapeutic concentration in the inner ear and a sustained release of the drug in order to reduce the number of injections. Ideally, it could offer precise release kinetics and specific targeting. Finally, it should be biodegradable and biocompatible without any negative effects on hearing or balance function. Similarly, a suitable device for intracochlear administration should be safe, minimally invasive and have appropriate dimensions for implantation. It should provide a controlled drug delivery over extended periods of time.

This review highlights successful inner ear drug delivery systems that have been tested either for clinical or research applications and discuss their benefits and potential drawbacks. First, we give a brief overview of the ear anatomy and physiology and other relevant biopharmaceutical aspects. Then, the different strategies for drug delivery to the inner ear are classified regarding the location of drug entry (intratympanic or intracochlear administration) and the nature of the delivery system (medical device, hydrogel, nanoparticulate system). This review discusses the promising systems for future clinical applications as well as the current hurdles that remain to be overcome for efficient inner ear therapy.

## 2. The ear

### 2.1. Anatomical and physiological issues

The ear is separated in three entities (**Fig. 1**): external, middle and inner ear. The external ear is represented by the pinna (visible part of the ear) and the external auditory canal. At the bottom of the external ear, the tympanic membrane (eardrum) creates a barrier with the middle ear. The middle ear consists of the tympanic cavity containing the ossicular chain formed by the malleus, the incus and the stapes. The Eustachian tube, which lies at an angle of  $\sim 45^\circ$  to the horizontal plane, allows the airing of the tympanic cavity *via* the nasopharynx. The inner ear is embedded deep in the petrous bone, one of the hardest bones of the body. It contains both the organ of hearing, the cochlea, and the organs of balance, the vestibuli (utricle and saccule) and the semicircular canals (Lee et al., 2003). The cochlea is a bony coiled tube of around 30 mm long in human, looking like a snail shell (Schuknecht and Gacek, 1993). The cochlea is divided in three fluid-filled compartments (**Fig. 2**). The middle compartment, called the *scala media*, is filled with endolymph, whereas the lower and upper compartments, the *scala tympani* and the *scala vestibuli* respectively, are both filled with perilymph. *Scala tympani* and *scala vestibuli* communicate at the apex of the cochlea through a structure known as the helicotrema (Igarashi et al., 1986). The basilar membrane supports the organ of Corti that is composed of highly organized mechano-sensory cells, the inner and the outer hair cells and their supporting cells (**Fig. 2**). Briefly, in the auditory process, sound waves are channeled by the pinna into the auditory canal causing vibration of the tympanic membrane. The vibrations cause motion of the ossicular chain and the piston-like motion of the stapes transfers the pressure wave to inner ear fluids *via* the oval window. Vibration of the stereocilia of the inner hair cells is responsible for the transformation of the acoustic information (pressure variation) into bioelectric signal (intracellular potential variation leading to neurotransmitters release) that is transferred to the spiral ganglion neurons. The structure of the basilar membrane and the sensory cells is tonotopically organized so that high frequencies stimulate the basal part of the cochlea whereas low frequencies stimulate the apex. Finally, this signal is transmitted to the brainstem *via* the cochlear nerve and ultimately to the cerebral cortex where the information is translated into auditory sensations (Lee et al., 2003).

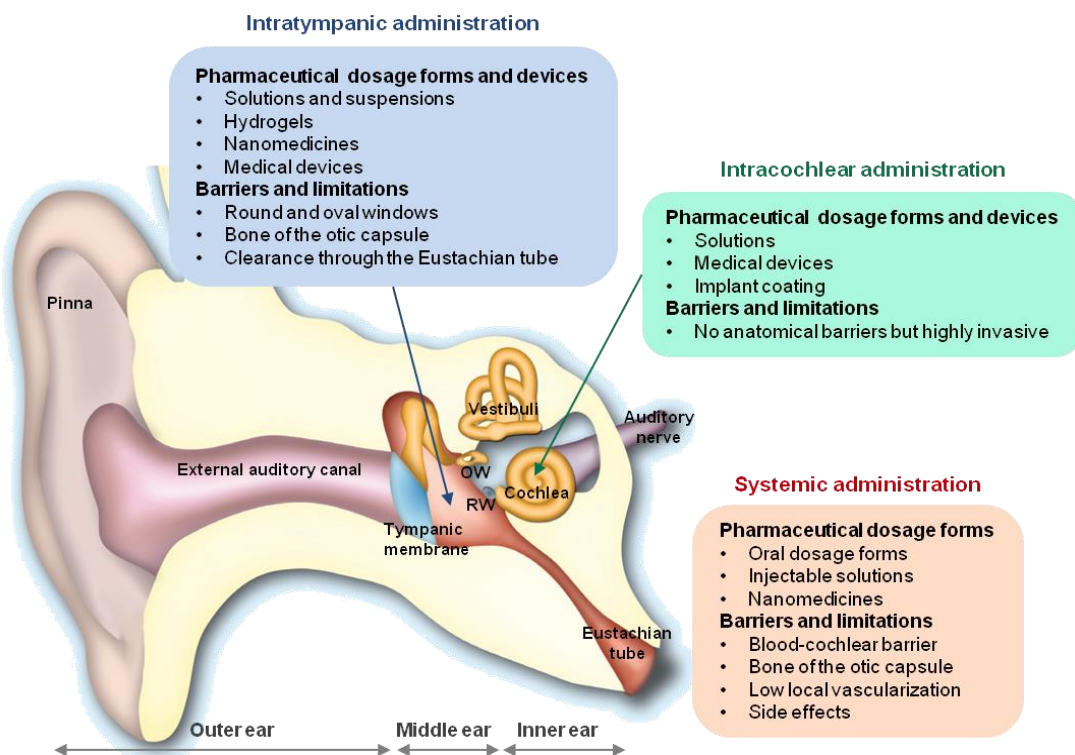


**Fig.1.** Coronal view of the ear demonstrating the outer, middle, inner ear components and the different strategies for local drug delivery to the inner ear. Image was adapted from Hoskinson *et al.* 2013 and is reproduced here with kind permission of Future Science Ltd.

RW: round window; OW: oval window.

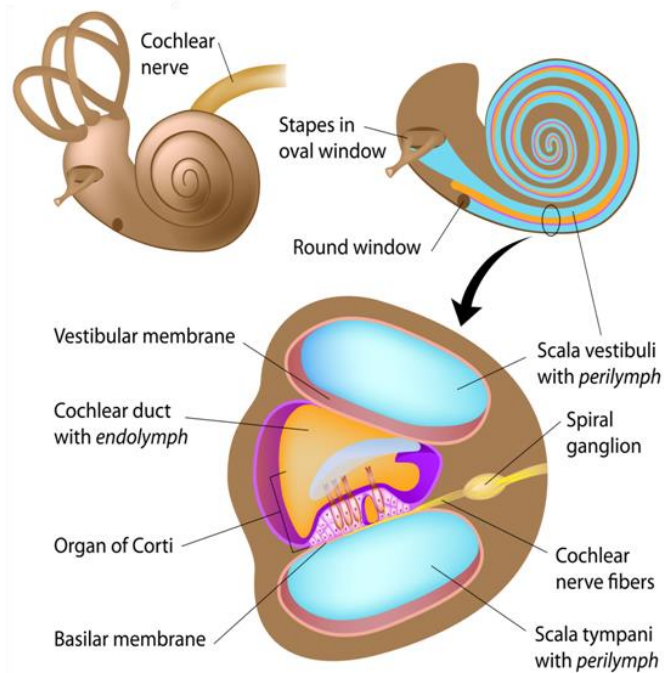


**Fig.2.** Anatomy of the cochlea.

## 2.2. Inner ear fluids

Mechanoelectrical transduction of sound and motion by the inner ear is highly dependent on the ionic composition of inner ear fluids bathing the auditory hair cells (Ghanem et al., 2008). Endolymph ( $\sim 8 \mu\text{L}$  in human), that bathes the apical surface of hair cells, is an unusual extracellular fluid with a high potassium concentration ( $[\text{K}^+] \sim 160 \text{ mM}$ ) and a low sodium concentration ( $[\text{Na}^+] < 1 \text{ mM}$ ) and is positively polarized ( $\sim + 80 \text{ mV}$ ) compared to cerebrospinal fluid or plasma (Table 1). Conversely, perilymph ( $\sim 70 \mu\text{L}$  in human), at the basolateral side of hair cells, has a high  $[\text{Na}^+]$  ( $\sim 150 \text{ mM}$ ) and a low  $[\text{K}^+]$  ( $\sim 4 \text{ mM}$ ) (Sterkers et al., 1988, Ferrary and Sterkers, 1998). The electrochemical gradients between apical endolymph and intracellular space on the one hand, and the basolateral perilymph on the other hand, drive  $\text{K}^+$  transport into hair cells for mechano-bio-transduction of the signal (Ghanem et al., 2008). Small changes from the normal state of perilymph and endolymph (composition, pH, osmolality, potential, volume) result in a decrease of hearing sensitivity (Juhn et al., 2001). Proteomic analysis of perilymph showed that more than 33% of the proteins comprised protease inhibitors (Swan et al., 2009). 16% were apolipoproteins and 15% were enzymes such as prostaglandin synthase, carboxylesterase, creatine kinase, and phosphodiesterase indicating a metabolic activity in perilymph. Albumin was the most abundant single protein (14%). Thus, the large amounts of albumin, apolipoproteins and glycoproteins may bind acidic/basic and lipophilic drugs and then, act as a reservoir.

**Table 1**

Composition and characteristics of cochlear fluids (Scheibe and Haupt, 1985, Anniko and Wroblewski, 1986, Igarashi et al., 1986, Ferrary and Sterkers, 1998, Shinomori et al., 2001).

Composition/characteristics	Perilymph	Endolymph
$\text{Na}^+$ (mM)	160	1
$\text{K}^+$ (mM)	4 - 5	150
$\text{Cl}^-$ (mM)	120	130
$\text{H}_2\text{CO}_3$ (mM)	20	30
$\text{Ca}^{2+}$ (mM)	1.2	0.02
Proteins (g/L)	1	0.15
Glucose (mM)	4	0.5
pH	7.4	7.4
Osmolality (mOsm/kg)	290	315
Potential (mV)	0	+ 80
Volume ( $\mu\text{L}$ )	8.9*	1.5*
	70**	8**

\* in guinea pig, \*\* in human

### 2.3. Ear barriers

#### 2.3.1. Blood-perilymph barrier

The blood-perilymph barrier (BPLB), also called blood-cochlear barrier, is formed by a continuous capillary endothelium lining blood vessels in the cochlea. The endothelial cells are connected with tight junctions and there are no fenestrations (Jahnke, 1980, Juhn, 1988). This structure maintains the microhomeostasis of the inner ear fluids and cells and protects the inner ear integrity (Juhn and Rybak, 1981, Juhn et al., 2001). The BPLB acts not only as a physical barrier but also as a biochemical one with efflux pump systems such as P-glycoprotein and multidrug resistance-related protein-1 (Saito et al., 2001). As the blood-brain barrier, the BPLB is only permeable to small liposoluble molecules, whereas high molecular weight, water-soluble and charged molecules are unlikely to diffuse passively (Swan et al., 2008). For these reasons, the BPLB is considered as a major barrier for the passage of drugs from the systemic circulation to the cochlea. For example, the single intracardial injection of dexamethasone in guinea pig (0.2 mg/mL) yielded very low perilymph concentrations (0.03 µg/mL in perilymph after 1 h versus 2.76 mg/mL in plasma) (Yang et al., 2008). Similarly, after systemic administration of lipoic acid in guinea pig (100 mg/mL), the maximal concentration detected in perilymph was 33 µg/mL, whereas the perilymphatic concentration of this compound was 5-fold higher after intratympanic administration (Zhou et al., 2009).

However, a number of conditions can modify the passage of molecules through the BPLB including noise exposure (Suzuki et al., 2002), inflammation (Kastenbauer et al., 2001), diuretics (McFadden et al., 2002) and osmotic agents such as glycerol (Juhn et al., 1976).

#### 2.3.2. Tympanic membrane

The tympanic membrane or eardrum is elliptical and slightly conical in shape and separates the middle from the external ear. It is around 0.6 mm in thickness and is composed of three layers: an outer epidermal layer, an inner mucosal layer and a middle fibrous layer with collagen giving the tympanic membrane its structural integrity (Lee et al., 2003). Its surface area is around 80 mm<sup>2</sup> in adult. The main function of the tympanic membrane is the transmission of sound waves to the ossicular chain. It acts as a barrier for drug delivery to the middle and inner ear and therefore must be artificially breached if intact (transtympanic injection) (Hoskison et al., 2013).

### 2.3.3. Round and oval windows

The round window and the oval window are semi-permeable membranous interfaces between the cochlea and the middle ear (**Fig. 1**). Both are located at the base of the cochlea. The round window and the oval window can be considered either as barriers or as pathways regarding drug delivery to the cochlea.

The round window, located towards the *scala tympani*, is composed of three layers: the outer epithelium, facing the middle ear, contains a single layer of cells with sparse microvilli. The inner epithelium, bounding the inner ear, consists of squamous cells with long lateral extensions sometimes overlapping, large extracellular spaces and rare microvilli. These two layers are separated by a core of connective tissue made of fibroblasts, blood vessels, collagen and elastic fibers. The round window has an average thickness of 70 µm in human and between 10 and 14 µm in rodents (Kawabata and Paparella, 1971, Goycoolea et al., 1988, Goycoolea and Lundman, 1997). Its surface area is around 2.2 mm<sup>2</sup> in human (Okuno and Sando, 1988) and 1 mm<sup>2</sup> in guinea pig (Ghiz et al., 2001).

The round window vibrates thanks to its elastic properties with opposite phase to vibrations entering the inner ear through the oval window, allowing fluid movement in the cochlea (Wever and Lawrence, 1948). Anatomic observations suggest that it also could participate in secretion and/or absorption of molecules (Richardson et al., 1971, Miriszlai et al., 1978). Consequently, the round window is able to transport drugs into the cochlea and is used as the main passage for drug delivery to the inner ear from the middle ear (Salt et al., 2012, Zou et al., 2012).

Factors impacting the permeability of the round window include size, concentration, solubility and electrical charge of the molecule being transported (Goycoolea et al., 1988, Juhn et al., 1989, Goycoolea and Lundman, 1997). However, round window permeability of different molecular weight substances depends more likely on the specific pathway involved for transmembrane transport (passive diffusion, facilitated diffusion, active transport or phagocytosis) (Goycoolea, 2001) than on the molecular weight itself. Indeed, both low-molecular weight substances such as aminoglycoside antibiotics and corticosteroids (around 500 Da) and large molecules such as horseradish peroxidase (45 kDa) (Kim et al., 1990) and golimumab, a monoclonal antibody (150 kDa) (Ghossaini et al., 2013) were able to diffuse through the round window. Conversely, albumin (70 kDa) was not able to cross the round window unless it was altered or in case of inflammation (Hamaguchi et al., 1988). Otherwise, cationic ferritin (450 kDa) was observed to pass easily through the normal round window

while anionic ferritin did not (Goycoolea et al., 1997). Lipophilic steroids are more likely to diffuse passively through the round window compared to hydrophilic steroids (Wang et al., 2011). Besides drug characteristics, other factors, including the thickness and the integrity of the round window, osmolality of the formulation and the presence of preservatives (benzyl alcohol) can affect round window permeability (Mikulec et al., 2008). These authors estimated that benzyl alcohol enhanced round window permeability by a factor of 3 to 5 and elevating osmolality from 300 to 620 mOsm/kg increased its permeability by a factor of 2 to 3. Moreover, Shih et al., (2013) successfully tested ultrasound-aided microbubbles to temporarily increase round window permeability to fluorescently labelled biotin and gentamicin. Interestingly, this approach did not alter the integrity of the round window and did not affect the hearing function of guinea pigs. Finally, other factors that may alter round window permeability are anatomic obstacles, such as plugs of connective or adipose tissue, or so-called pseudomembranes of the round window niche. It has been estimated that approximately one third of patients have obstructions of the round window (Alzamil and Linthicum, 2000).

Recent studies have shown that, in rodents, drugs can also enter the inner ear *via* the oval window (Salt et al., 2012, King et al., 2013). The oval window contains the footplate of the stapes and the annular ligament and is located towards the *scala vestibuli* (**Fig. 1**). A histological study in rat demonstrated that the annular ligament across the stapedio-vestibular joint has a porous structure composed of fibrillin, 36 kDa microfibril-associated glycoprotein and hyaluronic acid (Ohashi et al., 2008). The amount of drug entering by this route, however, remains uncertain and is likely to depend on drug size and charge. Nevertheless, it is thought to be less effective than the pathway through the round window (Zou et al., 2012). Salt et al., (2012) estimated that 65% of the total ionic marker trimethylphenylammonium (applied in the round window niche of guinea pig) entered through the round window and 35% entered the vestibule directly in the vicinity of the stapes. Moreover, Mikulec et al., (2009) showed that following intratympanic administration in guinea pig, molecules may enter in the inner ear through the bone of the otic capsule.

### 3. Main inner ear diseases and therapies

Hearing loss, tinnitus and balance disorders are common inner ear diseases affecting individuals of different ages and have significant impact on quality of life. Sensorineural hearing loss is one of the most common sensory impairments in humans and results from

damaged hair cells or damaged spiral ganglion neurons (Ayoob and Borenstein, 2015). Several factors may alter hair cells and spiral ganglion neurons including aging, aminoglycoside drugs, Meniere's disease, viral infection, autoimmune diseases, genetic anomalies, acute or long-term noise exposure. Currently, most hearing-impaired patients receive either hearing aids or cochlear implants for hearing improvement (Ayoob and Borenstein, 2015). In parallel, systemic or local administration of corticosteroids is frequently used for the management of sudden sensorineural hearing loss. In severe cases of vertigo attacks due to Meniere's disease, systemic or local aminoglycoside antibiotics may be considered to purposefully damage the inner ear but are usually a last resort treatment (McCall et al., 2010, Huon et al., 2012, Bear and Mikulec, 2014). However, the clinical effectiveness of drugs after systemic administration is limited by side effects arising from the high doses required to achieve an appropriate concentration in the inner ear (because of the BPLB, see section 2.3.1). It is noteworthy that the treatment of inner ear diseases is now moving towards local drug delivery, which allows to obtain therapeutic concentration of drugs in the inner ear fluids with limited systemic side effects (Staecker and Rodgers, 2013) (**Table 2**).

Moreover, most of the drugs employed in clinical practice for inner ear therapy have a broad rather than targeted effect (i.e. corticosteroids, gentamicin, antioxydants) (Staecker and Rodgers, 2013). Interestingly, an expanding number of pharmacological compounds are now in development either in pre-clinical or clinical research and are demonstrating promising results for the treatment of sensorineural hearing loss and other auditory diseases (**Table 2**). Indeed, advances in molecular biology and identification of regeneration pathways of sensory and neural cells in the inner ear should allow the future treatment of inner ear diseases in a more efficient and targeted manner. It includes the use of apoptosis inhibitors, growth factors, neurotrophins, gene therapy and stem cells therapy (**Table 2**). Several regenerative compounds designed to treat sensorineural hearing loss, Menière's disease and tinnitus are now in clinical trials (Ayoob and Borenstein, 2015).

#### 4. Local drug delivery to the inner ear

Topical treatments applied through the external auditory canal such as ear drops are not detailed in this review. Such approaches do not allow to treat inner ear diseases because of the barriers described previously (tympanic membrane, bone, round window, oval window) between external and inner ear (**Fig. 1**). Outer ear and some middle ear diseases with perforated eardrum are commonly treated by topical antibiotics, steroids and antifungal

formulations which were reviewed elsewhere (Hoskison et al., 2013). The present review focuses on local drug delivery for the treatment of inner ear diseases. There are two main strategies based on the location of drug entry (**Fig. 1**): intratympanic and intracochlear drug administrations. Intratympanic administration is minimally invasive but relies on diffusion of the active molecule through the round window for access to the inner ear, whereas intracochlear administration offers direct access to the cochlea but is highly invasive (**Fig. 1**). These two approaches are compared in **Table 3**.

Since the cochlea is extremely sensitive to changes in fluid volume and ionic composition, any formulation intended for intratympanic or intracochlear administration should maintain the homeostasis of inner fluids. It should have a physiological pH (7.38 - 7.42) and an osmolality around 300 mOsm/kg. Furthermore, according to the monography for parenteral preparations in the European Pharmacopoeia (European Pharmacopoeia Commission), the formulation must be sterile and under the limit accepted for the bacterial endotoxin test. As the local administration in the middle or inner ear is a route that gives access to the cerebrospinal fluid, the use of preservatives for such applications is not permitted. Consequently, preparations for local administration in the middle or inner ear must be presented in single-dose containers. In addition, the presence of preservatives in the middle ear affects round window permeability and those molecules may concentrate in the inner ear potentially leading to toxicity on cochlear cells (Mikulec et al., 2008). Finally, the excipients have to be safe (i.e. be biocompatible, have low immunogenicity and minimize the inflammatory response).

**Table 2**

Main therapeutic molecules intended for the treatment of inner ear diseases.

Type	Therapeutic molecule(s)	Disease(s)	Route of administration	Use	Reference(s)
<b>Corticosteroid</b>	Dexamethasone, methylprednisolone	SNHL, Menière's disease, AIED, NIHL, tinnitus	systemic	Clinical practice	(McCall et al., 2010, Li et al., 2013)
			local	Clinical practice, clinical and pre-clinical research	(Alles et al., 2006, McCall et al., 2010, Bear and Mikulec, 2014)
<b>Aminoglycoside antibiotic</b>	Gentamicin, streptomycin, kanamycin	Menière's disease	systemic	Clinical practice	(Berryhill and Graham, 2002)
			local	Clinical practice, clinical and pre-clinical research	(Huon et al., 2012)
<b>Antioxydant</b>	n-acetyl cysteine, d-methionine, thiourea	NIHL, otoprotection	local	Clinical practice, clinical and pre-clinical research	(Darrat et al., 2007, Eastwood et al., 2010, Mukherjea et al., 2011)
<b>Local anesthetic</b>	Lidocaine	Tinnitus	local	Clinical and pre-clinical research	(Horie et al., 2010)
<b>n-methyl-d-aspartate receptor antagonist</b>	Esketamine, gacyclidine, ifenprodil	Tinnitus	local	Clinical and pre-clinical research	(Guitton and Dudai, 2007, Wenzel et al., 2010, van de Heyning et al., 2014)
<b>Antiviral</b>	Cidofovir, ganciclovir	Congenital SNHL due to CMV infection, Menière's disease	local	Clinical and pre-clinical research	(Guyot et al., 2008, Ward et al., 2014)
<b>Apoptosis inhibitor</b>	AM-111 peptide (JNK inhibitor)	NIHL	local	Clinical and pre-clinical research	(Coleman et al., 2007, Suckfuell et al., 2007, Omotehara et al., 2011)
<b>Neurotrophin</b>	BDNF, neurotrophic factor-3, growth factors	SNHL	local	Pre-clinical research	(Richardson et al., 2008)
<b>Monoclonal antibody</b>	Infliximab, Golimumab (TNF $\alpha$ inhibitor), Anakinra (IL-1 antagonist), Rituximab (CD20 antagonist)	AIED	local	Clinical and pre-clinical research	(Ghossaini et al., 2013, Lobo et al., 2013)
<b>Gene therapy</b>	Plasmids, siRNA	SNHL	local	Pre-clinical research	(Fukui and Raphael, 2013)
<b>Stem cell therapy</b>		SNHL	local	Pre-clinical research	(Almeida-Branco et al., 2014)

**Table 3**

Comparison between intratympanic and intracochlear administration: benefits and limitations.

	<b>Intratympanic administration</b>	<b>Intracochlear administration</b>
<b>Benefits</b>	<ul style="list-style-type: none"> <li>- Treatment of middle ear and inner ear diseases</li> <li>- Minimized systemic exposure</li> <li>- Short and middle term local drug delivery (several days to weeks)</li> <li>- Minimally invasive</li> <li>- Usually outpatient procedure</li> <li>- Adapted for nanocarriers, hydrogels and medical devices</li> </ul>	<ul style="list-style-type: none"> <li>- Treatment of inner ear diseases</li> <li>- Minimized systemic exposure</li> <li>- Long term local drug delivery (several months to years)</li> <li>- Avoids the diffusion through the round window, direct access to the cochlea</li> <li>- Adapted for nanocarriers, liquid formulations and medical devices</li> <li>- Drugs can be delivered along with a cochlear implant</li> </ul>
<b>Limitations</b>	<ul style="list-style-type: none"> <li>- Require diffusion through the round window for access to the cochlea</li> <li>- High inter-individual variability (variable thickness of the round window, potential obstruction of the round window)</li> <li>- Clearance through the Eustachian tube</li> <li>- Not adapted for liquid formulations</li> <li>- Risk of introducing pathogens in the middle ear</li> <li>- Risk of tympanic membrane perforation</li> </ul>	<ul style="list-style-type: none"> <li>- Invasive</li> <li>- Requires hospitalization</li> <li>- Potential toxicity of a high drug concentration in the cochlea</li> <li>- Risk of introducing pathogens in the inner ear</li> </ul>

#### 4.1. Intratympanic administration

The principle of intratympanic administration consists in using the middle ear as a reservoir for drugs that can diffuse through the round window for access to the inner ear. It involves the administration of drugs into the middle ear either by a transtympanic injection or by a direct injection in the tympanic cavity or the round window niche after a retro-auricular surgery. The key parameter influencing drug concentration in perilymph after intratympanic administration is the time the drug remains in contact with the round window (Hahn et al., 2006). In addition, drug distribution along the three turns of the cochlea is dominated by passive diffusion as shown by Salt and Plontke (2005; 2009) resulting in a large longitudinal gradient from base to apex when drugs enter the cochlea through the round window: the concentration of the drug will be highest in the basal turn of the cochlea (high frequency region) and will probably not reach the apical turn (low frequency region) (Mynatt et al., 2006, Plontke et al., 2007). The conventional transtympanic injection of liquid drug solutions is still in use and is described in section (4.1.1). To increase drug concentration in perilymph and to reduce variability of perilymph drug levels, the residence time of the drug in contact with the round window should be sustained and controlled as closely as possible. It can be achieved by using drug delivery systems that are classified into two categories: implantable medical drug delivery devices (4.1.2) and injectable drug delivery systems (4.1.3).

#### 4.1.1. *Transtympanic injection of liquid solutions*

In practice, transtympanic injection is performed under local anesthesia in outpatient clinic. This method was introduced 60 years ago (Schuknecht, 1956). Briefly, the tympanic membrane is perforated using a long and fine needle (spinal puncture needles from 22 to 25 G in human (Herraiz et al., 2010) and from 27 to 30 G in animals (Wang et al., 2009, Salt et al., 2011). Then, a volume of 0.4 to 0.6 mL in humans (Herraiz et al., 2010) or 50 to 200 µL in animals (Wang et al., 2009) of drug solution is injected and fills the middle ear cavity ensuring that the drug is in contact with the round window. The main adverse reactions related to transtympanic administration are pain or vertigo after injection. But, these symptoms are generally limited to 1 to 2 hours after injection and are strongly dependent on the drug administered, its concentration, its temperature and on individual susceptibility (Herraiz et al., 2010). Transtympanic injection of conventional drug solutions such as corticosteroids is routinely used in clinical practice. However, this technique generally requires repeated injections, 2 to 5 times a week (Alles et al., 2006), because the injected liquid is rapidly eliminated from the middle ear *via* the Eustachian tube.

Recently, Kanzaki et al., (2012) developed and tested a novel otoendoscopy device that allows the visualization of the round window for the purpose of transtympanic injection. The otoendoscope consists of a fiber optic lens for viewing and two working channels, a catheter channel equipped with a fine needle for delivering drugs and a suction channel for removing adhesions when the round window is obstructed. The otoendoscope is used to apply drugs directly on the surface of the round window and the correct placement of an inner ear drug delivery system, ensuring that it is safely in place and in contact with the round window.

#### 4.1.2. *Medical drug delivery devices*

Several implantable medical devices were developed for intratympanic administration. They include the microwick, microcatheters and several biodegradable or non-biodegradable polymer devices (**Table 4**).

##### 4.1.2.1. *MicroWick<sup>®</sup>*

The Silverstein MicroWick<sup>®</sup> is an absorbent polyvinyl acetate wick with a length of 9 mm and a diameter of 1 mm. This device is inserted through a ventilation tube in the tympanic membrane and placed overlying the round window. The insertion procedure requires only local anesthesia. Then, the patient instills the drug solution into the external ear canal, usually

several times a day and for several weeks. The drug absorbed by the wick is delivered in contact with the round window for a passive diffusion to the inner ear (Silverstein, 1999, Silverstein et al., 2004).

#### 4.1.2.2. Microcatheter ( $\mu$ Cat<sup>®</sup>) and osmotic pump

The microcatheter has been evaluated both in clinical and animal studies. The microcatheter has two lumens, one for infusion of drugs and another for fluid withdrawal. The bulbous tip of 1.5, 2.0 or 2.5 mm diameter is placed and compressed in the round window niche. General anesthesia is required to expose the round window niche after performing a tympanomeatal flap. The other end of the catheter exits from the outer ear canal and can be connected to various pumping systems for infusion of drugs such as micropumps and osmotic pumps (Swan et al., 2008, McCall et al., 2010). Osmotic pumps have been used both for intratympanic and intracochlear administration in animal studies. These devices have small volumes allowing reservoir capacities of 0.1 to 2 mL and flow rates from 0.1 to 10  $\mu$ L/h (Brown et al., 1993). The pump operates with osmotic pressure. Briefly, a semi-permeable outer membrane surrounds an osmotic driving agent. Inside this compartment, an impermeable and flexible reservoir contains the drug. Once *in vivo*, water flows into the compartment holding the osmotic agent, pressure is exerted on the flexible drug reservoir and the drug is pushed through the cannula (Brown et al., 1993) providing continuous infusion for 1 day to 6 weeks. Osmotic pumps have been used to test therapies for many inner ear disorders and have been reviewed elsewhere (Swan et al., 2008, Pararas et al., 2012).

This device was also employed to evaluate the biodistribution of nanocarriers in the cochlea such as liposomes after transtympanic injection (Zou et al., 2014) or polymersomes (Zhang et al., 2010, Zhang et al., 2011) after direct infusion into the cochlea. The versatility and ease of use of osmotic pumps in rodents make them very attractive for the study of novel therapies applied to the inner ear.

#### 4.1.2.3. Polymeric-based devices

Polymer-based systems are solid sponges, beads or discs soaked with a drug solution (**Table 4**). The use of such devices involves surgery to perform a tympanomeatal skin flap to place the device next to the round window. The surgical removing can be avoided when the polymer is biodegradable such as gelfoam<sup>®</sup> or seprapack<sup>®</sup>. Gelfoam<sup>®</sup> is a sterile compressed sponge intended for application to bleeding surfaces as a hemostatic. It is composed of purified porcine gelatin and is able to absorb many times its weight of fluids (Pfizer product

detail, 2014). Seprapack<sup>®</sup> (carboxymethylcellulose and hyaluronic acid discs) is a bioresorbable device primarily developed for nasal surgery by Genzyme that can be a potential vehicle for drug delivery to the inner ear after round window application (James et al., 2008, Eastwood et al., 2010).

Several works have reported the use of  $\mu$ Cat<sup>®</sup>, MicroWick<sup>®</sup> and biodegradable polymeric-based devices for clinical and animal studies. They are summarized in **Table 4**. MicroWick<sup>®</sup>,  $\mu$ Cat<sup>®</sup>, gelfoam<sup>®</sup> and seprapack<sup>®</sup> were efficient to deliver different drugs into the inner ear and resulted in therapeutic efficacy with different administration protocols on Menière's disease and hearing loss in human (**Table 4**). Moreover, BDNF loaded into Gelfoam<sup>®</sup> resulted in a significant preservation of spiral ganglion neurons in guinea pig (Havenith et al., 2011). Seprapack<sup>®</sup> bearing either dexamethasone or n-acetyl cysteine allowed residual hearing preservation during cochlear implantation in guinea pigs when applied on the round window 30 to 120 min prior to surgery (James et al., 2008, Eastwood et al., 2010). Hashimoto et al., (2007) confirmed that kanamycin distribution in the cochlea depends on both the drug concentration and the administration time (using  $\mu$ Cat<sup>®</sup> along with an osmotic pump). When the initial dose of kanamycin, an ototoxic drug, was higher or administered over a longer period, the damage region of the cochlea was wider. In addition, drug kinetic following intratympanic administration of drugs using polymeric devices is dependent upon the specific polymer chemistry and its degradation characteristics (Noushi et al., 2005). Generally, the rate of drug release from polymer based devices cannot be controlled to the same degree as with a  $\mu$ Cat<sup>®</sup> associated with an osmotic pump (Richardson et al., 2006).

Potential drawbacks with medical drug delivery devices include the need for patient compliance (i.e. microwick<sup>®</sup>) and often a subsequent surgery to remove the device if non-biodegradable. These devices were also associated with a risk of a persistent tympanic perforation (microcathether and microwick<sup>®</sup>) (McCall et al., 2010), infection of the middle or external ear and potential tissue ingrowth (Plontke et al., 2006, Van Wijck et al., 2007).

**Table 4**

Pre-clinical and clinical studies evaluating medical devices (Microwick®, µCath®, Gelfoam®, Seprapack®) implanted in the middle ear for inner ear therapy.

Device	Pre-clinical / clinical study	Disease / aim of the study	Drug	Administration protocol	Main outcome	References
<b>Microwick®</b>	Clinical study (n = 69)	Menière's disease	Gentamicin	10 mg/mL, 3 drops, 3 times/day, 2 weeks	Good control of vertigo symptoms in 76% of cases, good tolerance	(Hill et al., 2006)
	Clinical study (n = 50)	Menière's disease	Dexamethasone	3 times/day, 2 weeks	Hearing improvement in 40% of cases	(Hillman et al., 2003)
	Clinical study (n = 17)	Menière's disease	Ganciclovir	50 mg/mL, 10 days	Good control of vertigo in 80% of cases	(Guyot et al., 2008)
	Clinical study (n = 12 or n = 26)	Sudden SNHL	Methylprednisolone	62 or 56 mg/mL, 3 drops, 2 times/day, 3 weeks	Hearing improvement	(Van Wijk et al., 2007, Barriat et al., 2012)
	Clinical study (n = 9)	AIED	Infliximab	0.3 mL Remicade® once a week, 4 weeks	Hearing improvement and reduced relapse	(Van Wijk et al., 2006)
<b>µCath®</b>	Clinical study (n= 22)	Menière's disease	Gentamicin	10 mg/mL, 5 µL/h, 10 days	Long-term vertigo control and preservation of hearing and vestibular function	(Suryanarayanan and Cook, 2004)
	Clinical study (n = 6)	Sudden SNHL	Methylprednisolone	62.5 mg/mL, 10 µL/h, 8-10 days	Significant recovery of hearing	(Lefebvre and Staeker, 2002)
	Clinical trial (n = 23)	Sudden SNHL	Dexamethasone phosphate	4 mg/mL, 6µL/h, 14 days	Average hearing improvement	(Plontke et al., 2009)
	Clinical study (n = 136)	Refractory SNHL	Dexamethasone	5 mg/mL, 10 µL/min, twice a day, 7 days	40% hearing improvement	(Li et al., 2013)
	Animal study (Guinea pig, n = 18)	Evaluation of ototoxicity	Kanamycin	172.5 or 345 mg/mL 0.1 mL/h, 1 or 2 h	Control of the region and severity of ototoxicity by changing the drug concentration and the administration time	(Hashimoto et al., 2007)
	Animal study (Rat, n = 25)	PK	Radiolabeled D-methionine and thiourea	1h infusion	Permeability of the RW to the tested molecules. Substantial amount in the perilymph of <i>sacra tympani</i> and tissues of the basal turn of the cochlea	(Laurell et al., 2002)

**Table 4** (continued)

<b>Device</b>	<b>Pre-clinical/clinical study</b>	<b>Disease / aim of the study</b>	<b>Drug</b>	<b>Administration protocol</b>	<b>Main outcome</b>	<b>References</b>
<b>Gelfoam®</b>	Clinical study (n= 56)	Menière's disease	Gentamicin	Single application	Controlled vertigo in 81% of cases with acceptable hearing loss	(Flanagan et al., 2006)
	Animal study (Guinea pig, n = 24)	Protection of spiral ganglion neurons	BDNF	Single application: 1 mm <sup>3</sup> , 1 mg/mL	Significant protection of the spiral ganglion neurons in the basal turn of the cochlea	(Havenith et al., 2011)
<b>Serapack®</b>	Animal study (Guinea pig, n = 26)	PK, preservation of residual hearing during cochlear implantation	Dexamethasone	2 or 20% dexamethasone	Higher and sustained drug concentration in perilymph. Protection of residual hearing across the entire frequency domain	(James et al., 2008, Eastwood et al., 2010)
	Animal study (Guinea pig)	Preservation of residual hearing during cochlear implantation	N-acetyl cysteine	40 mg/mL N-acetyl cysteine	Protection of residual hearing. Reduction in the chronic inflammatory changes associated with implantation. Osseoneogenesis associated to local N-acetyl cysteine delivery	(Eastwood et al., 2010)

#### 4.1.3. Injectable drug delivery systems

Injectable drug delivery systems are expected to deliver the drug with specific kinetic profiles depending on the physicochemical properties of the vehicle. Injectable drug delivery systems used for inner ear therapy can be categorized into hydrogels and nanoparticulate systems.

##### 4.1.3.1. Hydrogels

Hydrogels have a high viscosity and viscoelastic properties that should avoid rapid flow through the Eustachian tube thus allowing longer residence times in the middle ear. Therefore, the use of hydrogels for transtympanic injection seems to be an interesting strategy to reduce the number of injections. Research investigations on hydrogel-based delivery systems in otology concern polymers of different natures: synthetic thermo-sensitive polymers such as poloxamer 407 and natural polymers as for example chitosan, hyaluronic acid, collagen or gelatin (**Table 5**).

**Poloxamer 407** is a triblock copolymer composed of a central hydrophobic chain of polypropylene glycol and two hydrophilic side chains of polyethylene glycol. Poloxamer hydrogel was extensively studied as a drug delivery system for several local applications (Dumortier et al., 2006, Almeida et al., 2013). Upon increasing the temperature, when their concentration is high enough, poloxamer 407 molecules self-assemble into micelles which subsequently organize themselves to form a semi-solid hydrogel (Dumortier et al., 2006). Thus, poloxamer 407 is an *in situ* forming thermoreversible system. Between 15.5 and 20% (w/v), poloxamer 407 has a gelation temperature below 37°C (Wang et al., 2009, Engleter et al., 2014). This property is very attractive as a drug delivery approach: poloxamer 407 solutions are fluid at room temperature. Easily injectable, they gelyfy at body temperature allowing a long residence time into the middle ear. In addition, the administration of poloxamers is considered as safe in humans (Singh-Joy and McLain, 2008), including the middle ear (Wang et al., 2009).

**Hyaluronic acid** is a natural mucoadhesive, biodegradable and biocompatible polymer that is one of the main components of the extracellular matrix of the connective tissue. It is a negatively charged polysaccharide composed of D-glucuronic acid and N-acetyl-D-glucosamine (Balazs, 2008). Depending on its concentration and molecular weight,

hyaluronic acid may form highly viscous gels when dissolved into aqueous media. High molecular weight hyaluronic acid (~ 1.5 MDa) offer mucoadhesive properties that should allow prolonged contact with the middle ear mucosa (Girish and Kemparaju, 2007). Moreover, animal studies have shown that hyaluronic acid itself exerts beneficial effects on the tympanic membrane perforation healing (Ozturk et al., 2006).

**Chitosan** is a non-toxic biodegradable cationic polymer with low immunogenicity, prepared by deacetylation of chitin that is obtained from the exoskeleton of crustaceans (Sreenivas and Pai, 2008). Chitosan is degraded by lysozyme and other glycosidases (Lai and Lin, 2009). The safety profile of chitosan along with the possibility for further chemical modifications makes this biopolymer attractive for a variety of biomedical and pharmaceutical applications including drug delivery (Dutta Gupta et al., 2015). Some chitosan derivatives such as chitosan glycerophosphate form thermoreversible hydrogels. As previously explained for poloxamer 407, this is an interesting property for injectability. In addition, the positively charged nature of chitosan provides attractive electrostatic interactions with the negatively charged mucosal surfaces of the middle ear allowing a prolonged residence time in contact with the round window (Sreenivas and Pai, 2008).

Other hydrogels forming polymers such as **collagen**, **gelatin** or a thermosensitive copolymer composed of **PLGA-PEG-PLGA** were used as biodegradable drug delivery systems to the inner ear (**Table 5**).

During the past decade, many pre-clinical studies have evaluated the hydrogels mentioned above for drug delivery to the inner ear and are summarized in **Table 5**.

**Table 5**

Pre-clinical evaluation of hydrogels for intratympanic administration.

Polymer	Drug	Gel composition	Animal model	Aim of the study	Outcome	References
<b>Poloxamer 407</b>	Triamcinolone acetonide	Poloxamer 407 20% (w/v) Triamcinolone acetonide 30% (m/v)	Guinea pig	PK and tolerability	Significant level of corticoid in perilymph until 10 days. Transient hearing loss solved within 10 days. No histological changes	(Engleder et al., 2014, Honeder et al., 2014)
	Dexamethasone	Poloxamer 407	Guinea pig	PK	Insoluble corticoids increased the degree and the duration of exposure in the inner ear compared to soluble corticoids	(Wang et al., 2011)
	Dexamethasone acetate	17% (w/w)				
	Dexamethasone phosphate	Corticoids 1.5 or 2% (w/w)				
	Methylprednisolone					
	Methylprednisolone succinate					
	Dexamethasone	Poloxamer 407 17% (w/w) Dexamethasone 4.5% (w/w)	Guinea pig	PK and cochlear function assessment	Conductive hearing loss induced by the gel resolved within 24 h. Hydrogel provides more uniform distribution of drug in the cochlea	(Salt et al., 2011)
	Dexamethasone	Poloxamer 407 17 or 15.5% (w/w) Dexamethasone 4.5, 1.5 or 0.15% (w/w)	Guinea pig	PK, tolerability and hearing function assessment	Transient hearing loss resolved within 7 days. No histological changes. Release profile depending on the concentration of both poloxamer and dexamethasone. Sustained release for at least 10 days	(Wang et al., 2009)
	Dexamethasone phosphate	Thiol-modified HA/gelatin 90/10 [HA] = 0.6% (w/v) Dexamethasone phosphate 1% (w/v)	Guinea pig	PK	Dexamethasone measurable in perilymph up to 72 h. Higher concentration of dexamethasone in perilymph with the gel than with the solution	(Borden et al., 2011)
	Neomycin	HA 0.5% (w/w) Neomycin 15, 5 and 2% (w/w)	Guinea pig	Ototoxicity assessment (hair cell loss and RW thickness)	Important hair cell loss with the gel but similar to the control solution. Dose-dependence. Transient increase in the RW thickness resolved within 28 days	(Saber et al., 2009)

Polymer	Drug	Gel composition	Animal model	Aim of the study	Outcome	References
<b>Hyaluronic acid</b>	AM-111 peptide	HA 2.6% (w/v) AM-111 100, 10 or 1 µM	Chinchilla	Evaluation of hearing protection	Significant protection against permanent hearing loss after acoustic trauma and ischemic cochlear damages	(Coleman et al., 2007, Omotehara et al., 2011)
	None	1.9% (w/w) High MW HA	Rat	Ototoxicity assessment	Conductive hearing loss until 7 days post-injection, completely recovered after 15 days. No histological damages. Middle ear cavity filled with gel until 7 days post-injection and gel remained on the RW and oval window up to 30 days	(Martini et al., 1992)
<b>Chitosan</b>	Gentamicin	Chitosan-glycerophosphate 2% (w/v) Gentamicin 20% (w/v)	Mouse	PK and evaluation of a regulation mechanism using chitosanase	Gentamicin distribution in a time-dependent and basal-to-apical manner. More concentrated in the vestibule and the basal turn of the cochlea. Gentamicin concentration in perilymph significantly decreased after chitosanase application	(Luo and Xu, 2012, Lajud et al., 2013)
	Neomycin	3 different chitosans 2% (w/v) Ch1 (32kDa, desacetylated) Ch2 (148 kDa, 15% acetylated) Ch3 (11 kDa, glycosylated) Neomycin 2 or 5% (w/v)	Guinea pig	Comparison of different types of chitosan. Ototoxicity assessment	Diffusion of neomycin through the RW and ototoxicity depending on the drug concentration. Ch1 and Ch2 still in the middle ear up to 7 days. No significant differences between the 3 chitosans in releasing neomycin. No noxious effect of chitosan <i>per se</i>	(Saber et al., 2010)
	Dexamethasone	Chitosan-glycerophosphate 3.4% (w/w) Dexamethasone 0.7% (w/w)	Mouse	PK, tolerability and hearing function assessment	Dexamethasone detected in perilymph up to 5 days. Postoperative transient hearing loss solved within 10 days	(Paulson et al., 2008)
<b>Gelatin</b>	IGF-1 HGF	Growth factors: 1 mg/mL	Guinea pig	Evaluation of protection from NIHL	Sustained delivery of IGF-1 in perilymph with the hydrogel. Reduced hearing loss after acoustic trauma and reduced outer hair cell loss with the hydrogel	(Lee et al., 2007, Inaoka et al., 2009)
<b>Collagen</b>	BDNF	Glutaraldehyde crosslinked type-1 porcine collagen	Guinea pig	Evaluation of protection from spiral ganglion neurons degeneration	Enhanced and sustained delivery of BDNF in perilymph with the hydrogel up to 7 days. Functional and histologic protection of the spiral ganglion neurons with the hydrogel	(Endo et al., 2005)
<b>PLGA-PEG-PLGA</b>	None		Guinea pig	Ototoxicity assessment	No hearing loss when 50 µL was injected while transient hearing loss after the injection of 100 µL hydrogel	(Feng et al., 2014)

### ***Characteristics of hydrogel-based drug delivery systems for the inner ear***

Important points to consider when using hydrogels for intratympanic administration are the injectability through long and fine needles (Herraiz et al., 2010), the residence time in the middle ear, the ability to deliver the drug into the inner ear and to sustain its release and finally, the safety profile of the hydrogel itself.

#### *- Injectability*

Injectability of a formulation is its ability to be injected manually *via* a needle with a reasonable injection force. For this purpose, thermoreversible hydrogels such as poloxamer 407, chitosan glycerophosphate and PLGA-PEG-PLGA are very attractive for transtympanic injection since they are easily injected (as liquids) at room temperature and turn into viscous gels at body temperature (**Table 5**). In addition, shear-thinning and self-healing hydrogels such as hyaluronic acid are also interesting since their viscosity decreases under shear during injection and is rapidly recovered after injection (El Kechai et al., 2015).

#### *- Residence time*

The residence time of the hydrogel in the middle ear controls the drug concentration in the inner ear since it impacts the time the drug remains in contact with the round window. The viscosity of the hydrogel is both controlled by the concentration and the molecular weight of the polymer and should influence the residence time in the middle ear. Saber et al., (2010) showed that low (32.9 kDa) and middle (148 kDa) molecular weight chitosans remain in the middle ear until day 7 post-injection whereas oligomeric chitosan (MW 11.8 kDa) are rapidly cleared from the middle ear cavity. Mucoadhesive properties of hyaluronic acid and chitosan promote the contact with the round window and the middle ear mucosa for long periods of time. Indeed, at a concentration of 1.9%, hyaluronic acid hydrogel (MW > 1 MDa) completely filled the middle ear cavity 7 days after injection and remained at the round window and oval window until 30 days post-injection (Martini et al., 1992).

#### *- Drug release*

The studies presented in **Table 5** show that hydrogels of different nature are efficient vehicles to sustain the release of various drugs in perilymph, enhancing local bioavailability in the inner ear while minimizing systemic exposure. A single application of a 17% poloxamer hydrogel containing dexamethasone resulted in a 50-fold less dexamethasone concentration in plasma than in perilymph at different time points (Wang et al., 2009).

Similarly, the application of a chitosan glycerophosphate gel containing dexamethasone led to 2 to 30-fold less dexamethasone concentration in plasma (Paulson et al., 2008) and a 20% poloxamer hydrogel containing triamcinolone acetonide reduced the systemic exposure by 600-fold at day 1 and 30-fold at day 10 post-injection (Honeder et al., 2014). Overall, a single injection of hydrogel led to higher drug concentrations in perilymph over longer periods of time (several days) compared to drug in solution (few hours) administered by the same route. For example, dexamethasone was detected in perilymph with significant concentrations for at least 10 days with poloxamer 407 hydrogel (Wang et al., 2009, Wang et al., 2011), until 5 days with chitosan glycerophosphate (Paulson et al., 2008) and up to 72 h with thiol-modified hyaluronic acid hydrogel (Borden et al., 2011). On the contrary, with transtympanic injection of dexamethasone solution, dexamethasone was not detected for more than 24 h in perilymph (Wang et al., 2009, Borden et al., 2011). Beneficial therapeutic effects of dexamethasone in the inner ear is achieved over a concentration range of 30-40 ng/mL (Wang et al., 2011). In most studies described previously, perilymphatic drug levels are several orders of magnitude above therapeutic levels. The physicochemical properties and the concentration of the drug in the hydrogel as well as the polymer concentration influence final drug concentration in the inner ear. Indeed, drug concentration in perilymph was enhanced with higher concentration of drug within the hydrogel (Wang et al., 2009, Saber et al., 2010, Omotehara et al., 2011). Conversely, increasing poloxamer 407 concentration (from 15.5 to 17%) led to a decrease in dexamethasone concentration within perilymph (Wang et al., 2009). Finally, poorly soluble corticosteroids increased the concentration and the duration of exposure in the inner ear compared to soluble corticosteroids (Wang et al., 2011).

#### - Safety

In most studies, a conductive transient hearing loss was observed when the middle ear cavity was overfilled with gel. In all cases, the hearing function returned to normal within 7 to 10 days (Martini et al., 1992, Paulson et al., 2008, Wang et al., 2009, Honeder et al., 2014). The hearing loss depends on the amount of gel injected in the middle ear (Feng et al., 2014). However, the presence of chitosan (Saber et al., 2010), hyaluronic acid (Martini et al., 1992) or poloxamer 407 (Wang et al., 2009) hydrogels in the middle ear did not provoke any histological damages to the round window and the cochlea indicating that those hydrogels have no noxious effects by themselves. The hearing loss observed is thus conductive in nature, i.e. due to a reduction of the ossicular chain mobility because of the gel viscosity (Wang et al., 2009).

- *Therapeutic efficacy and clinical evaluation*

Hydrogels have proven their therapeutic efficacy in several animal models (**Table 5**) (Coleman et al., 2007, Lee et al., 2007, Inaoka et al., 2009, Omotehara et al., 2011). More interestingly, the safety and efficacy profiles of hydrogels for inner ear therapy were evaluated in humans (**Table 6**). A prospective clinical study using hyaluronic acid with dexamethasone for the treatment of sudden sensorineural hearing loss or Menière's disease, compared to systemic steroid and vasoactive therapy, have shown significant improvement of auditory function without systemic or local side effects (Gouveris et al., 2005, Selivanova et al., 2005). Nakagawa et al., (2014) examined the efficacy and safety of gelatin hydrogel containing IGF-1 in comparison to intratympanic corticosteroid therapy for the treatment of sudden sensorineural hearing loss. Transtympanic injection of IGF-1 within hydrogel showed a positive effect on hearing levels that was superior to intratympanic dexamethasone therapy and presented a favorable safety profile. Currently, some companies take an interest in medicines for local inner ear therapy based on hydrogel formulations (**Table 6**). Otonomy is developing OTO-104 (poloxamer 407 hydrogel containing dexamethasone) (Lambert et al., 2012). The Phase Ib clinical trial of a single transtympanic injection of OTO-104 in patients with Menière's disease demonstrated that OTO-104 was well tolerated. Furthermore, 12 mg of OTO-104 was associated with clinically meaningful improvements in both vertigo frequency and tinnitus compared to placebo three months after treatment. There were no serious adverse events observed during the clinical trial (Lambert et al., 2012). OTO-104 is currently in phase IIb (Otonomy, 2015). Another company, Auris Medical, is working on hydrogels based on hyaluronic acid: AM-101 for the treatment of acute inner ear tinnitus and AM-111 for the treatment of noise-induced hearing loss (**Table 6**). Both products showed promising benefits on tinnitus and hearing loss as well as good tolerance. AM-101 is in phase III and AM-111 received orphan drug designation from both FDA and EMA for the treatment of noise-induced hearing loss (Auris medical, 2015).

Pre-clinical and clinical studies evaluating hydrogels indicate that they can be considered as safe and effective carriers for inner ear therapy after transtympanic injection in the middle ear. However, animal studies point out that their efficacy can be strongly dependent on the physicochemical properties of the drug being delivered and polymer characteristics (Wang et al., 2009, Saber et al., 2010, Omotehara et al., 2011, Wang et al., 2011).

**Table 6**  
Clinical evaluation of hydrogels for inner ear therapy

Polymer	Medicine	Indication	Status	Company/ references
<b>HA</b>	AM-101 (esketamine)	Tinnitus	Clinical trial Phase III	Auris Medical (van de Heyning et al., 2014)
	AM-111 (JNK-inhibitor)	NIHL	Orphan drug designation	Auris Medical
	Dexamethasone	Sudden SNHL (idiopathic or associated with Menière's disease)	Clinical study	(Selivanova et al., 2005)
<b>Poloxamer 407</b>	OTO-104 (dexamethasone)	Menière's disease	Clinical trial Phase IIb	Otonomy (Lambert et al., 2012)
<b>Gelatin</b>	IGF-1	Sudden SNHL after failure of systemic steroids	Clinical trial	(Nakagawa et al., 2014)

#### 4.1.3.2. Nanoparticulate systems

Nanoparticulate systems, also called nanocarriers, have sizes below 1 µm and were primarily developed to carry a drug to a target site, thereby avoiding the potentially toxic effects on healthy tissues. Due to their numerous advantages, nanotechnologies have generated considerable interest in the past several years for drug delivery to the inner ear (Pritz et al., 2013, Staecker and Rodgers, 2013). Indeed, nanocarriers compensate drug properties in terms of low solubility, degradation and short half-life. Thus, the nanocarriers that are able to cross the round window offer the possibility of introducing drugs into the cochlea in a sustained and/or targeted manner avoiding surgical trauma to the inner ear (Pritz et al., 2013). Furthermore, it is possible to functionalize the surface of these systems to target specific cells in the cochlea (hair cells and spiral ganglion neurons). However, as previously mentioned for liquid solutions, nanocarrier suspensions injected in the middle ear will be rapidly cleared through the Eustachian tube due to their low viscosity. When intratympanic administration of nanovectors is considered, the residence time in the middle ear should be prolonged either by increasing the viscosity (i.e. incorporating the nanovectors in hydrogels) or by using a medical device (i.e. gelfoam®, osmotic pump).

The nanocarriers tested in otology have a broad variety of chemical compositions including phospholipids and polymers. The main nanovectors that may be interesting for intratympanic administration as well as their general physicochemical characteristics are reviewed below.

Major outcomes from *in vivo* studies evaluating these vectors after intratympanic administration are summarized in **Table 7**.

**Liposomes** are small vesicular structures formed by phospholipid bilayers surrounding an aqueous core. Liposomes exhibit a range of sizes (between 20 nm and few  $\mu\text{m}$ ) and morphologies depending on the phospholipid mixture, the bulk solution and the preparation method (Bozzuto and Molinari, 2015). Liposomes can encapsulate either hydrophobic molecules in the phospholipid bilayer, or hydrophilic molecules in the aqueous core (Wang et al., 2012, Bozzuto and Molinari, 2015). In addition, liposomes allow surface modification with PEG, antibodies, peptides, carbohydrates, chitosan, hyaluronic acid and folic acid (Bozzuto and Molinari, 2015). Finally, the biomimetic structure of liposomes offers low immunogenicity and good tolerance (Wang et al., 2012).

**Lipid nanocapsules** consist of a hydrophobic core generally made of triglycerides and mineral oil surrounded by an amphiphilic shell of nonionic surfactants (PEGylated or not) that can be functionalized (Roy et al., 2012). Their size varies from 20 to 100 nm (Huynh et al., 2009). Lipid nanocapsules can encapsulate only hydrophobic drugs into their core.

**GMO-based nanoparticles.** Glycerol monooleate (GMO) is an extensively studied lipid that forms lyotropic mesophases. GMO forms both bicontinuous cubic and hexagonal phases in excess of water over a wide temperature range (Liu et al., 2013, Liu et al., 2013). GMO has low cytotoxicity and improves the chemical and physical stability of incorporated drugs including biomacromolecules such as proteins, peptides and nucleic acids (Angelova et al., 2005). Additionally, GMO is biodegradable *via* esterase mediated lipolysis. Therefore, lipid nanoparticles made from GMO, also called cubosomes, are prospective candidates for drug delivery. Their surface can be modified using synthetic cationic lipids such as 1,2-dioleoyl-3-trimethylammoniumpropane (DOTAP) and didodecyldimethylammonium bromide (DDAB) to allow DNA complexation and gene delivery (Liu et al., 2013).

**Table 7**

Pre-clinical evaluation of nanocarriers for intratympanic administration.

Nanocarrier	payload	Diameter (nm)	$\zeta$ - potential (mV)	Model	Biodistribution, outcome	References
PLGA nanoparticle	Rhodamine B	140 -180	ns	Guinea pig	After local application, diffusion through the RW and detection of nanoparticles in the <i>scala tympani</i> . The number of nanoparticles after local application was approximately 10-fold higher than that after systemic application	(Tamura et al., 2005)
	Coumarin-6	135	ns	Guinea pig	4.7-fold higher AUC and 10.9-fold higher C <sub>max</sub> in perilymph with coumarin-nanoparticle compared to coumarin solution	(Cai et al., 2014)
	Salvianolic acid B (sal B) Tanshinone IIA (TSIIA) Panax-notoginsenoside (PNS)	154	ns		No significant differences between Sal B or TS IIA -nanoparticles and the compound solutions 3 to 7-fold higher AUC and 10 to 16.7-fold higher C <sub>max</sub> with PNS-nanoparticle compared to PNS solution	
PLGA SPION nanoparticle	None	160 - 280	-20	Chinchilla	Perilymph, endolymph and organ of Corti. Diffusion through the RW with or without magnetic forces	(Ge et al., 2007)
	Dexamethasone	324 - 640	-20	Guinea pig	Higher concentration of dexamethasone in perilymph with magnetic targeting compared with diffusion alone	(Du et al., 2013)
PEG-PCL polymersome	Carboxycyanine	53 - 71	ns	Rat	Spiral ligament (with TTI and RW application), organ of Corti (only with RW application), vestibuli (only with TTI, indicating possible passage of polymersomes trough the oval window after TTI)	(Zhang et al., 2011)
	Carboxycyanine	85 - 125	negatively charged	Rat	RW, <i>scala vestibuli</i> and <i>scala tympani</i> . Reduction of RW permeation with Tet1. Targeting of the cochlear nerve with Tet1 functionalized polymersomes when delivered by cochleostomy but not with TTI	(Zhang et al., 2012)
	Disulfiram	70 - 110	ns	Mouse	Spiral ganglion cells, hair cells throughout the cochlea polymersomes successfully transported disulfiram into the cochlea	(Buckiova et al., 2012)
PHEA polymersome	Nile red	11 - 43	-35	Mouse	Organ of Corti, inner hair cells. No ototoxicity	(Kim et al., 2015)
Liposome	Gadolinium	130	ns	Rat	Perilymph, <i>scala tympani</i> , <i>scala vestibuli</i> , until 24 h	(Zou et al., 2010)
	Gadolinium	95, 130 or 240	ns	Rat	Size-dependant diffusion through the RW. Diffusion of liposomes decreases with size, liposomes remain intact in perilymph	(Zou et al., 2012)

**Table 7** (Continued)

Nanocarrier	payload	Diameter (nm)	$\zeta$ - potential (mV)	Model	Biodistribution, outcome	References
<b>Liposome</b>	Disulfiram	85	ns	Mouse	Spiral ganglion cells, hair cells throughout the cochlea Liposomes successfully transported disulfiram into the cochlea	(Buckiova et al., 2012)
	Gadolinium	90 - 120	+ 14	Rat	The RW is the major pathway for liposomes entry into the inner ear. The oval window is not permeable to liposomes. Liposomes were detected in the cochlea within 6 days and in the RW up to 11 days Biocompatibility of liposomes: no inflammation observed in the inner ear up to 20 days post-injection	(Zou et al., 2014)
<b>LNC</b>	Nile red and FITC	50	ns	Rat	Hair cells, spiral ganglion neurons, nerve fibers and spiral ligament fibrocytes. LNCs remained in the cochlea 7 days post-injection. Paracellular passage through the RW	(Zou et al., 2008)
	None	50	-35	Rat	Biocompatibility of LNCs: no changes in hearing thresholds, no cell death and no morphological changes in the inner ear at up to 28 days	(Zhang et al., 2011)
	Nile red and FITC	55	ns	Human temporal bone	Hair cells, nerve fibers, diffusion across the RW	(Roy et al., 2012)
<b>GMO nanoparticle</b>	Rhodamine B	160 - 234	Positively or negatively charged	Guinea pig cochlea	Higher permeability of the RW for positively charged nanoparticles and broader distribution in the cochlea	(Liu et al., 2013)
<b>BSA nanoparticle</b>	Rhodamine B	636	+ 5	Guinea pig	Sustained release profile of rhodamine B with BSA nanoparticles. Particles penetrate into the cochlea through the RW and aggregate on the osseous spiral lamina (observed 3 days after injection)	(Yu et al., 2014)
<b>HBPL dendriplex</b>	None	10	ns	Rat	Biocompatibility: no changes in hearing thresholds and no hair cell loss	(Scheper et al., 2009)
	DNA plasmid	134 - 234	Positively charged	Rat	Organ of Corti, inner and outer hair cells, spiral ganglion cells 24h after injection. Gradient distribution through the different layers of the RW	(Zhang et al., 2011)
	None	10	ns	Human temporal bone	Hair cells, nerve fibers, diffusion across the RW	(Roy et al., 2012)
<b>CMAP dendriplex</b>	Atoh1 plasmid	110 - 150	+ 31	Rat	Gene transfer in hair cells, good tolerance: no changes in hearing thresholds 7 days after injection	(Wu et al., 2013)

**PLGA nanoparticles.** Poly(lactic-co-glycolic acid) (PLGA) is a negatively charged biodegradable copolymer composed of lactic and glycolic acid monomers and approved by FDA and EMA for parenteral administration (Kumari et al., 2010). PLGA nanoparticles have variable sizes (Danhier et al., 2012). Different molecules, either hydrophilic or hydrophobic, were successfully encapsulated and delivered with PLGA nanoparticles (protein, steroids, antibiotics, nucleic acids) (Grottka et al., 2013). In addition, PLGA with different degradation rates are available and these polymers offer the possibility for nanoparticle surface modification such as PEGylation, chitosan adsorption, antibody and oligopeptide ligands (Danhier et al., 2012, Grottka et al., 2013). Therefore, PLGA nanoparticles are an interesting drug delivery system for the inner ear regarding their high versatility and ability to adapt to specific requirement in terms of drug properties and target tissue (Pritz et al., 2013).

**Polymersomes** are formed by the self-assembly of amphiphilic block copolymers such as poly(ethyleneglycol)-*b*-poly( $\epsilon$ -caprolactone) (PEG-*b*-PCL) (Roy et al., 2012) or poly(2-hydroxyethyl aspartamide (PHEA) (Kim et al., 2015) in an aqueous solution. They have a hydrophobic membrane surrounding an aqueous core and a hydrophilic corona. Their biomimetic structure enables a good tolerance regarding the immune system. Hydrophilic drugs are loaded in the core and hydrophobic ones in the membrane.

**Dendrimer-based nanoparticles.** Dendrimers are randomly branched dendritic polymers consisting in the repetition of a unique molecule. Hyperbranched poly-L-lysine (HBPL) is a widely used dendrimer for non-viral gene delivery due to its high cationic charge that permits DNA complexation (Roy et al., 2012). Another dendrimer was used in otology and consists of polyamidoamine (PAMAM) activated and modified with Na-carboxymethyl- $\beta$ -cyclodextrins (CM- $\beta$ -CD) in sequence resulting in CPAM (CM- $\beta$ -CD modified activated PAMAM) nanoparticles suitable for DNA delivery (Wu et al., 2013). Dendrimers present small sizes between 10 and 100 nm and are generally polydisperse (Roy et al., 2012, Wu et al., 2013). Upon complexation with DNA and formation of the so-called dendriplexes, their size increases significantly.

**Superparamagnetic iron oxide nanoparticles (SPIONs)** consist of Fe<sub>3</sub>O<sub>4</sub> magnetized by an external magnetic field. SPIONs by themselves are not usual drug carriers since they are not able to encapsulate drugs. They are usually coated with a polymer layer such as PLGA containing the drug (Ge et al., 2007). SPIONs are expected to be magnetically driven through the round window into the cochlea where the drug will be released from the PLGA coating.

The magnetic field consists in a magnet placed on the contralateral ear (Ge et al., 2007, Du et al., 2013).

### ***Characteristics of nanoparticulate systems for drug delivery to the inner ear***

The key parameters to consider for nanocarrier-mediated drug delivery after intratympanic administration are the round window permeability to the carrier, the distribution of the carrier in the cochlea and potential targeting, the ability to carry a drug into the inner ear and to release it in a sustained manner. Finally, the toxicity of the nanocarrier regarding the sensitive inner ear must be taken into account. All these parameters were evaluated with different nanoparticulate systems *ex vivo* or *in vivo* (**Table 7**). However, there are no therapeutic efficacy studies documented yet after intratympanic administration of such systems.

- *Round window permeability*

Nanocarriers of different nature with a size ranging from 10 to 640 nm were able to diffuse through the round window (**Table 7**). Nevertheless, very few quantitative data are available in the literature about this passage. Both the surface characteristics and the size are important factors that affect the diffusion of nanocarriers from the middle ear to the inner ear. Zou et al., (2012) demonstrated that the transport percentage across the round window decreased with liposome size. Positively charged GMO-based nanoparticles allowed higher uptake in the round window and broader distribution in the cochlea compared to neutral or negatively charged nanoparticles (Liu et al., 2013). In addition, the surface grafting of a peptide on polymersomes reduced round window permeation (Zhang et al., 2012).

The diffusion of nanocarriers through the round window was initially believed to be by the paracellular pathway as described for lipid nanocapsules (Zou et al., 2008). However, more recent studies suggest that the passage of liposomes may occur either *via* paracellular or transcellular pathways involving clathrin- and caveolin-mediated endocytic mechanisms present in rat round window (Buckiova et al., 2012, Zou et al., 2012). The round window is considered as the major pathway for access to the inner after administration in the middle ear but entry could also occur through the oval window as shown for PEG-PCL polymersome (Zhang et al., 2011).

- *Distribution of the carrier in the cochlea*

**Table 7** shows the regions of the cochlea or the cells reached by the nanocarriers after transtympanic injection or round window application. In most of the studies, nanocarriers

were loaded or labeled either with a fluorescent dye (rhodamine B, carboxycyanine, nile red) or a contrast agent (gadolinium) allowing visualization of the particles in the cochlear cells or fluids by imaging techniques. Consequently, very few quantitative data are available about the amount of nanovectors distributed in the cochlea. Interestingly, the nanocarriers tested were able to reach different cell populations in the cochlea including the sensorineural cells (hair cells, spiral ganglion neurons) which are the main targets for the treatment of sensorineural hearing loss (Pritz et al., 2013). Liposomes were detected in the round window up to 11 days and in the cochlea until 6 days post-injection (Zou et al., 2014). Lipid nanocapsules remained visible in the cochlea until 7 days post-injection (Zou et al., 2008). However, the internalization of the non-functionalized nanocarriers by the cochlear cells was not specific for any cellular population *in vivo* (**Table 7**). Conversely, specific targeting of spiral ganglion neurons and nerve fibers was successfully tested *in vitro* and *ex vivo* using nanoparticles functionalized with Nerve Growth Factor-derived peptide (Roy et al., 2010). A specific targeting of outer hair cells *ex vivo* (rat cochlear explants) was obtained with PEG-PCL polymersomes functionalized with A665 prestin binding peptide (Surovtseva et al., 2012).

#### - Drug release

The ability of nanovectors to carry drugs into the cochlea *via* the round window was demonstrated *in vivo* (**Table 7**). However, no long-term study of drug release from nanoparticles has been conducted yet. PLGA SPION nanoparticles enabled the entry of dexamethasone into the inner ear *via* magnetic targeting through the round window resulting in higher concentration of dexamethasone in perilymph compared with passive diffusion (Du et al., 2013). 10% of the injected amount of dexamethasone was delivered 60 min after injection. Recently, Cai et al., (2014) showed that PLGA nanoparticles enhanced the local bioavailability of the encapsulated drugs in the inner ear compared to drug solutions (3 to 7 higher area under the curve (AUC) and 10 to 17 higher  $C_{max}$  in perilymph). Liposomes and polymersomes were evaluated using disulfiram, a neurotoxic agent, as a model. Disulfiram-loaded liposomes and polymersomes delivery resulted in a significant decrease in the number of spiral ganglion cells starting 2 days post-administration. On the contrary, no effect was observed in controls when a solution of free disulfiram was similarly tested. This demonstrates that liposomes and polymersomes are efficient nanocarriers for cochlear delivery of disulfiram (Buckiova et al., 2012). However, in this study, the state of the drug in perilymph (still encapsulated, free or both) was not evaluated.

- *Safety*

Nanoparticulate systems tested in animals following a single intratympanic administration showed a good safety profile. They did not exhibit negative effects on the hearing function and did not provoke any hair cell loss or histological damages (Scheper et al., 2009, Zhang et al., 2011, Wu et al., 2013, Kim et al., 2015) or inflammation (Zou et al., 2014). However, SPIONs exhibited a neurotoxic effect by disturbing the electrical activity even at low particle concentrations (Gramowski et al., 2010, Pritz et al., 2013). Liposomes were tested for up to 20 days after injection (Zou et al., 2014) and LNC were evaluated until 28 days post-injection (Zhang et al., 2011). As no long-term delivery in the inner ear has been documented yet, the potential long-term toxicity of nanovectors remains to be tested.

The use of nanoparticulate systems to target drugs to the inner ear after their administration in the middle ear shows potential for the future. Until today, no clinical trials are ongoing with these systems for intratympanic administration. This method requires extensive pre-clinical tests to evaluate more quantitatively the passage of nanocarrier/drug through the round window, the long-term drug release and the safety. The design of more targetable nanocarriers is also promising to improve the therapeutic efficacy on inner ear diseases.

## *4.2. Intracochlear administration*

Intracochlear administration (**Table 3**) consists in introducing the drug directly into the cochlea avoiding middle ear barriers and thus, the limitations of diffusion based-therapies. A risk of introducing pathogens in the inner ear exists when the cochlea is opened *via* a cochleostomy (**Table 3**). Besides the simple intracochlear injection, a variety of tools including cochlear implant coating and advanced devices has been employed for intracochlear administration.

### *4.2.1. Intracochlear injection*

The access to the cochlea is created *via* a cochleostomy in the basal turn of the cochlea or through the round window. Very small volumes of drug solutions (few  $\mu\text{L}$ ) are injected using fine gauge needles (i.e. 30G) (Stover et al., 1999). However, the applied amount of drug is difficult to control since some liquid leaks out of the cochlea during the procedure. In addition, the high concentration of drugs injected directly in the cochlea might be toxic for some cells and drug concentration will decrease constantly over time. Many strategies have been explored in order to have a more constant drug concentration in the cochlea over long

periods and were reviewed elsewhere (Pararas et al., 2012, Ayoob and Borenstein, 2015). In current clinical practice, direct intracochlear injection is performed only during surgery. However, in research studies, it is a convenient way to assess the pharmacological effects of new compounds.

#### 4.2.2. *Cochlear implant coating*

A cochlear implant is a hearing device with an array implanted in the *scala tympani* that can stimulate directly the spiral ganglions neurons on a damaged cochlea (Bouccara et al., 2012). Cochlear implantation is usually indicated in patients with profound sensorineural hearing loss. Nevertheless, the surgery may lead to histological damages during insertion, inflammation and fibrous tissue formation that result in residual hearing decrease when hearing persisted at low frequencies (Nguyen et al., 2015). Many efforts have been made to reduce local trauma such as the application of a protective pharmacological agent during surgery to avoid inflammatory reaction (Quesnel et al., 2011, Bas et al., 2012) and growth factors to promote sensorineural cell growth (Quesnel et al., 2011). Biodegradable polymeric coating on cochlear implant surface represents an interesting strategy to deliver drug along with the implant. The electrode can be embedded within a polymeric matrix containing a drug that will be released into the *scala tympani* for a prolonged period of time (ideally several months up to years) (Krenzlin et al., 2012). Kikkawa et al., (2014) showed that gelatin coated electrodes containing growth factors (IGF1 or HGF) reduced the insertion trauma and promoted the recovery from it up to 28 days in guinea pig. Chikar et al., (2012) developed a dual coating, composed of (arginine-glycine-aspartic acid)-functionalized alginate and the conducting polymer poly(3,4-ethylenedioxythiophene) and aimed to improve the performance of the implant and its biological stability in the cochlea. Both *in vitro* and *in vivo* studies demonstrated improvements in electrode performance such as reduction of electrode impedance and significant release of trophic factor (BDNF) in the cochlear fluid without any cytotoxic effects. A biocompatible silicone elastomer (Krenzlin et al., 2012), Poly(L-lactide) and poly(4-hydroxybutyrate) could also be used as potential coating matrices for cochlear implants (Ceschi et al., 2014). Interestingly, Bohl et al., (2012) showed that a combination of poly(4-hydroxybutyrate) and silicone coating resulted in a biphasic dexamethasone release: initial burst release from the first polymer to treat the acute response and a slow release from the silicone to prevent long-term inflammatory reactions. The drug release kinetic from polymer coated electrodes was evaluated *in vitro*. The drug release can be sustained up to several months (Astolfi et al., 2014, Kikkawa et al., 2014, Wrzeszcz et al., 2014) or years

(Krenzlin et al., 2012) depending on the nature of the coating polymer and the drug concentration. However, *in vivo* long-term effectiveness of this strategy in preventing damages caused by cochlear implantation remains to be tested.

#### 4.2.3. Microfluidic reciprocating reservoir

Reciprocating drug delivery consists in delivering soluble drugs to closed fluid spaces in the body such as the cochlea *via* a single cannula without consequent fluid volume change. The core of the microfluidic reciprocating reservoir is a system for perfusion of drugs into the cochlear perilymph through a single hole in the basal turn of the cochlea (Sewell et al., 2009). The single cannula is directly implanted in the *scala tympani* and acts as inlet and outlet. The principle consists in using the endogenous perilymph as a carrier for highly concentrated drug solutions. The system injects repeatedly small volumes (0.2 to few  $\mu\text{L}$ ) of drug solution into the cochlea over a short period of time (1 to 10 s). Drug delivery occurs through the diffusion and mixing of the high concentrated drug with perilymph in the *scala tympani*. During withdrawal, the same volume of less concentrated fluid is returned in the device. This method may protect the sensitive hair cells from damaging changes in perilymph volume and pressure while the drug concentration in the cochlea increases (Pararas et al., 2012). The system has been tested for the delivery of DNQX, a glutamate receptor blocker, in guinea pig (Chen et al., 2005). Perfusion of the control artificial perilymph showed no effect on the hearing function indicating the safety of the device, whereas the injection of DNQX resulted in a reversible, dose-dependent increase in hearing thresholds. The effect was also dependent on the location along the cochlea representing a gradient basal-to-apical concentration. Increasing in flow rate distributed the drug more extensively in the apical region (Pararas et al., 2011). A critical issue for using this device consists in obtaining an overall size consistent with surgical implantation into the mastoid cavity behind the ear. The wearable device used for guinea pig studies measured 5.5 x 4.0 x 3.8 cm (Handzel et al., 2009, Sewell et al., 2009). Therefore, future directions are focused on miniaturization while preserving and/or increasing the functionality for such devices.

#### 4.3. Combination of local drug delivery systems

Combining different drug delivery systems seems to be an attractive strategy to overcome the limitations of each system alone either for intratympanic or intracochlear drug administration. For example, the incorporation of nanoparticulate systems into hydrogels

should increase the residence time of the nanocarriers in the middle ear and thus, enhance their concentration in the inner ear, while preserving potential targeting of inner ear cells. Some examples in the literature explored this possibility:

Thaler et al., (2011) tested a "ferrogel" consisting of SPIONs dispersed within a poloxamer 407 hydrogel, in post-mortem human temporal bone and in organotypic explants of mouse inner ear. More recently, Lajud et al., (2015) developed a "nanohydrogel" where fluorescently labeled liposomes incorporated into a chitosan hydrogel were evaluated *in vitro* and *in vivo* in mouse. *In vitro* experiments showed that the nanohydrogel can carry and release intact liposomes in a controlled and sustained manner. *In vivo* study demonstrated that intact liposomes were delivered into the perilymphatic space and reached cellular structures in the scala media.

For intracochlear drug administration, Hutten et al., (2014) tested a combination of a hydrogel with a medical device for cochlear implantation. The drug delivery device consists of a silicone reservoir which is refillable with a PEG-based hydrogel carrying dexamethasone. This device was implanted into the cochlea in guinea pig *via* a cochleostomy resulting in a significant protection of residual hearing and a reduced fibrosis. The hydrogel-filled reservoir could be used as a drug delivery device on its own or in combination with cochlear implants providing sustained drug delivery.

#### 4.4. Current hurdles to overcome

Whereas local drug delivery for inner ear therapy showed a great potential in research and clinic over the past decade, in practice, there are still several hurdles to overcome. Difficulties are mainly related to the ear anatomy. Considering the location of the cochlea in the petrous bone, its complexity, its highly differentiated cellular populations and the fact that any surgical approach is responsible for hearing loss, the study of cochlear function requires the use of animal models (usually rodents) where *in vivo* microsurgical techniques and microsampling of inner ear fluids are required. Both the withdrawal and the analysis of perilymph samples represent considerable technical challenges (Salt and Plontke, 2005). Because the fluid volumes in the inner ear are extremely small and especially in animals (around 10 µL for total cochlear perilymph in guinea pig), it is difficult to provide adequate sample volumes for analysis by conventional methods such as UV-HPLC. Highly sensitive techniques such as LC-MS are more adapted for assays in perilymph samples (Wang et al., 2009, Honeder et al., 2014) but are more complex and rather expensive. In addition, the

sampling method could cause the contamination of the fluid samples, taken from *scala tympani*, with cerebrospinal fluid (Salt and Plontke, 2005; 2009). Based on measurements with marker ions, it was estimated that 10 µL samples taken from the basal turn of the guinea pig cochlea contained 85% cerebrospinal fluid and 1 µL samples contained 20% cerebrospinal fluid (Salt et al., 2003). However, by using proper techniques, it is possible to minimize perilymph contamination with cerebrospinal fluid.

In most studies, applied doses, application protocols and drug delivery systems are empirically justified leading to varying results. It is thus difficult to compare the different studies and to conclude on quantitative data about drug pharmacokinetics in the inner ear using different drug delivery systems. In addition, the pharmacokinetics of drugs in the inner ear is not well defined and there is a lack of quantitative data about local bioavailability, drug distribution and round window permeability. However, a basic understanding of the mechanisms of drug distribution in the inner ear has emerged. Salt and Plontke (2009) described the pharmacokinetic processes of the inner ear according to the LADME concept (Liberation, Absorption, Distribution, Metabolism, Elimination). They also provided a finite-element computer model (Cochlear Fluids Simulator V3.083) that considers the anatomy of the inner ear in human and rodents, general pharmacokinetic principles and solute distribution processes. Based on experimental data, this model permits the calculation of solute movements associated with a variety of delivery protocols.

A high inter-individual variability of drug levels in perilymph was also reported with over 10-fold differences between animals in the same group (Salt and Plontke, 2009). This variability is probably caused by inherent variations in round window permeability, possibly associated with variations in thickness or cellular permeability properties between individuals (Hahn et al., 2006, Mikulec et al., 2008). Round window permeability can also be affected by potential round window obstruction in some persons (see section 2.2.2). Consequently, important differences in pharmacokinetic profiles in animal experiments considerably limit their extrapolation to human. Furthermore, recent studies demonstrated that drug entry in the inner ear following intratympanic administration in guinea pig may occur through the bone of the otic capsule which is thinner in rodents than in humans (Mikulec et al., 2009). Drug entry through the bone is thus not likely to be significant in human. These observations have to be considered carefully when analyzing results from animal studies that involve applying drugs to the bulla and when translating these data for the human situation.

## **5. Conclusions**

Inner ear therapy is undergoing rapid progress and a wide range of drug delivery systems were developed in the last decade in research. Significant evolution towards efficacious inner ear local drug delivery allowed the development of systems where therapeutics agents can be introduced in the cochlea in a sustained manner either by intratympanic or intracochlear administration. These systems include hydrogels and nanoparticulate systems as injectable drug delivery systems and several implantable devices such as osmotic pumps and reciprocating reservoirs. Some clinical trials are ongoing for inner ear diseases (e.g. hydrogels based on poloxamer 407 (OTO-104) or hyaluronic acid (AM-111 and AM-101)) demonstrating the transposition of the strategies developed in research during the past decade to the clinical practice. A hydrogel-based drug delivery system is likely to become the first inner ear disease-specific medicine on the market. The future of inner ear treatments depends on the development of further minimally invasive strategies (e.g. miniaturized devices), safe and highly controlled delivery systems, combining different drug delivery systems and targeting of sensory and neural cells.

## **Acknowledgments**

Naila El Kechai acknowledges the Ministère de l'Education Nationale, de l'Enseignement Supérieur et de la Recherche for her PhD grant.

## References

- Alles, M.J., der Gaag, M.A., Stokroos, R.J., 2006. Intratympanic steroid therapy for inner ear diseases, a review of the literature. *Eur Arch Otorhinolaryngol.* 263, 791-797.
- Almeida-Branco, M.S., Cabrera, S., Lopez-Escamez, J.A., 2014. Perspectives for the treatment of sensorineural hearing loss by cellular regeneration of the inner ear. *Acta Otorrinolaringol Esp.* Doi: 10.1016/j.otorri.2014.07.009.
- Almeida, H., Amaral, M.H., Lobao, P., Sousa Lobo, J.M., 2013. Applications of poloxamers in ophthalmic pharmaceutical formulations: an overview. *Expert Opin Drug Deliv.* 10, 1223-1237.
- Alzamil, K.S., Linthicum, F.H., Jr., 2000. Extraneous round window membranes and plugs: possible effect on intratympanic therapy. *Ann Otol Rhinol Laryngol.* 109, 30-32.
- Angelova, A., Angelov, B., Papahadjopoulos-Sternberg, B., Ollivon, M., Bourgaux, C., 2005. Proteocubosomes: nanoporous vehicles with tertiary organized fluid interfaces. *Langmuir.* 21, 4138-4143.
- Anniko, M., Wroblewski, R., 1986. Ionic environment of cochlear hair cells. *Hear Res.* 22, 279-293.
- Astolfi, L., Guarani, V., Marchetti, N., Olivetto, E., Simoni, E., Cavazzini, A., Jolly, C., Martini, A., 2014. Cochlear implants and drug delivery: In vitro evaluation of dexamethasone release. *J Biomed Mater Res B Appl Biomater.* 102, 267-273.
- Auris medical, 2015, Auris medical: product candidates. <http://www.aurismedical.com/product-candidates/pipeline> (30/04/2015).
- Ayoob, A.M., Borenstein, J.T., 2015. The role of intracochlear drug delivery devices in the management of inner ear disease. *Expert Opin Drug Deliv.* 12, 465-479.
- Balazs, E.A., 2008. Hyaluronan as an ophthalmic viscoelastic device. *Curr Pharm Biotechnol.* 9, 236-238.
- Barriat, S., van Wijck, F., Staeker, H., Lefebvre, P.P., 2012. Intratympanic Steroid Therapy Using the Silverstein Microwick (TM) for Refractory Sudden Sensorineural Hearing Loss Increases Speech Intelligibility. *Audiology and Neuro-Otology.* 17, 105-111.
- Bas, E., Dinh, C.T., Garnham, C., Polak, M., Van de Water, T.R., 2012. Conservation of hearing and protection of hair cells in cochlear implant patients' with residual hearing. *Anat Rec (Hoboken).* 295, 1909-1927.
- Bear, Z.W., Mikulec, A.A., 2014. Intratympanic steroid therapy for treatment of idiopathic sudden sensorineural hearing loss. *Mo Med.* 111, 352-356.
- Berryhill, W.E., Graham, M.D., 2002. Chemical and physical labyrinthectomy for Meniere's disease. *Otolaryngol Clin North Am.* 35, 675-682.
- Bohl, A., Rohm, H.W., Ceschi, P., Paasche, G., Hahn, A., Barcikowski, S., Lenarz, T., Stover, T., Pau, H.W., Schmitz, K.P., Sternberg, K., 2012. Development of a specially tailored local drug delivery system for the prevention of fibrosis after insertion of cochlear implants into the inner ear. *J Mater Sci Mater Med.* 23, 2151-2162.
- Borden, R.C., Saunders, J.E., Berryhill, W.E., Krempl, G.A., Thompson, D.M., Queimado, L., 2011. Hyaluronic acid hydrogel sustains the delivery of dexamethasone across the round window membrane. *Audiol Neurootol.* 16, 1-11.

- Bouccara, D., Mosnier, I., Bernardeschi, D., Ferrary, E., Sterkers, O., 2012. Cochlear implant in adults. *Rev Med Interne.* 33, 143-149.
- Bozzuto, G., Molinari, A., 2015. Liposomes as nanomedical devices. *Int J Nanomedicine.* 10, 975-999.
- Brown, J.N., Miller, J.M., Altschuler, R.A., Nuttall, A.L., 1993. Osmotic pump implant for chronic infusion of drugs into the inner ear. *Hear Res.* 70, 167-172.
- Buckiova, D., Ranjan, S., Newman, T.A., Johnston, A.H., Sood, R., Kinnunen, P.K., Popelar, J., Chumak, T., Syka, J., 2012. Minimally invasive drug delivery to the cochlea through application of nanoparticles to the round window membrane. *Nanomedicine (Lond).* 7, 1339-1354.
- Cai, H., Wen, X., Wen, L., Tirelli, N., Zhang, X., Zhang, Y., Su, H., Yang, F., Chen, G., 2014. Enhanced local bioavailability of single or compound drugs delivery to the inner ear through application of PLGA nanoparticles via round window administration. *Int J Nanomedicine.* 9, 5591-5601.
- Ceschi, P., Bohl, A., Sternberg, K., Neumeister, A., Senz, V., Schmitz, K.P., Kietzmann, M., Scheper, V., Lenarz, T., Stover, T., Paasche, G., 2014. Biodegradable polymeric coatings on cochlear implant surfaces and their influence on spiral ganglion cell survival. *J Biomed Mater Res B Appl Biomater.* 102, 1255-1267.
- Chen, Z., Kujawa, S.G., McKenna, M.J., Fiering, J.O., Mescher, M.J., Borenstein, J.T., Swan, E.E., Sewell, W.F., 2005. Inner ear drug delivery via a reciprocating perfusion system in the guinea pig. *J Control Release.* 110, 1-19.
- Chikar, J.A., Hendricks, J.L., Richardson-Burns, S.M., Raphael, Y., Pfingst, B.E., Martin, D.C., 2012. The use of a dual PEDOT and RGD-functionalized alginate hydrogel coating to provide sustained drug delivery and improved cochlear implant function. *Biomaterials.* 33, 1982-1990.
- Cochlear Fluids Simulator V3.083, <http://oto2.wustl.edu/cochlea/model3.html> (23/02/2015).
- Coleman, J.K., Littlesunday, C., Jackson, R., Meyer, T., 2007. AM-111 protects against permanent hearing loss from impulse noise trauma. *Hear Res.* 226, 70-78.
- Danhier, F., Ansorena, E., Silva, J.M., Coco, R., Le Breton, A., Preat, V., 2012. PLGA-based nanoparticles: an overview of biomedical applications. *J Control Release.* 161, 505-522.
- Darrat, I., Ahmad, N., Seidman, K., Seidman, M.D., 2007. Auditory research involving antioxidants. *Curr Opin Otolaryngol Head Neck Surg.* 15, 358-363.
- Du, X., Chen, K., Kuriyavar, S., Kopke, R.D., Grady, B.P., Bourne, D.H., Li, W., Dormer, K.J., 2013. Magnetic targeted delivery of dexamethasone acetate across the round window membrane in guinea pigs. *Otol Neurotol.* 34, 41-47.
- Dumortier, G., Grossiord, J.L., Agnely, F., Chaumeil, J.C., 2006. A review of poloxamer 407 pharmaceutical and pharmacological characteristics. *Pharm Res.* 23, 2709-2728.
- Dutta Gupta, D.S., Jadhav, V.M., Kadam, V.J., 2015. Chitosan: A Propitious Biopolymer for Drug Delivery. *Curr Drug Deliv.*
- Eastwood, H., Chang, A., Kel, G., Sly, D., Richardson, R., O'Leary, S.J., 2010. Round window delivery of dexamethasone ameliorates local and remote hearing loss produced by cochlear implantation into the second turn of the guinea pig cochlea. *Hear Res.* 265, 25-29.

- Eastwood, H., Pinder, D., James, D., Chang, A., Galloway, S., Richardson, R., O'Leary, S., 2010. Permanent and transient effects of locally delivered n-acetyl cysteine in a guinea pig model of cochlear implantation. *Hear Res.* 259, 24-30.
- El Kechai, N., Bochot, A., Huang, N., Nguyen, Y., Ferrary, E., Agnely, F., 2015. Effect of liposomes on rheological and syringeability properties of hyaluronic acid hydrogels intended for local injection of drugs. *Int J Pharm.* 487, 187-196.
- Endo, T., Nakagawa, T., Kita, T., Iguchi, F., Kim, T.S., Tamura, T., Iwai, K., Tabata, Y., Ito, J., 2005. Novel strategy for treatment of inner ears using a biodegradable gel. *Laryngoscope.* 115, 2016-2020.
- Engleider, E., Honeder, C., Klobasa, J., Wirth, M., Arnoldner, C., Gabor, F., 2014. Preclinical evaluation of thermoreversible triamcinolone acetonide hydrogels for drug delivery to the inner ear. *Int J Pharm.* 471, 297-302.
- European Pharmacopoeia Commission. Parenteral preparations. In European Pharmacopoeia 8.4, 2015, European Directorate for the Quality of Medicines (EDQM), 4691-4693.
- Feng, L., Ward, J.A., Li, S.K., Tolia, G., Hao, J., Choo, D.I., 2014. Assessment of PLGA-PEG-PLGA copolymer hydrogel for sustained drug delivery in the ear. *Curr Drug Deliv.* 11, 279-286.
- Ferrary, E., Sterkers, O., 1998. Mechanisms of endolymph secretion. *Kidney Int Suppl.* 65, S98-103.
- Flanagan, S., Mukherjee, P., Tonkin, J., 2006. Outcomes in the use of intra-tympanic gentamicin in the treatment of Meniere's disease. *J Laryngol Otol.* 120, 98-102.
- Fukui, H., Raphael, Y., 2013. Gene therapy for the inner ear. *Hear Res.* 297, 99-105.
- Ge, X., Jackson, R.L., Liu, J., Harper, E.A., Hoffer, M.E., Wassel, R.A., Dorner, K.J., Kopke, R.D., Balough, B.J., 2007. Distribution of PLGA nanoparticles in chinchilla cochleae. *Otolaryngol Head Neck Surg.* 137, 619-623.
- Ghanem, T.A., Breneman, K.D., Rabbitt, R.D., Brown, H.M., 2008. Ionic composition of endolymph and perilymph in the inner ear of the oyster toadfish, *Opsanus tau*. *Biol Bull.* 214, 83-90.
- Ghiz, A.F., Salt, A.N., DeMott, J.E., Henson, M.M., Henson, O.W., Jr., Gewalt, S.L., 2001. Quantitative anatomy of the round window and cochlear aqueduct in guinea pigs. *Hear Res.* 162, 105-112.
- Ghossaini, S.N., Liu, J.P., Phillips, B., 2013. Round window membrane permeability to golimumab in guinea pigs: a pilot study. *Laryngoscope.* 123, 2840-2844.
- Girish, K.S., Kemparaju, K., 2007. The magic glue hyaluronan and its eraser hyaluronidase: a biological overview. *Life Sci.* 80, 1921-1943.
- Gouveris, H., Selivanova, O., Mann, W., 2005. Intratympanic dexamethasone with hyaluronic acid in the treatment of idiopathic sudden sensorineural hearing loss after failure of intravenous steroid and vasoactive therapy. *Eur Arch Otorhinolaryngol.* 262, 131-134.
- Goycoolea, M.V., 2001. Clinical aspects of round window membrane permeability under normal and pathological conditions. *Acta Otolaryngol.* 121, 437-447.
- Goycoolea, M.V., Lundman, L., 1997. Round window membrane. Structure function and permeability: a review. *Microsc Res Tech.* 36, 201-211.

- Goycoolea, M.V., Muchow, D., Martinez, G.C., Aguilà, P.B., Goycoolea, H.G., Goycoolea, C.V., Schachern, P., Knight, W., 1988. Permeability of the human round-window membrane to cationic ferritin. *Arch Otolaryngol Head Neck Surg.* 114, 1247-1251.
- Goycoolea, M.V., Muchow, D., Schachern, P., 1988. Experimental studies on round window structure: function and permeability. *Laryngoscope.* 98, 1-20.
- Gramowski, A., Flossdorf, J., Bhattacharya, K., Jonas, L., Lantow, M., Rahman, Q., Schiffmann, D., Weiss, D.G., Dopp, E., 2010. Nanoparticles induce changes of the electrical activity of neuronal networks on microelectrode array neurochips. *Environ Health Perspect.* 118, 1363-1369.
- Grottkau, B.E., Cai, X., Wang, J., Yang, X., Lin, Y., 2013. Polymeric nanoparticles for a drug delivery system. *Curr Drug Metab.* 14, 840-846.
- Guitton, M.J., Dudai, Y., 2007. Blockade of cochlear NMDA receptors prevents long-term tinnitus during a brief consolidation window after acoustic trauma. *Neural Plast.* 2007, 80904.
- Guyot, J.P., Maire, R., Delaspre, O., 2008. Intratympanic application of an antiviral agent for the treatment of Meniere's disease. *ORL J Otorhinolaryngol Relat Spec.* 70, 21-26; discussion 26-27.
- Hahn, H., Kammerer, B., DiMauro, A., Salt, A.N., Plontke, S.K., 2006. Cochlear microdialysis for quantification of dexamethasone and fluorescein entry into scala tympani during round window administration. *Hear Res.* 212, 236-244.
- Hamaguchi, Y., Morizono, T., Juhn, S.K., 1988. Round window membrane permeability to human serum albumin in antigen-induced otitis media. *Am J Otolaryngol.* 9, 34-40.
- Handzel, O., Wang, H., Fiering, J., Borenstein, J.T., Mescher, M.J., Swan, E.E., Murphy, B.A., Chen, Z., Peppi, M., Sewell, W.F., Kujawa, S.G., McKenna, M.J., 2009. Mastoid cavity dimensions and shape: method of measurement and virtual fitting of implantable devices. *Audiol Neurotol.* 14, 308-314.
- Hashimoto, Y., Iwasaki, S., Mizuta, K., Arai, M., Mineta, H., 2007. Pattern of cochlear damage caused by short-term kanamycin application using the round window microcatheter method. *Acta Otolaryngol.* 127, 116-121.
- Havenith, S., Versnel, H., Agterberg, M.J., de Groot, J.C., Sedee, R.J., Grolman, W., Klis, S.F., 2011. Spiral ganglion cell survival after round window membrane application of brain-derived neurotrophic factor using gelfoam as carrier. *Hear Res.* 272, 168-177.
- Herraiz, C., Miguel Aparicio, J., Plaza, G., 2010. Intratympanic drug delivery for the treatment of inner ear diseases. *Acta Otorrinolaringol Esp.* 61, 225-232.
- Hill, S.L., 3rd, Digges, E.N., Silverstein, H., 2006. Long-term follow-up after gentamicin application via the Silverstein MicroWick in the treatment of Meniere's disease. *Ear Nose Throat J.* 85, 494-498.
- Hillman, T.M., Arriaga, M.A., Chen, D.A., 2003. Intratympanic steroids: do they acutely improve hearing in cases of cochlear hydrops? *Laryngoscope.* 113, 1903-1907.
- Holley, M.C., 2005. Keynote review: The auditory system, hearing loss and potential targets for drug development. *Drug Discov Today.* 10, 1269-1282.
- Honeder, C., Engleider, E., Schopper, H., Gabor, F., Reznicek, G., Wagenblast, J., Gstoettner, W., Arnoldner, C., 2014. Sustained release of triamcinolone acetonide from an

- intratympanically applied hydrogel designed for the delivery of high glucocorticoid doses. *Audiol Neurotol.* 19, 193-202.
- Horie, R.T., Sakamoto, T., Nakagawa, T., Tabata, Y., Okamura, N., Tomiyama, N., Tachibana, M., Ito, J., 2010. Sustained delivery of lidocaine into the cochlea using poly lactic/glycolic acid microparticles. *Laryngoscope.* 120, 377-383.
- Hoskison, E., Daniel, M., Al-Zahid, S., Shakesheff, K.M., Bayston, R., Birchall, J.P., 2013. Drug delivery to the ear. *Ther Deliv.* 4, 115-124.
- Huon, L.K., Fang, T.Y., Wang, P.C., 2012. Outcomes of intratympanic gentamicin injection to treat Meniere's disease. *Otol Neurotol.* 33, 706-714.
- Hutten, M., Dhanasingh, A., Hessler, R., Stover, T., Esser, K.H., Moller, M., Lenarz, T., Jolly, C., Groll, J., Scheper, V., 2014. In vitro and in vivo evaluation of a hydrogel reservoir as a continuous drug delivery system for inner ear treatment. *PLoS One.* 9, e104564.
- Huynh, N.T., Passirani, C., Saulnier, P., Benoit, J.P., 2009. Lipid nanocapsules: a new platform for nanomedicine. *Int J Pharm.* 379, 201-209.
- Igarashi, M., Ohashi, K., Ishii, M., 1986. Morphometric comparison of endolymphatic and perilymphatic spaces in human temporal bones. *Acta Otolaryngol.* 101, 161-164.
- Inaoka, T., Nakagawa, T., Kikkawa, Y.S., Tabata, Y., Ono, K., Yoshida, M., Tsubouchi, H., Ido, A., Ito, J., 2009. Local application of hepatocyte growth factor using gelatin hydrogels attenuates noise-induced hearing loss in guinea pigs. *Acta Otolaryngol.* 129, 453-457.
- Jahnke, K., 1980. Permeability barriers of the inner ear. Fine structure and function. *Fortschr Med.* 98, 330-336.
- James, D.P., Eastwood, H., Richardson, R.T., O'Leary, S.J., 2008. Effects of round window dexamethasone on residual hearing in a Guinea pig model of cochlear implantation. *Audiol Neurotol.* 13, 86-96.
- Juhn, S.K., 1988. Barrier systems in the inner ear. *Acta Otolaryngol Suppl.* 458, 79-83.
- Juhn, S.K., Hamaguchi, Y., Goycoolea, M., 1989. Review of round window membrane permeability. *Acta Otolaryngol Suppl.* 457, 43-48.
- Juhn, S.K., Hunter, B.A., Odland, R.M., 2001. Blood-labyrinth barrier and fluid dynamics of the inner ear. *Int Tinnitus J.* 7, 72-83.
- Juhn, S.K., Prado, S., Pearce, J., 1976. Osmolality changes in perilymph after systemic administration of glycerin. *Arch Otolaryngol.* 102, 683-685.
- Juhn, S.K., Rybak, L.P., 1981. Labyrinthine barriers and cochlear homeostasis. *Acta Otolaryngol.* 91, 529-534.
- Kanzaki, S., Saito, H., Inoue, Y., Ogawa, K., 2012. A new device for delivering drugs into the inner ear: otoendoscope with microcatheter. *Auris Nasus Larynx.* 39, 208-211.
- Kastenbauer, S., Klein, M., Koedel, U., Pfister, H.W., 2001. Reactive nitrogen species contribute to blood-labyrinth barrier disruption in suppurative labyrinthitis complicating experimental pneumococcal meningitis in the rat. *Brain Res.* 904, 208-217.
- Kawabata, I., Paparella, M.M., 1971. Fine structure of the round window membrane. *Ann Otol Rhinol Laryngol.* 80, 13-26.
- Kikkawa, Y.S., Nakagawa, T., Ying, L., Tabata, Y., Tsubouchi, H., Ido, A., Ito, J., 2014. Growth factor-eluting cochlear implant electrode: impact on residual auditory function, insertional trauma, and fibrosis. *J Transl Med.* 12, 280.

- Kim, C.S., Cho, T.K., Jinn, T.H., 1990. Permeability of the round window membrane to horseradish peroxidase in experimental otitis media. *Otolaryngol Head Neck Surg.* 103, 918-925.
- Kim, D.K., Park, S.N., Park, K.H., Park, C.W., Yang, K.J., Kim, J.D., Kim, M.S., 2015. Development of a drug delivery system for the inner ear using poly(amino acid)-based nanoparticles. *Drug Delivery.* 22, 367-374.
- King, E.B., Salt, A.N., Kel, G.E., Eastwood, H.T., O'Leary, S.J., 2013. Gentamicin administration on the stapes footplate causes greater hearing loss and vestibulotoxicity than round window administration in guinea pigs. *Hear Res.* 304, 159-166.
- Krenzlin, S., Vincent, C., Munzke, L., Gnansia, D., Siepmann, J., Siepmann, F., 2012. Predictability of drug release from cochlear implants. *J Control Release.* 159, 60-68.
- Kumari, A., Yadav, S.K., Yadav, S.C., 2010. Biodegradable polymeric nanoparticles based drug delivery systems. *Colloids Surf B Biointerfaces.* 75, 1-18.
- Lai, W.F., Lin, M.C.M., 2009. Nucleic acid delivery with chitosan and its derivatives. *Journal of Controlled Release.* 134, 158-168.
- Lajud, S.A., Han, Z., Chi, F.L., Gu, R., Nagda, D.A., Bezpaliko, O., Sanyal, S., Bur, A., Han, Z., O'Malley, B.W., Jr., Li, D., 2013. A regulated delivery system for inner ear drug application. *J Control Release.* 166, 268-276.
- Lajud, S.A., Nagda, D.A., Qiao, P., Tanaka, N., Civantos, A., Gu, R., Cheng, Z., Tsourkas, A., O'Malley, B.W.J., Li, D., 2015. A Novel Chitosan-Hydrogel-Based Nanoparticle Delivery System for Local Inner Ear Application. *Otology & Neurotology.* 36, 341-347.
- Lambert, P.R., Nguyen, S., Maxwell, K.S., Tucci, D.L., Lustig, L.R., Fletcher, M., Bear, M., Lebel, C., 2012. A randomized, double-blind, placebo-controlled clinical study to assess safety and clinical activity of OTO-104 given as a single intratympanic injection in patients with unilateral Meniere's disease. *Otol Neurotol.* 33, 1257-1265.
- Laurell, G., Teixeira, M., Sterkers, O., Bagger-Sjöback, D., Eksborg, S., Lidman, O., Ferrary, E., 2002. Local administration of antioxidants to the inner ear. Kinetics and distribution(1). *Hear Res.* 173, 198-209.
- Lee, K.J., Chan, Y., Das, S. 2003. Essential otolaryngology: head & neck surgery. McGraw-Hill, Medical Pub. Division.
- Lee, K.Y., Nakagawa, T., Okano, T., Hori, R., Ono, K., Tabata, Y., Lee, S.H., Ito, J., 2007. Novel therapy for hearing loss: delivery of insulin-like growth factor 1 to the cochlea using gelatin hydrogel. *Otol Neurotol.* 28, 976-981.
- Lefebvre, P.P., Staeker, H., 2002. Steroid perfusion of the inner ear for sudden sensorineural hearing loss after failure of conventional therapy: a pilot study. *Acta Otolaryngol.* 122, 698-702.
- Li, L., Ren, J., Yin, T., Liu, W., 2013. Intratympanic dexamethasone perfusion versus injection for treatment of refractory sudden sensorineural hearing loss. *Eur Arch Otorhinolaryngol.* 270, 861-867.
- Liu, H., Chen, S., Zhou, Y., Che, X., Bao, Z., Li, S., Xu, J., 2013. The effect of surface charge of glycerol monooleate-based nanoparticles on the round window membrane permeability and cochlear distribution. *J Drug Target.* 21, 846-854.
- Liu, H., Wang, Y., Wang, Q., Li, Z., Zhou, Y., Zhang, Y., Li, S., 2013. Protein-bearing cubosomes prepared by liquid precursor dilution: inner ear delivery and

- pharmacokinetic study following intratympanic administration. *J Biomed Nanotechnol.* 9, 1784-1793.
- Lobo, D., Garcia-Berrocal, J.R., Trinidad, A., Verdaguer, J.M., Ramirez-Camacho, R., 2013. Review of the biologic agents used for immune-mediated inner ear disease. *Acta Otorrinolaringol Esp.* 64, 223-229.
- Luo, J., Xu, L., 2012. Distribution of gentamicin in inner ear after local administration via a chitosan glycerophosphate hydrogel delivery system. *Ann Otol Rhinol Laryngol.* 121, 208-216.
- Martini, A., Rubini, R., Ferretti, R.G., Govoni, E., Schiavinato, A., Magnavita, V., Perbellini, A., Fiori, M.G., 1992. Comparative ototoxic potential of hyaluronic acid and methylcellulose. *Acta Otolaryngol.* 112, 278-283.
- McCall, A.A., Swan, E.E., Borenstein, J.T., Sewell, W.F., Kujawa, S.G., McKenna, M.J., 2010. Drug delivery for treatment of inner ear disease: current state of knowledge. *Ear Hear.* 31, 156-165.
- McFadden, S.L., Ding, D., Jiang, H., Woo, J.M., Salvi, R.J., 2002. Chinchilla models of selective cochlear hair cell loss. *Hear Res.* 174, 230-238.
- Mikulec, A.A., Hartsock, J.J., Salt, A.N., 2008. Permeability of the round window membrane is influenced by the composition of applied drug solutions and by common surgical procedures. *Otol Neurotol.* 29, 1020-1026.
- Mikulec, A.A., Plontke, S.K., Hartsock, J.J., Salt, A.N., 2009. Entry of substances into perilymph through the bone of the otic capsule after intratympanic applications in guinea pigs: implications for local drug delivery in humans. *Otol Neurotol.* 30, 131-138.
- Miriszlai, E., Benedeczky, I., Csapo, S., Bodanszky, H., 1978. The ultrastructure of the round window membrane of the cat. *ORL J Otorhinolaryngol Relat Spec.* 40, 111-119.
- Mukherjea, D., Rybak, L.P., Sheehan, K.E., Kaur, T., Ramkumar, V., Jajoo, S., Sheth, S., 2011. The design and screening of drugs to prevent acquired sensorineural hearing loss. *Expert Opin Drug Discov.* 6, 491-505.
- Mynatt, R., Hale, S.A., Gill, R.M., Plontke, S.K., Salt, A.N., 2006. Demonstration of a longitudinal concentration gradient along scala tympani by sequential sampling of perilymph from the cochlear apex. *J Assoc Res Otolaryngol.* 7, 182-193.
- Nakagawa, T., Kumakawa, K., Usami, S., Hato, N., Tabuchi, K., Takahashi, M., Fujiwara, K., Sasaki, A., Komune, S., Sakamoto, T., Hiraumi, H., Yamamoto, N., Tanaka, S., Tada, H., Yamamoto, M., Yonezawa, A., Ito-Ihara, T., Ikeda, T., Shimizu, A., Tabata, Y., Ito, J., 2014. A randomized controlled clinical trial of topical insulin-like growth factor-1 therapy for sudden deafness refractory to systemic corticosteroid treatment. *BMC Med.* 12, 219.
- Nguyen, Y., Bernardeschi, D., Kazmitcheff, G., Miroir, M., Vauchel, T., Ferrary, E., Sterkers, O., 2015. Effect of embedded dexamethasone in cochlear implant array on insertion forces in an artificial model of scala tympani. *Otol Neurotol.* 36, 354-358.
- Noushi, F., Richardson, R.T., Hardman, J., Clark, G., O'Leary, S., 2005. Delivery of neurotrophin-3 to the cochlea using alginate beads. *Otol Neurotol.* 26, 528-533.
- Ohashi, M., Ide, S., Sawaguchi, A., Suganuma, T., Kimitsuki, T., Komune, S., 2008. Histochemical localization of the extracellular matrix components in the annular ligament of rat stapediovestibular joint with special reference to fibrillin, 36-kDa

- microfibril-associated glycoprotein (MAGP-36), and hyaluronic acid. *Med Mol Morphol.* 41, 28-33.
- Okuno, H., Sando, I., 1988. Anatomy of the round window. A histopathological study with a graphic reconstruction method. *Acta Otolaryngol.* 106, 55-63.
- Omotehara, Y., Hakuba, N., Hato, N., Okada, M., Gyo, K., 2011. Protection against ischemic cochlear damage by intratympanic administration of AM-111. *Otol Neurotol.* 32, 1422-1427.
- Otonomy, 2015, Otonomy: Pipeline. <http://www.otonomy.com/pipeline/oto-104> (30/04/2015).
- Ozturk, K., Yaman, H., Cihat Avunduk, M., Arbag, H., Keles, B., Uyar, Y., 2006. Effectiveness of MeroGel hyaluronic acid on tympanic membrane perforations. *Acta Otolaryngol.* 126, 1158-1163.
- Pararas, E.E., Borkholder, D.A., Borenstein, J.T., 2012. Microsystems technologies for drug delivery to the inner ear. *Adv Drug Deliv Rev.* 64, 1650-1660.
- Pararas, E.E., Chen, Z., Fiering, J., Mescher, M.J., Kim, E.S., McKenna, M.J., Kujawa, S.G., Borenstein, J.T., Sewell, W.F., 2011. Kinetics of reciprocating drug delivery to the inner ear. *J Control Release.* 152, 270-277.
- Paulson, D.P., Abuzeid, W., Jiang, H., Oe, T., O'Malley, B.W., Li, D., 2008. A novel controlled local drug delivery system for inner ear disease. *Laryngoscope.* 118, 706-711.
- Pfizer product detail, 2014, Gelfoam®: absorbable gelatin compressed sponge, USP. <http://labeling.pfizer.com>ShowLabeling.aspx?id=573> (26/04/2015).
- Plontke, S.K., Lowenheim, H., Mertens, J., Engel, C., Meisner, C., Weidner, A., Zimmermann, R., Preyer, S., Koitschev, A., Zenner, H.P., 2009. Randomized, double blind, placebo controlled trial on the safety and efficacy of continuous intratympanic dexamethasone delivered via a round window catheter for severe to profound sudden idiopathic sensorineural hearing loss after failure of systemic therapy. *Laryngoscope.* 119, 359-369.
- Plontke, S.K., Mynatt, R., Gill, R.M., Borgmann, S., Salt, A.N., 2007. Concentration gradient along the scala tympani after local application of gentamicin to the round window membrane. *Laryngoscope.* 117, 1191-1198.
- Plontke, S.K., Zimmermann, R., Zenner, H.P., Lowenheim, H., 2006. Technical note on microcatheter implantation for local inner ear drug delivery: surgical technique and safety aspects. *Otol Neurotol.* 27, 912-917.
- Pritz, C.O., Dudas, J., Rask-Andersen, H., Schrott-Fischer, A., Glueckert, R., 2013. Nanomedicine strategies for drug delivery to the ear. *Nanomedicine (Lond).* 8, 1155-1172.
- Quesnel, S., Nguyen, Y., Campo, P., Hermine, O., Ribeil, J.A., Elmaleh, M., Grayeli, A.B., Ferrary, E., Sterkers, O., Couloigner, V., 2011. Protective effect of systemic administration of erythropoietin on auditory brain stem response and compound action potential thresholds in an animal model of cochlear implantation. *Ann Otol Rhinol Laryngol.* 120, 737-747.

- Quesnel, S., Nguyen, Y., Elmaleh, M., Grayeli, A.B., Ferrary, E., Sterkers, O., Couloigner, V., 2011. Effects of systemic administration of methylprednisolone on residual hearing in an animal model of cochlear implantation. *Acta Otolaryngol.* 131, 579-584.
- Richardson, R.T., Noushi, F., O'Leary, S., 2006. Inner ear therapy for neural preservation. *Audiol Neurotol.* 11, 343-356.
- Richardson, R.T., Wise, A.K., Andrew, J.K., O'Leary, S.J., 2008. Novel drug delivery systems for inner ear protection and regeneration after hearing loss. *Expert Opin Drug Deliv.* 5, 1059-1076.
- Richardson, T.L., Ishiyama, E., Keels, E.W., 1971. Submicroscopic studies of the round window membrane. *Acta Otolaryngol.* 71, 9-21.
- Roy, S., Glueckert, R., Johnston, A.H., Perrier, T., Bitsche, M., Newman, T.A., Saulnier, P., Schrott-Fischer, A., 2012. Strategies for drug delivery to the human inner ear by multifunctional nanoparticles. *Nanomedicine (Lond).* 7, 55-63.
- Roy, S., Johnston, A.H., Newman, T.A., Glueckert, R., Dudas, J., Bitsche, M., Corbacella, E., Rieger, G., Martini, A., Schrott-Fischer, A., 2010. Cell-specific targeting in the mouse inner ear using nanoparticles conjugated with a neurotrophin-derived peptide ligand: potential tool for drug delivery. *Int J Pharm.* 390, 214-224.
- Saber, A., Laurell, G., Brammer, T., Edsman, K., Engmer, C., Ulfendahl, M., 2009. Middle ear application of a sodium hyaluronate gel loaded with neomycin in a Guinea pig model. *Ear Hear.* 30, 81-89.
- Saber, A., Strand, S.P., Ulfendahl, M., 2010. Use of the biodegradable polymer chitosan as a vehicle for applying drugs to the inner ear. *Eur J Pharm Sci.* 39, 110-115.
- Saito, T., Zhang, Z.J., Tokuriki, M., Ohtsubo, T., Noda, I., Shibamori, Y., Yamamoto, T., Saito, H., 2001. Expression of p-glycoprotein is associated with that of multidrug resistance protein 1 (MRP1) in the vestibular labyrinth and endolymphatic sac of the guinea pig. *Neurosci Lett.* 303, 189-192.
- Salt, A.N., Hartsock, J., Plontke, S., LeBel, C., Piu, F., 2011. Distribution of dexamethasone and preservation of inner ear function following intratympanic delivery of a gel-based formulation. *Audiol Neurotol.* 16, 323-335.
- Salt, A.N., Kellner, C., Hale, S., 2003. Contamination of perilymph sampled from the basal cochlear turn with cerebrospinal fluid. *Hear Res.* 182, 24-33.
- Salt, A.N., King, E.B., Hartsock, J.J., Gill, R.M., O'Leary, S.J., 2012. Marker entry into vestibular perilymph via the stapes following applications to the round window niche of guinea pigs. *Hear Res.* 283, 14-23.
- Salt, A.N., Plontke, S.K., 2005. Local inner-ear drug delivery and pharmacokinetics. *Drug Discov Today.* 10, 1299-1306.
- Salt, A.N., Plontke, S.K., 2009. Principles of local drug delivery to the inner ear. *Audiol Neurotol.* 14, 350-360.
- Scheibe, F., Haupt, H., 1985. Biochemical differences between perilymph, cerebrospinal fluid and blood plasma in the guinea pig. *Hear Res.* 17, 61-66.
- Scheper, V., Wolf, M., Scholl, M., Kadlecova, Z., Perrier, T., Klok, H.A., Saulnier, P., Lenarz, T., Stover, T., 2009. Potential novel drug carriers for inner ear treatment: hyperbranched polylysine and lipid nanocapsules. *Nanomedicine (Lond).* 4, 623-635.

- Schuknecht, H.F., 1956. Ablation therapy for the relief of Meniere's disease. *Laryngoscope*. 66, 859-870.
- Schuknecht, H.F., Gacek, M.R., 1993. Cochlear pathology in presbycusis. *Ann Otol Rhinol Laryngol.* 102, 1-16.
- Selivanova, O.A., Gouveris, H., Victor, A., Amedee, R.G., Mann, W., 2005. Intratympanic dexamethasone and hyaluronic acid in patients with low-frequency and Meniere's-associated sudden sensorineural hearing loss. *Otol Neurotol.* 26, 890-895.
- Sewell, W.F., Borenstein, J.T., Chen, Z., Fiering, J., Handzel, O., Holmboe, M., Kim, E.S., Kujawa, S.G., McKenna, M.J., Mescher, M.M., Murphy, B., Swan, E.E., Peppi, M., Tao, S., 2009. Development of a microfluidics-based intracochlear drug delivery device. *Audiol Neurotol.* 14, 411-422.
- Shih, C.P., Chen, H.C., Chen, H.K., Chiang, M.C., Sytwu, H.K., Lin, Y.C., Li, S.L., Shih, Y.F., Liao, A.H., Wang, C.H., 2013. Ultrasound-aided microbubbles facilitate the delivery of drugs to the inner ear via the round window membrane. *J Control Release*. 167, 167-174.
- Shinomori, Y., Spack, D.S., Jones, D.D., Kimura, R.S., 2001. Volumetric and dimensional analysis of the guinea pig inner ear. *Ann Otol Rhinol Laryngol.* 110, 91-98.
- Silverstein, H., 1999. Use of a new device, the MicroWick, to deliver medication to the inner ear. *Ear Nose Throat J.* 78, 595-598.
- Silverstein, H., Thompson, J., Rosenberg, S.I., Brown, N., Light, J., 2004. Silverstein MicroWick. *Otolaryngol Clin North Am.* 37, 1019-1034.
- Singh-Joy, S.D., McLain, V.C., 2008. Safety assessment of poloxamers 101, 105, 108, 122, 123, 124, 181, 182, 183, 184, 185, 188, 212, 215, 217, 231, 234, 235, 237, 238, 282, 284, 288, 331, 333, 334, 335, 338, 401, 402, 403, and 407, poloxamer 105 benzoate, and poloxamer 182 dibenzoate as used in cosmetics. *Int J Toxicol.* 27 Suppl 2, 93-128.
- Sreenivas, S.A., Pai, K.V., 2008. Thiolated Chitosans: Novel Polymers for Mucoadhesive Drug Delivery - A Review. *Tropical Journal of Pharmaceutical Research.* 7, 1077-1088.
- Staecker, H., Rodgers, B., 2013. Developments in delivery of medications for inner ear disease. *Expert Opin Drug Deliv.* 10, 639-650.
- Sterkers, O., Ferrary, E., Amiel, C., 1988. Production of inner ear fluids. *Physiol Rev.* 68, 1083-1128.
- Stover, T., Yagi, M., Raphael, Y., 1999. Cochlear gene transfer: round window versus cochleostomy inoculation. *Hear Res.* 136, 124-130.
- Suckfuell, M., Canis, M., Strieth, S., Scherer, H., Haisch, A., 2007. Intratympanic treatment of acute acoustic trauma with a cell-permeable JNK ligand: a prospective randomized phase I/II study. *Acta Otolaryngol.* 127, 938-942.
- Surovtseva, E.V., Johnston, A.H., Zhang, W., Zhang, Y., Kim, A., Murakoshi, M., Wada, H., Newman, T.A., Zou, J., Pyykkö, I., 2012. Prestin binding peptides as ligands for targeted polymersome mediated drug delivery to outer hair cells in the inner ear. *Int J Pharm.* 424, 121-127.
- Suryanarayanan, R., Cook, J.A., 2004. Long-term results of gentamicin inner ear perfusion in Meniere's disease. *J Laryngol Otol.* 118, 489-495.
- Suzuki, M., Yamasoba, T., Ishibashi, T., Miller, J.M., Kaga, K., 2002. Effect of noise exposure on blood-labyrinth barrier in guinea pigs. *Hear Res.* 164, 12-18.

- Swan, E.E., Mescher, M.J., Sewell, W.F., Tao, S.L., Borenstein, J.T., 2008. Inner ear drug delivery for auditory applications. *Adv Drug Deliv Rev.* 60, 1583-1599.
- Swan, E.E., Peppi, M., Chen, Z., Green, K.M., Evans, J.E., McKenna, M.J., Mescher, M.J., Kujawa, S.G., Sewell, W.F., 2009. Proteomics analysis of perilymph and cerebrospinal fluid in mouse. *Laryngoscope.* 119, 953-958.
- Tamura, T., Kita, T., Nakagawa, T., Endo, T., Kim, T.S., Ishihara, T., Mizushima, Y., Higaki, M., Ito, J., 2005. Drug delivery to the cochlea using PLGA nanoparticles. *Laryngoscope.* 115, 2000-2005.
- Thaler, M., Roy, S., Fornara, A., Bitsche, M., Qin, J., Muhammed, M., Salvenmoser, W., Rieger, G., Fischer, A.S., Glueckert, R., 2011. Visualization and analysis of superparamagnetic iron oxide nanoparticles in the inner ear by light microscopy and energy filtered TEM. *Nanomedicine (Lond).* 7, 360-369.
- van de Heyning, P., Muehlmeier, G., Cox, T., Lisowska, G., Maier, H., Morawski, K., Meyer, T., 2014. Efficacy and safety of AM-101 in the treatment of acute inner ear tinnitus--a double-blind, randomized, placebo-controlled phase II study. *Otol Neurotol.* 35, 589-597.
- Van Wijck, F., Staeker, H., Lefebvre, P.P., 2007. Topical steroid therapy using the Silverstein Microwick in sudden sensorineural hearing loss after failure of conventional treatment. *Acta Otolaryngol.* 127, 1012-1017.
- Van Wijk, F., Staeker, H., Keithley, E., Lefebvre, P.P., 2006. Local perfusion of the tumor necrosis factor alpha blocker infliximab to the inner ear improves autoimmune neurosensory hearing loss. *Audiol Neurotol.* 11, 357-365.
- Wang, A.Z., Langer, R., Farokhzad, O.C., 2012. Nanoparticle delivery of cancer drugs. *Annu Rev Med.* 63, 185-198.
- Wang, X., Dellamary, L., Fernandez, R., Harrop, A., Keithley, E.M., Harris, J.P., Ye, Q., Lichter, J., LeBel, C., Piu, F., 2009. Dose-dependent sustained release of dexamethasone in inner ear cochlear fluids using a novel local delivery approach. *Audiol Neurotol.* 14, 393-401.
- Wang, X., Dellamary, L., Fernandez, R., Ye, Q., LeBel, C., Piu, F., 2011. Principles of inner ear sustained release following intratympanic administration. *Laryngoscope.* 121, 385-391.
- Ward, J.A., Sidell, D.R., Nassar, M., Reece, A.L., Choo, D.I., 2014. Safety of cidofovir by intratympanic delivery technique. *Antivir Ther.* 19, 97-105.
- Wenzel, G.I., Warnecke, A., Stover, T., Lenarz, T., 2010. Effects of extracochlear gacyclidine perfusion on tinnitus in humans: a case series. *Eur Arch Otorhinolaryngol.* 267, 691-699.
- Wever, E.G., Lawrence, M., 1948. The functions of the round window. *Ann Otol Rhinol Laryngol.* 57, 579-589.
- Wrzeszcz, A., Dittrich, B., Haamann, D., Aliuos, P., Klee, D., Nolte, I., Lenarz, T., Reuter, G., 2014. Dexamethasone released from cochlear implant coatings combined with a protein repellent hydrogel layer inhibits fibroblast proliferation. *J Biomed Mater Res A.* 102, 442-454.
- Wu, N., Li, M., Chen, Z.T., Zhang, X.B., Liu, H.Z., Li, Z., Guo, W.W., Zhao, L.D., Ren, L.L., Li, J.N., Yi, H.J., Han, D., Yang, W.Y., Wu, Y., Yang, S.M., 2013. In vivo delivery of

- Atoh1 gene to rat cochlea using a dendrimer-based nanocarrier. *J Biomed Nanotechnol.* 9, 1736-1745.
- Wu, T.H., Liu, C.P., Chien, C.T., Lin, S.Y., 2013. Fluorescent hydroxylamine derived from the fragmentation of PAMAM dendrimers for intracellular hypochlorite recognition. *Chemistry.* 19, 11672-11675.
- Yang, J., Wu, H., Zhang, P., Hou, D.M., Chen, J., Zhang, S.G., 2008. The pharmacokinetic profiles of dexamethasone and methylprednisolone concentration in perilymph and plasma following systemic and local administration. *Acta Otolaryngol.* 128, 496-504.
- Yu, Z., Yu, M., Zhang, Z., Hong, G., Xiong, Q., 2014. Bovine serum albumin nanoparticles as controlled release carrier for local drug delivery to the inner ear. *Nanoscale Res Lett.* 9, 343.
- Zhang, W., Zhang, Y., Lobler, M., Schmitz, K.P., Ahmad, A., Pykkö, I., Zou, J., 2011. Nuclear entry of hyperbranched polylysine nanoparticles into cochlear cells. *Int J Nanomedicine.* 6, 535-546.
- Zhang, Y., Zhang, W., Johnston, A.H., Newman, T.A., Pykkö, I., Zou, J., 2011. Comparison of the distribution pattern of PEG-b-PCL polymersomes delivered into the rat inner ear via different methods. *Acta Otolaryngol.* 131, 1249-1256.
- Zhang, Y., Zhang, W., Johnston, A.H., Newman, T.A., Pykkö, I., Zou, J., 2010. Improving the visualization of fluorescently tagged nanoparticles and fluorophore-labeled molecular probes by treatment with CuSO<sub>4</sub> to quench autofluorescence in the rat inner ear. *Hear Res.* 269, 1-11.
- Zhang, Y., Zhang, W., Johnston, A.H., Newman, T.A., Pykkö, I., Zou, J., 2012. Targeted delivery of Tet1 peptide functionalized polymersomes to the rat cochlear nerve. *Int J Nanomedicine.* 7, 1015-1022.
- Zhang, Y., Zhang, W., Lobler, M., Schmitz, K.P., Saulnier, P., Perrier, T., Pykkö, I., Zou, J., 2011. Inner ear biocompatibility of lipid nanocapsules after round window membrane application. *Int J Pharm.* 404, 211-219.
- Zhou, C.H., Sun, J.J., Gong, S.S., Gao, G., 2009. Comparison of the antioxidants lipoic acid pharmacokinetics in inner ear between intravenous and intratympanic administration in guinea pigs. *Zhonghua Er Bi Yan Hou Tou Jing Wai Ke Za Zhi.* 44, 1034-1037.
- Zou, J., Poe, D., Ramadan, U.A., Pykkö, I., 2012. Oval window transport of Gd-dOTA from rat middle ear to vestibulum and scala vestibuli visualized by in vivo magnetic resonance imaging. *Ann Otol Rhinol Laryngol.* 121, 119-128.
- Zou, J., Saulnier, P., Perrier, T., Zhang, Y., Manninen, T., Toppila, E., Pykkö, I., 2008. Distribution of lipid nanocapsules in different cochlear cell populations after round window membrane permeation. *J Biomed Mater Res B Appl Biomater.* 87, 10-18.
- Zou, J., Sood, R., Ranjan, S., Poe, D., Ramadan, U.A., Kinnunen, P.K., Pykkö, I., 2010. Manufacturing and in vivo inner ear visualization of MRI traceable liposome nanoparticles encapsulating gadolinium. *J Nanobiotechnology.* 8, 32.
- Zou, J., Sood, R., Ranjan, S., Poe, D., Ramadan, U.A., Pykkö, I., Kinnunen, P.K., 2012. Size-dependent passage of liposome nanocarriers with preserved posttransport integrity across the middle-inner ear barriers in rats. *Otol Neurotol.* 33, 666-673.

Zou, J., Sood, R., Zhang, Y., Kinnunen, P.K., Pyykko, I., 2014. Pathway and morphological transformation of liposome nanocarriers after release from a novel sustained inner-ear delivery system. *Nanomedicine (Lond)*. 9, 2143-2155.

# **Travaux expérimentaux**

*Première partie*

**Étude physicochimique**

## **Première partie**

### **Etude physicochimique**

#### **Introduction**

L'objectif de cette première partie est de caractériser d'un point de vue physicochimique et de façon approfondie les propriétés du gel d'acide hyaluronique contenant différentes formulations de liposomes afin d'en faire une plateforme de formulation pour différentes voies locales. En effet, en partant d'une formulation qui a été testée précédemment au laboratoire pour l'injection intra-vitréenne en ophtalmologie et qui s'est montrée très prometteuse (Lajavardi et al. Journal of Controlled Realease, 2009), nous avons fait varier les paramètres de formulation des liposomes afin d'étendre l'utilisation du système « gel de liposomes » à d'autres applications telles que : l'injection transtympanique en otologie et l'injection intra-articulaire en rhumatologie. Nous avons préparé pour cela des liposomes neutres, chargés positivement ou négativement, ou bien recouverts de chaînes de polyéthylène glycol (PEG) de différentes longueurs et de différentes densités de recouvrement. Nous avons également préparé des liposomes de tailles différentes et fait varier la concentration de lipides dans le gel et enfin, la concentration en acide hyaluronique.

Le **Chapitre I** s'intéresse à l'effet des liposomes (composition, concentration, taille) sur les propriétés rhéologiques et de seringabilité des gels d'acide hyaluronique. Le **Chapitre II** présente, d'une part, une caractérisation approfondie de la compatibilité du système gel de liposomes ainsi que de sa microstructure et, d'autre part, une étude de la mobilité des liposomes au sein du gel d'HA à l'échelle macro- et microscopique.

# **Chapitre I**

**Propriétés rhéologiques et seringabilité de gels  
d'acide hyaluronique contenant des liposomes pour  
l'injection par voie locale**

# **Chapitre I**

## **Propriétés rhéologiques et seringabilité de gels d'acide hyaluronique contenant des liposomes pour l'injection par voie locale**

### **Introduction - résumé**

L'objectif de ce premier chapitre est d'étudier de façon approfondie l'effet de ces différents types de liposomes (neutres, chargés positivement ou négativement, ou bien PEGylés) sur les propriétés des gels d'acide hyaluronique. Pour cela, les formulations ont été caractérisées par microscopie électronique, par une étude rhéologique et par des tests de seringabilité. Les résultats montrent que quelles que soient les caractéristiques des liposomes dispersés dans le gel (propriétés de surface et taille), la viscosité et l'élasticité du gel d'acide hyaluronique augmentent avec la concentration en lipides. En effet, les liposomes interagissent avec l'acide hyaluronique entraînant un renforcement du réseau 3D des chaînes de polymère. La nature et les effets résultant de ces interactions dépendent à la fois de la composition et de la concentration des liposomes. Malgré une viscosité élevée au repos, toutes les formulations ont été facilement injectables avec différentes aiguilles utilisées pour des injections intra-oculaires, intra-articulaires et transtympaniques et, cela, grâce au comportement rhéofluidifiant de l'acide hyaluronique. Par ailleurs, cette étude démontre que les mesures rhéologiques ainsi que les tests de seringabilité sont à la fois nécessaires et complémentaires pour élucider le comportement de ces systèmes pendant et après l'injection. Enfin, le gel de liposomes apparaît comme une plate-forme de formulation modulable et prometteuse qui pourrait servir pour différentes applications dans l'administration locale de substances actives lorsqu'une injection est requise.

Dans une étude complémentaire, nous avons évalué de façon plus détaillée l'influence de la viscosité des gel avec ou sans liposomes sur leurs propriétés de seringabilité. L'objectif était d'étudier la possibilité de prédire l'injectabilité des gels à partir des données rhéologiques.

La première partie de ce chapitre a été publiée dans ***International Journal of Pharmaceutics*** :

El Kechai, N., Bochot, A., Huang, N., Nguyen, Y., Ferrary, E., Agnely, F\*. **2015**. Volume 487, 187-196.

## **Publication 2**

### **Effect of liposomes on rheological and syringeability properties of hyaluronic acid hydrogels intended for local injection of drugs**

*Naila El Kechai<sup>a</sup>, Amélie Bochot<sup>a</sup>, Nicolas Huang<sup>a</sup>, Yann Nguyen<sup>b</sup>, Evelyne Ferrary<sup>b</sup>,  
Florence Agnely<sup>a\*</sup>*

<sup>a</sup> Université Paris-Sud, Faculté de pharmacie, Institut Galien Paris-Sud, CNRS UMR 8612, 5 Rue J-B Clément, 92290 Châtenay-Malabry, France.

<sup>b</sup> UMR-S 1159 Inserm “Minimally Invasive Robot-based Hearing Rehabilitation”, Université Paris VI Pierre et Marie Curie, 46 rue Henri Huchard, 75018 Paris, France.

#### **\* Corresponding Author**

Florence Agnely: +33 1 46 83 56 26; [florence.agnely@u-psud.fr](mailto:florence.agnely@u-psud.fr)

## Abstract

The aim of this work was to thoroughly study the effect of liposomes on the rheological and the syringeability properties of hyaluronic acid (HA) hydrogels intended for the local administration of drugs by injection. Whatever the characteristics of the liposomes added (neutral, positively or negatively charged, with a corona of polyethylene glycol chains, size), the viscosity and the elasticity of HA gels increased in a lipid concentration-dependent manner. Indeed, liposomes strengthened the network formed by HA chains due to their interactions with this polymer. The nature and the resulting effects of these interactions depended on liposome composition and concentration. The highest viscosity and elasticity were observed with liposomes covered by polyethylene glycol chains while neutral liposomes displayed the lowest effect. Despite their high viscosity at rest, all the formulations remained easily injectable through needles commonly used for local injections thanks to the shear-thinning behavior of HA gels. The present study demonstrates that rheological and syringeability tests are both necessary to elucidate the behavior of such systems during and post injection. In conclusion, HA liposomal gels appear to be a promising and versatile formulation platform for a wide range of applications in local drug delivery when an injection is required.

## Keywords

Hyaluronic acid; hydrogel; liposomes; local injection; rheology; syringeability

## Abbreviations

Chol, cholesterol; DSPE-PEG2000, 1,2-distearoyl-sn-glycero-3-phosphoethanolamine-N-[methoxy-poly-(ethyleneglycol)-2000]; DSPE-PEG5000, 1,2-distearoyl-sn-glycero-3-phosphoethanolamine-N-[methoxy-poly-(ethyleneglycol)-5000]; EPC, egg phosphatidylcholine; HA, hyaluronic acid; PEG, polyethylene glycol; PG, L- $\alpha$ -phosphatidylglycerol; SA, sterylamine.

## 1. Introduction

Local drug delivery is being developed instead of systemic drug delivery in ophthalmology (Ludwig, 2005; Kang-Mieler et al., 2014), rheumatology (Chevalier et al., 2010; Szabo et al., 2012) and otology (McCall et al., 2010; Staeker et al., 2013). In such applications, systemic administration induces side effects and leads to a very low amount of the drug at the target site mainly because of biological barriers and poor local vascularization. Therefore, intraocular, intraarticular and transtympanic administrations are more efficient approaches for drug delivery to the posterior segment of the eye (Kang-Mieler et al., 2014), the joint (Chevalier et al., 2010) and the inner ear (McCall et al., 2010) respectively. However, there is a need to develop local drug delivery systems suitably designed to ensure long residence times and controlled drug release to reduce the frequency of injections. Such systems also require to be easily injectable, safe and well-tolerated. In this context, the physico-chemical properties of hydrogels have sparked interest in their use for drug delivery (Hoare et al., 2008). Among the different hydrogel forming polymers, hyaluronic acid (HA) is particularly attractive. This negatively charged polysaccharide composed of D-glucuronic acid and N-acetyl-D-glucosamine is mucoadhesive, biodegradable and biocompatible (Liao et al., 2005; Girish et al., 2007). Medically, high molecular weight HA is commonly used for its viscosupplementation and anti-inflammatory properties (Lapcik et al., 1998) and as a surgical aid in ophthalmology and wound healing (Goa et al., 1994). This polymer has also by itself a therapeutic potential in the treatment of arthritis (Goa et al., 1994; Ray, 2013) and for the preservation of residual hearing during cochlear implantation (Friedland et al., 2009). Otherwise, HA hydrogels have demonstrated their potential as drug delivery systems alone (Peattie, 2012) or combined with another polymer such as poloxamer 407 (Mayol et al., 2008; Seol et al., 2013) or HPMC (Hoare et al., 2010) and with colloids such as DNA-PEI polyplexes (Lei et al., 2011) or liposomes (Lajavardi et al., 2009; Dong et al., 2013; Widjaja et al., 2014). Indeed, the addition of PEGylated liposomes containing Vasoactive Intestinal Peptide into HA gel protected this peptide from degradation and sustained its release after intraocular injection resulting in a therapeutic efficacy on inflammation in rats (Lajavardi et al., 2009). Interestingly, PEGylated liposomes increased both the viscosity and the elasticity of the gels in a concentration-dependent manner (Lajavardi et al., 2009). Considering the properties of HA reported previously, the administration of HA liposomal hydrogels is not limited to the intraocular route. Indeed, such systems have a great potential for other local routes requiring an injection. Regarding the formulation, HA liposomal gel offers further

advantages: the dispersion of liposomes in HA gel is simple to prepare and does not require the use of organic solvents. High concentration of drug could be obtained by adjusting the amount of liposomes in HA gels. Finally, the composition of the liposomes could be adapted to the physico-chemical properties of the drug. However, it appears necessary to identify the key parameters affecting the gel behavior by performing a thorough and systematic study of their rheological and syringeability properties in presence of different unloaded liposome formulations. Some studies (Bochot et al., 1998; Ruel-Gariepy et al., 2002; Boulmedarat et al., 2005; Mourtas et al., 2008) have previously evaluated the effect of liposomes on the rheological properties of hydrogels with different polymers (HA, carbopol®, poloxamer, chitosan). Various effects of liposomes were reported depending on the polymer used. Overall, the lipid concentrations were lower (1.25 to 25 mM) than those used in this study. Recently, Hurler et al. (2013) studied the effect of lipid composition (neutral, negative or positive surface charge, 2.6 mM) and liposome size on the release properties, the rheological and textural behaviors of liposomes in chitosan hydrogels but they evaluated neither the effect of PEG nor that of lipid concentration. In the present study, the effects of lipid concentration on a large range (10 to 80 mM) and liposome characteristics (neutral, positively or negatively charged, with a corona of polyethylene glycol (PEG) chains of different lengths, size) were systematically assessed related to the HA gel behavior. Besides, the interactions observed between HA and PEGylated liposomes were further investigated and compared to the interactions of HA with free PEG chains or poloxamer 407. All this knowledge will be useful in the future to adapt the formulation to the specific requirements of the foreseen final applications (injection site, appropriate viscosity, therapeutic dose needed).

## 2. Materials and methods

### 2.1. Materials

Egg phosphatidylcholine (EPC, Purity 96%) was provided by Lipoid GmbH (Ludwigshafen, Germany). Cholesterol (Chol), Egg L- $\alpha$ -phosphatidylglycerol (PG) and stearylamine (SA) were purchased from Sigma-Aldrich Co. (St. Louis, USA). 1,2-distearoyl-sn-glycero-3-phosphoethanolamine-N-[methoxy-poly-(ethyleneglycol)-2000] (DSPE-PEG2000) and

1,2-distearoyl-sn-glycero-3-phosphoethanolamine-N-[methoxy-poly-(ethyleneglycol)-5000] (DSPE-PEG5000) were obtained from Avanti Polar Lipids, inc. (Alabaster, USA). The purities of Chol, PG, SA, DSPE-PEG2000 and DSPE-PEG5000 were > 99%. Sodium

hyaluronate (HA, Mw 1.5 MDa, purity 95%) was provided by Acros Organics (New Jersey, USA). Polyethyleneglycol (PEG1500 and PEG6000, purity > 97%) were obtained from Prolabo (West Chester, USA). Poloxamer 407 (Lutrol F127<sup>®</sup>, Mw 12600 Da, purity 98%) was purchased from BASF (Ludwigshafen, Germany). All other chemicals used in the experiments were of analytical grade.

## 2.2. Preparation of liposomes

Liposomes were prepared by the thin film method (Bangham et al., 1965). Their composition and denomination are presented in **Table 1**. Lipid ratios were chosen according to the values commonly used in classical liposome formulations. Briefly, lipids dissolved in chloroform were introduced in a round bottom flask. The organic phase was evaporated under vacuum using rotary evaporation resulting in a dry lipid film. The film was hydrated with HEPES/NaCl buffer (10/145 mM, pH 7.4) to achieve a 100 mM final lipid concentration. The suspensions were subsequently extruded 10 times through 0.2 µm polycarbonate filters set in a LIPEX extruder (Whitley, Vancouver, Canada). Non-extruded liposomes were prepared as described previously avoiding the extrusion step.

**Table 1**

Denomination and composition of liposome formulations.

Denomination	Liposome composition	Lipid ratio (mole%)
Lip	EPC:Chol	65:35
Lip SA	EPC:Chol:SA	55:35:10
Lip PG	EPC:Chol:PG	55:35:10
Lip PG-5% PEG <sub>2000</sub>	EPC:Chol:PG:DSPE-PEG2000	50:35:10:5
Lip-5% PEG <sub>2000</sub>	EPC:Chol:DSPE-PEG2000	60:35:5
Lip PG-5% PEG <sub>2000</sub> <sup>a</sup>	EPC:Chol:PG:DSPE-PEG2000	50:35:10:5
Lip PG-1% PEG <sub>2000</sub>	EPC:Chol:PG:DSPE-PEG2000	54:35:10:1
Lip PG-5% PEG <sub>5000</sub>	EPC:Chol:PG:DSPE-PEG5000	50:35:10:5
Lip PG-1% PEG <sub>5000</sub>	EPC:Chol:PG:DSPE-PEG5000	54:35:10:1

<sup>a</sup> non-extruded liposomes

## 2.3. Physicochemical characterization of liposomes

The hydrodynamic diameter and the zeta potential of liposomes were determined in triplicate at 25°C using a Zetasizer Nano ZS (Malvern, Worcestershire, UK) following a 1/50 (v/v) dilution in milliQ water.

The concentration of EPC in liposomes was evaluated after extrusion through an enzymatic phospholipid assay (Biolabo SA, Maizy, France). The assay is based on the enzymatic cleavage of EPC in a quinoneimine derivative which is quantified by spectrophotometry at 500 nm using a Lambda 25 spectrophotometer (Perkin Elmer, Waltham, USA). The total amount of lipids in liposome suspensions was then calculated from EPC concentration by assuming that lipid composition was unchanged during the different liposome preparation steps. Lipid concentration was determined for each formulation prepared. Then, the liposome suspensions were diluted into HEPES/NaCl buffer to obtain the desired final lipid concentration.

#### *2.4. Gel formulation*

##### *2.4.1. Preparation of HA gels and Liposomes-HA gels*

All gels were prepared at a final HA concentration of 2.28% (w/v). For Liposomes-HA gels, HA was dissolved under magnetic stirring into liposome suspensions (7 mL) at various lipid concentrations: 10, 30, 50, 80 mM for Lip, Lip SA, Lip PG, Lip PG-5%PEG<sub>2000</sub> and Lip PG-5%PEG<sub>5000</sub>, or 10 and 80 mM for Lip-5%PEG<sub>2000</sub>, Lip PG-5%PEG<sub>2000</sub> (non-extruded), Lip PG-1%PEG<sub>2000</sub> and Lip PG-1%PEG<sub>5000</sub>. HA gels (without liposomes) were prepared as described above by replacing the liposome suspension with 7 mL HEPES/NaCl (10/145 mM) buffer, pH 7.4.

##### *2.4.2. Preparation of HA gels containing free PEG1500 or PEG6000 chains*

The appropriate amount of PEG1500 or PEG6000 was initially dissolved in HEPES/NaCl buffer, pH 7.4 (7 mL). Following complete dissolution of PEG, HA (2.28% w/v) was added under magnetic stirring which was maintained for two hours at room temperature. The final concentration of PEG1500 in HA gel was 0.6% w/v (4 mM) or 6% w/v (40 mM) and that of PEG6000 was 2.4% w/v (4 mM) or 24% w/v (40 mM).

##### *2.4.3. Preparation of HA/poloxamer gels*

Poloxamer 407 solutions were prepared by dissolving gradually the poloxamer 407 powder (20% w/v) in HEPES/NaCl buffer, pH 7.4 (7 mL) under magnetic stirring in an ice bath until a clear solution was obtained. HA/poloxamer gels were prepared by adding HA (2.28% w/v) to poloxamer 407 solution. The stirring was maintained for two hours in the ice bath.

Different batches of gels were prepared: three for Lip PG-5%PEG<sub>2000</sub>-HA gel, two for Lip SA-HA, Lip-HA and Lip PG-5%PEG<sub>5000</sub>-HA gels and one for Lip PG-HA and other HA gels

containing the other PEGylated liposomes, poloxamer or free PEG. All gels were stored at 4°C for at least 12 h prior to analysis to obtain a complete hydration of the polymers.

### *2.5. Freeze-fracture electron microscopy (FF-EM)*

HA gels and Liposomes-HA gels at 80 mM final lipid concentration (Lip, Lip SA, Lip PG, Lip PG-5%PEG<sub>2000</sub> or Lip PG-5%PEG<sub>5000</sub>) were analyzed by transmission electron microscopy after freeze-fracture. Briefly, a drop of the gel was put between two copper holders and rapidly plunged in liquid nitrogen. The sandwiches were transferred in a home-made freeze-fracture apparatus and maintained under high vacuum and at liquid nitrogen temperature. After fracturing, a thin layer of platinum (2 nm) was deposited under a 45° angle and reinforced with a 20 nm thick carbon layer at 90°. After bringing back to room temperature under a dry nitrogen stream, the replicas were extensively washed by acidic treatment and picked up on 400 mesh copper grids. The grids were observed at 200 kV in a Tecnai G2 transmission electron microscope and the images were acquired with an Eagle 2K2K CDD camera.

### *2.6. Rheological study*

All rheological measurements were carried out on a rotational rheometer ARG2 (TA instruments, New Castle, USA). The geometry was an aluminum cone/plate (diameter 4 cm, angle 1° and cone truncation 28 µm) equipped with a solvent trap. TRIOS software was used for data analysis.

#### *2.6.1. Flow measurements*

Flow properties of the gels mentioned previously were determined at 19°C and 37°C by a stress sweep. After a 2-minute equilibration time, the shear stress was increased gradually from 0 to 300 Pa (upward curve). Then, the shear stress was maintained at 300 Pa for 2 minutes (plateau) and subsequently decreased gradually from 300 to 0 Pa (downward curve). Measurements were performed in triplicate on each gel batch under steady state conditions. The viscosity curves were fitted according to the Cross equation (Cross, 1968) (Eq. 1):

$$\eta = \eta_\infty + \frac{\eta_0 - \eta_\infty}{1 + (C \dot{\gamma})^n} \quad (1)$$

$\eta$  represents the apparent viscosity at a given shear rate (Pa.s),  $\dot{\gamma}$  is the shear rate ( $s^{-1}$ ),  $\eta_0$  is the zero-shear rate viscosity (Pa.s),  $\eta_\infty$  is the infinite-shear rate viscosity (Pa.s), C is a multiplicative parameter (s) and n is a dimensionless exponent.

### 2.6.2. Oscillatory measurements

Viscoelastic properties of the gels were evaluated at 37°C under a stress value of 10 Pa which belonged to the viscoelastic linear regime, where the samples did not undergo irreversible structural modifications. A frequency sweep was performed in a frequency range from 0.01 to 10 Hz. The elastic (or storage) modulus  $G'$  (Eq. 2) as well as the viscous (or loss) modulus  $G''$  (Eq. 3) were measured as a function of frequency. When an oscillatory shear stress is applied to the gel,  $G'$  is related to the elasticity or the energy stored and recovered in the material per deformation cycle, whereas  $G''$  describes the viscous character or the energy dissipated during the cycle.

$$G' = \frac{\tau_0}{\gamma_0} \cos \delta \quad (2)$$

$$G'' = \frac{\tau_0}{\gamma_0} \sin \delta \quad (3)$$

$$\tan \delta = \frac{G''}{G'} \quad (4)$$

$\tau_0$  and  $\gamma_0$  are the maximal amplitudes of the stress and the strain respectively.  $\delta$ , the phase angle varies between 0° and 45° ( $\tan \delta < 1$ ,  $G' > G''$ ) for a rather elastic material and between 45° and 90° ( $\tan \delta > 1$ ,  $G'' > G'$ ) for a predominantly viscous material (Eq. 4). Measurements were performed in triplicate on each gel batch.

### 2.7. Behavior of HA gels and Liposomes-HA gels over time and after injection

HA gels and Liposomes-HA gels containing 80 mM neutral (Lip) or PEGylated liposomes (Lip PG-5% PEG<sub>2000</sub>) were stored at 4°C for 3 months. Their behavior over time or after injection through a 29G needle (see section 2.8) was followed by macroscopic observation and by measuring their flow properties at 37°C.

### 2.8. Syringeability tests

The syringeability is the force required for the injection of a formulation at a given injection rate *via* a needle of predetermined gauge and length. Syringeability of the gels was studied using a home-made device described previously by Burckbuchler et al. (2010). This device was coupled to a texture analyzer TAXT2 (Stable MicroSystems, Godalming, UK) in compression mode which was equipped with a force transducer calibrated with a 30 kg sensor. The principle consists in applying a given displacement rate to the plunger of the syringe filled with the gel and in measuring the resulting injection force.

HA gels and 10, 30, 50 or 80 mM Liposomes-HA gels were filled into 1mL Plastipak syringes and stored at 4°C for 12h. They were kept at room temperature at least 10 minutes before measurement. The syringes were equiped with 27G (diameter,  $d = 0.19$  mm and length,  $l = 20$  mm, Terumo), 29G ( $d = 0.16$  mm;  $l = 88$  mm, B.Braun) or 30G ( $d = 0.14$  mm;  $l = 13$  mm, BD Microlance) needles. The displacement rate of the plunger was 0.5 mm/s corresponding to a flow rate of 0.4 mL/min, which is similar to a manual injection rate (Burckbuchler et al., 2010). All measurements were performed in triplicate at room temperature on each gel batch. The feasability of the manual injection of all formulations with the different needles was also checked systematically.

### 3. Results

#### 3.1. Physicochemical characterization of liposomes

Liposome formulations were rather monodisperse (polydispersity index, PdI < 0.2) with a mean diameter between 136 and 178 nm except for non-extruded liposomes which had a diameter of 1089 nm (**Table 2**). Zeta potential values were almost neutral (-1 mV) for Lip, positive (+54 mV) for Lip SA and negative (between -19 and -62 mV) for the formulations containing either PG or DSPE-PEG or both. The final lipid concentration after extrusion varied between 90 and 95 mM for all the formulations (**Table 2**).

**Table 2**

Physicochemical characterization (hydrodynamic diameter, PdI, zeta potential, final lipid concentration after extrusion) of liposome formulations.

Denomination	Diameter (nm)	PdI	$\zeta$ -Potential (mV)	[lipids] (mM)
Lip	178 ± 64	0.16	-1 ± 5	90
Lip SA	150 ± 56	0.09	+54 ± 9	94
Lip PG	146 ± 62	0.10	-62 ± 8	90
Lip PG-5%PEG <sub>2000</sub>	136 ± 47	0.08	-29 ± 8	93
Lip-5%PEG <sub>2000</sub>	148 ± 46	0.08	-20 ± 7	93
Lip PG-5%PEG <sub>2000</sub> <sup>a</sup>	1089 ± 270	0.20	-49 ± 8	95
Lip PG-1%PEG <sub>2000</sub>	148 ± 54	0.08	-47 ± 9	94
Lip PG-5%PEG <sub>5000</sub>	140 ± 47	0.08	-19 ± 11	94
Lip PG-1%PEG <sub>5000</sub>	142 ± 49	0.08	-31 ± 12	94

<sup>a</sup> non-extruded liposomes

### 3.2. Microscopic aspect of HA gels and Liposomes-HA gels

Transmission electron microscopy images showed a high number of vesicle-like shapes only in HA gels containing liposomes (**Fig. 1B, C, D, E and F**) and some of them were non spherical. Their size was comparable to that of the liposomes prepared.

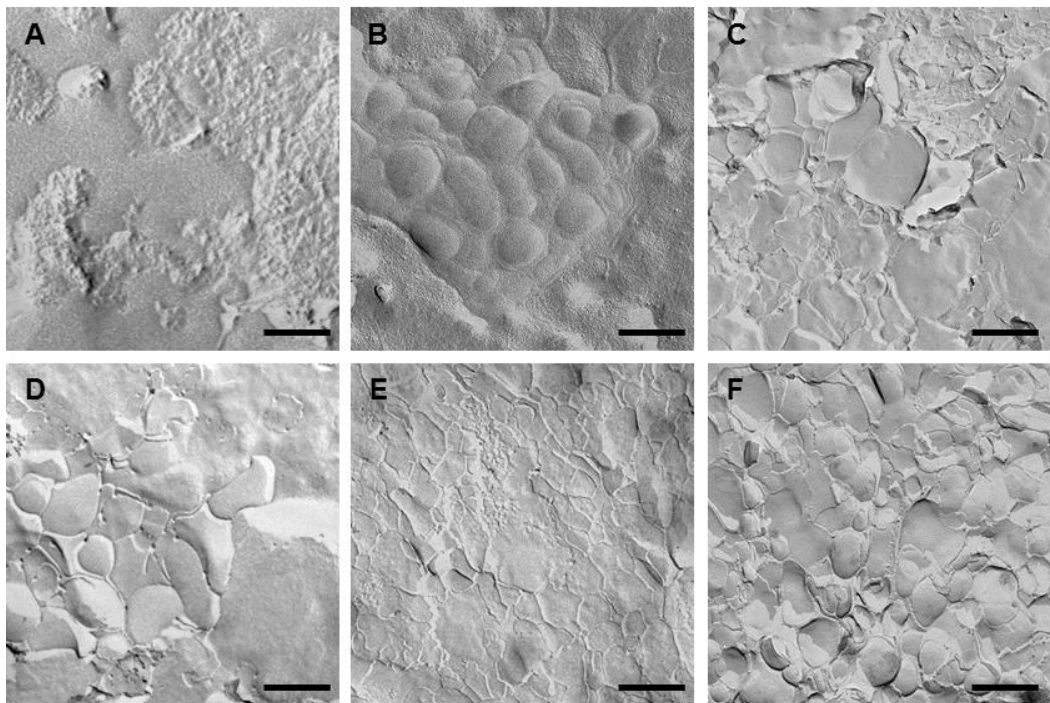


**Fig. 1.** Transmission electron micrographs of freeze-fractured HA gels (A) and 80 mM Liposomes-HA gels: Lip (B), Lip SA (C), Lip PG (D), Lip PG-5%PEG<sub>2000</sub> (E) and Lip PG-5%PEG<sub>5000</sub> (F). Scale bar = 200 nm.

### 3.3. Rheological behavior of HA gels

HA gel presented a shear-thinning behavior (**Fig. 2A**). Rheograms were fitted with the Cross model with good correlation coefficient values ( $R^2 > 0.998$ ). A constant viscosity was obtained for very low shear rates (zero-shear rate viscosity, determined with the Cross model,  $\eta_0 = 120 \pm 6$  Pa.s at 19°C and  $\eta_0 = 75 \pm 5$  Pa.s at 37°C), then, the viscosity decreased with shear rate and with temperature. HA gel also displayed a non-thixotropic behavior shown by the overlay of downward and upward curves (**Fig. 2A**). In addition, HA gel presented a viscoelastic behavior at 37°C (**Fig. 2B**). G' and G'' frequency sweep curves exhibited a crossover point at 0.90 Hz. For this frequency,  $G' = G'' = 74$  Pa. Below this frequency, the gel had mainly a viscous behavior, whereas above this frequency, the gel had a predominant

elastic character. For example, at a frequency of 1 Hz, this system behaved as an elastic gel ( $G' = 78 \pm 7$  Pa and  $\tan \delta = 0.92 \pm 0.02$ ).

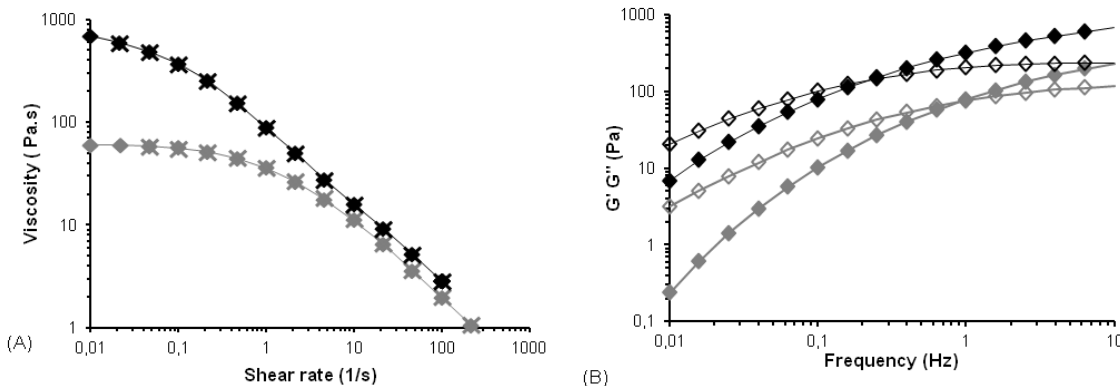


**Fig. 2.** Rheological behavior of HA gels and Liposomes-HA gels. (A) Viscosity as a function of shear rate at 37°C: HA gel, upward curve (◆) and downward curve (×). 80 mM Lip PG-5%PEG<sub>2000</sub>-HA gel, upward curve (◆) and downward curve (×). (B) Elastic ( $G'$ ) and viscous ( $G''$ ) moduli as a function of frequency at 37°C: (◆)  $G'$  HA gel, (◇)  $G''$  HA gel, (◆)  $G'$  80 mM Lip PG-5%PEG<sub>2000</sub>-HA gel, (◇)  $G''$  80 mM Lip PG-5%PEG<sub>2000</sub>-HA gel.

### 3.4. Rheological behavior of Liposomes-HA gels

Upon addition of liposomes, the shear-thinning, the non-thixotropic and the viscoelastic behaviors of HA gels were preserved. This observation was done for all kinds of Liposomes-HA gels tested and Lip PG-5%PEG<sub>2000</sub>-HA gel is given as an example in **Fig. 2**. However, the presence of liposomes provoked a pronounced increase of the zero-shear rate viscosity ( $\eta_0 = 1045 \pm 50$  Pa.s at 19°C and  $\eta_0 = 720 \pm 85$  Pa.s at 37°C) (**Fig. 2A**); overall, the viscosity was higher for Liposomes-HA gels than for HA gels. Liposomes also increased  $G'$  and  $G''$  values, and this was associated to a decrease of the frequency at the crossover point ( $G' = G''$  and  $\tan \delta = 1$ ), from 0.90 Hz to 0.2 Hz in this example (**Fig. 2B**). Liposomes-HA gels behaved predominately like elastic materials on a larger frequency range than HA gels.

#### 3.4.1. Effect of the concentration and composition of liposomes

HA gels containing the different liposome formulations were compared based on the zero-shear rate viscosity (for viscosity) and based on  $G'$  and  $\tan \delta$  at 1 Hz (for elasticity). Also, these values were normalized to the HA gel values according to the following equations (Eqs.

5, 6, 7) to determine a relative increase in the viscosity and the elasticity of Liposomes-HA gels:

$$\text{Normalized } \eta_0 = \frac{\eta_0(\text{sample}) - \eta_0(\text{HA})}{\eta_0(\text{HA})} \quad (5)$$

$$\text{Normalized } G' = \frac{G'(\text{sample}) - G'(\text{HA})}{G'(\text{HA})} \quad (6)$$

$$\text{Normalized } \tan \delta = \frac{\tan \delta(\text{sample}) - \tan \delta(\text{HA})}{\tan \delta(\text{HA})} \quad (7)$$

Whatever the composition, liposomes at low lipid concentration (10 mM) within HA gels had only few impact on the viscosity. However, higher concentrations (from 30 to 80 mM) dramatically increased the viscosity of the gels, except for Lip-HA gels for which only a slight viscosity increase was observed starting from 50 mM (**Fig. 3A**). An enhanced elastic behavior in the presence of liposomes was also observed in a concentration-dependent manner (**Fig. 3B** and **3C**). It appeared that liposome composition had a significant impact on gel properties. Indeed, the presence of a charge or PEG chains on the surface of liposomes led to a higher increase in viscosity and elasticity compared to neutral liposomes (Lip). Cationic liposomes (Lip SA) had less effect than anionic ones (Lip PG). The most significant variations were obtained with PEGylated anionic liposomes (Lip PG-5% PEG<sub>5000</sub> and Lip PG-5% PEG<sub>2000</sub>).

The addition of liposomes in the gel shifted the G' and G'' versus frequency curves towards lower frequencies and higher moduli compared to HA gel (**Fig. 4**). Taking HA gel as a reference, shift factors were calculated based on the crossover point (G' = G'') for the different liposomes-HA gel formulations (at 10, 30, 50, 80 mM lipids). This allowed to obtain a master curve with all lipid concentrations and for the different liposome formulations. The master curve obtained for Lip PG-5%PEG<sub>2000</sub>-HA gel as well as the corresponding shift factors are displayed as an example in **Fig. 4**.

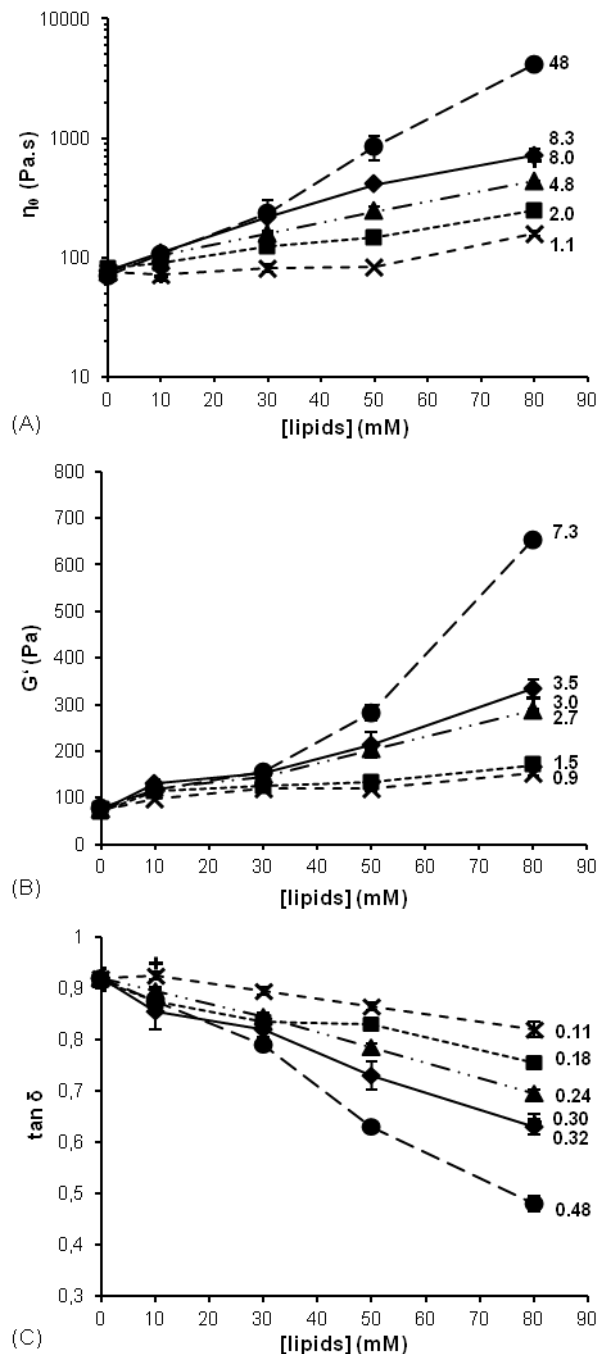


**Fig. 3.** Influence of liposome composition and lipid concentration on the rheological properties of Liposomes-HA gels: (x) Lip, (■) Lip SA, (▲) Lip PG, (+) Lip-5%PEG<sub>2000</sub>, (◆) Lip PG-5%PEG<sub>2000</sub>, (●) Lip PG-5%PEG<sub>5000</sub>. Zero-shear rate viscosity (A), elastic modulus  $G'$  (B) and  $\tan \delta$  (C) measured at 37°C. Numbers on the right of the curves refer to normalized zero-shear rate viscosity (A), elastic modulus  $G'$  (B) and  $\tan \delta$  (C) values at 80 mM lipid concentration.

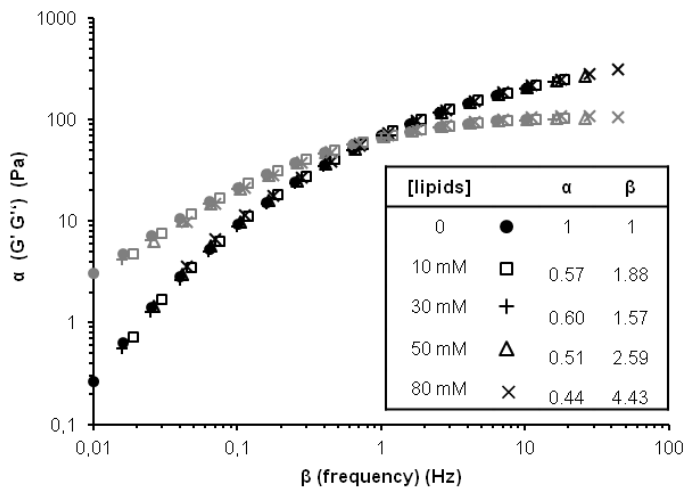


**Fig. 4.** Master curve of rescaled  $G'$  (black) and  $G''$  (grey) versus rescaled frequency for Lip PG-5%PEG<sub>2000</sub>-HA gel (10, 30, 50, 80 mM lipids). HA gel was taken as a reference.  $\alpha$ :  $G'$  and  $G''$  shift factor.  $\beta$ : frequency shift factor. Data are based on oscillatory measurements at 37°C.

#### 3.4.2. Effect of PEG chain length and concentration

Two different PEG chain lengths (DSPE-PEG2000 and DSPE-PEG5000) were incorporated in liposome formulations at 1 or 5 mole%. The viscosity and the elasticity of the gels were significantly increased when the PEG chain was longer (Fig. 3). The effect on the viscosity was more pronounced when PEG concentration was higher (Fig. 5).

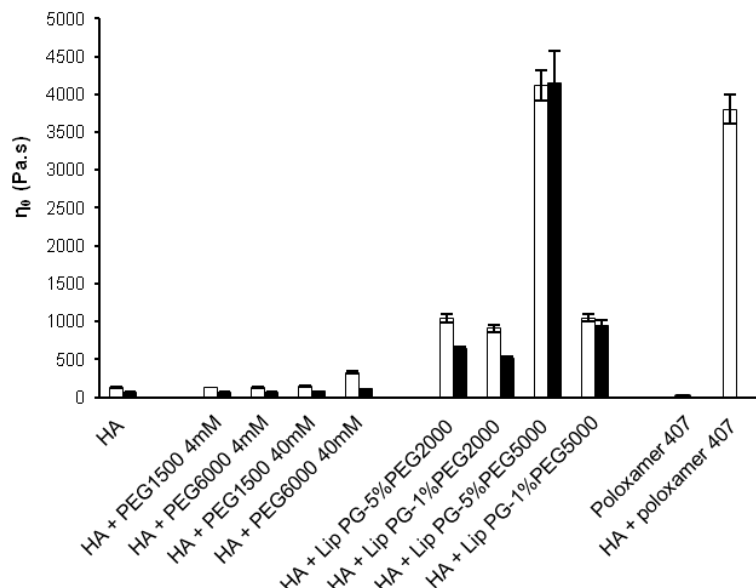


**Fig. 5.** Zero-shear rate viscosity measurements of HA gels containing 80 mM PEGylated liposomes (Lip PG-5%PEG<sub>2000</sub>, Lip PG-5%PEG<sub>5000</sub>), free PEG (PEG1500, PEG6000) or poloxamer 407 20% (w/v) at 19°C (white bars) and 37°C (black bars).

### 3.4.3. Effect of PEGylated liposomes, free PEG and poloxamer 407 on the viscosity of HA gels

HA gels containing 80 mM PEGylated liposomes were compared to those containing PEG1500 or PEG6000 at two different concentrations: 4 mM which corresponds to PEG content in 80 mM PEGylated liposomes (5 mole%) or 40 mM which is 10-fold higher than PEG content in those liposomes. Interestingly, the addition of free PEG chains into HA gels had no significant effects on the viscosity of the gels, compared to the addition of PEGylated liposomes into HA gels (**Fig. 5**). Overall, the viscosity of the gels at 19°C was higher than their viscosity at 37°C except for Lip PG-5%PEG<sub>5000</sub> and Lip PG-1%PEG<sub>5000</sub>-HA gels where the temperature had no effect on the viscosity.

Moreover, PEGylated liposomes-HA gels were compared with a HA/poloxamer 407 blend. Poloxamer 407 at 20% (w/v) had a gelation temperature around 27°C determined from rheological experiments (results not shown). At 37°C, the rheological properties of the HA/poloxamer 407 gels were governed by poloxamer 407. Thus, to avoid the gelation of poloxamer 407, the viscosity of all HA gels containing the different PEG systems were compared at 19°C (**Fig. 5**). At this temperature, HA/poloxamer 407 system led to a 29-fold increased viscosity of HA gel which is quite similar to the 31-fold increase in the viscosity obtained with 80 mM Lip PG-5% PEG<sub>5000</sub>-HA gel.

### 3.4.4. Effect of liposome size

The impact of liposome size on gel properties was studied using non-extruded liposomes ( $1089 \pm 270$  nm) which were compared to extruded ones ( $136 \pm 47$  nm). At a lipid concentration of 80 mM, the viscosity and the elasticity were significantly lower with the largest liposomes, whereas almost no difference was observed at 10 mM (**Fig. 6**).

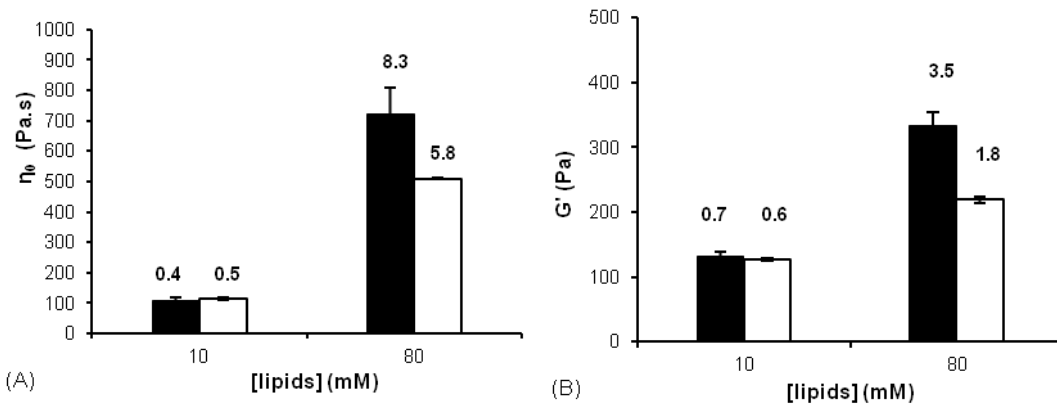


**Fig. 6.** Influence of liposome size on the viscosity and the elasticity of Lip PG-5%PEG<sub>2000</sub>-HA gels (10 and 80 mM), non-extruded (white bars) or extruded (black bars) liposomes. Zero-shear rate viscosity (A) and elastic modulus G' (B) measured at 37°C. Numbers refer to normalized zero-shear rate viscosity (A) and elastic modulus G' (B).

#### 3.4.5. Behavior of HA gels and Liposomes-HA gels over time and after injection

There was no modification of the macroscopic aspect of the gels over 3-month storage at 4°C and after injection through a 29G needle. The gels exhibited a colorless (HA gels) or white (Liposomes-HA gels) homogeneous aspect. There was also no significant modification of the rheograms (not shown) and the zero-shear rate viscosity after a 3-month storage or after injection (**Fig. 7**).

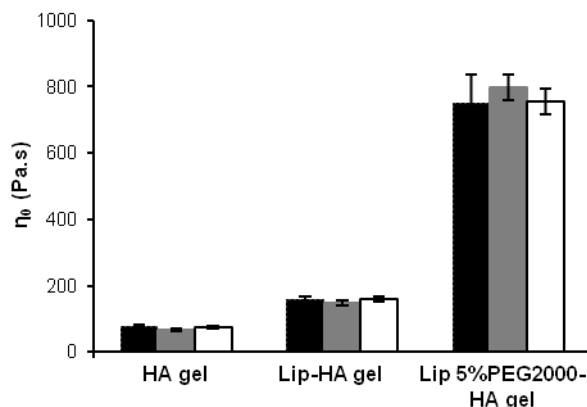


**Fig. 7.** Zero-shear rate viscosity measured at 37°C for HA gel, 80mM Lip-HA gel and 80mM Lip PG-5%PEG<sub>2000</sub>-HA gel one day after preparation (black bars), after a 3-month storage at 4°C (grey bars), after syringeability test at 19°C using 29G needle (white bars). No significant differences for each gel (One-way ANOVA, p > 0.05).

### 3.5. Syringeability tests

Syringeability experiments were first performed at 19°C on HA gels using three different needles to evaluate the effect of needle characteristics (diameter and length) on the injection force (**Fig. 8A**). The injection force measured with the three needles was lower than 10 N. The highest injection forces were found for the thinnest needles. On the other hand, the injection force was higher when the needle was longer even if the diameter of this needle was larger (29G compared to 30G).

Since 29G needles exhibited the most difficult injection conditions, this needle type was chosen to assess the syringeability of Liposomes-HA gels. The addition of liposomes into HA gel had a moderate impact on the injection forces which varied between 8 and 15 N (**Fig. 8B**). The increase in liposome concentration led to more important injection forces. Moreover, as in the rheological study, PEGylated liposomes-HA gels at 80 mM displayed the highest injection forces. Nevertheless, this effect is significantly lower than the one observed in the rheological study on the zero-shear rate viscosity and on the elasticity.

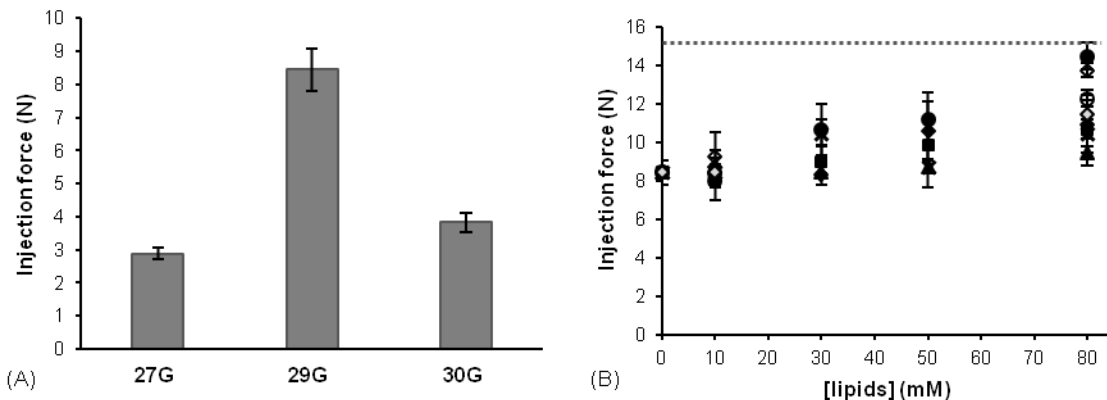


**Fig. 8.** Syringeability of HA gels and Liposomes-HA gels performed at room temperature (19°C). (A) Maximal injection force measured for HA gels using three different needles (diameter; length): 27G (0.19; 20 mm), 29G (0.16; 88 mm), 30G (0.14; 13 mm). (B) Variations of the injection force as a function of lipid concentration using 29G needle for Liposomes-HA gels: (×) Lip, (■) Lip SA, (▲) Lip PG, (+) Lip-5%PEG<sub>2000</sub>, (◆) Lip PG-5%PEG<sub>2000</sub>, (◆) non-extruded Lip PG-5%PEG<sub>2000</sub>, (◇) Lip PG-1%PEG<sub>2000</sub>, (●) Lip PG-5%PEG<sub>5000</sub>, (○) Lip PG-1%PEG<sub>5000</sub>.

### 3. Discussion

The aim of this study was to evaluate the rheological and syringeability properties of hyaluronic acid gels containing different formulations of unloaded liposomes to design a flexible drug delivery system intended for local injections. In this study, the concentration of HA (2.28% w/v) was the same for all the gels tested. This concentration provides consistent gels with a viscosity comparable to that of a commercial HA gel used in ophthalmic surgery (Provisc®) (Lajavardi et al., 2009). In the present study, the concentration and the composition of liposomes were varied to identify the key parameters of liposome formulation that could influence HA gel properties. Therefore, depending on the physicochemical properties of the drug to be encapsulated, liposome composition and concentration could be adapted according to the drug loading and the therapeutic dose needed. On the other hand, regarding the interactions between liposomes and HA, which is an anionic polyelectrolyte, the composition and the concentration of liposomes could also be adjusted to modulate the rheological properties of the gel and thus, the release profile of the drug. Liposome size was fixed (around 150 nm) for all formulations to specifically assess liposome concentration and composition effects. Besides, for one formulation and at a similar lipid concentration, the size of liposomes was increased to evaluate the impact of the surface area.

Despite their high viscosity at rest, Liposomes-HA gels were easily injected both manually and using our home-made device. 30 N is considered as the maximal force for a manual injection (Burckbuchler et al., 2010). Since injection forces varied between a quarter and a half of this value, whatever the needle used (**Fig. 8**), all gels are suitable for injection by different routes of administration (Adler, 2012; Reeff et al., 2013). 29G needles (88 mm) were the most challenging needles. This kind of thin and long needles are typically used for the administration of medicines to the inner ear by transtympanic injection both in human and animal (Wang et al., 2011). Generally, smaller or larger needles are required for other applications such as intraarticular injection (23G, 20 mm needles (Reeff et al., 2013) or intravitreal injection (30G, 13 mm (Lajavardi et al., 2009) or 27G, 20 mm needles (Anayol et al., 2014).

Syringeability results can be explained by the shear-thinning behavior of HA (Krause et al., 2001; Falcone et al., 2006) (**Fig. 2**). The viscosity decrease observed when increasing shear rate is due to a temporary destructuration of the polymer network under shear and to the alignment of HA molecules in the flow direction. Thus, when the gel flows through the needle, it undergoes a very high shear rate resulting in a low viscosity that allows the gel to be

injected with a reasonable injection force. The shear rate in the 29G needle (estimated between 15000 and 25000 s<sup>-1</sup> using Poiseuille or Mooney-Rabinowitsch equations (Rabinowitsch, 1929) exceeds the technical limit specified for the rheometer and the geometry used (6000 s<sup>-1</sup>). Consequently, it was not possible to measure experimentally the viscosity under such shear rates. Furthermore, there was no correlation between the viscosity under high shear (calculated from Cross equation using the estimated shear rates above) and the measured injection forces. Thus, the injectability of our gels cannot be predicted from the rheological data. This highlights the need to perform both rheological and syringability studies to assess the gels behavior during injection at 19°C and after injection (*i.e.* at rest at 37°C).

Liposomes-HA gels were able to recover their initial viscosity after injection (**Fig. 7**) indicating that there was no irreversible destructuration of the gels during injection. These results can be explained by the non-thixotropic property (**Fig. 2A**), also called self-healing property of HA (Nejadnik et al., 2014). HA rheological properties are thus very advantageous for local drug delivery. Indeed, the shear-thinning behavior allows an easy injectability of the gel, while the self-healing property provides a fast recovery of the high initial viscosity at the injection site. Moreover, the high viscosity and the elasticity of the gel combined with the adhesive properties of HA (Girish et al., 2007) should favor an increased residence time and a sustained release of the drug.

Interestingly, liposomes increased the viscosity and reinforced the elasticity of HA gels depending on the lipid concentration. These results are in agreement with those previously published by our group using PEGylated liposomes (EPC:Chol:PG:DSPE-PEG2000 50:35:10:5) (Lajavardi et al., 2009). In the present study, we demonstrate that the composition and the size of liposomes are also controlling the rheological properties of HA gels due to interactions between HA chains and liposome surface. The increase in lipid concentration enhances the number of liposomes and therefore the surface area between liposomes and HA chains as well as their interactions. Conversely, an increase in the size of liposomes decreases the surface area and thus the interactions. The effect of liposome size on hydrogel properties was previously reported by Hurler et al. (2013) had shown that liposomes with a size below 200 nm and composed of PC, PC:PG or PC:SA, enhanced the textural characteristics of chitosan hydrogels compared to larger liposomes (*i.e.* > 1 μm). Therefore, lipid concentration and liposome size can be used to adapt the surface developed between HA chains and liposomes and subsequently, to modulate their interactions.

These interactions could be of different nature depending on liposome composition. Phosphatidylcholine (EPC) contained in liposomes should interact with HA by hydrophobic interactions (Ghosh et al., 1994; Taglienti et al., 2006). EPC could bind to HA by competing for the hydrophobic regions along the HA chain (patches of –CH groups over three neighboring sugar units (Heatley et al., 1988) which are normally responsible for the inter- and intra-chain interactions between HA molecules resulting in the network structure of HA (Scott et al., 1991). EPC and HA could also interact through hydrogen bounds as described by Ionov et al. (2004). Interaction between high molecular weight HA (0.3% w/v) and liposomes composed of Di-palmitoyl phosphatidylcholine (DPPC) (0.1 or 1% w/v) was reported by Crescenzi et al. (2004) that showed the destructuration of the vesicles and the formation of a supramolecular complex (aggregates, cylinders, or lipidic sheets) between HA and DPPC resulting in a viscosity decrease due to the collapse of HA chains (Pasquali-Ronchetti et al., 1997; Crescenzi et al., 2004). In the present study, we obtained different results from Crescenzi et al. (2004). This might be explained by the presence of 35 mole% cholesterol (Chol) in all our liposome formulations which confers stiffness to the lipid bilayer and decreases its permeability (Lee et al., 2005). In this work, vesicles were visualized by FF-EM with a size comparable to that of the liposomes prepared (**Fig. 1** and **Table 2**). The non-spherical shape observed for some liposomes was due to the high concentration of liposomes (80 mM of lipids) in the gels leading to their close-packing and deformation. Any significant change in the size or the number of liposomes during time (fusion of vesicles or degradation) should impact the viscosity of Liposomes-HA gels. On the contrary, the viscosity remained stable over time, which confirms the stability of liposomes in HA gels. These results are in good agreement with those of Mourtas et al. (2008) who have shown the integrity of liposomes containing EPC and Chol dispersed within HA gel. Hydrophobic interactions and hydrogen bounds are likely to take place especially with the neutral liposomes (Lip, EPC:Chol) but probably for all the other formulations tested in this study in addition to specific interactions that may occur with charged and/or PEGylated liposomes.

Since HA is an anionic polyelectrolyte, the interactions with positively or negatively charged liposomes could be electrostatic attractions or repulsions, respectively, with the carboxylate groups of HA molecule (Taglienti et al., 2006; Quemeneur et al., 2008). The addition of anionic liposomes (Lip PG) resulted in a higher viscosity of the gels compared to that of cationic ones (Lip SA). The electrostatic repulsions may modify the HA molecule conformation resulting in a more stretched and expended HA network. Another hypothesis

could be a micro-phase separation between HA chains and liposomes leading to an increased local concentration of HA in some regions. Similar interactions between liposomes and charged polymers were described in the literature. Indeed, attractive interactions between positively charged liposomes and Carbopol® 974P NF (anionic polymer) increased the gel viscosity in a concentration-dependent manner (Boulmedarat et al., 2005), while, anionic liposomes reduced the gelation time and the elasticity of chitosan thermo-sensitive gel (cationic polymer) (Ruel-Gariepy et al., 2002). Hurler et al. (2013) demonstrated that both positively and negatively charged liposomes enhanced the hardness, cohesiveness and adhesiveness of chitosan hydrogels compared to neutral liposomes. Apparently, the impact of charged liposomes on rheological properties of polyelectrolytes depends on both electrostatic interactions between the two components and their physicochemical properties. In parallel, we studied the effect of the ionic strength on HA gel properties using liposomes prepared in milliQ water. Surprisingly, the ionic strength of the preparation medium had no effect on the viscosity of HA gels containing charged liposomes while it affected the viscosity of HA gel without liposomes (data not shown). It can be assumed that, in the buffer, the ions partially shielded the negative charges of HA leading to a more contracted conformation of the polymer (Dobrynin et al., 1995). It resulted in a reduced viscosity of HA in buffer compared to its viscosity in water. In the presence of liposomes, the conformation of polymer chains seems to be mostly governed by the interactions with liposome surface rather than by the ions present in the aqueous medium.

The most important effect on the rheological properties of HA was observed with PEGylated liposomes. Since the increase in the viscosity and the elasticity depends on both the concentration and the length of the PEG chain at the surface of the liposomes, PEGylated liposomes are likely to interact with HA by steric repulsions between the two polymers (PEG and HA). These repulsions may result in a more expanded HA network or in an increased local concentration of HA by regions as proposed for anionic liposomes. In order to dissociate the effect of the negative charge from that of PEG itself, Lip PG-5%PEG2000 was compared to Lip-5%PEG2000 (**Fig. 3**). Viscosity, G' and tan δ values at 80 mM are almost the same for these two formulations, which means that the PEG effect is predominant. Interestingly, the addition of free PEG molecules had no effect on HA gel viscosity even at high concentration of PEG (**Fig. 5**). However, mixing poloxamer 407 with HA led to a viscosity increase similar to that obtained with PEGylated liposomes. Poloxamer 407 is a triblock copolymer composed of a central hydrophobic chain and two hydrophilic side chains (PEG). When the

concentration of poloxamer 407 is higher than 15%, the monomers assemble to form micelles with a diameter around 20 nm (Dumortier et al., 2006) (much smaller than liposomes). As PEGylated liposomes, they are colloidal objects with a hydrophilic corona composed of oxyethylene groups. These results suggest that the interactions with HA entail enhanced rheological properties only in the presence of colloidal objects such as liposomes or micelles.

Depending on the interactions (hydrophobic interactions, hydrogen bounds, electrostatic repulsions or attractions, steric repulsions), liposomes provoke a specific reorganization of HA network, resulting in a stronger 3D structure of the gel. This structure is stable over time at a 2.28% HA concentration (**Fig. 7**). However, the viscosity increase in the presence of liposomes occurs from a 30 mM lipid concentration (**Fig. 3**). This means that at low lipid concentration (low number of liposomes), these interactions are not significant enough to modify the organization of HA network. In addition, the master curve (**Fig. 4**) obtained for the different liposome formulations and at different lipid concentrations, suggests that HA controls the rheological behavior of the liposomal gels and that liposomes slow down only the dynamic of the system. This observation might reinforce our hypothesis concerning the micro-phase separation between HA chains and liposomes leading to an apparent increase of local HA concentration.

Since the interactions between HA and liposomes are non-covalent, liposome effect could be assimilated to a physical reversible crosslinking of HA gel (Hoare et al., 2008; Nejadnik et al., 2014). Interestingly, G' values obtained with HA gels containing 80 mM Lip PG-5%PEG5000 (G' around 650 Pa) are similar to those reported for the chemically crosslinked injectable HA gels used as dermal fillers such as Restylane® and Perlane®. These gels are lightly crosslinked but highly structured to provide the best resistance to deformation (G' between 600 and 700 Pa, initial HA molecular weight around 6 kDa and concentration around 2% w/v) (Kablik et al., 2009). Therefore, PEGylated liposomes-HA gels could be an interesting alternative to the soft chemically crosslinked HA gels to obtain biocompatible and biodegradable systems, with similar viscoelasticity and good mechanical properties, while avoiding the toxicity related to residual crosslinking agents and proinflammatory low molecular weight HA (Noble, 2002).

#### 4. Conclusion

This study provides a better understanding of the effect of liposomes on HA gel behaviors. It also highlights the complementarity of rheological and syringeability studies to fully assess the *in-use* properties of such formulations during and post injection. The shear-thinning behavior of HA liposomal gels allowed suitable injectability whatever the needles tested. In addition, the viscoelasticity and the self-healing property of these gels should favor a fast immobilization and a long residence time after injection. We demonstrated that liposome composition and size as well as lipid concentration are key parameters governing Liposomes-HA gel behavior. Lipid vesicle integrity is preserved in HA gels which should favor a sustained release of encapsulated drugs. The reinforcement of the 3D structure of the formulations strongly depends on interactions between liposomes and HA chains. Further physico-chemical investigations are required to fully elucidate the structure of liposomes-HA gels. Finally, this work evidences that HA liposomal gels can be considered as a safe and flexible formulation platform for a wide range of applications in the field of local drug delivery. Further experiments are ongoing for the evaluation of HA gel with PEGylated liposomes encapsulating dexamethasone phosphate for transtympanic injection.

#### Acknowledgments

Naila El Kechai acknowledges the Ministère de l'Education Nationale, de l'Enseignement Supérieur et de la Recherche for her PhD grant. Authors gratefully thank Marc Schmutz (PHI) from Institut Charles Sadron, Strasbourg University, for freeze-fracture transmission electron microscopy experiments, Jean-Jacques Vachon for the design of the syringeability device, Giovanni Tonelli and Erica Leite-Delquignies for preliminary data and one of the reviewers for his/her valuable suggestion to look for a master curve.

## References

- Adler, M., 2012. INJECTABLES-Challenges in the Development of Pre-filled Syringes for Biologics from a Formulation Scientist's Point of View. American Pharmaceutical Review. 15, 96.
- Anayol, M.A., Toklu, Y., Kamberoglu, E.A., Raza, S., Arifoglu, H.B., Simavli, H., Altintas, A.G., Simsek, S., 2014. Short-term effects of intravitreal triamcinolone acetonide injection on ocular blood flow evaluated with color Doppler ultrasonography. Int J Ophthalmol. 7, 811-815.
- Bangham, A.D., Standish, M.M., Watkins, J.C., 1965. Diffusion of univalent ions across the lamellae of swollen phospholipids. J Mol Biol. 13, 238-252.
- Bochot, A., Fattal, E., Gulik, A., Couarrazé, G., Couvreur, P., 1998. Liposomes dispersed within a thermosensitive gel: a new dosage form for ocular delivery of oligonucleotides. Pharm Res. 15, 1364-1369.
- Boulmedarat, L., Piel, G., Bochot, A., Lesieur, S., Delattre, L., Fattal, E., 2005. Cyclodextrin-mediated drug release from liposomes dispersed within a bioadhesive gel. Pharm Res. 22, 962-971.
- Burckbuchler, V., Mekhloufi, G., Giteau, A.P., Grossiord, J.L., Huille, S., Agnely, F., 2010. Rheological and syringeability properties of highly concentrated human polyclonal immunoglobulin solutions. Eur J Pharm Biopharm. 76, 351-356.
- Chevalier, X., Jerosch, J., Goupille, P., van Dijk, N., Luyten, F.P., Scott, D.L., Bailleul, F., Pavelka, K., 2010. Single, intra-articular treatment with 6 ml hylan G-F 20 in patients with symptomatic primary osteoarthritis of the knee: a randomised, multicentre, double-blind, placebo controlled trial. Ann Rheum Dis. 69, 113-119.
- Crescenzi, V., Taglienti, A., Pasquali-Ronchetti, I., 2004. Supramolecular structures prevailing in aqueous hyaluronic acid and phospholipid vesicles mixtures: an electron microscopy and rheometric study. Colloids Surf., A. 245, 133-135.
- Cross, M.M., 1968. Polymer Systems: Deformation and Flow; Wetton, R.E. and Whorlow, R.W., Eds.; Macmillan: London, p. 263.
- Dobrynin, A.V., Colby, R.H., Rubinstein, M.R., 1995. Scaling Theory of Polyelectrolyte Solutions. Macromolecules. 28, 1859-1871.
- Dong, J., Jiang, D., Wang, Z., Wu, G., Miao, L., Huang, L., 2013. Intra-articular delivery of liposomal celecoxib-hyaluronate combination for the treatment of osteoarthritis in rabbit model. Int J Pharm. 441, 285-290.
- Dumortier, G., Grossiord, J.L., Agnely, F., Chaumeil, J.C., 2006. A review of poloxamer 407 pharmaceutical and pharmacological characteristics. Pharm Res. 23, 2709-2728.
- Falcone, S.J., Palmeri, D.M., Berg, R.A., 2006. Rheological and cohesive properties of hyaluronic acid. J Biomed Mater Res A. 76, 721-728.
- Friedland, D.R., Runge-Samuelson, C., 2009. Soft cochlear implantation: rationale for the surgical approach. Trends Amplif. 13, 124-138.

- Ghosh, P., Hutadilok, N., Adam, N., 1994. Interations of hyaluronan (hyaluronic acid) with phospholipids as determined by gel permeation chromatography, multi-angle laser-light-scattering photometry and H-NMR spectroscopy. *Int. J. Biol. Macromol.* 16, 237.
- Girish, K.S., Kemparaju, K., 2007. The magic glue hyaluronan and its eraser hyaluronidase: a biological overview. *Life Sci.* 80, 1921-1943.
- Goa, K.L., Benfield, P., 1994. Hyaluronic acid. A review of its pharmacology and use as a surgical aid in ophthalmology, and its therapeutic potential in joint disease and wound healing. *Drugs.* 47, 536-566.
- Heatley, F., Scott, J.E., 1988. A water molecule participates in the secondary structure of hyaluronan. *Biochem J.* 254, 489-493.
- Hoare, T., Zurakowski, D., Langer, R., Kohane, D.S., 2010. Rheological blends for drug delivery. I. Characterization in vitro. *J Biomed Mater Res A.* 92, 575-585.
- Hoare, T.R., Kohane, D.S., 2008. Hydrogels in drug delivery: Progress and challenges. *Polymer.* 49, 1993-2007.
- Hurler, J., Zakelj, S., Mravljak, J., Pajk, S., Kristl, A., Schubert, R., Skalko-Basnet, N., 2013. The effect of lipid composition and liposome size on the release properties of liposomes-in-hydrogel. *Int J Pharm.* 456, 49-57.
- Ionov, R., El-Abed, A., Goldmann, M., Peretti, P., 2004. Interactions of lipid monolayers with the natural biopolymer hyaluronic acid. *Biochim Biophys Acta.* 1667, 200-207.
- Kablik, J., Monheit, G.D., Yu, L., Chang, G., Gershkovich, J., 2009. Comparative physical properties of hyaluronic acid dermal fillers. *Dermatol Surg.* 35 Suppl 1, 302-312.
- Kang-Mieler, J.J., Osswald, C.R., Mieler, W.F., 2014. Advances in ocular drug delivery: emphasis on the posterior segment. *Expert Opin Drug Deliv.* 11, 1647-1660.
- Krause, W.E., Bellomo, E.G., Colby, R.H., 2001. Rheology of sodium hyaluronate under physiological conditions. *Biomacromolecules.* 2, 65-69.
- Lajavardi, L., Camelo, S., Agnely, F., Luo, W., Goldenberg, B., Naud, M.C., Behar-Cohen, F., de Kozak, Y., Bochot, A., 2009. New formulation of vasoactive intestinal peptide using liposomes in hyaluronic acid gel for uveitis. *J Control Release.* 139, 22-30.
- Lapcik, L., Jr., Lapcik, L., De Smedt, S., Demeester, J., Chabrecek, P., 1998. Hyaluronan: Preparation, Structure, Properties, and Applications. *Chem Rev.* 98, 2663-2684.
- Lee, S.C., Lee, K.E., Kim, J.J., Lim, S.H., 2005. The effect of cholesterol in the liposome bilayer on the stabilization of incorporated Retinol. *J Liposome Res.* 15, 157-166.
- Lei, Y., Rahim, M., Ng, Q., Segura, T., 2011. Hyaluronic acid and fibrin hydrogels with concentrated DNA/PEI polyplexes for local gene delivery. *J Control Release.* 153, 255-261.
- Liao, Y.H., Jones, S.A., Forbes, B., Martin, G.P., Brown, M.B., 2005. Hyaluronan: pharmaceutical characterization and drug delivery. *Drug Deliv.* 12, 327-342.
- Ludwig, A., 2005. The use of mucoadhesive polymers in ocular drug delivery. *Adv Drug Deliv Rev.* 57, 1595-1639.
- Mayol, L., Quaglia, F., Borzacchiello, A., Ambrosio, L., La Rotonda, M.I., 2008. A novel poloxamers/hyaluronic acid in situ forming hydrogel for drug delivery: rheological, mucoadhesive and in vitro release properties. *Eur J Pharm Biopharm.* 70, 199-206.

- McCall, A.A., Swan, E.E., Borenstein, J.T., Sewell, W.F., Kujawa, S.G., McKenna, M.J., 2010. Drug delivery for treatment of inner ear disease: current state of knowledge. *Ear Hear.* 31, 156-165.
- Mourtas, S., Duraj, S., Fotopoulou, S., Antimisiaris, S.G., 2008. Integrity of liposomes in presence of various formulation excipients, when dispersed in aqueous media and in hydrogels. *Colloids Surf B Biointerfaces.* 61, 270-276.
- Mourtas, S., Haikou, M., Theodoropoulou, M., Tsakiroglou, C., Antimisiaris, S.G., 2008. The effect of added liposomes on the rheological properties of a hydrogel: a systematic study. *J Colloid Interface Sci.* 317, 611-619.
- Nejadnik, M.R., Yang, X., Bongio, M., Alghamdi, H.S., van den Beucken, J.J., Huysmans, M.C., Jansen, J.A., Hilborn, J., Ossipov, D., Leeuwenburgh, S.C., 2014. Self-healing hybrid nanocomposites consisting of bisphosphonated hyaluronan and calcium phosphate nanoparticles. *Biomaterials.* 35, 6918-6929.
- Noble, P.W., 2002. Hyaluronan and its catabolic products in tissue injury and repair. *Matrix Biol.* 21, 25-29.
- Pasquali-Ronchetti, I., Quaglino, D., Mori, G., Bacchelli, B., 1997. Hyaluronan-Phospholipid interactions. *J. Struct. Biol.* 120, 1-10.
- Peattie, R.A., 2012. Release of growth factors, cytokines and therapeutic molecules by hyaluronan-based hydrogels. *Curr Pharm Biotechnol.* 13, 1299-1305.
- Quemeneur, F., Rinaudo, M., Pepin-Donat, B., 2008. Influence of polyelectrolyte chemical structure on their interaction with lipid membrane of zwitterionic liposomes. *Biomacromolecules.* 9, 2237-2243.
- Rabinowitsch, B., 1929. Über die Viskosität und Elastizität von solen. *Zeit Phys Chem Abt A.* 145, 1-26.
- Ray, T.R., 2013. Using viscosupplementation to treat knee osteoarthritis. *Phys Sportsmed.* 41, 16-24.
- Reeff, J., Gaignaux, A., Goole, J., Siepmann, J., Siepmann, F., Jerome, C., Thomassin, J.M., De Vries, C., Amighi, K., 2013. Characterization and optimization of GMO-based gels with long term release for intraarticular administration. *Int J Pharm.* 451, 95-103.
- Ruel-Gariepy, E., Leclair, G., Hildgen, P., Gupta, A., Leroux, J.C., 2002. Thermosensitive chitosan-based hydrogel containing liposomes for the delivery of hydrophilic molecules. *J Control Release.* 82, 373-383.
- Scott, J.E., Cummings, C., Brass, A., Chen, Y., 1991. Secondary and tertiary structures of hyaluronan in aqueous solution, investigated by rotary shadowing-electron microscopy and computer simulation. Hyaluronan is a very efficient network-forming polymer. *Biochem J.* 274, 699-705.
- Seol, D., Magnetta, M.J., Ramakrishnan, P.S., Kurriger, G.L., Choe, H., Jang, K., Martin, J.A., Lim, T.H., 2013. Biocompatibility and preclinical feasibility tests of a temperature-sensitive hydrogel for the purpose of surgical wound pain control and cartilage repair. *J Biomed Mater Res B Appl Biomater.* 101, 1508-1515.
- Staecker, H., Rodgers, B., 2013. Developments in delivery of medications for inner ear disease. *Expert Opin Drug Deliv.* 10, 639-650.
- Szabo, A., Szabo, B., Balogh, E., Zelko, R., Antal, I., 2012. Modified release intra-articular drug delivery systems. *Acta Pharm Hung.* 82, 69-74.

- Taglienti, A., Cellesi, F., Crescenzi, V., Sequi, P., Valentini, M., Tirelli, N., 2006. Investigating the interactions of hyaluronan derivatives with biomolecules. The use of diffusional NMR techniques. *Macromol Biosci.* 6, 611-622.
- Wang, X., Dellamary, L., Fernandez, R., Ye, Q., LeBel, C., Piu, F., 2011. Principles of inner ear sustained release following intratympanic administration. *Laryngoscope*. 121, 385-391.
- Widjaja, L.K., Bora, M., Chan, P.N., Lipik, V., Wong, T.T., Venkatraman, S.S., 2014. Hyaluronic acid-based nanocomposite hydrogels for ocular drug delivery applications. *J Biomed Mater Res A*. 102, 3056-3065.

## **Etude complémentaire : influence des dimensions de l'aiguille et de la viscosité des gels sur les propriétés de seringabilité.**

Afin de déterminer l'influence de la viscosité du gel sur ses propriétés de seringabilité et d'évaluer la possibilité de prédire son injectabilité à partir des données de rhéologie, nous avons estimé la vitesse de cisaillement que subit le gel dans l'aiguille. Pour cela, des aiguilles de différentes dimensions ont été utilisées et la vitesse de cisaillement  $\dot{\gamma}$  dans l'aiguille a été calculé par deux méthodes :

- En utilisant la loi de Poiseuille (**Equation 1**) qui est valable pour les liquides newtoniens (Cumaraze et al., 2014) :

$$\dot{\gamma} = \frac{32 Q}{\pi d^3} \quad (1)$$

où Q représente le débit volumique ( $m^3.s^{-1}$ ) et d le diamètre interne de l'aiguille (m).

- En utilisant l'équation de Mooney-Rabinowitsch (**Equation 2**) qui est valable pour des matériaux rhéofluidifiants (Rabinowitsch, 1929) :

$$\dot{\gamma} = \frac{4n+1}{4n} \frac{32 Q}{\pi d^3} \quad (2)$$

où Q représente le débit volumique ( $m^3.s^{-1}$ ) et d le diamètre interne de l'aiguille (m). n est un exposant obtenu par l'ajustement des courbes représentant la contrainte de cisaillement ( $\tau$ ) en fonction de la vitesse de cisaillement ( $\dot{\gamma}$ ) à l'aide de la loi de puissance (**Equation 3**) :

$$\tau = K \dot{\gamma}^n \quad (3)$$

où K est une constante de proportionnalité.

Pour un débit constant de 0,4 mL/min, la vitesse de cisaillement est plus importante lorsque l'aiguille est plus fine (**Tableau 1**).

Des mesures de la viscosité en écoulement à 19°C ont été effectuées sur l'ensemble des gels présentés dans la publication 2. Cette température est celle à laquelle les mesures de seringabilité ont été effectuées (publication 2). Les courbes d'écoulement ont ensuite été ajustées en utilisant le modèle de Cross comme décrit dans la publication 2. A partir des paramètres ajustables déterminés avec cette équation, il est possible de calculer la viscosité du gel à une vitesse de cisaillement comparable à celle qu'il subit dans l'aiguille.

**Tableau 1**

Seringabilité des gels HA 2,28% sans liposomes avec des aiguilles 27G, 29G, et 30G : vitesse de cisaillement dans l'aiguille, viscosité du gel (calculée) à la vitesse de cisaillement dans l'aiguille, résistance hydrodynamique calculée et force d'injection mesurée avec l'analyseur de texture.

Aiguilles	Débit (mL/min)	Vitesse de cisaillement $\dot{\gamma}$ calculée (s <sup>-1</sup> )	Viscosité à $\dot{\gamma}$ dans l'aiguille (Pa.s)	Résistance hydrodynamique calculée (Pa.s.m <sup>-3</sup> )	Force d'injection mesurée (N)
<b>27 G</b> (d = 0,19 mm, l = 20 mm)	0,4	9200	0,05	$3 \times 10^{13}$	$2,9 \pm 0,2$
<b>29 G</b> (d = 0,16 mm, l = 88 mm)	0,4	15670	0,04	$2 \times 10^{14}$	$8,5 \pm 0,6$
<b>30 G</b> (d = 0,14 mm, l = 13 mm)	0,4	23400	0,03	$5 \times 10^{13}$	$3,8 \pm 0,3$

En utilisant la loi de Poiseuille (équation 1), la vitesse de cisaillement calculée dans l'aiguille 29G est de 15670 s<sup>-1</sup> pour tous les gels présentés dans le **tableau 2**. Avec l'équation de Mooney-Rabinowitsch (**Equation 2**), cette valeur est de 22945 s<sup>-1</sup> pour le gel HA 2.28% sans liposomes et elle atteint un maximum de 24810 s<sup>-1</sup> pour le gel HA-Lip PG-5%PEG<sub>5000</sub> à 80 mM de lipides. C'est pour ce dernier que la valeur maximale de force d'injection (15 N) a été obtenue lors des tests de seringabilité (publication 2). De telles vitesses de cisaillement ne peuvent être atteintes expérimentalement avec le rhéomètre et la géométrie utilisée. La viscosité des gels à ces vitesses de cisaillement a été calculée par extrapolation à l'aide du modèle de Cross. Les valeurs de viscosités calculées à la vitesse de cisaillement dans l'aiguille se situent probablement au deuxième plateau newtonien puisque que celles-ci sont équivalentes quelle que soit l'équation utilisée (**Equation 1 ou 2**) pour calculer la vitesse de cisaillement et ce pour chacun des gels avec ou sans liposomes.

Dans les résultats ci-dessous, la vitesse de cisaillement est celle obtenue avec **l'équation 1** tirée de loi de Poiseuille. Afin de comparer les différentes aiguilles entre elles, la résistance hydrodynamique dans ces aiguilles a été calculée en utilisant **l'équation 4** :

$$R_h = \frac{128 \eta l}{\pi d^4} \quad (4)$$

où l est la longueur de l'aiguille (m), d le diamètre interne de l'aiguille (m) et  $\eta$  la viscosité du gel à la vitesse de cisaillement dans l'aiguille (Pa.s). La résistance hydrodynamique dépend

des caractéristiques géométriques de l'aiguille et des caractéristiques physiques du gel (viscosité).

La courbe représentant la force d'injection mesurée en fonction de la résistance hydrodynamique calculée (**Fig. 1**) est une droite. Ceci signifie que la viscosité à elle seule ne permet pas de prédire la seringabilité du gel car la force d'injection dépend à la fois des propriétés rhéologiques du gel et des dimensions de l'aiguille (longueur et diamètre interne).

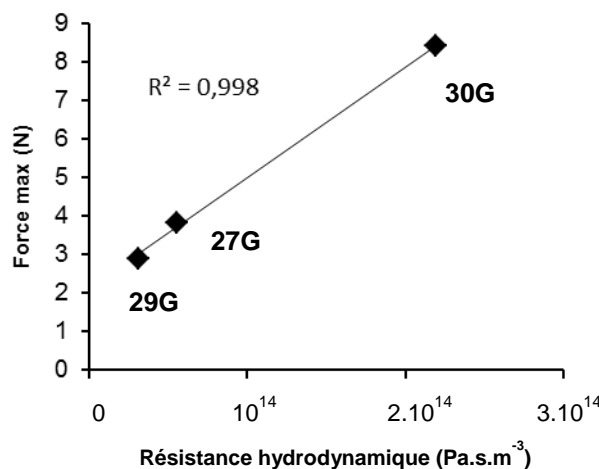


**Fig. 1.** Variations de la force maximale d'injection mesurée en fonction de la résistance hydrodynamique dans l'aiguille pour un gel d'HA à 2,28% sans liposomes en utilisant des aiguilles 27G (20 mm), 29G (88 mm) et 30G (13 mm).

Connaissant la vitesse de cisaillement dans l'aiguille 29G ( $\dot{\gamma} = 15670 \text{ s}^{-1}$ ), la viscosité à cette vitesse de cisaillement (calculée à partir des paramètres du modèle de Cross) ainsi que les dimensions de l'aiguille, il est possible de calculer une force théorique d'injection. L'**équation 5** qui est dérivée de la loi de Poiseuille a été utilisée pour calculer la force d'injection théorique. Cette équation tient compte à la fois du diamètre et de la longueur de l'aiguille.

$$F = \frac{32 D^2 l}{d^4} Q \eta \quad (5)$$

Q représente le débit volumique ( $\text{m}^3 \cdot \text{s}^{-1}$ ), D le diamètre interne de la seringue (m), l la longueur de l'aiguille (m), d le diamètre interne de l'aiguille (m) et  $\eta$  la viscosité du gel à la vitesse de cisaillement dans l'aiguille (Pa.s).

Les forces d'injection théoriques et expérimentales (**Tableau 2**) ne sont pas du même ordre de grandeur. La force d'injection calculée semble fortement dépendante de la viscosité du gel et de la concentration en lipides. Une valeur théorique de 603 N est obtenue (pour le gel HA-Lip PG-5%PEG5000 à 80 mM) alors que les forces d'injection mesurées ne dépassent pas 15 N.

### Tableau 2

Seringabilité des gels d'HA 2,28% contenant des liposomes avec des aiguilles 29G (88 mm) : viscosité calculée à la vitesse de cisaillement dans l'aiguille, force d'injection théorique et force d'injection mesurée avec l'analyseur de texture.

Composition	Concentration lipides (mM)	Viscosité à 15670 s <sup>-1</sup> (Pa.s)	Force mesurée (N)	Force calculée (N)
HA	0	0,04	8,5 ± 0,6	17
HA-Lip SA	10	0,04	8,1 ± 0,4	17
	30	0,07	9,0 ± 0,8	30
	50	0,10	9,8 ± 0,1	43
	60	0,11	10,9 ± 0,3	47
	80	0,14	10,6 ± 0,2	60
HA-Lip PG-5%PEG <sub>2000</sub>	10	0,56	8,7 ± 0,1	38
	30	0,97	8,3 ± 0,1	215
	50	1,21	10,6 ± 1,5	521
	80	1,11	10,9 ± 1,5	478
HA-Lip PG-5%PEG <sub>5000</sub>	10	0,11	8,4 ± 0,1	47
	30	0,21	10,6 ± 1,4	90
	50	0,70	11,2 ± 1,3	301
	80	1,40	14,5 ± 0,7	603
HA-Lip 5%PEG <sub>2000</sub>	10	0,04	7,8 ± 0,3	17
	80	0,78	10,7 ± 0,4	336
HA-Lip PG-1%PEG <sub>5000</sub>	10	0,05	8,0 ± 0	21
	80	0,12	12,3 ± 0,4	51

En conclusion, nous n'avons pas montré de corrélation entre la viscosité des systèmes extrapolée à forte vitesse de cisaillement et la force d'injection pour les gels d'HA contenant ou non des liposomes. Ainsi, les données de rhéologie ainsi que les dimensions de l'aiguille ne suffisent pas pour prédire la valeur de la force d'injection de nos gels. L'extrapolation de la viscosité aux vitesses de cisaillement mises en jeu dans l'aiguille avec le modèle de Cross est probablement trop éloignée des valeurs expérimentales.

## Références

- Couaraze G., Grossiord J.L., Huang, N., 2014. Initiation à la rhéologie. Bases théoriques et applications expérimentales (4<sup>e</sup> ed), Edition Tec & Doc Lavoisier. 310 p.
- Rabinowitsch, B., 1929. Über die viskosität und elastizität von soien. Zeit Phys Chem Abt A. 145, 1-26.

## **Chapitre II**

**Mélanges d'acide hyaluronique et de liposomes en  
milieu aqueux : compatibilité, microstructure et  
mobilité des liposomes**

## **Chapitre II**

### **Mélanges d'acide hyaluronique et de liposomes en milieu aqueux : compatibilité, microstructure et mobilité des liposomes**

#### **Introduction - résumé**

Après avoir caractérisé de façon approfondie les propriétés rhéologiques et la seringabilité des systèmes HA-Liposomes (Chapitre I), nous nous sommes intéressés dans ce deuxième chapitre à la compatibilité entre HA et liposomes, à la microstructure des mélanges ainsi qu'à la mobilité des liposomes dans ces systèmes. Les mélanges colloïdes-polymères ont plusieurs applications technologiques et sont très utilisés dans le domaine biomédical, notamment pour l'administration de substances actives encapsulées dans les particules colloïdales. Dans cette dernière application, la diffusion des liposomes est un point clé puisque celle-ci va déterminer leur devenir après injection. S'ils sont immobiles, les liposomes vont servir de réservoir de substance active au niveau du site d'injection. Si, au contraire, les liposomes peuvent diffuser à travers l'HA, ils pourront alors quitter le site d'injection pour éventuellement atteindre les tissus ou les cellules cibles. Cependant, la compatibilité des liposomes et de l'HA est un point crucial qui pourrait affecter de manière significative leurs propriétés d'usage.

Ce chapitre a un double objectif. Le premier est d'évaluer la microstructure et la compatibilité à l'échelle macroscopique de mélanges à base d'acide hyaluronique (HA) et de liposomes en faisant varier la concentration en HA ainsi que les propriétés de surface des liposomes (chargée positivement ou négativement, neutre, PEGylée). Le deuxième, est de déterminer l'influence de la concentration en HA ainsi que la composition et la concentration des liposomes sur leur mobilité dans la solution d'HA.

Nous avons, dans un premier temps, caractérisé les propriétés rhéologiques des solutions d'HA sans liposomes sur une large gamme de concentrations afin de déterminer les régimes de concentrations de ce polyélectrolyte. Ensuite, la compatibilité des systèmes HA-Liposomes en présence de différentes formulations de liposomes à une concentration fixe de 80 mM, pour des concentrations variables en HA, a été évaluée au cours du temps par une observation macroscopique. La structure microscopique de l'HA à forte concentration contenant les différentes formulations de liposomes a été analysée par microscopie confocale et par

microscopie de force atomique. Enfin, la mobilité des liposomes, dans des solutions semi-diluées non enchevêtrées et concentrées en HA, a été étudiée à l'échelle macroscopique par une analyse optique au Turbiscan® et à l'échelle microscopique par vidéomicroscopie.

La concentration d'enchevêtrement critique de l'HA a été estimée à 0,4% (m/v). A l'exception des liposomes chargés positivement, la dispersion des autres liposomes dans l'HA présentait une séparation de phases macroscopique lorsque la concentration en HA était en dessous de sa concentration d'enchevêtrement critique. La séparation de phases est probablement induite par un effet de déplétion entre l'HA et les liposomes. Les liposomes chargés positivement sont, quant à eux, susceptibles d'interagir avec l'HA chargé négativement par des attractions électrostatiques en plus de l'effet de déplétion. A forte concentration en HA (2.28% m/v), aucune séparation de phases n'a été observée macroscopiquement mais la formulation contenant des liposomes cationiques a monté une légère synérèse. La microstructure de ces systèmes semble formée par des agrégats de liposomes dispersés de façon homogène au sein du réseau d'HA. Cependant, le mélange HA et liposomes PEGylés se distingue des autres formulations par une microstructure formée d'un réseau bicontinu d'HA et d'agrégats de liposomes. La diffusion des liposomes est contrôlée aussi bien par la concentration en HA que par la concentration et les caractéristiques de surface des liposomes. Enfin, liposomes PEGylés ont montré une mobilité plus importante dans l'HA, même à forte concentration, et ce aux échelles macro- et microscopique.

Une version ultérieure de ce chapitre sera soumise à publication.

## **Projet de publication**

### **Mixtures of hyaluronic acid and liposomes in aqueous media: phase behavior, microstructure and mobility of liposomes**

*Naila El Kechai<sup>a</sup>, Sandrine Geiger<sup>a</sup>, Arianna Fallacara<sup>a</sup>, Ingrid Cañero Infante<sup>b</sup>, Valérie Nicolas<sup>c</sup>, Evelyne Ferrary<sup>d</sup>, Nicolas Huang<sup>a</sup>, Amélie Bochot<sup>a,#</sup>, Florence Agnely<sup>a,#,\*</sup>*

<sup>a</sup> *Institut Galien Paris-Sud, Université Paris-Sud, CNRS UMR 8612, Université Paris-Saclay, 92290 Châtenay-Malabry, France.*

<sup>b</sup> *SPMS, Ecole Centrale Paris, UMR 8580 CNRS, 92290 Châtenay-Malabry, France.*

<sup>c</sup> *UMS IPSIT, Plate-forme d'imagerie cellulaire, Faculté de Pharmacie, Université Paris-Sud, Châtenay-Malabry, France.*

<sup>d</sup> *UMR-S 1159 Inserm / Université Pierre et Marie Curie - Sorbonne Universités “Minimally Invasive Robot-based Hearing Rehabilitation”, Paris, France.*

<sup>#</sup> *These authors have contributed equally*

#### **\* Corresponding Author**

Florence Agnely: +33 1 46 83 56 26; [florence.agnely@u-psud.fr](mailto:florence.agnely@u-psud.fr)

## Abstract

Colloid-polymer mixtures have many technological and medical applications. However, the stability of such systems is a critical issue that could significantly impact and determine their use. The aim of this study was to evaluate the microstructure and the phase behavior of hyaluronic acid (HA) and liposomes mixtures at different HA concentrations and using liposomes characterized by different surface properties (positively or negatively charged, neutral, with a corona of polyethylene glycol). On the other hand, the influence of HA concentration and liposome composition was determined regarding the mobility of liposomes into HA solutions. The entanglement concentration of HA was determined to be 0.4% (w/v). Except the positively charged liposomes, the other ones dispersed within HA exhibited phase separation below this concentration. The phase separation is probably driven by depletion interactions whereas the positively charged liposomes are likely to interact with the negatively charged HA through electrostatic attractions. At high HA concentration, no macroscopic phase separation was observed. The microstructure showed aggregates of liposomes homogeneously distributed into a HA network for all liposome types except for the PEGylated ones, which seems to form bicontinuous interpenetrating networks. The diffusion of liposomes was controlled by the concentration of HA as well as the concentration and the surface characteristics of liposomes. Finally, PEGylated liposomes displayed the best mobility into HA at high concentration (2.28% w/v) both macro- and microscopically.

## Keywords

Atomic force microscopy, depletion, interactions, entanglement concentration, hyaluronic acid, liposomes, phase separation, single particle tracking.

## Abbreviations

AFM: atomic force microscopy, Chol: cholesterol, DSPE-PEG2000: 1,2-distearoyl-sn-glycero-3-phosphoethanolamine-N-[methoxy-poly-(ethyleneglycol)-2000], EPC: Egg phosphatidylcholine, HA: hyaluronic acid, Lip: liposome, MSD: mean square displacement, PE: phosphatidylethanolamine, PEG: polyethylene glycol, PG: phosphatidylglycerol, Rh: rhodamine, SA: stearylamine, SPT: single particle tracking.

## 1. Introduction

Nanoparticle dispersions into polymeric matrices have sparked interest for different technological applications such as the design of functional hybrid and nanocomposite materials (Lin et al., 2005, Hooper and Schweizer, 2006, Barber et al., 2009), polymer based solar-cells and dielectric coatings (Huynh et al., 2002, Hadipour et al., 2006, Yaklin et al., 2008). Colloids-polymer mixtures are also of great interest in the medical field, especially for drug delivery (Hamidi et al., 2008, Lajavardi et al., 2009, Hurler et al., 2013), as well as in the food industry and in cosmetics (Huh et al., 2011). However, the kinetic stability of colloidal suspensions is a key parameter that can be impacted by the addition of a polymer in the suspending media.

Mixtures of polymer and colloids exhibit complex structural and phase behaviors. For instance, a hard-sphere colloidal suspension in the presence of a non adsorbing polymer can exist as homogeneous fluid, can macroscopically phase separate, crystallize or form non equilibrium gels depending on the size and the concentration of the polymer (Hooper and Schweizer, 2005). The mechanism involved in the behavior of such systems is the polymer depletion. Indeed, polymer segments cannot penetrate the solid colloidal particles. This results in a reduction of polymer conformations and a loss of entropy, which can induce segregative phase separation into a colloid-rich phase and a colloid-poor phase (Pelissetto and Hansen, 2006). A key parameter that characterize the behavior of such mixtures is the size ratio ( $\lambda = R_c/R_g$ ) where  $R_c$  is the radius of the colloid and  $R_g$  is the radius of gyration of the individual polymer coil. The case  $\lambda \gg 1$  is referred to the colloid limit and is the best understood. It can be described through the Asakura and Oosawa (1954) and the Vrij (1976) models. The polymer is excluded from a layer  $\Delta$  around the particles with  $\Delta \approx R_g$  (Bolhuis et al., 2002). Theoretical simulations provide a good description of the phase diagrams obtained with nanoparticles (Bolhuis et al., 2002, Tuinier et al., 2003) but also with other colloidal systems such as emulsions (Meller and Stavans, 1996, Meller et al., 1999, Tuinier and De Kruif, 1999). The case  $\lambda < 1$  is less understood. The polymer can wrap around the smaller particles and phase separation can also be observed with such systems. The case  $\lambda \ll 1$  is called the protein limit and was also theoretically described. The mixture of a small globular protein with a water soluble polymer can even induce protein crystallization, which is an important step to determine the structure of the protein from X-ray scattering experiments. Pelissetto and Hansen (2006) have developed a simulation to semi-quantitatively predict the phase diagrams both in the colloid and the protein regimes. Yet, most of experimental and

theoretical studies on the mixtures of non adsorbing polymer and colloids were performed in dilute or in non entangled regimes. In the entangled semi-dilute regime, it is most likely that the correlation length  $\xi$  should come into play instead of  $R_g$  (de Gennes, 1979, Pelissetto and Hansen, 2006). Furthermore, when polymer melts and colloidal particles are mixed, it seems that the key parameter is the size ratio of the colloid to the polymer monomer (Hooper and Schweizer, 2005). Compared to the non adsorbing polymers described above, more complexity arises when the monomers are even weakly attracted to the particle surfaces. Indeed, both enthalpy and entropic effects are then involved. A steric stabilization of the colloidal suspension can be observed due to the adsorbed polymer layer. However, bridging attraction or depletion can also occur leading either to associative or segregative phase separation or physical gelation (Hooper and Schweizer, 2005).

In this work, hyaluronic acid (HA) was selected as it is a naturally occurring linear polysaccharide which is of particular interest in the medical field. HA is soluble in water at neutral pH and behaves as a negatively charged semi-rigid polyelectrolyte (Lapčík et al., 1998, Gatej et al., 2005). Its intrinsic persistence length was reported to be around 9 nm (Morfin et al., 2011). Due to its strong hydrophilic character and its high molecular weight in biological tissues, HA has important structural and functional roles on the body (Volpi et al., 2009). From a physicochemical point of view, high molecular weight HA forms a transient network in aqueous solution leading to an enhanced viscosity depending on HA concentration. HA chains start to overlap each other at a very low HA concentration (De Smedt et al., 1993, Krause et al., 2001) providing high macroscopic viscoelasticity even in dilute HA concentration (Lapčík et al., 1998, Scott and Heatley, 1999, Masuda et al., 2001). From a biological and a medical point of view, the diffusion of small molecules or nanoparticles in HA solutions has attracted interest (De Smedt et al., 1994, Masuda et al., 2001, Martens et al., 2013). Indeed, HA can be regarded as a model especially for drug delivery to biological tissues containing a high concentration of HA such as the vitreous humor in the eye and the synovial fluid in the joints (Barbucci et al., 2002, Martens et al., 2013, Xu et al., 2013).

In Chapter I, we thoroughly studied the effect of added liposomes on the rheological properties of hyaluronic acid (HA) solutions at a fixed concentration of 2.28% (w/v) (El Kechai et al., 2015). We demonstrated that liposomes strengthened the network formed by HA chains due to their interactions with this polymer resulting in a viscosity increase that was dependent on both liposome concentration and composition. The rheological analysis also

revealed that HA controls the rheological behavior of the liposomal HA mixture and that liposomes slow down the dynamic of the system. Moreover, those liposomal HA mixtures exhibited stable macroscopic properties.

In the present study, we have two primary goals. The first is to evaluate the microstructure and the stability of HA liposomal mixtures at different HA concentrations using liposomes characterized by different surface properties (positively or negatively charged, neutral, with a corona of polyethylene glycol). The second goal is to study the influence of HA concentration and liposome composition on their mobility into HA solutions. First, we analyzed the rheological properties of HA solutions over a wide concentration range in order to determine its entanglement concentration. Then, the phase behavior of HA in presence of different liposome formulations was followed macroscopically over time. The microscopic structure of highly concentrated HA containing different liposomes was investigated by confocal microscopy and atomic force microscopy. Finally, the mobility of liposomes with different surface properties, into semi-diluted non entangled and concentrated HA solutions, was determined both macroscopically using optical analysis and microscopically using single particle tracking.

## 2. Materials and methods

### 2. 1. Materials

Egg phosphatidylcholine (EPC, purity 96%) was provided by Lipoid GmbH (Ludwigshafen, Germany). Cholesterol (Chol), Egg L- $\alpha$ -phosphatidylglycerol (PG), stearylamine (SA) and fluoresceinamine (purities > 98%) were purchased from Sigma-Aldrich Co. (St. Louis, USA). 1,2-distearoyl-sn-glycero-3-phosphoethanolamine-N-[methoxy-poly-(ethyleneglycol)-2000] (DSPE-PEG2000) and phosphatidylethanolamine-N-(lissamine rhodamine B sulfonyl) (PE-Rh) (purities > 99%) were obtained from Avanti Polar Lipids, inc. (Alabaster, USA). Sodium hyaluronate (HA, M<sub>w</sub> 1.5 MDa, purity 95%) was provided by Acros Organics (New Jersey, USA). All other chemicals were of analytical grade.

## 2.2. Preparation and characterization of liposomes

The different liposome formulations -fluorescently labeled or not- were prepared by the thin film method as described previously (El Kechai et al., 2015) and are presented in **Table 1**. Briefly, lipid films of different compositions (**Table 1**) were prepared using rotary evaporation. The lipid film was hydrated with HEPES/NaCl buffer (10/145 mM, pH 7.4) to achieve total lipid concentration of 100 mM for unlabeled liposomes (Lip, Lip SA, Lip PG, Lip PEG) or 20 mM for fluorescently labeled liposomes (Lip-Rh, Lip SA-Rh, Lip PG-Rh, Lip PEG-Rh). The liposome suspensions were subsequently extruded 10 times through 0.2 µm polycarbonate filters set in a LIPEX extruder (Whitley, Vancouver, Canada).

The hydrodynamic diameter and the zeta potential of liposomes were determined in triplicate by dynamic light scattering (DLS) at 25°C using a Zetasizer Nano ZS (Malvern, Worcestershire, UK). The concentration of EPC in unlabeled liposomes was evaluated after extrusion through an enzymatic phospholipid assay (Biolabo SA, Maizy, France) (El Kechai et al., 2015). The total amount of lipids in liposome suspensions was then calculated from EPC concentration by assuming that lipid composition was unchanged during the different liposome preparation steps. Since rhodamine interferes with absorbance measurements, the lipid concentration of rhodamine-conjugated liposomes was estimated by taking into account the average percent of lipid loss after extrusion.

**Table 1**

Composition and physicochemical characterization of liposomes.

Liposomes	Composition Lipid ratios (mole%)	Diameter (nm)	PdI	ζ-Potential (mV)
Lip	EPC:Chol 65:35	167 ± 49	0.09	-0.8 ± 6
Lip-Rh	EPC:Chol:PE-Rh 64:35:1	163 ± 52	0.10	-8.5 ± 7
Lip SA	EPC:Chol:SA 55:35:10	153 ± 50	0.07	64 ± 12
Lip SA-Rh	EPC:Chol:SA:PE-Rh 54:35:10:1	164 ± 59	0.08	30 ± 7
Lip PG	EPC:Chol:PG 55:35:10	147 ± 62	0.11	-57 ± 10
Lip PG-Rh	EPC:Chol:PG:PE-Rh 54:35:10:1	158 ± 60	0.13	-41 ± 8
Lip PEG	EPC:Chol:DSPE-PEG <sub>2000</sub> 60:35:5:	132 ± 50	0.11	-25 ± 10
Lip PEG-Rh	EPC:Chol:DSPE-PEG <sub>2000</sub> :PE-Rh 59:35:5:1	134 ± 44	0.06	-22 ± 11

### 2.3. Fluorescein-labeling of HA

Labeling of HA with fluoresceinamine (Fl-HA) was performed as described previously (Lajavardi et al., 2009). Briefly, 25 mg of HA was dissolved into 20 mL MilliQ water and mixed with 20 mL dimethylsulfoxide. Then, fluoresceinamine (12.5 mg) dissolved in DMSO (0.25 mL) containing acetaldehyde (12.5 µL) and cyclohexyl isocyanide (12.5 µL) was added to the mixture and the pH was adjusted to 4.5. The solution was maintained for one night at room temperature under magnetic stirring and protected from light. Fl-HA was then precipitated in cold absolute ethanol by adding a saturated NaCl solution, centrifuged and resuspended in water. Centrifugation was repeated three times and the final pellet was resuspended in 12.5 mL MilliQ water and then purified by dialysis (cellulose dialysis membranes, M<sub>w</sub> cut off 50 kDa) against 2 L milliQ water for 48 h with repeated changes of water and protected from light. Fl-HA purified solution was finally freeze-dried and stored at 4 °C.

### 2.4. Preparation of HA liposomal formulations

#### *Formulations for rheological study and macroscopic observation*

HA solutions ranging from 0.05 to 2.28% (w/v) were prepared by dissolving HA powder into HEPES/NaCl buffer (10/145 mM, pH 7.4). HA liposomal mixtures (HA-Lip, HA-Lip SA or HA-Lip PEG) were prepared by dissolving HA (from 0.05 to 2.28% w/v) into unlabeled liposome suspensions at a fixed lipid concentration of 80 mM. HA solutions and HA-Liposomes mixtures were then homogenized by means of vortex for 5 min, maintained at room temperature for 1 h and then stored at 4°C for 12 h prior rheological measurements. Their homogeneity was assessed over time in storage conditions (4°C) by macroscopic observation 12, 24, and 36 hours after preparation.

#### *Formulations for confocal microscopy and atomic force microscopy (AFM)*

Fluorescent HA liposomal mixtures (HA-Lip, HA-Lip SA, HA-Lip PG, HA-Lip PEG) were prepared at a 2.28% (w/v) final HA concentration (containing 10% (w/w) HA-Fl and 90% (w/w) unlabeled HA) and an 80 mM final lipid concentration (containing 10% (w/w) Rhodamine-conjugated liposomes and 90% (w/w) unlabeled liposomes). Briefly, 8.2 mg Fl-HA (corresponding to 4.6 mg HA) was mixed with 41 mg of HA powder. Then, the HA/Fl-HA blend was dissolved into 2 mL of each liposome blend (Lip/Lip-Rh, Lip SA/Lip SA-Rh, Lip PG/Lip PG-Rh, Lip PEG/Lip PEG-Rh, 72/8 mM).

### *Formulations for videomicroscopy*

The concentration of Rhodamine-conjugated liposomes in HA-liposomes mixtures was optimized to obtain a suitable number of fluorescent particles for multiple particle tracking. The total concentration of lipids in each mixture (80 mM for Lip, Lip SA, Lip PG, Lip PEG and also 10 mM for Lip PEG) contained 0.01% (v/v) of rhodamine-conjugated liposomes (Lip-Rh, Lip SA-Rh, Lip PG-Rh, Lip PEG-Rh). The final HA concentration was 0.25% or 2.28% (w/v). HA-liposomes mixtures were prepared as described previously by dissolving HA powder into liposome suspension blends (see section: formulations for rheological study and macroscopic observation).

HA-Liposomes mixtures prepared as described above were then homogenized by means of vortex for 5 min, maintained at room temperature for 1 h and then stored at 4°C for 12 h prior to analysis.

### *2.5. Rheological measurements*

Flow measurements were carried out using a rotational rheometer ARG2 (TA instruments, Newcastle, UK) equipped with an aluminum cone/plate geometry (diameter 4 cm, angle 1° and cone truncation 28 µm). Flow measurements were performed at 37°C by a shear rate sweep. After a 2-minute equilibration time, the shear rate ( $\dot{\gamma}$ ) was increased gradually from 0.01 to 1000 s<sup>-1</sup>. Measurements were at least triplicated and performed under steady state conditions. The viscosity curves were fitted according to the Cross equation (Cross, 1968) to determine the zero-shear rate viscosity (El Kechai et al., 2015). For HA solutions from 0.05 to 2.28% (w/v), the specific viscosity ( $\eta_{sp}$ ) was calculated according to the following equation (**Eq. 1**):

$$\eta_{sp} = \frac{\eta_0 - \eta_{solv}}{\eta_{solv}} \quad (1)$$

where  $\eta_0$  is the zero-shear rate viscosity of the HA solution and  $\eta_{solv}$  is the viscosity of the solvent (HEPES/NaCl buffer 10/145 mM, pH 7.4,  $\eta_{solv} = 0.83$  mPa.s measured at 37°C).

### *2.6. Confocal microscopy*

Fluorescent HA liposomal mixtures (HA-Lip, HA-Lip SA, HA-Lip PG, HA-Lip PEG) and fluorescent HA, placed between glass slide and slip cover, were observed with an inverted confocal laser scanning microscope Leica TCS SP8 (Leica, Germany) using a HC PL APO CS2 63x/1.40 oil immersion objective lens. The excitation sources were provided by a white

light laser (WLL) (495 nm and 552 nm selected excitation wavelength). The corresponding fluorescence emission was collected in sequential mode using 504-542 nm (fluorescein) and 565-700 nm (rhodamine B) wide slits respectively. The pinhole was set at 1.0 Airy unit. 12-bit numerical images were obtained with Leica SP8 LAS AF software (Version 3.6; Leica, Germany).

### *2.7. Atomic force microscopy (AFM)*

AFM images were collected in air at room temperature (22°C) using a commercial Multimode-8 equipped with a NanoScope V controller and an “E” scanner (10 µm) from Bruker manufacturer (Bruker, AXS, France). Topographical and mechanical properties (dissipation) were imaged using the QNM (Quantitative NanoMechanical Property) mode with a nanoindentation frequency of 2 KHz. SCANASYST-AIR cantilevers of a nominal spring constant of 0.4 N/m were used (tip radius of about 8 nm). The scan rate was adjusted in the range of 1 Hz over a selected area in dimension of 1.0 µm x 1.0 µm and 10.0 µm x 10.0 µm. The samples (HA, HA-Lip, HA-Lip SA, HA-Lip PG, HA-Lip PEG) were deposited on clean mica surfaces fixed on a magnetic disk directly mounted on top of the AFM scanner. The samples were left to dry at room temperature for at least 1 h and were finally imaged. Data processing was performed with the WSxM and Bruker softwares.

### *2.8. Turbiscan® optical analysis*

A Turbiscan MA 2000 (Formulaction, L'Union, France) was used to optically assess the migration of the different liposome formulations (Lip, Lip SA, Lip PG, Lip PEG) prepared as described previously into HA solution. 4 mL of HA (2.28% w/v) samples were prepared in the cylindrical glass cells supplied by the manufacturer and analyzed prior to liposome addition. 1mL of each liposome suspension at 80 mM was subsequently placed in the cell in contact with HA solution and the sample was analyzed instantly ( $t_0$ ). All the samples were then incubated at 37°C for 10 days and acquisitions were performed at 1, 3, 7 and 10 days of incubation ( $t_1$ ,  $t_3$ ,  $t_7$ ,  $t_{10}$  respectively). The detection head of Turbiscan MA 2000 was composed of a pulsed near-infrared light source ( $\lambda=850$  nm) and two synchronous transmission and back scattering detectors. The transmission detector received the light which crosses the sample (at 180° from the incident beam), while the back scattering detector received the light scattered backward by the sample (at 45° from the incident beam). The

detection head scanned the entire height of the sample, acquiring transmission and back scattering data each 40 µm for each time point ( $t_0, t_1, t_3, t_7, t_{10}$ ).

### 2.9. Videomicroscopy and single particle tracking (SPT)

The mobility of the different liposomes (Lip, Lip SA, Lip PG, Lip PEG) into HA (0.25 or 2.28% w/v) was measured using videomicroscopy and SPT by analyzing the trajectories of the rhodamine-labeled liposomes. 100 µL HA-liposomes samples were deposited in 8-well glass chambers (Labtek, Campbell, CA) and incubated for 20 min in an XL incubator at 37°C before microscopic observation. 30 s movies with a 100 ms temporal resolution were acquired thanks to a charge-coupled device (CCD) HSm camera (9.9 µm pixel size) mounted on an inverted epifluorescence AxioObserver Z1-Colibri videomicroscope (Carl Zeiss, Germany). Time-lapse images were acquired with a 63x/1.4-numerical-aperture (NA) oil-immersion objective lens, a 555 nm light-emitting diode (LED) for excitation, and a band-pass 605/70 nm filter to collect the emission of fluorescence. Movies were analyzed using the 3D Tracking module of Image J and Matlab software. 3 independent experiments were performed and a total of  $100 < n < 300$  trajectories were analyzed for each condition. The coordinates of particle centroids were transformed into time-averaged mean square displacement (MSD) (Suh et al., 2005).

## 3. Results and discussion

### 3.1. Characterization of liposomes

All unlabeled liposomes (Lip, Lip SA, Lip PG, Lip PEG) and their equivalent rhodamine-conjugated liposomes (Lip-Rh, Lip SA-Rh, Lip PG-Rh, Lip PEG-Rh) showed narrow size distributions characterized by mean hydrodynamic diameters around 150 nm and a  $PdI \leq 0.2$  (**Table 1**). Zeta potential values were almost neutral for Lip and Lip-Rh, positive for Lip SA and Lip SA-Rh, negative for Lip PG, Lip PG-Rh, Lip PEG and Lip PEG-Rh (**Table 1**). Zeta potential values were not significantly different between unlabeled and rhodamine-labeled liposomes except for Lip SA and Lip SA-Rh (**Table 1**). These data indicate that the presence of rhodamine did not alter the surface properties of liposomes except for the positively charged ones in which rhodamine slightly decreased the zeta potential value. The final lipid concentration after extrusion varied between 90 and 95 mM (Lip, Lip SA, Lip PG, Lip PEG) corresponding to a percent of lipid loss after extrusion between 5 and 10 %.

### 3.2. Entanglement concentration of HA ( $C_e$ )

Variations of the apparent viscosity of HA in HEPES/NaCl buffer as function of shear rate at 37 °C are given in **Figure 1A**. The rheograms show a shear-thinning behavior of HA solutions all over the concentration range studied (0.05 to 2.28 % w/v). The specific viscosity ( $\eta_{sp}$ ) was calculated as described previously (Eq. 1) for each HA solution and the concentration dependence of  $\eta_{sp}$  was plotted in **Fig. 1B**. The entanglement concentration ( $C_e$ ) characterizes the transition between the semi-dilute unentangled regime and the concentrated entangled regime. It is represented by a change in the slope of the logarithmic  $\eta_{sp}$  versus concentration curve and was determined to be  $C_e = 0.4\%$  (w/v) for HA at 37°C (**Fig. 1B**). The HA solutions studied here are in the “high salt limit” since HA was dissolved in a HEPES/NaCl buffer (10/145 mM, pH 7.4). De Gennes theory (de Gennes, 1979) gives scaling laws for the specific viscosity of polyelectrolytes in the high salt limit and describes three concentration regions: dilute, semi-dilute and concentrated regions. The overlap concentration  $C^*$  characterizes the transition between the dilute and non entangled semi-dilute regime.

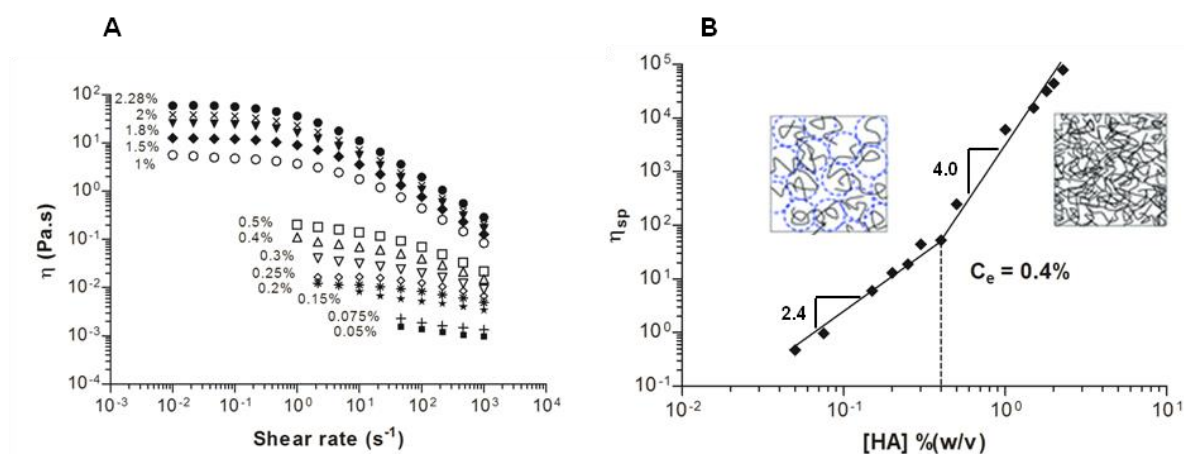


**Fig. 1.** Determination of the entanglement concentration ( $C_e$ ) of HA in HEPES/NaCl buffer (10/145 mM, pH 7.4) at 37°C. A: apparent viscosity as function of shear rate for HA solutions in the range 0.05-2.28% w/v. B: variations of specific viscosities ( $\eta_{sp}$ ) versus concentrations of HA. 2.4 and 4.0 represent the scaling exponents in semi-dilute non entangled and entangled regimes respectively.

As given in **Fig. 1B**, the scaling laws for the variation of specific viscosity were  $\eta_{sp} \sim C^{2.4}$  ( $C < C_e$ ) and  $\eta_{sp} \sim C^{4.0}$  ( $C > C_e$ ). For the semi-dilute unentangled regime ( $C^* < C < C_e$ ), the

exponent obtained in this study (2.4) is higher than the predicted one (1.25) whereas for the concentrated regime ( $C > C_e$ ), the exponent (4.0) is slightly higher but in the same order of magnitude than the theoretical one (3.75). Overall, our exponents are in good agreement with those previously reported in the literature for HA with  $M_w$  around 1.5 MDa, whereas the  $C_e$  value obtained here is different from those reported previously by Krause et al. (2001) and Oelschlaeger et al. (2013). Indeed, Oelschlaeger et al. (2013) obtained  $C_e = 0.7\%$  for HA at 20°C in 0.1 M NaCl and the scaling law for  $C > C_e$  was  $\eta_{sp} \sim C^{4.0}$ . The higher concentration dependence of  $\eta_{sp}$  compared to the theoretical predictions can be explained by the possible formation of aggregates at high HA concentration presumably due to the formation of hydrogen bonds or hydrophobic interactions between HA chains leading to an increase in the apparent molecular weight of HA (Scott et al., 1991, Esquenet and Buhler, 2002, Oelschlaeger et al., 2013). Oelschlaeger et al. (2013) also demonstrated that the scaling exponents were not dependent on the temperature (from 20 to 60°C) indicating that there is no change of polymer structure or conformation in this temperature range. Krause et al. (2001) reported a  $C_e = 0.24\%$  (w/v) and  $C^* = 0.059\%$  (w/v) for HA in phosphate buffered saline at 25°C (concentration range between 0.009 and 0.87% w/v). In our study, the overlap concentration  $C^*$  was not determined since our rheometer did not allow to accurately measure low viscosities. However, according to Krause et al. (2001) results, we supposed that the dilute region of HA would appear for HA concentrations below 0.05% approximamente.

De Gennes also made theoretical considerations on the transient network structure of semi-dilute polymer solutions. He assumed that the polymer solution can be considered as a collection of “blobs” which can be each characterized by a correlation length ( $\xi$ ). This parameter describes the average distance between the entanglement points of HA chains and can be considered as a measure of the mesh size of the transient network. This theory is supported by the following equations:

$$C^* \cong \frac{M}{\frac{4}{3}\pi R_g^3 N_A} \quad (2)$$

$$\xi \cong R_g \left( \frac{C^*}{C} \right)^{3/4} \quad (3)$$

where  $M$  is the molecular weight of the polymer,  $R_g$  is the radius of gyration of the polymer,  $N_A$  is the number of Avogadro.

The radius of gyration of HA in our experimental conditions was calculated from **equation 2** by estimating  $C^* = 0.05\%$  (w/v) and was found to be  $R_g = 100$  nm. By taking a  $\frac{3}{4}$  exponent, which

characterizes polymers in good solvent, the mesh size, at a 2.28% HA concentration, calculated from **equation 3** is  $\xi = 7$  nm. By taking the exponent (0.58) reported by De Smedt et al. (1994) for HA in phosphate buffered saline, the correlation length was found to be  $\xi = 11$  nm. Masuda et al. (2001) estimated the mesh size for HA to be  $\xi = 9$  nm (at 1.4 % w/v, HEPES/NaCl buffer 50/100 mM, pH 7). Other studies with HA of different molecular weights and different concentrations in the high salt limit reported mesh sizes between 10 and 20 nm using FRAP technique (De Smedt et al., 1994) and around 11 nm using electron spin resonance technique (Shenoy et al., 1995).

### 3.3. Phase behavior of HA liposomal mixtures

HA solutions between 0.05 and 2.28% (w/v) containing 80 mM unlabeled liposomes (Lip, Lip SA, Lip PEG) were macroscopically examined regarding their homogeneity at three different time points after preparation (30 min, 12 h, 36 h) (**Fig. 2**). Interestingly, whatever the liposome formulation or HA concentration, there was no phase separation observed 30 min after preparation indicating that HA liposomal mixtures did not undergo instantaneous phase separation. Only HA-Lip SA exhibited a homogeneous white opaque aspect over the whole HA concentration range and at each time point (**Fig. 2B**). Nevertheless, for Lip SA into HA at 2.28%, a thin water layer was observed at the surface of the sample 36 h after preparation suggesting syneresis. HA-Lip and HA-Lip PEG showed a macroscopic phase separation between 0.05 to 0.25 % (w/v) for Lip at 36 h and between 0.075 and 0.4% (w/v), observed starting from 12 h for Lip PEG (**Fig. 2**). HA-Lip PG was not studied over the entire HA concentration range but the sample at 0.25% (w/v) also showed a phase separation. The phase separation was characterized by a higher opacity at the bottom of the sample whereas its surface became more transparent suggesting sedimentation of liposomes. Furthermore, there was no sedimentation of liposomes observed when no HA was added (data not shown). Liposome suspensions without HA remained homogeneous for at least 15 days except for Lip suspension that showed a reversible aggregation and sedimentation. Indeed, for unloaded liposomes, the density of the suspension is very close to that of the suspending media (i.e. 1g/mL for HEPES/NaCl buffer) (Bucher et al., 1980) allowing a good stability of the suspension if no spontaneous aggregation of liposomes occurs (Torchilin and Weissig, 2003). Thus, the phase separation observed in **Figure 2** for low HA concentrations is due to the addition of HA.

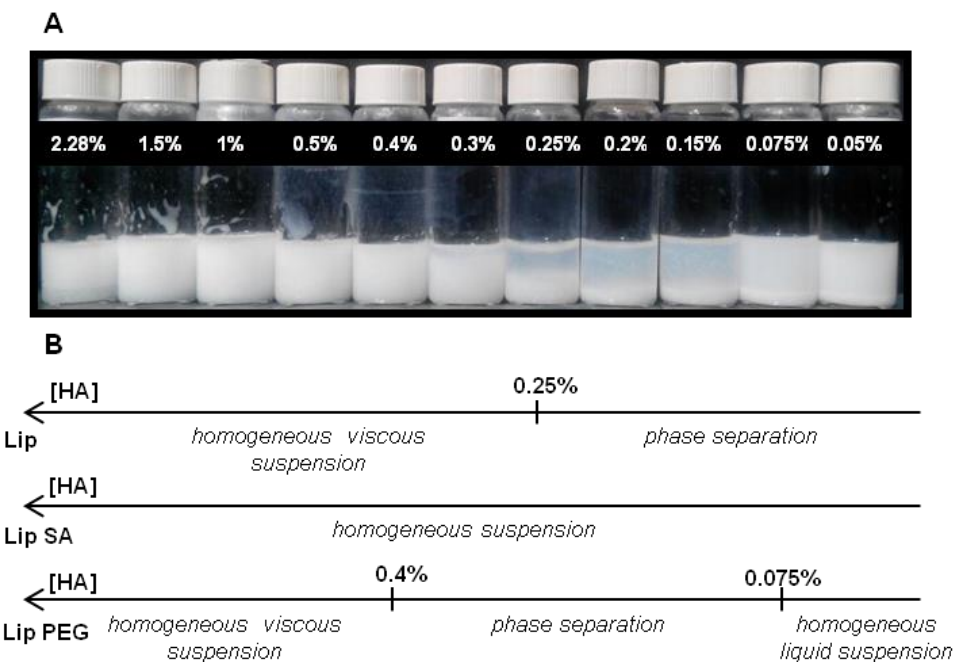


**Fig. 2.** Phase behavior of HA liposomal formulations. A: image taken 36 h after preparation of HA solutions (0.05 to 2.28% w/v) containing 80 mM Lip showing phase separation below a 0.25% HA concentration. B: Macroscopic observation of phase behavior for HA (0.05 to 2.28%) containing 80 mM of each Lip, Lip SA and Lip PEG 36 h after preparation. No phase separation observed with HA-Lip SA over the whole HA concentration range but a thin water layer was observed at 2.28% at the surface of the sample. Phase separation was observed with HA-Lip PEG between 0.075 and 0.4% of HA. The samples were stored at 4°C.

Phase separation was widely described for different colloid-polymer mixtures such as nanocomposites or polymeric particles, lipid vesicles dispersed within polymer solutions as well as nanoemulsions (Poon, 1998, Tuinier et al., 2003, Hooper and Schweizer, 2006, Pelissetto and Hansen, 2006, Huh et al., 2007; 2011). As mentioned previously, a crucial parameter characterizing the mixture of colloids and polymers is the size ratio  $\lambda = R_c/R_g$  between the colloid ( $R_c$ ) and the polymer coil ( $R_g$ ). In the present study, the mixture of liposomes ( $R_c = 75$  nm) and HA ( $R_g = 100$  nm) is in the case  $\lambda < 1$  ( $\lambda = 0.75$ ). The phase separation can be explained by a depletion mechanism in which interparticle attractions can be induced *via* the polymer excluded from the space between particles that pushes them together by osmotic pressure (Asakura and Oosawa, 1954, Vrij, 1976). In our study, depletion effect is likely to cause segregative phase separation for HA-Lip, HA-Lip PG and HA-Lip PEG mixtures. However, there are electrostatic attractive interactions, in addition to depletion, between the positively charged liposomes (Lip SA) and the negatively charged HA for which

no segregative macroscopic phase separation was observed over the entire HA concentration range studied (HA-Lip SA, **Fig. 2B**), whereas a slight syneresis was observed for HA-Lip SA at 2.28% HA concentration.

The mixtures of vesicles and polymers described in the literature were usually polyelectrolytes and oppositely charged colloids or hydrophobically modified polymers (associative polymers) and lipid vesicles (Huh et al., 2007, Antunes et al., 2009, Huh et al., 2011). In most of the previous studies, the mixtures were in the dilute concentration regime of the polymer. In the present study, the mixtures of HA and liposomes were studied in the semi-dilute unentangled regime ( $C^* < C < C_e$ ) and in the entangled regime ( $C > C_e$ ).

Overall, no phase separation was observed macroscopically for HA liposomal mixtures at high HA concentration (above the entanglement concentration  $C_e = 0.4\%$  w/v) possibly because of the high viscosity of the formulations (**Table 2**) and their viscoelasticity (El Kechai et al., 2015) that significantly slow down the dynamic of the system thereby allowing kinetic stability. For this reason, the structure of HA at 2.28% containing different liposome formulations was also studied microscopically.

**Table 2**

Rheological and diffusion properties of HA liposomal formulations.

[HA] %	Liposomes	[Lipids] mM	$\eta_0^a$ (Pa.s)	$\alpha^b$	$D_w/D_{HA}^c$	Median $\log_{10}$ (MSD $\tau = 1s$ )
0.25	Lip	80	$0.04 \pm 0.01$	0.03	106	-2.12
	Lip SA	80	$0.05 \pm 0.01$	0.01	444	-2.22
	Lip PG	80	na	0.42	30	-0.33
	Lip PEG	80	$0.08 \pm 0.01$	0.31	67	-0.68
	Lip PEG	10	na	0.69	26	-0.21
2.28	Lip	80	$245 \pm 38$	$8.5 \times 10^{-4}$	7126	-3.23
	Lip SA	80	$319 \pm 33$	$9.8 \times 10^{-5}$	6613	-3.07
	Lip PG	80	$436 \pm 22$	$1.1 \times 10^{-3}$	1226	-2.75
	Lip PEG	80	$786 \pm 67$	$5.0 \times 10^{-3}$	946	-2.75
	Lip PEG	10	$109 \pm 11$	$7.1 \times 10^{-3}$	582	-2.03

<sup>a</sup>  $\eta_0$  is the zero-shear rate viscosity representing the viscosity at rest of the HA liposomal formulations at 37°C.

<sup>b</sup>  $\alpha$  is the slope of the logarithmic average MSD versus time scale curve. Brownian diffusion is represented by  $\alpha = 1$ , whereas a decrease in  $\alpha$  indicates an increased hindrance to diffusion. A particle is completely immobile when  $\alpha = 0$ .

<sup>c</sup>  $D_w$  is the theoretical diffusion of liposomes in water calculated from the Stokes-Einstein equation using the average liposome diameter of each liposome formulation.  $D_{HA}$  is the effective diffusion of liposomes in HA at a time scale of 1 s. The ratio  $D_w/D_{HA}$  indicates by which factor the movements of liposomes in HA are slower than in water.

### 3.4. Microscopic structure of HA liposomal mixtures

A micro-phase separation between HA and liposomes was observed with both confocal microscopy and AFM.

#### 3.4.1. Confocal microscopy

For confocal microscopy experiments, HA was labeled with fluorescein (green) and liposomes with rhodamine (red). For each HA liposomal mixture, three different samples were observed at different locations and with various magnifications. The microscopic aspect for each HA, HA-Lip, HA-Lip SA, HA-Lip PG and HA-Lip PEG samples analyzed was equivalent over the entire surface of the sample.

Confocal image of HA solution (2.28%) without liposomes (**Fig. 3A**), shows a homogeneous green fluorescence. In presence of neutral, negatively charged or PEGylated liposomes (HA-Lip, HA-Lip PG and HA-Lip PEG, **Fig. 3 B, D, E** respectively), distinguishable and non-overlapping red and green fluorescences are observed indicating segregation between HA and liposomes. In **Figure 3C** (Lip SA), beside the red and the green fluorescence, non-fluorescent zones were also observed. As mentioned previously, due to the attractive electrostatic interactions between negatively charged HA and positively charged liposomes, densely packed mixed aggregates are likely to be formed and might expulse some water that appears as non-fluorescent zones in **Figure 3C**. Moreover, the attractive attractions between HA and liposomes could increase the permeability of the lipid bilayer resulting in the release of a part of the aqueous content of the liposomes. This could explain the syneresis phenomenon observed macroscopically for HA-Lip SA (section 3.3).

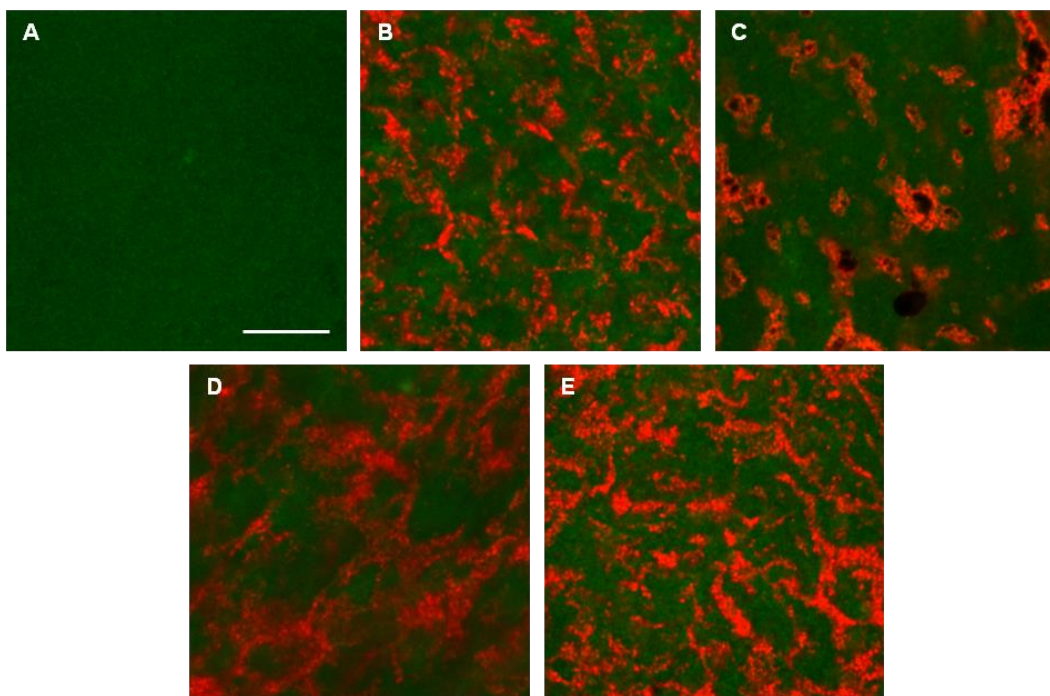


**Fig. 3.** Confocal images of HA liposomal formulations: HA without liposomes (A), HA-Lip (B), HA-Lip SA (C), HA-Lip PG (D) and HA-Lip PEG (E). HA was labeled with fluoresceinamine (green) and liposomes were labeled with rhodamine (red). The final concentrations were 2.28% for HA (10% HA-fl and 90% unlabeled HA) and 80 mM for liposomes (10% liposomes-Rh and 90% unlabeled liposomes). Scale bar = 10 µm.

#### 3.4.2. Atomic force microscopy (AFM)

1 x 1 µm AFM images showed vesicle-like shapes only in HA liposomal mixtures (data not shown). These objects were identified as liposomes as their size was comparable to that of the liposomes prepared (between 100 and 200 nm). From these data, the high dissipation property that appears as clear zones on AFM images in dissipation mode was attributed to liposomes, whereas the dark zones, corresponding to low dissipation areas, were attributed to HA (**Fig. 4**). In order to observe the segregation between HA and liposomes, the samples were imaged under a larger scale (**Fig. 4**). HA displayed uniform mechanical properties (**Fig. 4B**) represented by an unimodal dissipation peak (**Fig. 4C**). Conversely, all HA liposomal mixtures (HA-Lip, HA-Lip SA, HA-Lip PG, HA-Lip PEG) presented two zones with distinguishable mechanical properties: a liposome-rich area represented by clear (low dissipation) zones dispersed within a dark (high dissipation) network corresponding to HA (**Fig. 4B**). The segregation between HA and liposomes was represented by a bimodal distribution of the dissipation as shown in **Fig. 4C**. A dissipation profile was determined for

each formulation by taking a diagonal line in dissipation images (**Fig. 4B**). This allows measuring approximately the range of size of the liposome aggregates. If we compare the different liposomal mixtures, HA-Lip seems to exhibit more and smaller liposome-rich areas (between 0.14 and 0.57  $\mu\text{m}$ ), whereas HA-Lip SA presents larger liposome-rich areas (between 0.21 and 2.12  $\mu\text{m}$ ). Aggregate sizes of HA-Lip PG (between 0.14 and 0.68  $\mu\text{m}$ ) were close to that of HA-Lip. For Lip PEG, the contrast between the two kinds of areas is less clear than for the others and aggregate sizes were between 0.17 and 1.08  $\mu\text{m}$ .

The Young modulus measured from AFM experiments based on the DMT model (Derjaguin et al., 1975) was found to be 25-35 MPa for the liposome-rich phase and around 130-150 MPa for the HA-rich phase. These values were obtained by taking a Poisson's ratio  $\nu = 0.4$ .

From both confocal and AFM images, the microstructure of HA-Lip, HA-Lip SA and HA-Lip PG exhibits aggregates of liposomes homogeneously dispersed within a HA network. For HA-Lip PEG the microstructure seems to be slightly different on AFM images and could be assimilated to bicontinuous interpenetrating networks of HA and PEGylated liposomes. Huh et al. (2011) reported a similar organization for cationic vesicles of 256 nm diameter dispersed within a cationic polymer ( $R_g = 11.2 \text{ nm}$ ,  $C < C_e$ ) using confocal microscopy. They also demonstrated that the compactness of the polymer network and the size of the polymer-rich areas increase with the polymer concentration. For HA liposomal mixtures, the formation of this microstructure is probably due to the depletion effect mentioned previously that trigger the aggregation of liposomes upon addition of HA (Huh et al., 2011).

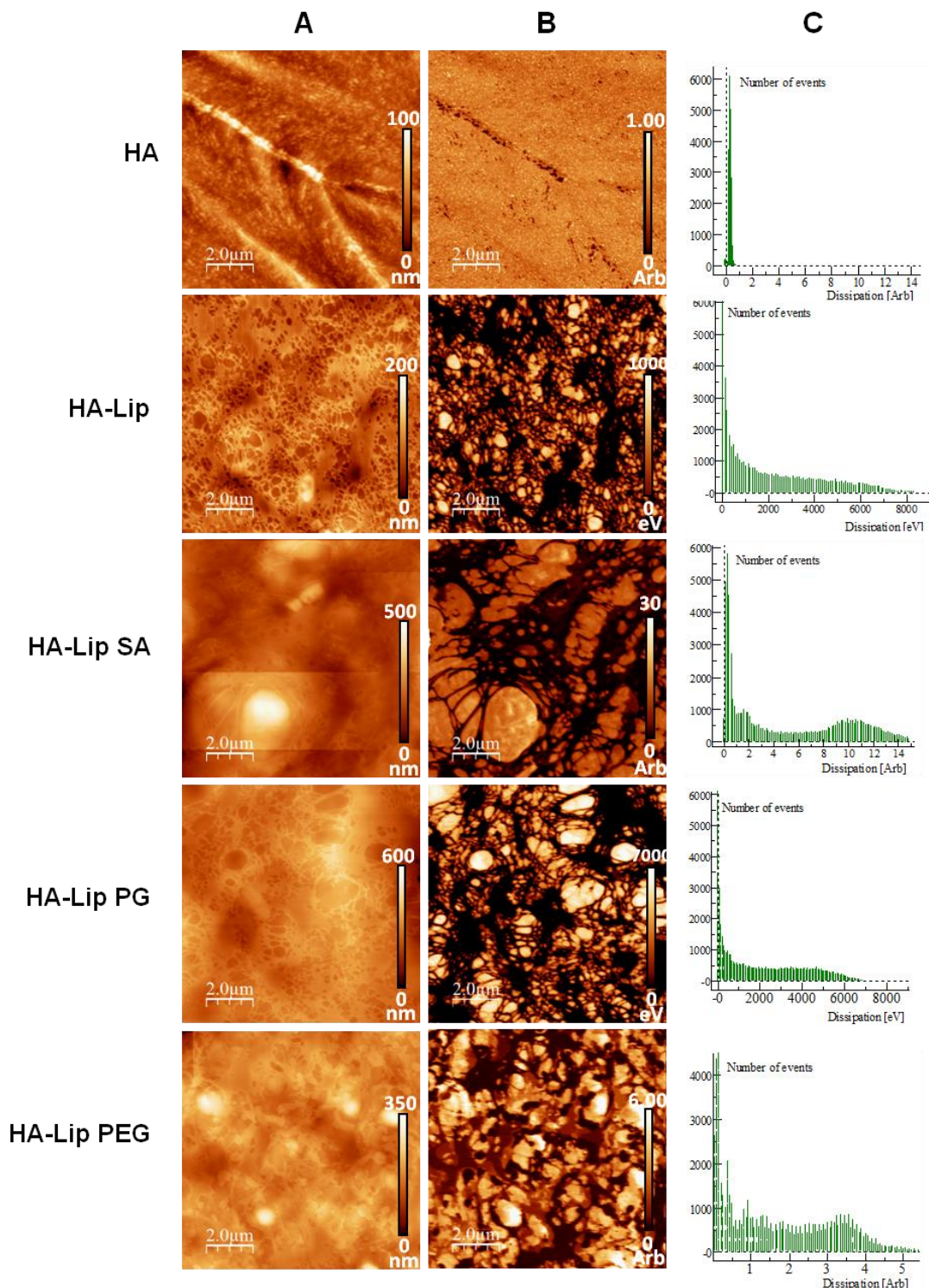


**Fig. 4.** AFM characterization of HA without liposomes and HA liposomal mixtures (HA-Lip, HA-Lip SA, HA-Lip PG, HA-Lip PEG). AFM images at a 10 μm scan range in topographic mode (A) and dissipation mode (B). The dissipation profile of the different samples was represented in column (C). Scale bar = 2 μm.

### 3.5. Mobility of liposomes into HA

The diffusion of liposomes with different surface characteristics was assessed both macroscopically using optical analysis and microscopically using single particle tracking.

#### 3.5.1. *Turbiscan® optical analysis of the migration of liposomes into HA*

The principle of the experiment was based on the migration of the liposomes deposited at the surface of a HA sample (2.28%), resulting in a variation of transmission and back scattering signals. **Figure 5B** gives the variations of the percent of light transmitted across the whole sample height. At  $t_0$ , the 4-mL transparent HA sample (height around 25 cm) resulted in almost 100% of light transmission (**Fig. 5B**). The addition of the white opaque liposome suspensions (Lip, Lip SA, Lip PG or Lip PEG, each at 80 mM) led to a sharp decrease in light transmission at the surface of the sample (height between 25 and 35 mm). Only PEGylated liposomes (Lip PEG) were able to migrate into HA. For this formulation, a migration front was observed macroscopically (**Fig. 5A**) and by optical analysis (**Fig. 5B**) starting from  $t_1$ . Lip PEG showed a rapid migration into HA within the first 24 h ( $t_1$ ) whereas their migration was slower between  $t_1$  and  $t_{10}$ . The other formulations showed no migration towards the bottom of the tube. However, a displacement of the liposome front towards the surface was observed starting from the first time point  $t_1$ , which was stable between  $t_1$  and  $t_{10}$ , and can be explained by swelling of HA because of the water in the liposome suspension deposited on its surface at  $t_0$  (**Fig. 5C**).

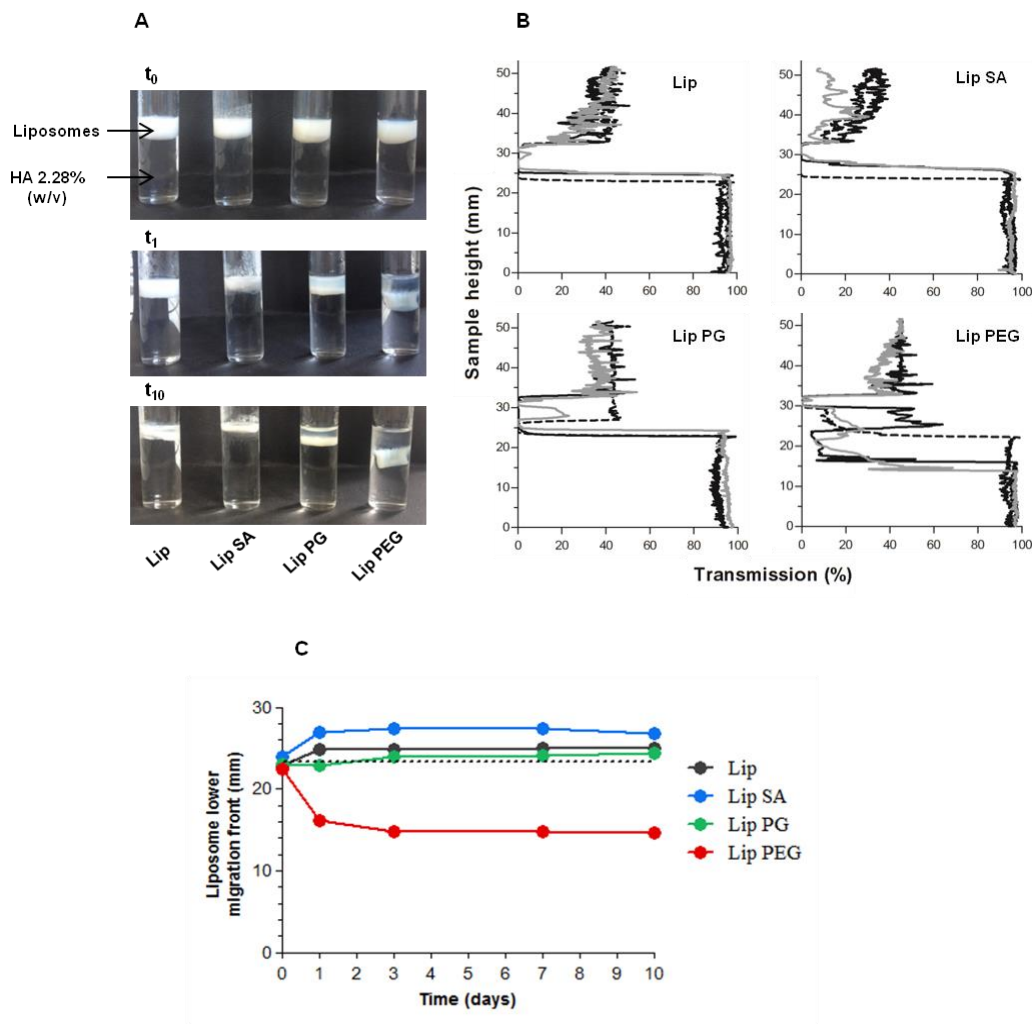


**Fig. 5.** Migration of the different liposome formulations into HA solution (2.28% w/v). A: Macroscopic observation. B: Turbiscan® optical analysis showing the % of light transmitted across the samples at  $t_0$  (discontinuous, black),  $t_1$  (continuous, black) and  $t_{10}$  (grey). C: Liposome lower migration fronts for the different liposomes as function of time obtained from optical analysis. The discontinuous line represents the position of liposomes at  $t_0$  (~ 23 mm).

### 3.5.2. Microscopic mobility of liposomes in HA

Single particle tracking was used to quantitatively assess the diffusion of neutral (Lip), positively (Lip SA) or negatively charged (Lip PG) and PEGylated liposomes (Lip PEG) into HA solution at two different concentrations. The lowest HA concentration (0.25% w/v) was below the entanglement concentration ( $C_e = 0.4\%$  w/v) whereas the highest one (2.28% w/v) was well above. Whatever their composition, liposome movements in HA 2.28% were strongly hindered compared to their movements in HA 0.25% (w/v). This was demonstrated

by significantly lower MSD and  $\alpha$  values in HA 2.28% (w/v) compared to 0.25% (Table 2, **Fig. 6C** compared to **6A**) and highly constrained trajectories in HA 2.28% (**Fig. 6D** compared to **6B**). The liposomes with different surface characteristics (80 mM) displayed different diffusion profiles but followed the same trend in both HA 0.25 and 2.28% (Lip PEG = Lip PG > Lip > Lip SA, **Fig. 6** and **Table 2**).

At 0.25% of HA, Lip PEG and Lip PG, which are both negatively charged, displayed the best diffusion properties, evidenced by their extended trajectories (**Fig. 6B**) and relatively high MSD (**Fig. 6A**). In addition,  $\alpha$  values for Lip PEG and Lip PG were 0.31 and 0.42 respectively and their diffusion in HA 0.25% was only 30- and 67-fold lower than their theoretical diffusion in water (**Table 2**). Conversely, neutral (Lip) and positively charged liposome (Lip SA) movements were hindered in HA 0.25% with the lowest mobility for Lip SA. This was demonstrated by constrained trajectories (**Fig. 6B**), reduced MSD (**Fig. 6A**) and  $\alpha$  values close to 0 (0.03 for Lip SA and 0.01 for Lip). Overall, the MSD plot for individual liposomes showed quite narrow distributions except for Lip and Lip SA in 0.25% HA where a wider distribution was obtained (**Fig. 7**).

Basically, two factors can influence the diffusion of molecules or particles in a polymeric network. First, the diffusion depend on physicochemical interactions between the diffusing molecule or particle and the polymer chains in the network. Second, diffusion is influenced by the steric hindrance which depends on both size and shape of the diffusing molecule or particle (Phillies and Clomenil, 1993) and the network structure of the polymer solutions (De Smedt et al., 1994). Indeed, particles that are smaller than the mesh size formed by the entangled polymer chains are supposed to rapidly diffuse through the polymer network, whereas particles larger than the pores are sterically trapped within the network (Braeckmans et al., 2010, Xu et al., 2013).

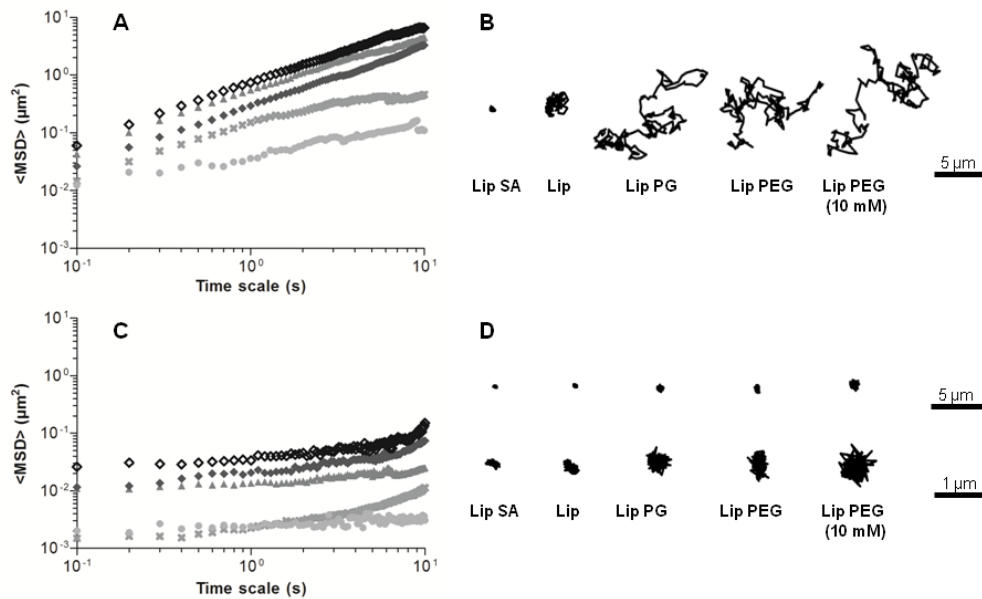


**Fig. 6.** Mobility of liposomes in HA solutions. A and C: averaged MSD as function of time scale for 80 mM Lip (●), Lip SA (x), Lip PG( ▲), Lip PEG( ◆) and 10 mM Lip PEG (◇) in HA solutions at 0.25% (A) or 2.28% (C). B and D: representative trajectories of the different liposomes in HA at 0.25% (B) or 2.28% (D).

At a concentration below the entanglement concentration of HA (0.25%), liposomes exhibited a more or less rapid diffusion, depending on the formulations, as their movement is slightly hindered by the non-entangled polymer chains that can be seen as obstacles. At 2.28% (above the entanglement concentration), the movement of liposomes was strongly hindered by the HA network. Regarding the microstructure described here for the mixture of liposomes and HA at 2.28% (w/v), and due to the depletion interactions, the liposomes are likely to form aggregates that are trapped into a highly viscoelastic HA network, which reduce their movements.

However, even at 2.28% HA, the PEGylated liposomes were the most mobile among the different liposome formulations both macro- and microscopically. This can be explained by steric repulsions between the PEG chain at the surface of liposomes and HA chains (Sanders et al., 2007) as well as steric repulsions between PEGylated liposomes in the liposome rich-phase allowing liposome movements even at short time scales. The microstructure observed for HA-Lip PEG, which appears to be bicontinuous interpenetrating networks of HA and PEGylated liposomes, can also favor the diffusion of PEGylated liposomes into the liposome network.

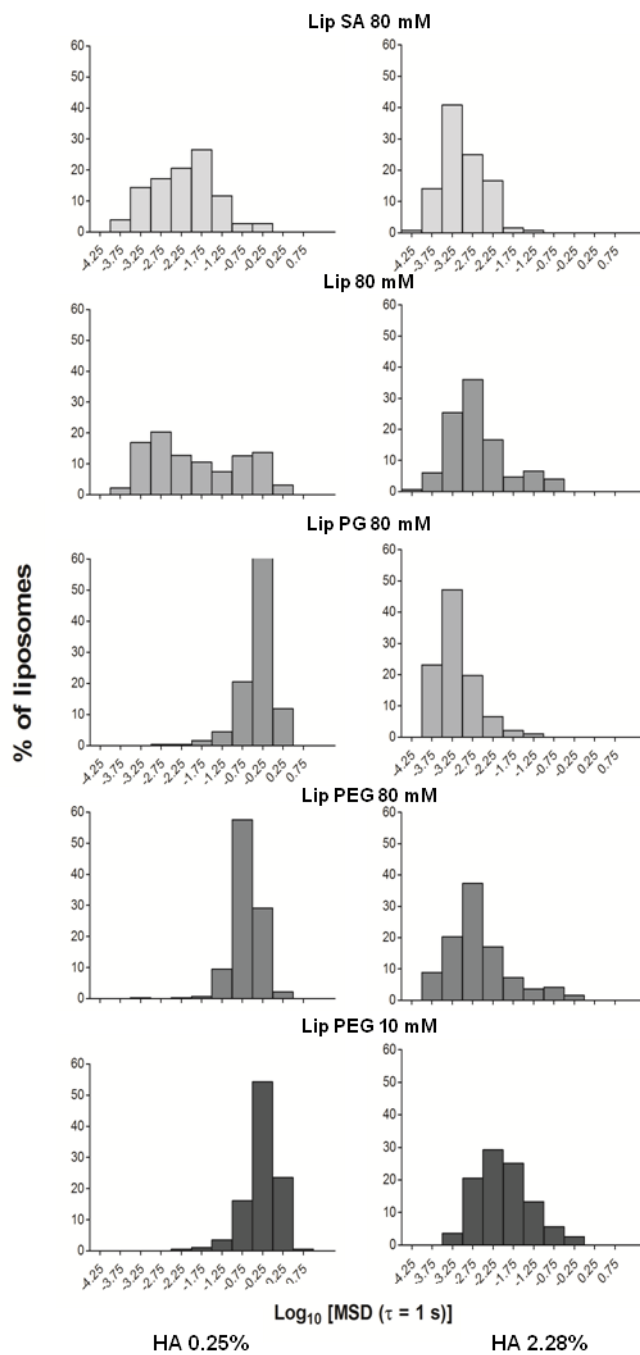


**Fig. 7.** Distributions of the individual logarithms of MSD at a time scale of 1 s for the different liposome formulations in HA at 0.25% (left graphs) or 2.28% (right graphs).

The negative charge at the surface of liposomes (Lip PG), providing electrostatic repulsions with the negatively charged carboxylate groups of HA, resulted in a diffusion profile close to that of the PEGylated liposomes microscopically and at short time scales. However, this was not confirmed macroscopically (Fig. 5). Conversely, positively charged liposomes should interact with HA by electrostatic attractions and complexation that led to an important

immobilization of those liposomes even at low HA concentration. The hydrophobic surface of neutral liposomes (Lip) can potentially interact with HA by binding the hydrophobic regions along the HA chain (Heatley and Scott, 1988, Scott et al., 1991), which also led to slow down the diffusion of those liposomes compared to the PEGylated and/or negatively charged liposomes.

These results are in good agreement with those of Martens et al. (2013) and Xu et al. (2013) who both demonstrated *ex vivo* that PEG-coated or negatively charged nanoparticles freely diffused in the vitreous, which contains a high concentration of HA, while positively charged nanoparticles with similar size were completely immobilized. Lajavardi et al. (2009) also observed the mobility of PEGylated liposomes into the vitreous *in vivo*. PEGylation is a well-known strategy to improve the colloidal stability of nanoparticles and to reduce interactions with biopolymers (Sanders et al., 2007). Furthermore, PEGylated nanoparticles are also known as “mucus penetrating particles” due to their ability to overcome the mucus barrier for drug and gene delivery (Lai et al., 2009). The mucus is mainly composed of mucine, which is a high molecular weight glycoprotein that provides to the mucus a high negative charge.

On the other hand, we assessed the effect of lipid concentration on PEGylated liposomes mobility into HA. For both HA concentrations, the reduction of lipid concentration from 80 to 10 mM led to a 2-fold increase in liposome mobility for HA 0.25% and a 1.5-fold increase for HA 2.28% (**Table 2**). This can be explained by a reduced number of liposomes at 10 mM resulting in less steric hindrance due to the close-packing of concentrated liposomes at 80 mM.

It is worth noting that HA chains in solution form a transient network where they are in permanent movement (De Smedt et al., 1994, Masuda et al., 2001). Thus, the mesh size and the shape of the HA network will continuously change within its lifetime and thus, may adapt depending on the interactions with molecules or colloids dispersed within the network. Due to this dynamical effect, the effective pore size for the diffusion of liposomes may be significantly larger than the theoretical one (7 - 11 nm for HA 2.28%). This also indicates that the microstructure formed by the mixtures of liposomes and HA is transient and in permanent movement. Thus, depending on the nature of the interactions between HA and liposomes, this dynamic structure may allow a better diffusion of liposomes at longer time scales.

#### **4. Conclusion**

The aim of this work was to characterize the physicochemical properties of HA-liposomal mixtures in aqueous media regarding phase behavior, microstructure and mobility of liposomes. The entanglement concentration of HA was determined to be 0.4% (w/v). Liposomes dispersed within HA exhibited phase separation at low HA concentration except for the positively charged ones. At high HA concentration, the microstructure seems to be either aggregates of liposomes into HA network (HA-Lip, HA-Lip SA, HA-Lip PG) or bicontinuous interpenetrating networks of HA and liposome aggregates (HA-Lip PEG) probably driven by depletion interactions. The diffusion of liposomes was controlled by the concentration of HA, the concentration and the surface characteristics of liposomes. Finally, PEGylated liposomes displayed the best mobility into HA at high concentration both macro- and microscopically. The diffusion of liposomes is a key parameter for drug delivery since their migration into HA, as a suspending or a biological media, allows them either to serve as a reservoir of drug at the injection site or to reach the target cells or tissues to deliver the encapsulated drug. The microstructure of the HA-liposomes mixtures, especially the influence of HA on the structure of liposomes, could be further investigated using X-ray scattering (SAXS) or neutron scattering (SANS).

#### **Acknowledgments**

This work was supported by a PhD grant (Naila El Kechai) from the French Ministry of National Education and Research. Authors wish to thank “la Région Ile-de-France” for the purchase of the confocal microscope that served in this study.

## References

- Antunes, F.E., Marques, E.F., Miguel, M.G., Lindman, B., 2009. Polymer–vesicle association. *Advances in Colloid and Interface Science.* 147, 18-35.
- Asakura, S., Oosawa, F., 1954. On interaction between two bodies immersed in a solution of macromolecules. *Chemical Physics.* 1255-1256.
- Barber, P., Balasubramanian, S., Anguchamy, Y., Gong, S., Wibowo, A., Gao, H., Ploehn, H., Zur Loyer, H.-C., 2009. Polymer Composite and Nanocomposite Dielectric Materials for Pulse Power Energy Storage. *Materials.* 2, 1697.
- Barbucci, R., Lamponi, S., Borzacchiello, A., Ambrosio, L., Fini, M., Torricelli, P., Giardino, R., 2002. Hyaluronic acid hydrogel in the treatment of osteoarthritis. *Biomaterials.* 23, 4503-4513.
- Bolhuis, P., Louis, A., Hansen, J., 2002. Influence of polymer-excluded volume on the phase-behavior of colloid-polymer mixtures. *Physical Review Letters.* 89, 128302.
- Braeckmans, K., Buyens, K., Bouquet, W., Vervaet, C., Joye, P., Vos, F.D., Plawinski, L., Doeuvre, L., Angles-Cano, E., Sanders, N.N., Demeester, J., Smedt, S.C.D., 2010. Sizing Nanomatter in Biological Fluids by Fluorescence Single Particle Tracking. *Nano Letters.* 10, 4435-4442.
- Bucher, D.J., Kharitonenkova, I.G., Zakomirdin, J.A., Grigoriev, V.B., Klimenko, S.M., Davis, J.F., 1980. Incorporation of influenza virus M-protein into liposomes. *Journal of Virology.* 36, 586-590.
- Cross, M.M. 1968. Polymer systems: deformation and flow. London, MacMillan.
- de Gennes, P.-G. 1979. Scaling concepts in polymer physics. Cornel University Press.
- De Smedt, S.C., Dekeyser, P., Ribitsch, V., Lauwers, A., Demeester, J., 1993. Viscoelastic and transient network properties of hyaluronic acid as a function of the concentration. *Biorheology.* 30, 31-41.
- De Smedt, S.C., Lauwers, A., Demeester, J., Engelborghs, Y., De Mey, G., Du, M., 1994. Structural information on hyaluronic acid solutions as studied by probe diffusion experiments. *Macromolecules.* 27, 141-146.
- Derjaguin, B.V., Muller, V.M., Toporov, Y.P., 1975. Effect of contact deformations on the adhesion of particles. *Journal of Colloid and Interface Science.* 53, 314-326.
- El Kechai, N., Bochot, A., Huang, N., Nguyen, Y., Ferry, E., Agnely, F., 2015. Effect of liposomes on rheological and syringeability properties of hyaluronic acid hydrogels intended for local injection of drugs. *Int J Pharm.* 487, 187-196.
- El Kechai, N., Bochot, A., Huang, N., Nguyen, Y., Ferry, E., Agnely, F., 2015. Effect of liposomes on rheological and syringeability properties of hyaluronic acid hydrogels intended for local injection of drugs. *International Journal of Pharmaceutics.* 487, 187-196.
- Esquenet, C., Buhler, E., 2002. Aggregation Behavior in Semidilute Rigid and Semirigid Polysaccharide Solutions. *Macromolecules.* 35, 3708-3716.
- Gatej, I., Popa, M., Rinaudo, M., 2005. Role of the pH on Hyaluronan Behavior in Aqueous Solution. *Biomacromolecules.* 6, 61-67.

- Hadipour, A., de Boer, B., Wildeman, J., Kooistra, F.B., Hummelen, J.C., Turbiez, M.G.R., Wienk, M.M., Janssen, R.A.J., Blom, P.W.M., 2006. Solution-Processed Organic Tandem Solar Cells. *Advanced Functional Materials.* 16, 1897-1903.
- Hamidi, M., Azadi, A., Rafiei, P., 2008. Hydrogel nanoparticles in drug delivery. *Adv Drug Deliv Rev.* 60, 1638-1649.
- Heatley, F., Scott, J.E., 1988. A water molecule participates in the secondary structure of hyaluronan. *Biochem J.* 254, 489-493.
- Hooper, J.B., Schweizer, K.S., 2005. Contact aggregation, bridging, and steric stabilization in dense polymer-particle mixtures. *Macromolecules.* 38, 8858-8869.
- Hooper, J.B., Schweizer, K.S., 2006. Theory of Phase Separation in Polymer Nanocomposites. *Macromolecules.* 39, 5133-5142.
- Huh, J.Y., Lynch, M.L., Furst, E.M., 2007. Microscopic structure and collapse of depletion-induced gels in vesicle-polymer mixtures. *Physical Review E.* 76, 051409.
- Huh, J.Y., Lynch, M.L., Furst, E.M., 2011. Poroelastic Consolidation in the Phase Separation of Vesicle-Polymer Suspensions. *Industrial & Engineering Chemistry Research.* 50, 78-84.
- Hurler, J., Zakelj, S., Mravljak, J., Pajk, S., Kristl, A., Schubert, R., Skalko-Basnet, N., 2013. The effect of lipid composition and liposome size on the release properties of liposomes-in-hydrogel. *Int J Pharm.* 456, 49-57.
- Huynh, W.U., Dittmer, J.J., Alivisatos, A.P., 2002. Hybrid nanorod-polymer solar cells. *Science.* 295, 2425-2427.
- Krause, W.E., Bellomo, E.G., Colby, R.H., 2001. Rheology of Sodium Hyaluronate under Physiological Conditions. *Biomacromolecules.* 2, 65-69.
- Lai, S.K., Wang, Y.-Y., Hanes, J., 2009. Mucus-penetrating nanoparticles for drug and gene delivery to mucosal tissues. *Adv Drug Deliv Rev.* 61, 158-171.
- Lajavardi, L., Camelo, S., Agnely, F., Luo, W., Goldenberg, B., Naud, M.-C., Behar-Cohen, F., de Kozak, Y., Bochot, A., 2009. New formulation of vasoactive intestinal peptide using liposomes in hyaluronic acid gel for uveitis. *Journal of Controlled Release.* 139, 22-30.
- Lapčík, L., Lapčík, L., De Smedt, S., Demeester, J., Chabreček, P., 1998. Hyaluronan: Preparation, Structure, Properties, and Applications. *Chem Rev.* 98, 2663-2684.
- Lin, Y., Boker, A., He, J., Sill, K., Xiang, H., Abetz, C., Li, X., Wang, J., Emrick, T., Long, S., Wang, Q., Balazs, A., Russell, T.P., 2005. Self-directed self-assembly of nanoparticle/copolymer mixtures. *Nature.* 434, 55-59.
- Martens, T.F., Vercauteren, D., Forier, K., Deschout, H., Remaut, K., Paesen, R., Ameloot, M., Engbersen, J.F.J., Demeester, J., De Smedt, S.C., Braeckmans, K., 2013. Measuring the intravitreal mobility of nanomedicines with single-particle tracking microscopy. *Nanomedicine (Lond).* 8, 1955-1968.
- Masuda, A., Ushida, K., Koshino, H., Yamashita, K., Kluge, T., 2001. Novel Distance Dependence of Diffusion Constants in Hyaluronan Aqueous Solution Resulting from Its Characteristic Nano-Microstructure. *Journal of the American Chemical Society.* 123, 11468-11471.
- Meller, A., Gisler, T., Weitz, D.A., Stavans, J., 1999. Viscoelasticity of depletion-induced gels in emulsion-polymer systems. *Langmuir.* 15, 1918-1922.

- Meller, A., Stavans, J., 1996. Stability of emulsions with nonadsorbing polymers. *Langmuir*. 12, 301-304.
- Morfin, I., Buhler, E., Cousin, F., Grillo, I., Boué, F., 2011. Rodlike complexes of a polyelectrolyte (hyaluronan) and a protein (lysozyme) observed by SANS. *Biomacromolecules*. 12, 859-870.
- Oelschlaeger, C., Cota Pinto Coelho, M., Willenbacher, N., 2013. Chain Flexibility and Dynamics of Polysaccharide Hyaluronan in Entangled Solutions: A High Frequency Rheology and Diffusing Wave Spectroscopy Study. *Biomacromolecules*. 14, 3689-3696.
- Pelissetto, A., Hansen, J.-P., 2006. An Effective Two-Component Description of Colloid-Polymer Phase Separation. *Macromolecules*. 39, 9571-9580.
- Phillies, G.D.J., Clomenil, D., 1993. Probe diffusion in polymer solutions under  $\Theta$  and good conditions. *Macromolecules*. 26, 167-170.
- Poon, W.C.K., 1998. Phase separation, aggregation and gelation in colloid-polymer mixtures and related systems. *Current Opinion in Colloid & Interface Science*. 3, 593-599.
- Sanders, N.N., Peeters, L., Lentacker, I., Demeester, J., De Smedt, S.C., 2007. Wanted and unwanted properties of surface PEGylated nucleic acid nanoparticles in ocular gene transfer. *Journal of Controlled Release*. 122, 226-235.
- Scott, J.E., Cummings, C., Brass, A., Chen, Y., 1991. Secondary and tertiary structures of hyaluronan in aqueous solution, investigated by rotary shadowing-electron microscopy and computer simulation. Hyaluronan is a very efficient network-forming polymer. *Biochem J*. 274 ( Pt 3), 699-705.
- Scott, J.E., Heatley, F., 1999. Hyaluronan forms specific stable tertiary structures in aqueous solution: A  $^{13}\text{C}$  NMR study. *Proceedings of the National Academy of Sciences*. 96, 4850-4855.
- Shenoy, V., Rosenblatt, J., Vincent, J., Gaigalas, A., 1995. Measurement of mesh sizes in concentrated rigid and flexible polyelectrolyte solutions by an electron spin resonance technique. *Macromolecules*. 28, 525-530.
- Suh, J., Dawson, M., Hanes, J., 2005. Real-time multiple-particle tracking: applications to drug and gene delivery. *Adv Drug Deliv Rev*. 57, 63-78.
- Torchilin, V., Weissig, V. 2003. Liposomes: a practical approach. Oxford University Press.
- Tuinier, R., De Kruif, C., 1999. Phase separation, creaming, and network formation of oil-in-water emulsions induced by an exocellular polysaccharide. *Journal of Colloid and Interface Science*. 218, 201-210.
- Tuinier, R., Rieger, J., de Kruif, C.G., 2003. Depletion-induced phase separation in colloid-polymer mixtures. *Advances in Colloid and Interface Science*. 103, 1-31.
- Volpi, N., Schiller, J., Stern, R., Soltes, L., 2009. Role, Metabolism, Chemical Modifications and Applications of Hyaluronan. *Current Medicinal Chemistry*. 16, 1718-1745.
- Vrij, A., 1976. Polymers at interfaces and the interactions in colloidal dispersions. *Pure and Applied Chemistry*. 48, 471-483.
- Xu, Q., Boylan, N.J., Suk, J.S., Wang, Y.-Y., Nance, E.A., Yang, J.-C., McDonnell, P.J., Cone, R.A., Duh, E.J., Hanes, J., 2013. Nanoparticle diffusion in, and microrheology of, the bovine vitreous *ex vivo*. *Journal of Controlled Release*. 167, 76-84.

Yaklin, M.A., Duxbury, P.M., Mackay, M.E., 2008. Control of nanoparticle dispersion in thin polymer films. *Soft Matter.* 4, 2441-2447.

# **Travaux expérimentaux**

*Deuxième partie*

**Évaluation *in vivo* du gel de liposomes  
encapsulant un corticoïde**

## ***Deuxième partie***

### **Evaluation *in vivo* du gel de liposomes encapsulant un corticoïde**

#### **Introduction**

A l'issue de la caractérisation physicochimique du gel d'acide hyaluronique contenant différentes formulations de liposomes (première partie), la formulation de liposomes PEGylés (EPC:Chol:DSPE-PEG2000, 60:35:5 mole %) a été retenue pour encapsuler la dexamethasone phosphate (DexP) et pour développer un système pour l'administration intratympanique. En effet, dispersés au sein du gel d'acide hyaluronique, les liposomes PEGylés ont permis d'obtenir une viscosité et une élasticité plus élevées comparées aux autres formulations et ce, tout en restant injectables à travers des aiguilles fines et longues (Chapitre I). De plus, cette formulation de liposomes a montré une aptitude à diffuser au sein du gel d'HA 2.28% aux échelles macro- et microscopique (Chapitre II), ce qui nous permettra d'évaluer par la suite leur aptitude à diffuser à travers la fenêtre ronde. La concentration de lipides choisie (80 mM) est une concentration élevée. Celle-ci permet, d'une part, d'augmenter davantage la viscosité du gel (Chapitre I) afin de permettre un temps de résidence prolongé dans l'oreille moyenne et, d'autre part, de maximaliser le taux d'encapsulation de la molécule active pour ainsi optimiser la dose de substance active administrée.

Le dexamethasone phosphate (DexP) a été retenue comme substance active modèle pour l'évaluation *in vivo*. La dexamethasone est un corticoïde doté d'un puissant effet anti-inflammatoire qui est très utilisé en otologie clinique (McCall et al., 2010, Li et al., 2013). Cette molécule diffuse facilement à travers la fenêtre ronde et sert de molécule modèle en recherche préclinique (Swan et al., 2008) pour tester de nouveaux systèmes d'administration (Cf. Travaux antérieurs). C'est aussi la molécule pour laquelle la pharmacocinétique dans l'oreille interne est la mieux décrite sur des modèles animaux (Salt and Plontke, 2005, Salt, 2008, Borden et al., 2011, Wang et al., 2011). Nous avons choisi d'utiliser la dexamethasone phosphate qui est la forme soluble de la dexamethasone, afin que celle-ci soit encapsulée dans le cœur aqueux des liposomes plutôt que dans la bicouche lipidique. Ceci permet de ne pas modifier les propriétés de surface des liposomes et de préserver les interactions HA-liposomes

PEGylés qui sont à l'origine des propriétés intéressantes du système gel de liposomes PEGylés. Enfin, la DexP est une prodrogue qui devant être métabolisée *in vivo* par voie enzymatique en dexamethasone qui est la forme active responsable de l'effet pharmacologique (Hargunani et al., 2006).

Les études *in vivo* ont été conduites chez le cobaye Hartley albinos. Le cobaye est reconnu par la communauté scientifique internationale pour être l'animal de référence pour les études sur l'audition (Pracy et al., 1998). Ce modèle animal a déjà été validé et utilisé pour d'autres applications en otologie (Tamura et al., 2005, Swan et al., 2008, Eastwood et al., 2010, Wang et al., 2011). Le fait que ces animaux soient normo-entendants permet d'évaluer de façon plus précise l'innocuité des formulations vis-à-vis de la fonction auditive, la protection durant un traumatisme sonore et le traumatisme chirurgical lié à l'implantation cochléaire. Le cobaye présente également l'avantage de posséder une cochlée de taille suffisante (5 mm), avec un tour basal périlymphatique large, permettant d'insérer un porte-électrodes sur le modèle d'implantation cochléaire. Enfin, ces animaux sont résistants aux complications de l'anesthésie et de la chirurgie avec un pourcentage élevé de survie postopératoire.

Dans cette deuxième partie, le gel d'HA à 2.28% contenant 80 mM de liposomes PEGylés est appelé HA-Lip. Celui contenant la DexP encapsulée dans les liposomes PEGylés est appellé HA-DexP-Lip. D'abord, nous avons vérifié l'innocuité de ces formulations vis-à-vis de la fonction auditive des cobayes. Nous avons par la suite étudié la biodistribution des différents composants de la formulation après injection dans l'oreille moyenne. Ces deux études font l'objet du Chapitre III. Ensuite, l'efficacité thérapeutique du gel de liposomes a été évaluée sur deux modèles pathologiques : un modèle de surdité induite par le bruit (traumatisme sonore) (Chapitre IV) et un modèle d'implantation cochléaire (Chapitre V).

Ces expériences ont été réalisées en étroite collaboration avec l'équipe du Dr. Evelyne Ferrary (Chirurgie mini-invasive robotisée, UMR-S 1159 Inserm, Hôpital Bichât et Hôpital de la Pitié-Salpêtrière, Paris). Les études sur le traumatisme sonore ont été conduites en collaboration avec l'équipe du Dr. Jean-Marc Edeline (Laboratoire de Neurobiologie de l'Apprentissage, de la Mémoire et de la Communication, UMR CNRS 8620, Orsay).

## Références

- Borden, R.C., Saunders, J.E., Berryhill, W.E., Kreml, G.A., Thompson, D.M., Queimado, L., 2011. Hyaluronic acid hydrogel sustains the delivery of dexamethasone across the round window membrane. *Audiol Neurotol.* 16, 1-11.
- Eastwood, H., Pinder, D., James, D., Chang, A., Galloway, S., Richardson, R., O'Leary, S., 2010. Permanent and transient effects of locally delivered n-acetyl cysteine in a guinea pig model of cochlear implantation. *Hear Res.* 259, 24-30.
- Hargunani, C.A., Kempton, J.B., DeGagne, J.M., Trune, D.R., 2006. Intratympanic injection of dexamethasone: time course of inner ear distribution and conversion to its active form. *Otol Neurotol.* 27, 564-569.
- Li, L., Ren, J., Yin, T., Liu, W., 2013. Intratympanic dexamethasone perfusion versus injection for treatment of refractory sudden sensorineural hearing loss. *Eur Arch Otorhinolaryngol.* 270, 861-867.
- McCall, A.A., Swan, E.E., Borenstein, J.T., Sewell, W.F., Kujawa, S.G., McKenna, M.J., 2010. Drug delivery for treatment of inner ear disease: current state of knowledge. *Ear Hear.* 31, 156-165.
- Pracy, J., White, A., Mustafa, Y., Smith, D., Perry, M., 1998. The comparative anatomy of the pig middle ear cavity: a model for middle ear inflammation in the human? *Journal of anatomy.* 192, 359-368.
- Salt, A.N., 2008. Dexamethasone concentration gradients along scala tympani after application to the round window membrane. *Otology & neurotology: official publication of the American Otological Society, American Neurotology Society [and] European Academy of Otology and Neurotology.* 29, 401.
- Salt, A.N., Plontke, S.K., 2005. Local inner-ear drug delivery and pharmacokinetics. *Drug Discov Today.* 10, 1299-1306.
- Swan, E.E., Mescher, M.J., Sewell, W.F., Tao, S.L., Borenstein, J.T., 2008. Inner ear drug delivery for auditory applications. *Adv Drug Deliv Rev.* 60, 1583-1599.
- Tamura, T., Kita, T., Nakagawa, T., Endo, T., Kim, T.S., Ishihara, T., Mizushima, Y., Higaki, M., Ito, J., 2005. Drug delivery to the cochlea using PLGA nanoparticles. *Laryngoscope.* 115, 2000-2005.
- Wang, X., Dellamary, L., Fernandez, R., Ye, Q., LeBel, C., Piu, F., 2011. Principles of inner ear sustained release following intratympanic administration. *Laryngoscope.* 121, 385-391.

## **Chapitre III**

**Libération prolongée d'un corticoïde dans l'oreille  
interne à partir d'un gel de liposomes administré  
localement dans l'oreille moyenne**

## **Chapitre III**

### **Libération prolongée d'un corticoïde dans l'oreille interne à partir d'un gel de liposomes administré localement dans l'oreille moyenne**

#### **Introduction - résumé**

L'oreille interne peut être considérée comme l'un des organes les plus difficiles à atteindre lors de l'administration de substances actives par voie systémique (Cf. Travaux antérieurs). Ceci est principalement lié à l'anatomie complexe de l'oreille interne et à la présence de la barrière hémato-pérymphatique. Par conséquent, en otologie, des méthodes d'administration locales, telles que l'injection transtympanique, se développent de plus en plus en alternative à l'administration par voie générale (intraveineuse, intramusculaire, orale) responsable de nombreux effets indésirables. Dans ce chapitre, nous avons évalué l'intérêt du gel d'acide hyaluronique contenant des liposomes pour l'administration prolongée d'un corticoïde, la dexamethasone phosphate (DexP), dans l'oreille interne après administration locale dans l'oreille moyenne.

Lors de l'étude *in vitro*, nous avons déterminé le taux d'encapsulation de la DexP dans les liposomes PEGylés. Le taux obtenu a permis l'administration d'une dose de corticoïde suffisante pour l'étude chez l'animal. Les liposomes ont par ailleurs montré une bonne stabilité dans les conditions de conservation. Pour l'étude *in vivo*, les formulations ont été administrées dans l'oreille moyenne de cobayes en utilisant les aiguilles adaptées à l'injection transtympanique. Nous avons d'abord évalué l'innocuité du gel de liposomes sur la fonction auditive des cobayes. Ensuite, le temps de résidence du gel dans l'oreille moyenne ainsi que l'aptitude des liposomes PEGylés à traverser la fenêtre ronde pour atteindre l'oreille interne ont été étudiés. Enfin, pour déterminer si le système permet d'atteindre une dose thérapeutique dans l'oreille interne et pour évaluer la libération prolongée du corticoïde, la DexP ainsi que sa forme active (la dexamethasone, Dex) ont été quantifiées par LC-MS dans pérylympe à différents temps.

Le gel de liposomes a montré une parfaite innocuité vis-à-vis de la fonction auditive des cobayes. Il a également permis une persistance prolongée dans l'oreille moyenne et sur la fenêtre ronde. La présence de liposomes dans la formulation a abouti à une libération prolongée du corticoïde dans la périlymphe jusqu'à 30 jours avec un temps de persistance et une concentration périlymphatique supérieurs à ceux obtenus avec le gel sans liposomes. En outre, les liposomes semblent promouvoir la conversion de la prodrogue encapsulée (DexP) en sa forme active (Dex). Enfin, une faible quantité de liposomes intacts a été visualisée dans la périlymphe jusqu'à 30 jours. La majeure partie des liposomes semble plutôt retenue dans la fenêtre ronde qui jouerait ainsi un rôle de réservoir pour une libération prolongée du corticoïde dans l'oreille interne.

Ce chapitre est soumis à publication.

## Projet de publication

# Hyaluronic acid liposomal gel sustains the delivery of a corticoid to the inner ear

Naila El Kechai <sup>a</sup>, Elisabeth Mamelle <sup>b, c</sup>, Yann Nguyen <sup>b, c</sup>, Nicolas Huang <sup>a</sup>,  
Valérie Nicolas <sup>d</sup>, Pierre Chaminade <sup>e</sup>, Stéphanie Yen-Nicolay <sup>e</sup>, Claire Gueutin <sup>a</sup>, Benjamin  
Granger <sup>f</sup>, Evelyne Ferrary <sup>b</sup>, Florence Agnely <sup>a, #</sup>, Amélie Bochot <sup>a, #,\*</sup>

<sup>a</sup> Institut Galien Paris-Sud, Université Paris-Sud, CNRS UMR 8612, Université Paris-Saclay,  
92290 Châtenay-Malabry, France.

<sup>b</sup> UMR-S 1159 Inserm / Université Pierre et Marie Curie - Sorbonne Universités “Minimally  
Invasive Robot-based Hearing Rehabilitation”, 16 rue Henri Huchard, 75018 Paris, France.

<sup>c</sup> AP-HP, Pitié-Salpêtrière Hospital, Otolaryngology Department, Unit of Otology, Auditory  
Implants and Skull Base Surgery, Paris, France.

<sup>d</sup> UMS IPSIT, Plate-forme d'imagerie cellulaire, Faculté de Pharmacie, Université Paris-Sud,  
Châtenay-Malabry, France.

<sup>e</sup> UMS IPSIT, SAMM, Faculté de Pharmacie, Université Paris-Sud, Châtenay-Malabry,  
France.

<sup>f</sup> UPMC Univ Paris 06. AP-HP, Pitié Salpêtrière Hospital, Department of Public Health,  
Paris, France.

# these authors have contributed equally

\* Corresponding Author

Pr. Amélie BOCHOT: +33 1 46 83 55 79; [amelie.bochot@u-psud.fr](mailto:amelie.bochot@u-psud.fr)

## **Abstract**

The inner ear is one of the most challenging organs for drug delivery, mainly because of the blood-perilymph barrier. Therefore, local instead of systemic drug delivery methods such as transtympanic injection are being developed for inner ear therapy. In this work, we evaluated the benefit of a hyaluronic acid liposomal gel for the sustained delivery of a corticoid to the inner ear after local administration in the middle ear in a guinea pig model. The liposomal gel was easily injectable thanks to the shear-thinning behavior of hyaluronic acid. A prolonged residence time was achieved in the middle ear as well as in the round window without any negative effect on the hearing function of the animals. The presence of liposomes in the formulation resulted in a sustained release of the drug in perilymph until 30 days and promoted the conversion of the prodrug loaded within liposomes (dexamethasone phosphate) into its active form (dexamethasone). Therapeutic doses were thereby achieved in perilymph. A small amount of intact liposomes was visualized in perilymph whereas the main proportion of liposomes seemed to be trapped in the round window resulting in a reservoir effect. Thus, the administration of hyaluronic acid liposomal gel in the middle ear is an efficient strategy to deliver corticoids to the inner ear in a sustained manner.

## **Keywords**

Dexamethasone phosphate, drug delivery, hydrogel, liposomes, perilymph, round window.

## **Abbreviations**

Chol: cholesterol, DSPE-PEG2000: 1,2-distearoyl-sn-glycero-3-phosphoethanolamine-N-[methoxy-poly-(ethyleneglycol)-2000], Dex: dexamethasone, DexP: dexamethasone phosphate, EPC: Egg phosphatidylcholine, HA: hyaluronic acid, Lip: liposomes, LC-MS: liquid chromatography coupled to mass spectroscopy, PE: phosphatidylethanolamine, Rh: rhodamine, RW: round window.

## 1. Introduction

Inner ear therapy is moving towards local drug delivery methods such as transtympanic injection, which is a well-accepted procedure in otological outpatient clinic. It involves the injection of the drug into the middle ear and relies on diffusion through the middle inner ear barriers, such as the round window (RW), for accessing the inner ear (Herraiz et al., 2010). This minimally invasive method avoids the blood-perilymph barrier (similar to the blood-brain barrier) that isolates the inner ear from the blood (Juhn et al., 2001). Thus, it allows to maximize drug concentration in the inner ear while minimizing systemic exposure and side effects (Wang et al., 2009, Pararas et al., 2012, Honeder et al., 2014). In human, transtympanic injection of conventional drug solutions/suspensions such as corticosteroids is in widespread use for the management of common inner ear diseases such as noise-induced or sudden sensorineural hearing loss and Menière's disease (Alles et al., 2006, McCall et al., 2010, Bear and Mikulec, 2014). However, the use of liquid formulations requires repeated injections (Alles et al., 2006) because of their rapid elimination from the middle ear by flow through the Eustachian tube. In this context, injectable systems such as hydrogels and nanocarriers have sparked interest over the past decade in pre-clinical and clinical researches as they offer a potential sustained drug delivery to the inner ear (Wang et al., 2011, Du et al., 2013, Pritz et al., 2013, Honeder et al., 2014, van de Heyning et al., 2014, El Kechai et al., 2015). Some clinical trials are ongoing with hydrogels based on poloxamer 407 (Lambert et al., 2012) or hyaluronic acid (van de Heyning et al., 2014) for inner ear therapy. Conversely, the use of nanocarriers is still at the research stage but shows potential for future applications especially for targeted drug delivery to the inner ear with functionalized nanoparticles (Pritz et al., 2013). The incorporation of nanocarriers into hydrogels appears to be a promising strategy that was reported previously for local drug delivery to the eye, the joint and the skin (Jayachandra Babu et al., 2009, Lajavardi et al., 2009, Dong et al., 2013, Widjaja et al., 2014). Applied to inner ear drug delivery, a hydrogel should increase the residence time of the nanocarriers in the middle ear enhancing in this way their concentration in the inner ear and offering sustained and/or targeted drug delivery to inner ear cells.

A suitable drug delivery system for the inner ear should be easily injectable and provide a sustained release of the drug to minimize the number of injections. It should be biodegradable and biocompatible without negative effects on hearing or balance function and allow achieving a therapeutic concentration in the inner ear. Ideally, it could offer controlled release

kinetics and specific targeting (El Kechai et al., 2015). Regarding these specifications, the present work aimed to design a drug delivery system for the inner ear based on the combination of a hyaluronic acid (HA) gel and PEGylated liposomes loaded with dexamethasone phosphate (DexP). In this formulation, HA may allow a long residence time into the middle ear in contact with the RW thanks to its high viscosity (El Kechai et al., 2015) and mucoadhesive properties (Girish and Kemparaju, 2007) whereas liposomes could act as a reservoir for a sustained release of the corticoid.

First, *in vitro* studies were performed to determine DexP loading into liposomes and their stability over storage. HA gel containing DexP-loaded liposomes (HA-DexP-Lip) was also characterized regarding its rheological properties and injectability. Secondly, the potential of HA-DexP-Lip gel was evaluated *in vivo*. The formulations were administered into the middle ear of guinea pigs using the needles commonly employed for transtympanic injection. The effect of the liposomal gel on the hearing function was assessed. Then, the residence time of the liposomal gel in the middle ear and the ability of the PEGylated liposomes to reach the inner ear were investigated. Finally, to determine if a therapeutic dose and a sustained delivery of the corticoid can be achieved, DexP and its active form were quantified in perilymph over time.

## 2. Materials and methods

### 2. 1. Materials

Dexamethasone sodium phosphate (DexP, Mw 516.4 Da, purity 98%) was obtained from Fagron (Amsterdam, The Netherlands). Egg phosphatidylcholine (EPC, purity 96%) was provided by Lipoid GmbH (Ludwigshafen, Germany). Dexamethasone (Dex, Mw 392.4, purity > 99%), Flumethasone (Flu, Mw 410.4, purity > 99%), cholesterol (Chol), triton X-100, diamidino-2-phenylindole (DAPI), ammonium acetate, trichloroacetic acid (TCA), trifluoroacetic acid (TFA) and Fluoromount<sup>®</sup> were purchased from Sigma-Aldrich Co. (St. Louis, USA). 1,2-distearoyl-sn-glycero-3-phosphoethanolamine-N-[methoxy-poly(ethyleneglycol)-2000] (DSPE-PEG2000) and phosphatidylethanolamine-N-(lissamine rhodamine B sulfonyl) (PE-Rh) (purities > 99%) were obtained from Avanti Polar Lipids, inc. (Alabaster, USA). Sodium hyaluronate (HA, Mw 1.5 MDa, purity 95%) was provided by Acros Organics (New Jersey, USA). All other chemicals were of analytical grade.

## 2.2. Preparation and characterization of liposomes

DexP-loaded PEGylated liposomes (DexP-Lip), unloaded PEGylated liposomes (Lip) and fluorescently labeled PEGylated liposomes (Lip-Rh) were prepared by the thin film method as described previously (El Kechai et al., 2015). Briefly, lipid films composed of EPC:Chol:DSPE-PEG2000 (60:35:5 mole %) for Lip and DexP-Lip or EPC:Chol:DSPE-PEG2000:PE-Rh (59:35:5:1 mole%) for Lip-Rh, were prepared using rotary evaporation. The lipid film was hydrated either with 100 mg/mL DexP solution in milliQ water (DexP-Lip) or HEPES/NaCl buffer (10/115 mM, pH 7.4) (Lip and Lip-Rh). The liposome suspensions were subsequently extruded 10 times through 0.2 µm polycarbonate filters set in a LIPEX extruder (Whitley, Vancouver, Canada). Non-encapsulated DexP was eliminated by means of dialysis using cellulose dialysis membranes with a molecular weight cut-off of 15 kDa (Spectrum Labs, CA, USA) against HEPES/NaCl buffer (10/115 mM, pH 7.4) at 4°C for 48 h with repeated changes of buffer and protection from light.

The hydrodynamic diameter and the zeta potential of liposomes were determined in triplicate by dynamic light scattering (DLS) at 25°C using a Zetasizer Nano ZS (Malvern, Worcestershire, UK). The concentration of EPC in liposomes was evaluated through an enzymatic phospholipid assay (Biolabo SA, Maizy, France) (El Kechai et al., 2015) after extrusion (Lip) or after extrusion and dialysis (DexP-Lip). The total amount of lipids in liposome suspensions was then calculated from EPC concentration by assuming that lipid composition remains unchanged during the different steps of liposome preparation. Since rhodamine interferes with absorbance measurements, the lipid concentration for Lip-Rh was estimated by taking into account the average percent of lipid loss after extrusion.

The amount of DexP encapsulated in DexP-Lip ( $n = 5$ ) was determined using high-performance liquid chromatography (HPLC) (Waters, MA, USA) (Banciu et al., 2008) after solubilization of 200 µL DexP-Lip in 2.5% Triton X-100. The analysis was performed with a UV detector set at 240 nm using a Reverse Phase C18 column (5 µm, 250 x 4 mm) (Merck, Darmstadt, Germany) and a mobile phase composed of acetonitrile/water (25/75 v/v) acidified at pH2 with trifluoroacetic acid (10 mM) at a flow rate of 1 mL/min. The injection volume was set at 20 µL and DexP peak was obtained at a retention time of 11 min. The method shows satisfactory linearity between 0.5 and 30 µg/mL ( $R^2 = 0.999$ ) and the detection limit was 0.5 µg/mL. Each measurement was at least duplicated.

### 2.3. Stability of DexP-Lip

The stability of DexP-Lip stored at 4°C was assessed over time during 15 days by monitoring their size, polydispersity index (PdI), zeta potential and DexP release. The experiment was performed on three different DexP-Lip batches. For each experiment, a sample of 3 mL DexP-Lip was stored at 4°C protected from light. At each time point, a 100 µL aliquot was withdrawn from the same sample and analyzed by DLS. The DexP released from DexP-Lip was then separated from the DexP that was encapsulated using 0.5 mL Amicon Ultra centrifugal filters (Mw cut off 100 kDa, Millipore Co., Molsheim, France). Following a 1/10 dilution in HEPES/NaCl buffer, samples were centrifuged for 30 min at 12000 g with a tabletop Eppendorf centrifuge minispin® (Hamburg, Germany). The DexP concentration in the filtrate solution was quantified by HPLC.

### 2.4. Gel preparation

HA and HA-DexP gels were prepared by dissolving HA (2.28% w/v) into HEPES/NaCl buffer (10/115 mM, pH 7.4) and into 10 mg/mL DexP solution respectively (DexP dissolved into HEPES/NaCl buffer 10/115 mM, pH 7.4). For liposomal gel preparation (HA-Lip, HA-Lip-Rh or HA-DexP-Lip), HA (2.28% w/v) was dissolved into liposome suspensions (Lip, Lip-Rh or DexP-Lip each at 80 mM final lipid concentration). The gels were then homogenized by means of vortex for 5 min, maintained at room temperature for 1 h and then stored at 4°C for at least 12 h prior to analysis or *in vivo* injection.

### 2.5. Gel osmolality, pH and rheological characterization

The osmolality of the different gels was measured in triplicate using a micro-osmometer (Hermann Roebling MeBtechnik, Berlin, Germany). Their pH was measured using a pHmeter Mettler Toledo. Rheological measurements were carried out on a rotational rheometer ARG2 (TA instruments, New Castle, USA) using a cone/plate geometry (diameter 40 mm, angle 1°, 28 µm truncation). The zero-shear rate viscosity ( $\eta_0$  obtained from Cross model) of the gels were determined in triplicate at 37°C as described previously (El Kechai et al., 2015). The yield stress was assessed through oscillatory stress sweep experiments at 37°C by ramping the shear stress from 0.01 to 300 Pa at a constant frequency of 1 Hz. G' and G" were recorded as a function of shear stress. The yield stress was obtained at the cross over point of G' and G" *versus* stress curves (shear stress for which G' = G").

## 2.6. *In vivo study*

### 2.6.1. *Animals*

Forty-two male Hartley albinos guinea pigs (Charles River, L'Arbresles, France), weighing between 300 and 500 g, and with normal hearing were used in this study. Animal care and experimental procedures were conducted in accordance with the European legislation and were approved by the local ethical committee (CEEA n° 26) of Paris-Sud University (permission n° 2013-100). First, the effect of different formulations was assessed regarding the hearing function after injection in the middle ear (21 guinea pigs). Then, the biodistribution of the formulations injected in the middle ear and drug concentration in perilymph (inner ear fluid) was monitored over time (21 guinea pigs). The study design including the different parameters, methods, groups, time points and the corresponding number of ears tested for each condition are detailed in **Table 1**.

### 2.6.2. *Injection procedure*

For each part of the *in vivo* study, the injection of the gel (HA-Lip, HA-Lip-Rh, HA-DexP or HA-DexP-Lip) in the middle ear was performed under general anesthesia (xylazine 4 mg/kg, ketamine 60 mg/kg, IM). Spontaneous ventilation was achieved and body temperature was maintained with a heating table. To guarantee the adequate application of the gel on the RW, the gel was injected in the middle ear after a retro-auricular surgical approach instead of a direct transtympanic injection. Indeed, the retro-auricular approach allows a better visualization of the bulla and the RW in guinea pig. The retro-auricular skin was shaved and disinfected with povidone-iodine. A local anesthesia (0.5 mL lidocaine hydrochloride 1%) was injected in the retro-auricular subcutaneous tissues to complete general anesthesia. After a retro-auricular incision, retro-auricular muscles were removed from the bone and the bulla was carefully exposed using a 2 mm diamond bur to drill the bone (NSK, Nakashima, Japan) allowing visualization of the cochlea as well as the round window. The gel was injected through a 1 mL syringe equipped with a 29G needle (length = 88 mm, B. Braun). The skin was then sutured with 3.0 Vicryl suture (Ethicon, Cincinnati, OH). After the injection procedure, guinea pigs received an intra-muscular injection of antibiotic prophylaxis (Enrofloxacin Bayer, Leverkusen, Germany).

**Table 1**

*In vivo* study design. n represents the number of ears tested in each condition.

Aim of the study	Parameters studied	Methods	Gel injected	Days after injection	n		
<b>Gel effect on hearing</b>	Hearing function	ABR test	None (control)	0	6		
				2	6		
				7	6		
	(50 µL)	HA-Lip	0	6			
			2	6			
			7	6			
	(150 µL)	HA-Lip	0	3			
			2	3			
			7	3			
	(50 µL)	HA-DexP-Lip	0	6			
			2	6			
			7	6			
<b>Biodistribution</b>	Gel persistence in the middle ear	Macroscopic observation after opening the bulla	HA-Lip-Rh / HA-DexP-Lip	2	12		
				7	12		
				15	8		
		RW sampling and confocal microscopy		30	10		
			HA-Lip-Rh	2	1		
	Drug concentration in perilymph	Perilymph sampling and analysis with LC-MS		7	2		
				15	1		
			None	0	2		
			HA-DexP	2	4		
				7	5		
				15	4		
			HA-DexP-Lip	2	6		
				7	4		
				15	5		
				30	6		
Presence of liposomes in perilymph	Perilymph sampling and confocal microscopy	HA-Lip-Rh	2	3			
			7	3			
			15	3			
			30	3			

When hearing function was measured, the contralateral ear had a surgical labyrinthectomy to avoid transcranial sound conduction. The same surgical procedure was performed but instead of gel injection, a large cochleostomy (1 mm) in the basal turn of the cochlea was performed using a 0.5 mm micro perforator (Karl Storz, Tuttlingen, Germany) and was followed by the introduction of fragments of muscle to obtain a total hearing loss. In this way, Auditory Brainstem Response (ABR) measurements (section 2.6.3) were specifically assessed for the injected ear.

### 2.6.3. Hearing assessment with Auditory Brainstem Response (ABR)

The hearing function of guinea pigs was evaluated by recording the auditory brainstem response following an auditory stimulus. ABR test was performed, under gas general anesthesia (isoflurane), before surgery to confirm normal hearing and then 2 days and 7 days after injection. Click bursts of 100 µs were delivered at 2, 4, 8, 16 and 32 kHz, with a high frequency transducer connected to an external ear canal probe (HIS, Miami, FL). Needle electrodes (Medtronic Xomed, Jackson-ville, Florida) were placed subcutaneously in the leg, the vertex and the ipsilateral retro-auricular side of the analyzed ear. At each frequency, the hearing threshold was determined with 5 dB decreasing increments and corresponded to the minimal intensity for which one or several ABR waves were clearly recognized.

### 2.6.4. Perilymph sampling

To expose properly the cochlea, perilymph sampling were performed under general anesthesia and followed by a lethal intra-cardiac injection of pentobarbital (110 mg). The basal turn of the cochlea was set out with the retro-auricular approach described above. The bulla and the posterior wall of the meatus were drilled so that the middle ear was widely opened and totally accessible. The cochlea and the RW were visualized under a binocular surgical microscope. The persistence of the liposomal gel in the middle ear was systematically assessed -before perilymph or RW sampling- by macroscopic observation regarding the amount and the location of residual liposomal gel. The bulla was then dried with tissue wicks and rinsed several times with buffer solution and ethanol prior to perilymph withdrawal to avoid sample contamination with DexP or liposomes. The basal turn of the cochlea was again dried with tissue wicks and the mucosa was resected. To access the perilymph in the *scala tympani*, the bony shell was thinned with a 0.4 mm micro-perforator 2 mm under the RW niche. A unique microhole was made through the wall with a microcapillary pipette fixed on micromanipulator to perform a controlled puncture. The home-made microcapillary pipettes had a distal diameter below 10 µm. Perilymph was collected by a slow aspiration and a small volume of around 2 µl (precisely measured) was removed in order to limit sample contamination with cerebrospinal fluid from the cochlear duct (Salt et al., 2003). The sample volume was accurately measured after transfer in a calibrated 10 µL microcaps. The samples were stored at -20°C prior to analysis.

### 2.6.5. RW sampling

Following general anesthesia and euthanasia of the animal, the bulla was removed, fixed in 4% formaldehyde for 30 min, subsequently washed with tap water for 10 s and with PBS for 5 min. Then, the bulla was counter stained with DAPI (10 µg/mL) for 10 min and further washed with PBS for 2 x 5 min (protected from light). The bulla was opened under a stereomicroscope and the RW was finally removed, placed on a glass slide and mounted with 1 to 2 drops of Fluoromount® (Zou et al., 2008).

### 2.6.6. Confocal microscopy

Mount RW samples and perilymph samples were observed with an inverted confocal laser scanning microscope Leica TCS SP8 (Leica, Germany) using a HC PL APO CS2 63x/1.40 oil immersion objective lens. The excitation sources were provided by a 405 nm (blue) diode and a white light laser (WLL) with 552 nm (red) selected excitation wavelength. The corresponding fluorescence emission was collected in sequential mode using 430-480 nm (DAPI) and 565-700 nm (rhodamine B) wide slits respectively. The pinhole was set at 1.0 Airy unit. 12-bit numerical images were obtained with Leica SP8 LAS AF software (Version 3.6; Leica, Germany). In order to estimate liposome concentration in perilymph samples, standard liposome suspensions with lipid concentrations ranging between 0.05 and 5 µM were prepared in HEPES/NaCl buffer and the final lipid concentration was measured as described in section 2.2. Each perilymph sample (2 µL) or standard liposome suspensions (2 µL) was imaged for 60 s at 3 different locations. Liposomes, identified as red spots showing a Brownian motion, were counted and averaged on a total of 30 different images using Leica SP8 LAS AF software. This experiment performed on standard liposome suspensions allowed to obtain a calibration curve that was used to quantify lipid concentration in perilymph from the count of fluorescent liposomes.

### 2.6.7. Drug concentration in perilymph

The concentration of both DexP and its active form Dex were measured in perilymph samples using high-pressure liquid chromatography combined with mass spectrometry detection (LC-MS) as described by Zhang et al. (2011). The LC-MS system consisted of an HPLC Ultimate 3000 DGP3600 (Thermo Scientific Dionex, CA, USA) coupled to a triple quadrupole mass spectrometer (Waters, Milford, MA, USA). DexP, Dex and the internal standard flumethasone (Flu) were separated under gradient elution using a Luna C18 (5 µm,

50 x 2 mm) analytical column proceeded by a C18 (4 x 2 mm) guard column (Phenomenex, Torrance, CA, USA). The initial mobile phase consisted of 5 mM ammonium acetate/methanol (60/40 v/v) at a flow rate of 0.3 mL/min, increasing up to 90% of methanol within 1 min and hold for 2 min before returning to starting conditions. Chromatographic separation was obtained within 6 min, with retention times of DexP, Dex and Flu obtained at 2.22, 2.42 and 2.37 min respectively.

Electrospray ionization source was operated in positive ion mode. The source and desolvation gas temperatures were set to 120 and 300°C respectively; desolvation and cone gas flows were 500 and 20 L/h respectively; capillary and cone voltages were 3.5 kV and 40 V respectively. Multiple reaction monitoring (MRM) was optimized to follow the precursor to product transitions for Dex  $[M+H]^+$  at m/z 393→373 at a 10V collision energy (CE), DexP  $[M+3H-2Na]^+$  at m/z 473→435 at a 17V CE and Flu  $[M+H]^+$  at m/z 411→253 at a 15V CE. Data acquisition and processing were performed with MassLynx software (Waters).

For sample preparation, 10  $\mu$ L of Flu (50 ng/mL in mobile phase) was added to 2  $\mu$ L of each perilymph samples, blank, calibration curve or quality control spiking solutions. After adding 5  $\mu$ L of TCA (10%) to precipitate the proteins, the mixture was centrifuged (10 min at 14000xg) and 10  $\mu$ L of clear supernatant was mixed with 20  $\mu$ L of mobile phase. The method showed a good linearity between 1 to 100 ng/mL for DexP ( $R^2 = 0.9987$ ) and between 2 to 200 ng/mL for Dex ( $R^2 = 0.9996$ ). By taking into account the final dilution factor (1/25), the quantification limit in perilymph samples was 25 ng/mL for DexP and 50 ng/mL for Dex.

#### 2.6.8. Statistical analysis

GraphPad Prism software was used for statistical analysis. Non-parametric tests were performed and statistical analysis was conducted using two-way or one-way analysis of variance (Anova), with a Bonferroni post-test (ABR measurements) or a Wilcoxon post-test (DexP and Dex concentrations in perilymph). A p value < 0.05 was considered as significant.

### 3. Results and discussion

#### 3.1. Characterization of liposomes

DexP-loaded (DexP-Lip), unloaded (Lip) and rhodamine-conjugated liposomes (Lip-Rh) showed narrow size distributions characterized by a mean hydrodynamic diameter around 140 nm and a PdI  $\leq 0.1$  (**Table 2**). Zeta potential values were around -27 mV (**Table 2**) for all

the formulations indicating that the presence of DexP or rhodamine did not alter the surface properties of liposomes. The mean encapsulation efficiency for DexP-Lip was  $182 \pm 30$  mg DexP/g lipids (corresponding to  $26 \pm 4$  % mol/mol) and the encapsulation rate was  $10.9 \pm 1.9$  % ( $n = 6$ ). This drug loading provided a total DexP dose of 0.75 mg or 1.5 mg when 50  $\mu$ L or 150  $\mu$ L respectively of HA-DexP-Lip were injected in animals. This dose is similar to that employed for other studies evaluating the *in vivo* pharmacokinetic profiles of dexamethasone or dexamethasone phosphate in the inner ear (Wang et al., 2009, Borden et al., 2011, Wang et al., 2011).

**Table 2**

Physicochemical characterization of liposomes (hydrodynamic diameter, PdI, zeta potential) and final lipid concentration after extrusion.

Liposome denomination	Diameter (nm)	PdI	$\zeta$ -Potential (mV)	[lipids] (mM)	Drug loading (mg DexP/g lipids)	Encapsulation rate (%)
Lip	$139 \pm 43$	0.08	$-27 \pm 8$	$80 \pm 5$		
Lip-Rh	$146 \pm 52$	0.10	$-29 \pm 10$	na		
DexP-Lip	$145 \pm 50$	0.09	$-25 \pm 7$	$78 \pm 2$	$182 \pm 30$	$10.4 \pm 1.9$

na: not assessed. Values are means  $\pm$  SD.

The stability of DexP-Lip was followed over time by monitoring the size, the zeta potential and the DexP released from liposomes stored at 4°C. There was neither modification of the hydrodynamic diameter nor of the zeta potential of liposomes over 15 days (Fig. 1A). The amount of DexP released over this period was less than 3% (Fig. 1B), which corresponds to a concentration lower than 0.3 mg/mL, indicating a good stability of DexP-Lip in storage conditions (4°C). This allowed us to prepare the HA liposomal gels, which needs 12 h before complete hydration of HA, with DexP encapsulated into liposomes at least at 97%.

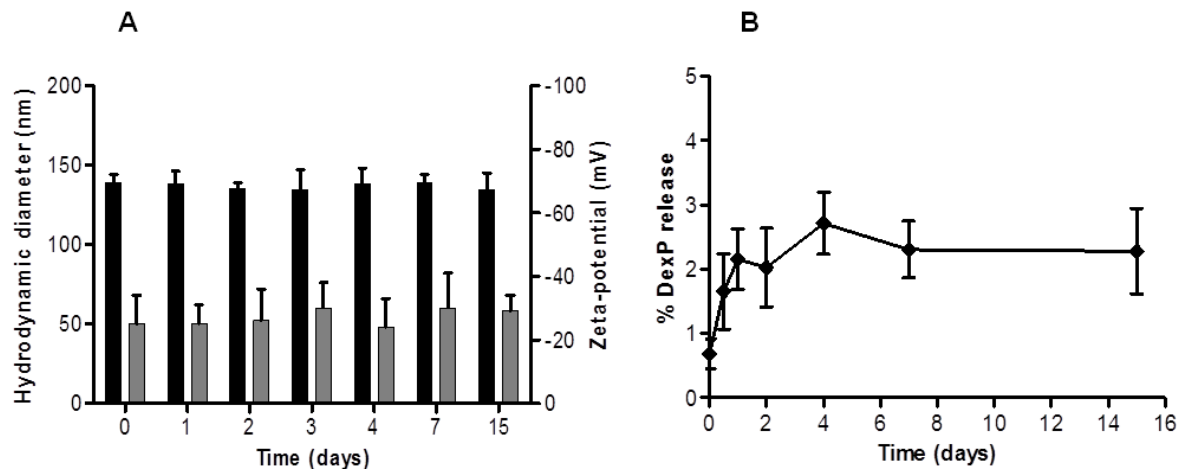


**Fig. 1.** Stability of DexP-Lip over time at 4°C. (A) Hydrodynamic diameter (black) and zeta potential (grey) of DexP-Lip and (B) % of DexP released over 15 days in storage conditions. Values are means  $\pm$  SD ( $n = 3$ ).

### 3.2. Characterization of gel formulations

#### 3.2.1. Osmolality

The cochlear function is strongly dependent on the ionic composition and the volume of the fluids filling the cochlea (perilymph and endolymph). As the formulations are intended to be in contact with the RW, and may have exchanges with the cochlear fluids, the osmolality and the pH of the different gel formulations designed for *in vivo* injection in the middle ear were adjusted around 300 mOsm/kg and pH between pH 7.1 to 7.4 to maintain the homeostasis of the cochlear fluids (**Table 3**).

**Table 3**

Osmolality, pH and rheological parameters (zero-shear rate viscosity ( $\eta_0$ ), elastic ( $G'$ ) and loss ( $G''$ ) moduli, yield stress) of the different gel formulations.  $G'$  and  $G''$  values were obtained at 10 Pa in the linear domain regime.

Gels	pH	Osmolality (mOsm/kg)	$\eta_0$ (Pa.s)	$G'$ (Pa)	$G''$ (Pa)	Yield stress (Pa)
HA	7.4	288 $\pm$ 20	78 $\pm$ 11	65 $\pm$ 4	62 $\pm$ 3	45 $\pm$ 1
HA-DexP	7.2	308 $\pm$ 17	82 $\pm$ 8	70 $\pm$ 3	64 $\pm$ 2	50 $\pm$ 1
HA-Lip	7.3	304 $\pm$ 20	747 $\pm$ 21	316 $\pm$ 6	201 $\pm$ 11	126 $\pm$ 1
HA-Lip-Rh	na	na	797 $\pm$ 35	na	na	na
HA-DexP-Lip	7.1	310 $\pm$ 12	734 $\pm$ 46	330 $\pm$ 11	217 $\pm$ 9	126 $\pm$ 1

na: not assessed. Values are means  $\pm$  SD.

### 3.2.2. Rheological behavior

As previously described by our group, HA gels containing or not liposomes displayed a shear-thinning, non-thixotropic and viscoelastic behavior (El Kechai et al., 2015). The shear-thinning property of all HA formulations allowed an easy injectability through the fine and long needles (29G, 88mm) used in this study to fill the bulla of guinea pigs after the retroauricular approach. Interestingly, the presence of DexP in HA gel -encapsulated into liposomes or not- did not change their rheological parameters (HA-DexP compared to HA, HA-DexP-Lip compared to HA-Lip) showing that there are no specific interactions between HA and DexP. However, the addition of PEGylated liposomes into HA gel resulted in a 10-fold increase in the viscosity at rest and a 5-fold increase in the elastic modulus G' (HA-Lip gel compared to HA gel, **Table 3**) due to the interactions between the surface of liposomes and HA (Lajavardi et al., 2009, El Kechai et al., 2015).

Furthermore, since HA was previously reported as a yield stress material (Hoare et al., 2010), the influence of PEGylated liposomes on this property was assessed. The yield stress is the critical stress that must first be applied to the material in order to destroy its 3D structure and to induce its flow as a viscous fluid. This property strongly affects the injectability of the system. Upon addition of liposomes (containing or not DexP) the yield stress of HA gel shifted from 45 to 126 Pa (**Table 3**), representing a 2.8-fold increase. This result is in agreement with our previous observations in which the addition of PEGylated liposomes at the same concentration led to a 1.5-fold increase in the injection force of HA gel (El Kechai et al., 2015). However, such yield stress values were not opposed to a good injectability, which was demonstrated both manually in this study, when the formulations were injected in animals, and by syringeability tests using the same needles (El Kechai et al., 2015). Indeed, the yield stress values obtained here are significantly below the compression stress applied during the injection (around  $2.4 \times 10^6$  Pa for HA-Lip). The compression stress was calculated by dividing the injection force recorded during syringeability tests (12 N for HA-Lip (El Kechai et al., 2015)) by the surface of the plunger (internal diameter of the syringe = 2.5 mm).

### 3.3. Hearing function assessment

The potential effect of the formulations (HA-Lip and HA-DexP-Lip) on the hearing function was evaluated using ABR tests. The gel was injected in the middle ear after surgery to fill either completely the bulla (150 µl) or only the RW niche (50 µL). The hearing

thresholds at 2 and 7 days post-surgery/injection were compared to the normal hearing function of the animals recorded 2 days before the experiment. The surgical procedure without injection had no impact on the hearing thresholds (control group, **Fig. 2**). Whatever the gels (HA-Lip or HA-Lip-DexP) or the volume injected (50 or 150 µL), there was no significant modification of the hearing thresholds 2 and 7 days after the injection (**Fig. 2**). It demonstrates that neither DexP nor the liposomal gel had a negative effect on the hearing function. Although 2 days and 7 days after the injection of 150 µL liposomal gel loaded or not with DexP, the middle ear cavity remained almost completely filled (day 2) or half filled (day 7) with gel (**Table 4**, section 3.4.1), this did not induce any subsequent hearing loss.

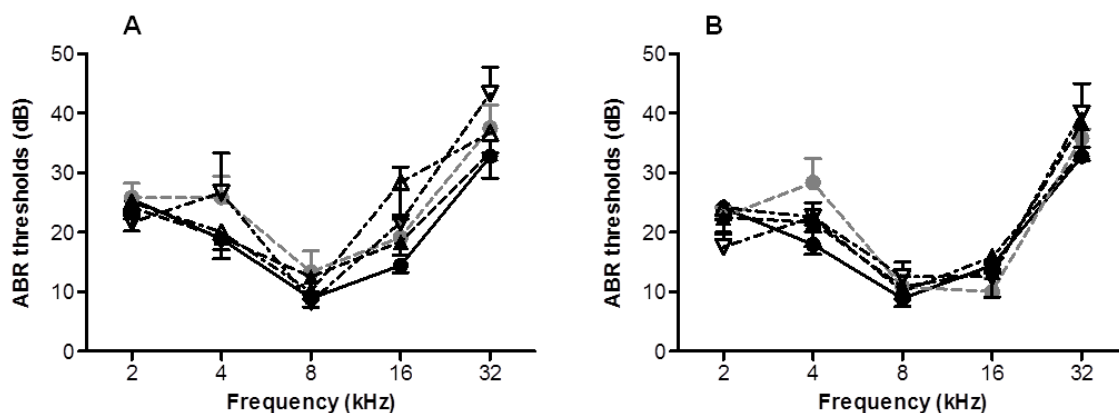


**Fig. 2.** ABR thresholds 2 days (A) and 7 days (B) after surgical procedure without injection (control group: ●, n = 6), after the injection of HA-Lip (50 µL: Δ, n = 6 or 150 µL: ∇, n = 3) or HA-DexP-Lip (50 µL: ▲, n = 6). Hearing thresholds 2 days before injection (●). No modification of the hearing thresholds for all groups, before surgery/injection and post-surgery/injection at 2 and 7 days (two-way Anova, ns). Values are represented as mean ± SEM.

Conversely, other studies have reported a transient conductive hearing loss up to 10 days, following administration of hydrogel-based formulations such as poloxamer 407 (Salt et al., 2011, Wang et al., 2009, Honeder et al., 2014) and chitosan-glycerophosphate (Paulson et al., 2008). The conductive hearing loss, which did not depend on the administration method (transtympanic injection or injection after a retro-auricular approach), was probably caused by the physical presence of these hydrogels in the middle ear that reduces the movement of the ossicular chain. In addition, Feng et al. (2014) demonstrated a volume-dependant transient

hearing loss after injection of 50 or 100  $\mu\text{L}$  of PLGA-PEG-PLGA thermosensitive hydrogel in the middle ear. This is not the case in the present study indicating that the presence of the HA liposomal gel in the middle ear did not alter the ossicular chain mobility. The impact of the gel on the ossicular chain mobility is likely to depend on its mechanical properties. Indeed, the elastic modulus of HA-DexP-Lip is  $G' = 330 \text{ Pa}$  (**Table 3**) whereas the elastic modulus of a poloxamer 407 gel (17% m/m) measured in the same conditions is around 10000 Pa (data not shown). Thus, HA-DexP-Lip display a 25-fold lower elasticity compared to poloxamer 407. This could explain the fact that the injection of the liposomal gel in the middle ear had no impact on the hearing thresholds.

**Table 4**

Macroscopic observation of the presence of HA-Lip-Rh (150  $\mu\text{L}$  injected at day 0) in the middle ear after opening the bulla at different time points. (++++) Gel completely filled the bulla. (++) Gel filled half of the bulla. (+/-) Traces of gel were sparsely distributed on the middle ear mucosa.

Time	Presence of gel
Day 2	++++
Day 7	++
Day 15	+/-
Day 30	+/-

### 3.4. *In vivo biodistribution study*

For the biodistribution study, a gel volume of 150  $\mu\text{L}$  (providing 1.5 mg DexP instead of 0.5 mg with 50  $\mu\text{L}$ ) was chosen in order to administrate a higher DexP dose and to ensure a prolonged contact of the formulation with the RW. The liposomal bilayer was fluorescently labeled with rhodamine to assess macroscopically and microscopically the biodistribution of liposomes after injection in the middle ear.

#### 3.4.1. *Gel persistence in the middle ear and presence of liposomes in the RW*

The aim of using highly viscous formulations such as the HA liposomal gel was to increase the persistence of the formulation in the middle ear in contact with the RW by avoiding flow through the Eustachian tube. Following the injection of HA-Lip-Rh or HA-DexP-Lip, the bulla was opened at different time points and observed under a stereomicroscope to assess the

presence and the location of the residual liposomal gel. The amount of gel in the middle ear decreased over time and traces of gel, sparsely distributed in the middle ear mucosa including on the RW, were observed in some animals up to 30 days (**Table 4**). It is not excluded that the gel or the liposomes remained longer on the middle ear mucosa as a thin film that was not visible macroscopically. Our results (**Table 4**) confirm those of Martini et al. (1992) (obtained with a 1.9% high molecular weight HA hydrogel) in which the gel completely filled the middle ear cavity of guinea pig 7 days after injection and remained at the RW and oval window until 30 days post-injection.

In parallel, confocal images of the RW (**Fig. 3**) after injection of HA-Lip-Rh, showed an abundant accumulation of liposomes in the RW at day 2 (**Fig. 3A**) whereas only few liposomes were visible at day 7 and 15 (**Fig. 3B** and **3C**). The aspect of the fluorescence in **Figure 3A** surrounding the nuclei suggests liposome endocytosis by RW cells. Regarding the different wash cycles required for RW sample preparation (section 2.6.5), any liposomal gel present at RW surface was probably eliminated. Thus, the liposomes observed in **Figure 3** are likely to be either in the RW cell cytoplasm or in the intercellular space. Similarly, Zou et al. (2008) explored the presence of lipid nanocapsules on the RW after a constant 24-h administration using a piece of gelfoam® or after a transient administration (30 min). The amount of visible particles on the RW was significantly higher with the constant administration during 24h. These data confirm that nanoparticle or liposome uptake by the RW is enhanced by increasing the time the drug delivery system remains in contact with the RW. Our results also showed that PEGylated liposomes are able to diffuse through HA gel to reach the RW. This is in agreement with the ability of PEGylated nanoparticles to diffuse in the vitreous (mainly composed of HA and collagen) *ex vivo* (Martens et al., 2013, Xu et al., 2013) and PEGylated liposomes to migrate in the vitreous *in vivo* (Lajavardi et al., 2009).

In the present study, the rheological properties of HA mentioned previously provided a long persistence of the liposomal gel in the middle ear. Indeed, the non-thixotropic property of the formulation allowed a fast recovery of the high initial viscosity after injection. Moreover, the high viscosity at rest and the viscoelasticity of the gel combined with the adhesive properties of high molecular weight HA (Girish and Kemparaju, 2007) favored a prolonged contact with the middle ear mucosa including the RW.

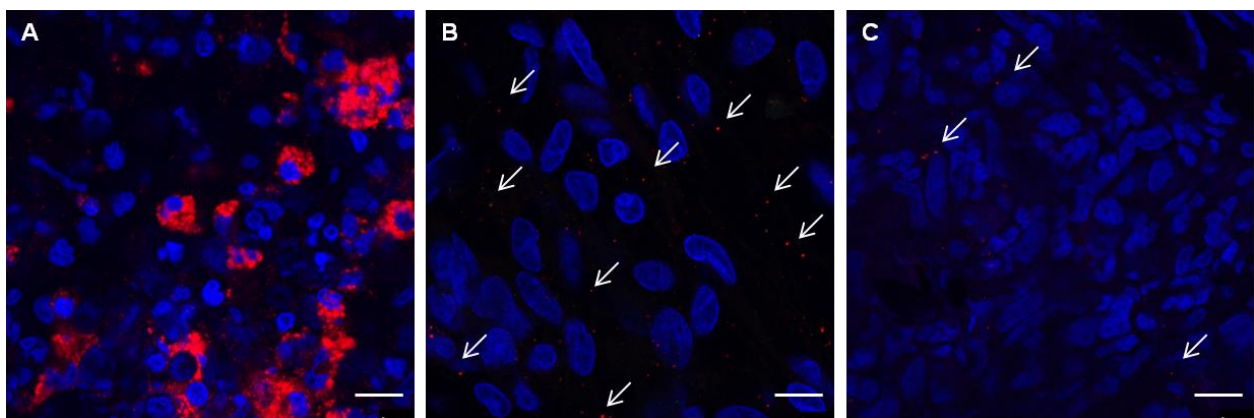


**Fig. 3.** Confocal images of the round window membrane sampled 2 days (A), 7 days (B) and 15 (C) days after injection of HA-Lip-Rh gel. Arrows on (B) and (C) show liposomes. Scale bar = 10 µm.

#### 3.4.2. Drug concentration in perilymph

DexP is a soluble form of Dex. It is also a prodrug that must be converted into its active form Dex for biological activity (Hargunani et al., 2006). For these reasons, both DexP and Dex were quantified in perilymph. HA gel allowed a sustained delivery of the corticoid up to 15 days whereas the HA liposomal gel sustained its delivery up to 30 days (**Fig. 4**). Interestingly, the conversion of DexP into Dex was promoted in presence of liposomes.

After injection of 150 µL HA-DexP, DexP concentration in perilymph was relatively constant between 2 and 15 days (**Fig. 4A**) (between 60 and 152 ng/mL) while Dex was detected only at days 2 and 7 in some animals (**Fig. 4B**). With HA-DexP-Lip group, no significant variations of DexP concentration was recorded over time (between 60 and 163 ng/mL) and DexP was detected until 30 days (**Fig. 4C**). Dex concentration did not show significant variations between day 2 and 15 (between 455 and 833 ng/mL) and then decreased between day 15 and 30. Dex was no more detectable at day 30 (**Fig. 4D**).

Although DexP concentrations in perilymph did not significantly differ between the two groups at all time points (**Fig. 4 A compared to C**), regarding Dex, the injection of HA-DexP-Lip resulted in higher concentrations in perilymph at days 2, 7 and 15 compared with HA-DexP (**Fig. 4 B compared to D**). In addition, HA-DexP-Lip yielded a 5-fold (day 2), 4-fold (day 7) and 25-fold (day 15) increase in total drug concentration (DexP + Dex) in comparison with HA-DexP.

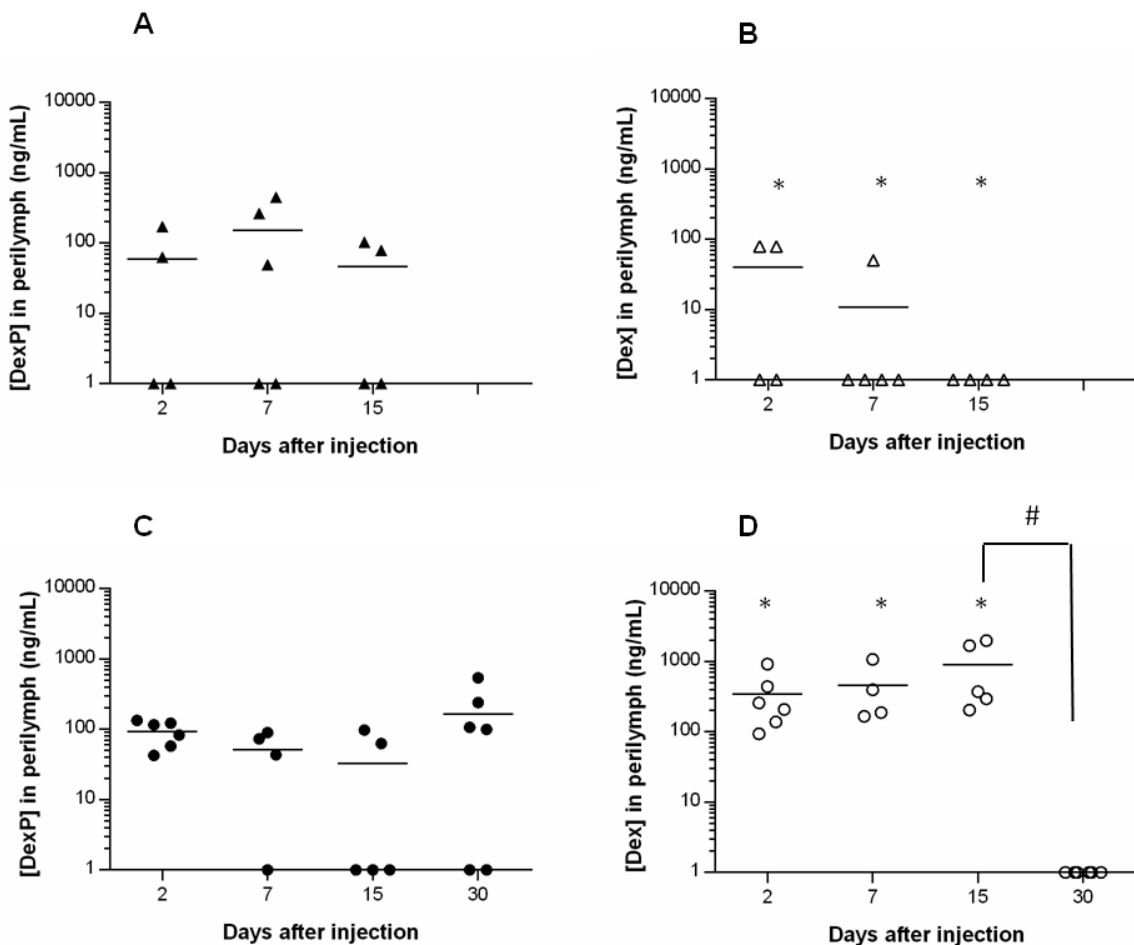


**Fig. 4.** Perilymphatic DexP and Dex concentrations over time after injection of DexP encapsulated in liposomes within HA gel (HA-DexP-Lip) or dissolved within HA gel (HA-DexP). (A) DexP concentration for HA-DexP group was monitored over 15 days. (B) Dex concentration for HA-DexP group over 15 days. (C) DexP concentration for HA-DexP-Lip group over 30 days. (D) Dex concentration for HA-DexP-Lip group over 30 days. The quantification limit in perilymph samples using LC-MS was 25 ng/mL for DexP and 50 ng/mL for Dex. A semi-logarithmic scale is used to represent drug levels. The black line represents the mean value. A, B, C: no significant difference in DexP or Dex concentration between the different time points (one-way Anova, ns). D: significant decrease in Dex concentration between 15 and 30 days (# post-test,  $p < 0.05$ ). Dex concentration was significantly higher in HA-DexP-Lip group compared to HA-DexP (\*post-test,  $p < 0.05$ , B compared to D) at day 2, day 7 and day 15. No significant differences in DexP concentration between HA-DexP and HA-DexP-Lip groups (A compared to C: two-way Anova, ns).

Dex was the major form in perilymph after the administration of the liposomal gel representing around 76 % (day 2), 90% (day 7) and 92% (day 15) of the total drug concentration (DexP + Dex) (**Fig. 4D**). This result is consistent with Hargunani et al. (2006) observations in which the conversion of DexP into Dex occurred rapidly in the inner ear. This conversion is mediated by esterases that are ubiquitous enzymes shown to be present in perilymph (Swan et al., 2009) and could be present also in the RW, which is composed of two epithelial layers separated by a connective tissue (Goycoolea and Lundman, 1997).

Interestingly, the perilymphatic drug levels obtained in both groups can be considered as suitable for therapeutic efficacy since they are above the Dex concentration (30-40 ng/mL) upon which therapeutic effects are achieved in the inner ear (Kim et al., 2009). Furthermore, the single injection of both gels (HA-DexP and HA-DexP-Lip) provided longer exposure times (15 and 30 days respectively) compared to those reported in the literature with other gels or with DexP solution. Following intratympanic injection of DexP solution (up to 2.25 mg), dexamethasone was not detected for more than 24 h in perilymph (Wang et al., 2009, Borden et al., 2011). Dexamethasone was detected for at least 10 days with poloxamer 407 hydrogel (Wang et al., 2009, Wang et al., 2011), up to 5 days with chitosan glycerophosphate (Paulson et al., 2008) and only until 72 h with thiol-modified HA/gelatin hydrogel (Borden et al., 2011).

Finally, a high inter-individual variability, which is also described in the literature (Salt and Plontke, 2009, Wang et al., 2009, Borden et al., 2011), was observed in the present study with sometimes a 10-fold difference between different animals under the same conditions. This can be explained by the variability in RW thickness and surface, in addition to variable cellular permeability between individuals (Hahn et al., 2006, Mikulec et al., 2008).

#### *3.4.3. Passage of liposomes in perilymph*

Since liposomes were observed on the RW (**Fig. 3**), their passage across this membrane up to perilymph was determined and perilymph samples were analyzed using confocal microscopy. Liposomes, represented by red spots showing a Brownian motion, were visualized on confocal time-lapse images on samples taken 2, 7, 15 and 30 days after injection of HA-Lip-Rh (**Fig. 5A**). Liposomes were thus able to cross the RW with preservation of their integrity and were detected in perilymph until 30 days. Liposome count on confocal images of

standard liposome suspensions allowed to obtain a calibration curve whose equation was (Eq 1,  $R^2 = 0.984$ ):

$$\text{Mean number of liposomes} = 24.5 [\text{Lipids}] - 0.73 \quad (1)$$

This equation was used to quantify lipid concentration in perilymph samples. To the best of our knowledge, this is the first study that evaluates the amount of liposomes in perilymph after administration in the middle ear. The lipid concentration varied between  $1.8 \pm 1.8 \text{ nmol/mL}$  (day 2) and  $0.18 \pm 0.04 \text{ nmol/mL}$  (day 30) (**Fig. 5C**), representing a very low percentage of liposomes delivered in perilymph, between  $3 \times 10^{-5} \%$  (day 2) and  $3 \times 10^{-6} \%$  (day 30). In addition, assuming that 100% of DexP is still encapsulated into liposomes in perilymph, the DexP concentration corresponding to the estimated lipid concentration in perilymph should be between 232 ng/mL (day 2) and 22 ng/mL (day 30). Despite the significant conversion of DexP into Dex (**Fig. 4**), these values are below the total drug concentrations measured by LC-MS, indicating that in perilymph, a large amount of DexP is not encapsulated into liposomes anymore.

Several studies have reported the passage of nanocarriers with a size ranging from 100 to 640 nm in the inner ear such as lipid nanocapsules (Zou et al., 2008), PLGA nanoparticles (Tamura et al., 2005), polymersomes (Zhang et al., 2012), dendriplexes (Zhang et al., 2011) and liposomes (Zou et al., 2010, Zou et al., 2014). Zou et al. (2012) described a size-dependent passage of liposomes through the RW in rat with increasing transportation efficacy by decreasing liposome size (from 240 to 95 nm). In addition, positively charged glycerol monooleate nanoparticles showed a better passage through the RW compared to neutral or negatively charged ones (Liu et al., 2013). Although the passage of nanocarriers through the RW is widely reported, these studies did not provide any quantitative data about the amount of nanocarriers in the inner ear. In the present study, we demonstrated that a small proportion of PEGylated liposomes bearing a negative charge (zeta potential -25 mV), with a diameter of 140 nm, was able to cross the RW with preservation of their integrity, whereas the main part of those liposomes remained trapped within the RW.

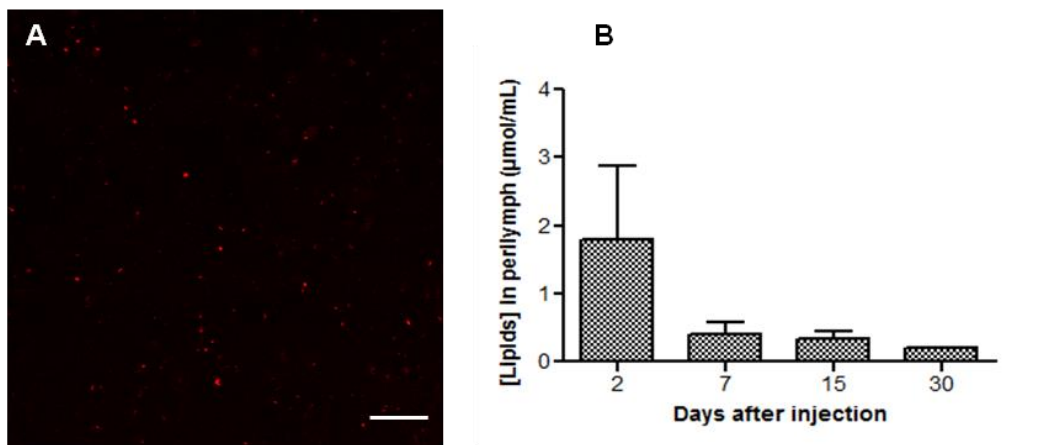


**Fig. 5.** Quantitative evaluation of lipid concentration in perilymph using confocal microscopy. A: Confocal image showing liposomes in a perilymph sample taken 2 days after injection of HA-Lip-Rh gel, scale bar = 10  $\mu\text{m}$ . B: Variations of lipid concentration in perilymph sampled 2, 7, 15 or 30 days post-injection. No significant differences between the different time points (one-way Anova, ns). The detection limit was 0.05  $\mu\text{mol/mL}$ . Values are represented as mean  $\pm$  SEM ( $n = 3$ ).

Two pathways that nanocarriers can use for passage through the RW are discussed in the literature: the transcellular pathway, involving events of endo- and exo-cytosis and the paracellular pathway (Zou et al., 2012, Pritz et al., 2013), which are both supposed to preserve the structural integrity of the nanocarriers (Zou et al., 2012, Pritz et al., 2013). Yet, the transcellular pathway does not seem consistent with the passage of intact liposomes through the three-layered RW structure (Goycoolea and Lundman, 1997). From our data, the following hypothesis can be expected: regarding the presence of liposomes in the RW (**Fig. 3**), the promoted conversion of DexP into Dex with liposomes and the relatively high concentration of non-encapsulated drug in perilymph, the RW is likely to act as a reservoir of liposomes that are either endocytosed and destabilized in the first epithelial layer or trapped in the connective tissue of the RW. DexP released from liposomes is thus converted in the RW resulting in a slow release of Dex in perilymph. On the other hand, the presence of intact vesicles in perilymph could be explained by the passage of a small fraction of liposomes by the paracellular pathway.

#### **4. Conclusions**

The combination of liposomes and HA gel appears to be a very promising approach to deliver drugs into the inner ear. The shear-thinning behavior of HA allowed a suitable injectability. Its non-thixotropic, viscoelastic and mucoadhesive properties provided a fast recovery of high initial viscosity after injection as well as a prolonged residence time in the middle ear in contact with the round window. Finally, the incorporation of PEGylated liposomes into HA gel sustained the delivery of the drug in perilymph up to 30 days.

#### **Acknowledgments**

This work was supported by a PhD grant (Naila El Kechai) from the French Ministry of National Education and Research. Authors wish to thank “la région Ile-de-France” for the purchase of the confocal microscope that served in this study, the SAMM (Service d'Analyse de Médicaments et Métabolites) where the LC-MS assays were performed with a valuable help from Audrey Solgadi. We are also grateful to Valérie Domergue at the Animex Plateform where the *in vivo* experiments were conducted.

## References

- Alles, M.J., der Gaag, M.A., Stokroos, R.J., 2006. Intratympanic steroid therapy for inner ear diseases, a review of the literature. *Eur Arch Otorhinolaryngol.* 263, 791-797.
- Banciu, M., Metselaar, J.M., Schiffelers, R.M., Storm, G., 2008. Liposomal glucocorticoids as tumor-targeted anti-angiogenic nanomedicine in B16 melanoma-bearing mice. *J Steroid Biochem Mol Biol.* 111, 101-110.
- Bear, Z.W., Mikulec, A.A., 2014. Intratympanic steroid therapy for treatment of idiopathic sudden sensorineural hearing loss. *Mo Med.* 111, 352-356.
- Borden, R.C., Saunders, J.E., Berryhill, W.E., Krempl, G.A., Thompson, D.M., Queimado, L., 2011. Hyaluronic acid hydrogel sustains the delivery of dexamethasone across the round window membrane. *Audiol Neurotol.* 16, 1-11.
- Dong, J., Jiang, D., Wang, Z., Wu, G., Miao, L., Huang, L., 2013. Intra-articular delivery of liposomal celecoxib-hyaluronate combination for the treatment of osteoarthritis in rabbit model. *International Journal of Pharmaceutics.* 441, 285-290.
- Du, X., Chen, K., Kuriyavar, S., Kopke, R.D., Grady, B.P., Bourne, D.H., Li, W., Dormer, K.J., 2013. Magnetic targeted delivery of dexamethasone acetate across the round window membrane in guinea pigs. *Otol Neurotol.* 34, 41-47.
- El Kechai, N., Agnely, F., Mamelle, E., Nguyen, Y., Ferrary, E., Bochot, A., 2015. Recent advances in local drug delivery to the inner ear. *Int J Pharm.* 494, 83-101.
- El Kechai, N., Bochot, A., Huang, N., Nguyen, Y., Ferrary, E., Agnely, F., 2015. Effect of liposomes on rheological and syringeability properties of hyaluronic acid hydrogels intended for local injection of drugs. *Int J Pharm.* 487, 187-196.
- Feng, L., Ward, J.A., Li, S.K., Tolia, G., Hao, J., Choo, D.I., 2014. Assessment of PLGA-PEG-PLGA copolymer hydrogel for sustained drug delivery in the ear. *Curr Drug Deliv.* 11, 279-286.
- Girish, K.S., Kemparaju, K., 2007. The magic glue hyaluronan and its eraser hyaluronidase: a biological overview. *Life Sci.* 80, 1921-1943.
- Goycoolea, M.V., Lundman, L., 1997. Round window membrane. Structure function and permeability: a review. *Microsc Res Tech.* 36, 201-211.
- Hahn, H., Kammerer, B., Di Mauro, A., Salt, A.N., Plontke, S.K., 2006. Cochlear microdialysis for quantification of dexamethasone and fluorescein entry into scala tympani during round window administration. *Hear Res.* 212, 236-244.
- Hargunani, C.A., Kempton, J.B., De Gagne, J.M., Trune, D.R., 2006. Intratympanic injection of dexamethasone: time course of inner ear distribution and conversion to its active form. *Otol Neurotol.* 27, 564-569.
- Herraiz, C., Miguel Aparicio, J., Plaza, G., 2010. [Intratympanic drug delivery for the treatment of inner ear diseases]. *Acta Otorrinolaringol Esp.* 61, 225-232.
- Hoare, T., Zurakowski, D., Langer, R., Kohane, D.S., 2010. Rheological blends for drug delivery. I. Characterization in vitro. *J Biomed Mater Res A.* 92, 575-585.
- Honeder, C., Engleider, E., Schopper, H., Gabor, F., Reznicek, G., Wagenblast, J., Gstötter, W., Arnoldner, C., 2014. Sustained release of triamcinolone acetonide from an intratympanically applied hydrogel designed for the delivery of high glucocorticoid doses. *Audiol Neurotol.* 19, 193-202.

- Jayachandra Babu, R., Ravis, W.R., Duran, S.H., Schumacher, J., Cox, E., Stahl, R., Jones, K., Jean Lin, Y.J., Phillip Lee, Y.H., Parsons, D.L., Portman, E.M., Brown, S.C.R., 2009. Enhancement of transdermal delivery of phenylbutazone from liposomal gel formulations through deer skin. *Journal of Veterinary Pharmacology and Therapeutics*. 32, 388-392.
- Juhn, S.K., Hunter, B.A., Odland, R.M., 2001. Blood-labyrinth barrier and fluid dynamics of the inner ear. *Int Tinnitus J*. 7, 72-83.
- Kim, S.H., Kim, K.X., Raveendran, N.N., Wu, T., Pondugula, S.R., Marcus, D.C., 2009. Regulation of ENaC-mediated sodium transport by glucocorticoids in Reissner's membrane epithelium. *Am J Physiol Cell Physiol*. 296, C544-557.
- Lajavardi, L., Camelo, S., Agnely, F., Luo, W., Goldenberg, B., Naud, M.-C., Behar-Cohen, F., de Kozak, Y., Bochot, A., 2009. New formulation of vasoactive intestinal peptide using liposomes in hyaluronic acid gel for uveitis. *Journal of Controlled Release*. 139, 22-30.
- Lajavardi, L., Camelo, S., Agnely, F., Luo, W., Goldenberg, B., Naud, M.C., Behar-Cohen, F., de Kozak, Y., Bochot, A., 2009. New formulation of vasoactive intestinal peptide using liposomes in hyaluronic acid gel for uveitis. *J Control Release*. 139, 22-30.
- Lambert, P.R., Nguyen, S., Maxwell, K.S., Tucci, D.L., Lustig, L.R., Fletcher, M., Bear, M., Lebel, C., 2012. A randomized, double-blind, placebo-controlled clinical study to assess safety and clinical activity of OTO-104 given as a single intratympanic injection in patients with unilateral Meniere's disease. *Otol Neurotol*. 33, 1257-1265.
- Liu, H., Chen, S., Zhou, Y., Che, X., Bao, Z., Li, S., Xu, J., 2013. The effect of surface charge of glycerol monooleate-based nanoparticles on the round window membrane permeability and cochlear distribution. *J Drug Target*. 21, 846-854.
- Martens, T.F., Vercauteren, D., Forier, K., Deschout, H., Remaut, K., Paesen, R., Ameloot, M., Engbersen, J.F., Demeester, J., De Smedt, S.C., Braeckmans, K., 2013. Measuring the intravitreal mobility of nanomedicines with single-particle tracking microscopy. *Nanomedicine (Lond)*. 8, 1955-1968.
- Martini, A., Rubini, R., Ferretti, R.G., Govoni, E., Schiavinato, A., Magnavita, V., Perbellini, A., Fiori, M.G., 1992. Comparative ototoxic potential of hyaluronic acid and methylcellulose. *Acta Otolaryngol*. 112, 278-283.
- McCall, A.A., Swan, E.E., Borenstein, J.T., Sewell, W.F., Kujawa, S.G., McKenna, M.J., 2010. Drug delivery for treatment of inner ear disease: current state of knowledge. *Ear Hear*. 31, 156-165.
- Mikulec, A.A., Hartsock, J.J., Salt, A.N., 2008. Permeability of the round window membrane is influenced by the composition of applied drug solutions and by common surgical procedures. *Otol Neurotol*. 29, 1020-1026.
- Pararas, E.E., Borkholder, D.A., Borenstein, J.T., 2012. Microsystems technologies for drug delivery to the inner ear. *Adv Drug Deliv Rev*. 64, 1650-1660.
- Paulson, D.P., Abuzeid, W., Jiang, H., Oe, T., O'Malley, B.W., Li, D., 2008. A novel controlled local drug delivery system for inner ear disease. *Laryngoscope*. 118, 706-711.

- Pritz, C.O., Dudas, J., Rask-Andersen, H., Schrott-Fischer, A., Glueckert, R., 2013. Nanomedicine strategies for drug delivery to the ear. *Nanomedicine (Lond)*. 8, 1155-1172.
- Salt, A.N., Hartsock, J., Plontke, S., LeBel, C., Piu, F., 2011. Distribution of dexamethasone and preservation of inner ear function following intratympanic delivery of a gel-based formulation. *Audiol Neurotol*. 16, 323-335.
- Salt, A.N., Plontke, S.K., 2009. Principles of local drug delivery to the inner ear. *Audiol Neurotol*. 14, 350-360.
- Swan, E.E., Peppi, M., Chen, Z., Green, K.M., Evans, J.E., McKenna, M.J., Mescher, M.J., Kujawa, S.G., Sewell, W.F., 2009. Proteomics analysis of perilymph and cerebrospinal fluid in mouse. *Laryngoscope*. 119, 953-958.
- Tamura, T., Kita, T., Nakagawa, T., Endo, T., Kim, T.S., Ishihara, T., Mizushima, Y., Higaki, M., Ito, J., 2005. Drug delivery to the cochlea using PLGA nanoparticles. *Laryngoscope*. 115, 2000-2005.
- van de Heyning, P., Muehlmeier, G., Cox, T., Lisowska, G., Maier, H., Morawski, K., Meyer, T., 2014. Efficacy and safety of AM-101 in the treatment of acute inner ear tinnitus--a double-blind, randomized, placebo-controlled phase II study. *Otol Neurotol*. 35, 589-597.
- Wang, X., Dellamary, L., Fernandez, R., Harrop, A., Keithley, E.M., Harris, J.P., Ye, Q., Lichter, J., LeBel, C., Piu, F., 2009. Dose-dependent sustained release of dexamethasone in inner ear cochlear fluids using a novel local delivery approach. *Audiol Neurotol*. 14, 393-401.
- Wang, X., Dellamary, L., Fernandez, R., Ye, Q., LeBel, C., Piu, F., 2011. Principles of inner ear sustained release following intratympanic administration. *Laryngoscope*. 121, 385-391.
- Xu, Q., Boylan, N.J., Suk, J.S., Wang, Y.Y., Nance, E.A., Yang, J.C., McDonnell, P.J., Cone, R.A., Duh, E.J., Hanes, J., 2013. Nanoparticle diffusion in, and microrheology of, the bovine vitreous ex vivo. *J Control Release*. 167, 76-84.
- Zhang, M., Moore, G.A., Jensen, B.P., Begg, E.J., Bird, P.A., 2011. Determination of dexamethasone and dexamethasone sodium phosphate in human plasma and cochlear perilymph by liquid chromatography/tandem mass spectrometry. *J Chromatogr B Analyt Technol Biomed Life Sci*. 879, 17-24.
- Zhang, W., Zhang, Y., Lobler, M., Schmitz, K.P., Ahmad, A., Pyykko, I., Zou, J., 2011. Nuclear entry of hyperbranched polylysine nanoparticles into cochlear cells. *Int J Nanomedicine*. 6, 535-546.
- Zhang, Y., Zhang, W., Johnston, A.H., Newman, T.A., Pyykko, I., Zou, J., 2012. Targeted delivery of Tet1 peptide functionalized polymersomes to the rat cochlear nerve. *Int J Nanomedicine*. 7, 1015-1022.
- Zou, J., Poe, D., Ramadan, U.A., Pyykko, I., 2012. Oval window transport of Gd-dOTA from rat middle ear to vestibulum and scala vestibuli visualized by in vivo magnetic resonance imaging. *Ann Otol Rhinol Laryngol*. 121, 119-128.
- Zou, J., Saulnier, P., Perrier, T., Zhang, Y., Manninen, T., Toppila, E., Pyykko, I., 2008. Distribution of lipid nanocapsules in different cochlear cell populations after round window membrane permeation. *J Biomed Mater Res B Appl Biomater*. 87, 10-18.

- Zou, J., Sood, R., Ranjan, S., Poe, D., Ramadan, U.A., Kinnunen, P.K., Pyykko, I., 2010. Manufacturing and in vivo inner ear visualization of MRI traceable liposome nanoparticles encapsulating gadolinium. *J Nanobiotechnology*. 8, 32.
- Zou, J., Sood, R., Ranjan, S., Poe, D., Ramadan, U.A., Pyykko, I., Kinnunen, P.K., 2012. Size-dependent passage of liposome nanocarriers with preserved posttransport integrity across the middle-inner ear barriers in rats. *Otol Neurotol*. 33, 666-673.
- Zou, J., Sood, R., Zhang, Y., Kinnunen, P.K., Pyykko, I., 2014. Pathway and morphological transformation of liposome nanocarriers after release from a novel sustained inner-ear delivery system. *Nanomedicine (Lond)*. 9, 2143-2155.

## **Chapitre IV**

**Efficacité thérapeutique de gels d'acide  
hyaluronique contenant un corticoïde sur un modèle  
de traumatisme sonore chez le cobaye**

## Chapitre IV

### **Efficacité thérapeutique de gels d'acide hyaluronique contenant un corticoïde sur un modèle de traumatisme sonore chez le cobaye**

#### **Introduction - résumé**

L'efficacité thérapeutique du gel d'acide hyaluronique contenant la dexamethasone phosphate encapsulée ou non dans les liposomes PEGylés a été évaluée sur un modèle de surdité secondaire à un traumatisme sonore chez le cobaye. Différentes formulations (gel d'acide hyaluronique seul, gel d'acide hyaluronique contenant le corticoïde libre à une concentration de 10 mg/mL, gel d'acide hyaluronique contenant la même concentration de corticoïde encapsulée dans les liposomes PEGylés) ont été administrées dans l'oreille moyenne des animaux 48 h après l'exposition au bruit (5 kHz, 100 dB, 1h) de façon à simuler la pratique clinique. Les gels ont été injectés après un abord chirurgical retro-auriculaire au lieu d'une injection transtympanique directe. Cet abord permet une meilleure visualisation de la fenêtre ronde chez le cobaye. Les seuils auditifs ont été évalués avant l'exposition au bruit (audition normale), 48 h après le traumatisme sonore (perte auditive induite par le bruit), puis 7 et 30 jours après l'injection du gel pour évaluer la récupération de l'audition.

Cette étude a permis de valider le modèle animal de traumatisme sonore dans nos conditions d'expérimentation. En effet, les résultats ont monté que la surexposition au bruit a entraîné une perte auditive à J<sub>30</sub> pour le groupe témoin d'environ 15 dB sur les fréquences 8 et 16 kHz. L'administration du corticoïde libre dans le gel d'acide hyaluronique a permis la récupération d'une audition normale sur ces deux fréquences. Le gel d'acide hyaluronique seul ou contenant le corticoïde encapsulé dans les liposomes a entraîné une récupération sur le 16 kHz mais pas sur le 8 kHz. Selon ces résultats préliminaires, le corticoïde libre semble avoir une efficacité supérieure à celle du corticoïde encapsulé. Cependant, des expériences complémentaires seront nécessaires pour confirmer ces résultats. Il serait par ailleurs intéressant d'élucider l'effet propre de l'acide hyaluronique sur ce modèle ainsi que les mécanismes responsables de l'effet du corticoïde pour la récupération de l'audition.

Chapitre non soumis à publication.



## **Therapeutic efficacy of a corticoid loaded into hyaluronic acid gels after noise-induced hearing loss in guinea pigs**

*Naila El Kechai<sup>a</sup>, Elisabeth Mamelle<sup>b, c</sup>, Victor Adenis<sup>d</sup>, Yann Nguyen<sup>b, c</sup>, Florence Agnely<sup>a</sup>, Amélie Bochot<sup>a</sup>, Jean-Marc Edeline<sup>d</sup>, Evelyne Ferrary<sup>b</sup>*

<sup>a</sup> Institut Galien Paris-Sud, Université Paris-Sud, CNRS UMR 8612, Université Paris-Saclay, 92290 Châtenay-Malabry, France.

<sup>b</sup> UMR-S 1159 Inserm / Université Pierre et Marie Curie - Sorbonne Universités “Minimally Invasive Robot-based Hearing Rehabilitation”, Paris, France.

<sup>c</sup> AP-HP, Pitié-Salpêtrière Hospital, Otolaryngology Department, Unit of Otology, Auditory Implants and Skull Base Surgery, Paris, France.

<sup>d</sup> Institut des Neurosciences Paris-Saclay (Neuro-PSI), Département Cognition-Comportement, URM 9197, Université Paris-Sud, 91405 Orsay cedex, France.

## Abstract

The therapeutic efficacy of a local treatment based on a corticoid (dexamethasone phosphate) loaded into hyaluronic acid gels after exposure to a traumatic sound was evaluated in guinea pigs under relatively realistic treatment conditions. Different formulations including hyaluronic acid gel without dexamethasone phosphate, hyaluronic acid gel containing free dexamethasone phosphate and hyaluronic acid gel containing dexamethasone phosphate encapsulated into liposomes were administered in the middle ear of the animals 48 h after noise-exposure (5 kHz, 100 dB, 1 h). The hearing thresholds were recorded by Auditory Brainstem Response test before acoustic trauma (normal hearing), 48 h after acoustic trauma (noise-induced hearing loss) and then, 7 and 30 days after gel injection, to evaluate the hearing recovery. This study allowed to validate our animal model of noise-induced hearing loss. Indeed, in the control animals at day 30, the noise overexposure resulted in a persistent hearing loss of around 15 dB at 8 and 16 kHz frequencies. Hearing recovery at both frequencies was observed with the local administration of the free corticoid solubilized in hyaluronic acid gel, whereas hyaluronic acid gel alone or containing the corticoid loaded into liposomes resulted in hearing recovery at 16 kHz but not at 8 kHz. Thus, the free corticoid dissolved in hyaluronic acid gel seems to be more efficient for hearing recovery than the encapsulated one. However, further experiments are required to confirm these results and to elucidate the effect of hyaluronic acid *per se* as well as the mechanisms underlying the effect of the corticoid.

## Keywords

Acoustic trauma, dexamethasone phosphate, hydrogel, liposomes, local treatment, round window permeability.

## Abbreviations

ABR: auditory brainstem response, Chol: cholesterol, DexP: dexamethasone phosphate, DSPE-PEG2000: 1,2-distearoyl-sn-glycero-3-phosphoethanolamine-N-[methoxy-poly-(ethyleneglycol)2000], EPC: Egg phosphatidylcholine, HA: hyaluronic acid, Lip: liposomes.

## 1. Introduction

Hearing loss affects about 10% of the world population at different degrees. It causes disability in 360 to 538 million people, and moderate to severe disability in 124 million people (Lasak et al., 2014, Olusanya et al., 2014). In industrial societies, exposure to noise is one of the major causes of hearing loss in adults. The traumatizing noise may be continuous and repetitive (industrial noises), or pure impulsive (explosions, gunshots) (Sendowski et al., 2006). Acute acoustic trauma leads to mechanical and metabolic damages into the cochlea. The mechanical damages are due to excessive movements of the basilar membrane leading to impaired stereocilia, hair cells loss and collapse of supporting cells (Wang et al., 2002, Plontke and Zenner, 2004, Coleman et al., 2007). The subsequent metabolic damages in sensory cells are ionic disorders, involving an intracellular influx of potassium or calcium, excitotoxicity following excessive release of glutamate, and oxidative stress due to the production of free radicals (Puel et al., 1998). These mechanisms can provoke more or less rapid cell death due to necrosis or apoptosis (Yang et al., 2004). A part of the initial noise-induced hearing loss can be only transitory and may recover thanks to cochlear repair mechanisms (Puel et al., 1998, Kopke et al., 1999, Wang et al., 2002). However, the exposure to impulse noise typically results in substantial permanent hearing loss.

The recommended treatment in clinic after severe noise-induced hearing loss consists in the placement in silent environment, administration of corticoids associated or not with vasodilator substances, hyperbaric oxygenotherapy or normovolemic hemodilution (Sendowski et al., 2006). Recently, various pharmacologic compounds such as corticosteroids (Sendowski et al., 2006, Ozdogan et al., 2012, Bao et al., 2013, Chen et al., 2014), apoptosis inhibitors (Coleman et al., 2007, Wang et al., 2007) and antioxidants (Darrat et al., 2007, Mukherjea et al., 2011) have been tested in animal models for the protection from noise-induced hearing loss. The therapies have been administered either before, or immediately after the noise exposure, and resulted in various efficacies regarding hearing recovery.

In Chapter III, we demonstrated that a liposomal hyaluronic acid gel loaded with dexamethasone phosphate (DexP) injected in the middle ear of guinea pigs resulted in a therapeutic drug concentration in perilymph as well as a sustained release of the corticoid until 30 days. The aim of the present study was to evaluate the protective efficacy of this local treatment, under relatively realistic acoustic trauma and treatment conditions, in a guinea pig model. Different formulations including hyaluronic acid gel (HA), hyaluronic acid gel

containing free DexP (HA-DexP) and hyaluronic acid gel containing DexP loaded into liposomes (HA-DexP-Lip) were administered in the middle ear of the animals 48 h after noise-exposure (5 kHz, 100 dB, 1h). The hearing recovery from the acoustic trauma was recorded over 30 days.

## 2. Materials and methods

### 2.1. Materials

Dexamethasone sodium phosphate (DexP, Mw 516.4 Da, purity 98%) was obtained from Fagron (Amsterdam, The Netherlands). Egg phosphatidylcholine (EPC, purity 96%) was provided by Lipoid GmbH (Ludwigshafen, Germany). Cholesterol (Chol) was purchased from Sigma-Aldrich Co. (St. Louis, USA). 1,2-distearoyl-sn-glycero-3-phosphoethanolamine-N-[methoxy-poly-(ethyleneglycol)-2000] (DSPE-PEG2000, purity > 99%) was obtained from Avanti Polar Lipids, inc. (Alabaster, USA). Sodium hyaluronate (HA, Mw 1.5 MDa, purity 95%) was provided by Acros Organics (New Jersey, USA). All other chemicals were of analytical grade.

### 2.2. Preparation of HA gels containing or not liposomes (HA, HA-DexP, HA-DexP-Lip)

First, DexP-loaded PEGylated liposomes (DexP-Lip) were prepared by the thin film method as described previously (Chapter III). Briefly, lipid films composed of EPC:Chol:DSPE-PEG2000 (60:35:5 mole %) were prepared using rotary evaporation. The lipid film was hydrated with 100 mg/mL DexP solution in milliQ water and subsequently extruded 10 times through 0.2 µm polycarbonate filters set in a LIPEX extruder (Whitley, Vancouver, Canada). Non-encapsulated DexP was eliminated by means of dialysis (Chapter III). The mean hydrodynamic diameter and the zeta potential measured using a Zetasizer Nano ZS (Malvern, Worcestershire, UK) were  $145 \pm 50$  nm and  $-27 \pm 8$  mV respectively. The final lipid concentration was evaluated by a colorimetric enzymatic assay (Biolabo SA, Maizy, France) (El Kechai et al., 2015) after extrusion and dialysis. The amount of DexP encapsulated in DexP-Lip, determined using UV-HPLC, was  $10 \pm 2$  mg/mL.

Then, HA, HA-DexP and HA-DexP-Lip gels were prepared by dissolving HA (2.28% w/v) in HEPES/NaCl buffer (10/115 mM, pH 7.4), in 10 mg/mL DexP solution or into liposome suspension (DexP-Lip at 80 mM final lipid concentration), respectively. The gels were then

homogenized by means of vortex for 5 min, maintained at room temperature for 1 h and then stored at 4°C for at least 12 h prior to *in vivo* injection.

### 2.3. Animals

Ten male Hartley albinos guinea pigs (Charles River, L'Arbresles, France) weighing between 300 and 500 g, and with normal hearing were used in this study. Animal care and experimental procedures were conducted in accordance with the guidelines established by the European Communities Council Directive (2010/63/EU Council Directive Decree) and were approved by the local ethical committee (CEEA n° 59) of Paris-Sud University (permission n° AP 2014-23). All the animals were subjected to noise-exposure at D<sub>-2</sub> after that their normal hearing has been checked using Auditory Brainstem Response test (ABR). At D<sub>0</sub>, the hearing threshold determinations were again assessed to evaluate the hearing loss induced by the acoustic overexposure. Following this ABR test, animals were assigned randomly to four experimental groups: control (n = 3), HA (n = 6), HA-DexP (n = 6), HA-DexP-Lip (n = 5). n represents the number of ears per group. HA, HA-DexP and HA-DexP-Lip gels were injected in the middle ear after a surgical procedure. The control group had no surgical procedure and no gel injection. The hearing function was followed over time at D<sub>7</sub> and D<sub>30</sub> for all groups (Fig. 1). In order to minimize the use of animals, both ears were used for each animal and each ear was considered as an independent repetition. In preliminary experiments, we checked that no detectable ABR signal was observed when stimulating the contralateral ear with sound less than 80 dB SPL (Mamelle, Adenis, Edeline; unpublished data).

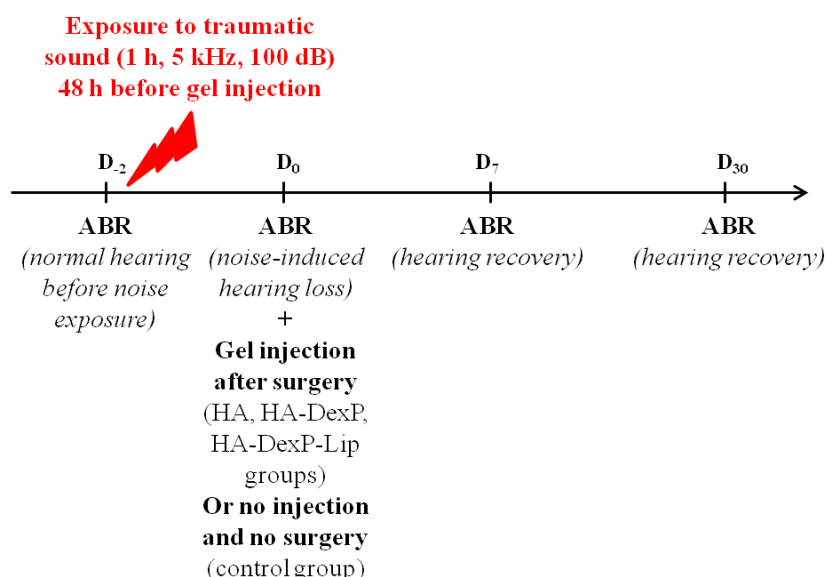


**Fig. 1.** Study design.

### 2.3.1. Exposure to traumatic sound

Animals, placed individually in a wire mesh cage (23 x 23 x 15 cm), were exposed for 1 h to a traumatic tone (pure tone of 5 kHz at 100 dB sound pressure level (SPL)) in an acoustically isolated chamber (IAC model AC2). The pure tone was generated by a wave generator (Hewlett-Packard, model HP 8903B), amplified (Prism-Audio, model LA-150M) and sent to two piezoelectric tweeters (Motorola, model KSN 1005) located on each side of the cage. The sound delivery system was calibrated to obtain  $100 \pm 5$  dB at various locations in the cage using a calibrated type I precision sound level meter (B&K model 2235). Visual inspection of the animal during exposure indicated that there was no preferred orientation of the animal regarding the speakers.

### 2.3.2. Injection procedure

Gel injection in the middle ear (HA, HA-DexP or HA-DexP-Lip) was performed two days after the noise trauma ( $D_0$ ) under general anesthesia (xylazine 4 mg/kg, ketamine 60 mg/kg, IM). Spontaneous ventilation was achieved and body temperature was maintained with a heating table. To guarantee the adequate application of the gel on the RW, the gel was injected in the middle ear after a retro-auricular surgical approach instead of a direct transtympanic injection. The retro-auricular skin was shaved and disinfected with povidone-iodine. A local anesthesia (0.5 mL lidocaine hydrochloride 1%) was injected in the retro-auricular subcutaneous tissues to complete general anesthesia. After a retro-auricular incision, retro-auricular muscles were removed from the bone, and the bulla was carefully exposed using a 2 mm diamond bur to drill the bone (NSK, Nakashima, Japan) allowing visualization of the cochlea as well as the round window. The gel was injected through a 1 mL syringe equipped with a 29G needle (length = 88 mm, B. Braun). The volume of gel injected was ~ 150 µL, [130-170] (DexP dose ~ 1.5 mg, [1.3-1.7]). The skin was then sutured with 3.0 Vicryl suture (Ethicon, Cincinnati, OH). After the injection procedure, guinea pigs received an intra-muscular injection of antibiotic prophylaxis (Enrofloxacin Bayer, Leverkusen, Germany).

### 2.3.3. Hearing thresholds determined by Auditory Brainstem Response recording (ABR)

The hearing function of guinea pigs was evaluated by recording the auditory brainstem response following auditory stimulus. ABR test was performed under gas general anesthesia (isoflurane) before acoustic trauma ( $D_{-2}$ ) and after trauma at  $D_0$ ,  $D_7$  and  $D_{30}$ . Tone bursts of

100 µs were delivered at 1, 4, 8, 16, 24 and 32 kHz, with a high frequency transducer (Etymotic Research ER1) connected to an external ear canal probe. The ABR were recorded via subcutaneous electrodes (SC25, Neuro-Services) placed subcutaneously in the leg (ground electrode), the vertex (active electrode), and the ipsilateral retro-auricular side of the analyzed ear (reference electrode). The ABR were collected with a commercialized interface and software (RT Otophy Lab, Echodia, France) and were determined with 5 dB decreasing increments at each frequency. The hearing threshold corresponded to the minimal intensity for which at least one ABR wave was clearly recognized. The accuracy of the ABR threshold measurement was ± 5 dB.

#### 2.3.4. Statistical analysis

GraphPad Prism software was used for statistical analysis. Non-parametric tests were performed and statistical analysis of the hearing thresholds was conducted using two-way or one-way analysis of variance (Anova), with a Sidak's post-test. A *p* value < 0.05 was considered as significant. Results were expressed as mean ± SEM.

## 2. Results and discussion

### 2.1. Hearing loss induced by the traumatic sound ( $D_0$ )

Auditory thresholds before noise exposure ( $D_{-2}$ ) appeared normal in the frequency range 1-32 kHz and were equivalent among individuals and between groups (**Fig. 2**). ABR results comparing the normal hearing and the hearing after noise exposure ( $D_{-2}$  vs  $D_0$ ) demonstrated a noise-induced threshold shift that was not equivalent among the frequency range (**Fig. 2**). The highest shift ~ 30-40 dB was recorded for 8 and 16 kHz frequencies. For 4, 24 and 32 kHz, ~ 10-15 dB shift was observed and there was no modification of the hearing thresholds at 1 kHz. The hearing threshold shifts after noise-exposure were equivalent between the different experimental groups (Two-way Anova, ns). These results allowed us to validate the guinea pig model of noise-induced hearing loss in the sound exposure conditions used (5 kHz at 100 dB for 1 h). 8 and 16 kHz are the frequencies that are the best heard by the guinea pig (i.e. frequencies for which hearing thresholds are around 0 dB (**Fig. 2**)). In human, the best detected frequencies are between 1 and 2 kHz corresponding to conversational frequencies.

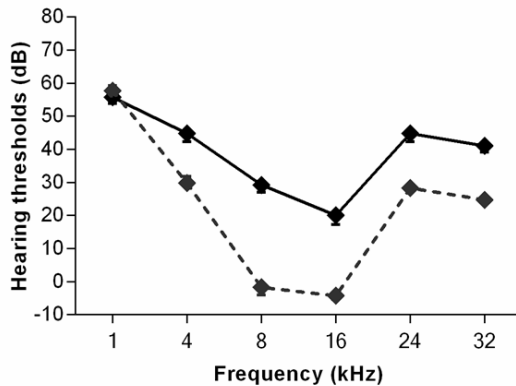


**Fig. 2.** Average noise-induced hearing loss in all the animals of the 4 groups. ABR thresholds were recorded before (discontinue line, D<sub>-2</sub>) and after (continue line, D<sub>0</sub>) the noise exposure (5 kHz, 100 dB, 1h). Results are expressed as mean ± SEM (n = 20). The noise-exposure induced threshold shifts between 10 to 40 dB at all frequencies (two-way Anova, p < 0.0001) except at 1 kHz (post-test, ns).

## 2.2. Hearing recovery at D<sub>7</sub>

Average ABR thresholds at D<sub>-2</sub>, D<sub>0</sub>, D<sub>7</sub> and D<sub>30</sub> for each group (Control, HA, HA-DexP and HA-DexP-Lip) are plotted in **Figure 3**. For the control group (no surgical procedure and no gel injection), a transient hearing recovery was observed at D<sub>7</sub> for all the frequencies except at 8 kHz (**Fig. 3A**). As previously mentioned, a part of the initial noise-induced hearing loss can recover thanks to cochlear repair mechanisms, such as neosynaptogenesis at the inner hair cell synaptic complex (Puel et al., 1998), recovery of outer hair cells (Chan et al., 1998) as well as supporting cells (Wang et al., 2002) and the reactions of intracellular antioxidant defense mechanisms (Kopke et al., 1999). However, the hearing threshold at 16 kHz increased again between D<sub>7</sub> and D<sub>30</sub>. This result may be explained by a delayed free radical formation, peaking 7-10 days following noise exposure as described previously by Le Prell et al. (2007). For the other groups (HA, HA-DexP, HA-DexP-Lip), there was no hearing recovery at D<sub>7</sub> (**Fig. 3**). Surprisingly, on the opposite to what was observed for the control group, the hearing thresholds appear to slightly increase at D<sub>7</sub> compared to D<sub>0</sub> (**Fig. 3B, 3C, 3D**). However, this increase was not statistically significant. This may be explained by the additional stress experienced by the animals in the treated groups (HA, HA-DexP, HA-DexP-Lip) due to the surgical procedure for the local gel injection at D<sub>0</sub> (*i.e.* 2 days after the acoustic trauma). The surgical procedure itself (retro-auricular surgery) is unlikely to directly cause damages to the inner ear (Takemura et al., 2004). However, this result needs to be further investigated by

adding another control group in which a surgical procedure will be performed but without gel injection.

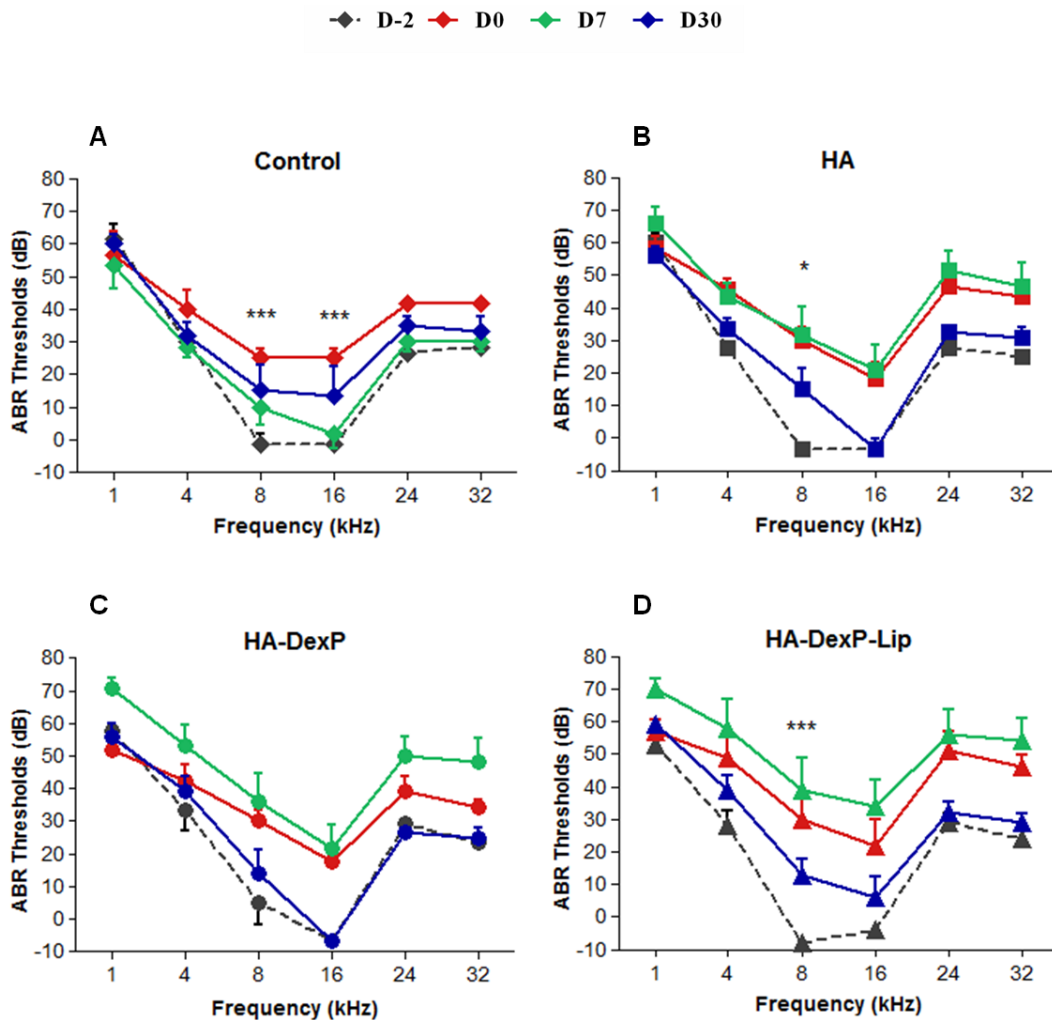


**Fig. 3.** ABR thresholds at D<sub>-2</sub> (black), D<sub>0</sub> (red), D<sub>7</sub> (green), D<sub>30</sub> (blue) for control (**A**, n = 3), HA (**B**, n = 6), HA-DexP (**C**, n = 6), HA-DexP-Lip (**D**, n = 5) groups. Results are expressed as mean ± SEM. Difference between D<sub>-2</sub> and D<sub>30</sub> (two-way Anova, post-test: \* p < 0.01, \*\*\* p < 0.0001).

### 2.3. Hearing recovery at D<sub>30</sub>

In the control group (**Fig. 3A**), the acoustic trauma caused threshold shift at D<sub>30</sub> of  $17 \pm 8$  dB (n=3) at 8 kHz, and of  $15 \pm 7$  dB (n=3) at 16 kHz, whereas the other frequencies returned to normal within 30 days (two-way Anova). In HA and HA-DexP-Lip groups (**Fig. 3B** and **3D**), at D<sub>30</sub>, the hearing thresholds returned to normal for all frequencies except 8 kHz for which a threshold shift around 20 dB persisted. In HA-DexP group, all frequencies returned to normal within 30 days (**Fig. 3C**). From these data, the free DexP dissolved in HA

gel seems to be more efficient for hearing recovery than the encapsulated one. Interestingly, HA gel itself appears to have a positive effect. Similarly, Lajavardi et al. (2009) reported that HA gel *per se* showed a trend to decrease endotoxin-induced uveitis in rat. This could be explained by the role of hyaluronic acid on the immune function reported previously (Termeer et al., 2003, Schwertfeger et al., 2015). Indeed, in addition to regulating pro-inflammatory cytokine production, high molecular weight HA was shown to modulate the expression of anti-inflammatory cytokines such as IL-10 in the tumor microenvironment (Schwertfeger et al., 2015). Besides, HA could be able to inhibit polymorphonuclear leucocyte and macrophage ability to produce active oxygen, or could act as an active-oxygen scavenger (Lym et al., 2004). Based on these data and regarding the high molecular weight HA (~ 1.5 MDa) used in this study and its high degree of entanglement at 2.28% w/v (Chapter II), HA is unlikely to diffuse through the round window. Thus, the effect of HA on the hearing thresholds could be due to a local anti-inflammatory action in the middle ear that positively affected the inner ear structures.

Hearing recovery between D<sub>0</sub> and D<sub>30</sub> was compared between the different groups in **Figure 4**. At a 4-32 kHz frequency range, all the groups, including the control, have shown a hearing recovery between D<sub>0</sub> and D<sub>30</sub> (**Fig. 4**). However, even if the hearing recovery seems to be higher in the treated groups compared to the control at 8, 16 and 24 kHz, the statistical analysis showed no significant differences between the groups (Two-way Anova, ns).

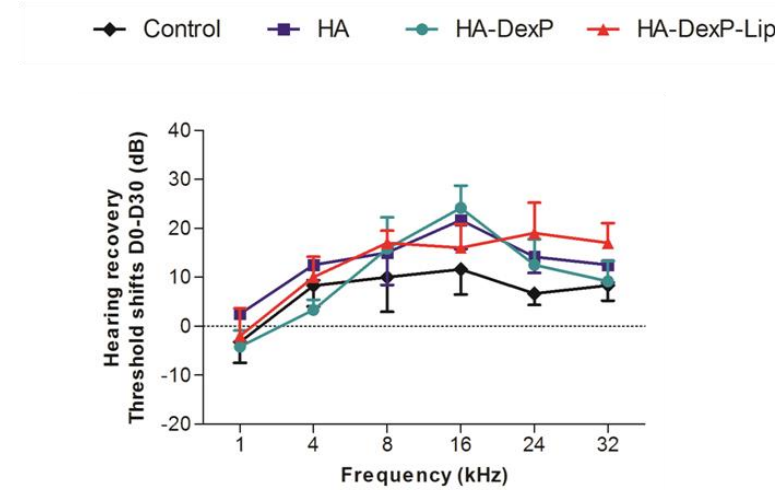


**Fig. 4.** Hearing recovery between D<sub>0</sub> and D<sub>30</sub> (thresholds D<sub>0</sub> - D<sub>30</sub>) for control (black diamond, n = 3), HA (purple square, n = 6), HA-DexP (green circle, n = 6) and HA-DexP-Lip (red triangle, n = 5) groups. Results are expressed as mean ± SEM. No difference between the groups (two-way Anova, ns).

Thereafter, in order to assess if the animals were able to recover a normal hearing function, we compared the noise-induced threshold shifts between D<sub>2</sub> and D<sub>30</sub> in the different groups specifically at 8 and 16 kHz (Fig. 5) since those frequencies were the most impacted by the acoustic trauma (Fig. 2). The lowest threshold shift was observed for HA-DexP at both frequencies but it was almost equivalent between the other groups at 8 kHz (Fig. 5A). At 16 kHz (Fig. 5B), the three treated groups (HA, HA-DexP, HA-DexP-Lip) showed a better recovery compared to the control. However, despite this trend, the statistical analysis showed no differences between the groups neither at 8 kHz nor at 16 kHz. The number of repetitions per group (number of ears, n between 3 and 6) is probably not sufficient to detect statistical differences and should be increased in future experiments.

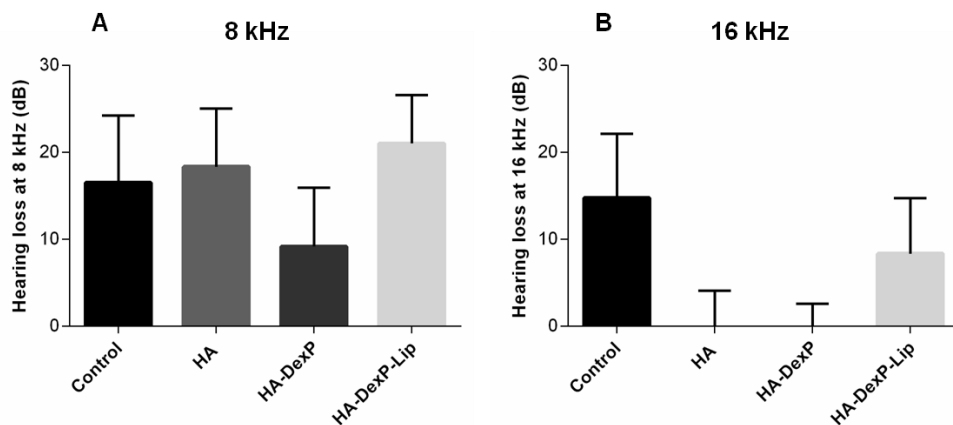


**Fig. 5.** Noise-induced hearing loss at D<sub>30</sub> (thresholds D<sub>30</sub> - D<sub>2</sub>) at 8 kHz (A) and 16 kHz (B) for the control (n = 3), HA (n = 6), HA-DexP (n = 6) and HA-DexP-Lip (n = 5) groups. Hearing loss was calculated individually for each animal and results are expressed as mean ± SEM for each group. There were no significant differences between the groups at both 8 and 16 kHz (two-way Anova, ns).

#### 2.4. Benefit of corticoids for hearing recovery after noise-induced hearing loss

The use of corticoids for hearing protection during noise overexposure is widely described in the literature in animal models. However, some of the animal studies reported limited success regarding hearing recovery. Sendowski et al. (2006) demonstrated that direct infusion of methylprednisolone in the cochlea reduces hair cell loss, accelerated hearing recovery, but did not limit permanent threshold shifts. Similarly, Ozdogan et al. (2012) showed that intratympanically administered methylprednisolone following an acoustic trauma reduced outer hair cell loss but had no impact on hearing loss after 2 weeks. Conversely, some other

studies have reported efficient hearing recovery after local administration of dexamethasone or methylprednisolone (Takemura et al., 2004, Zhou et al., 2009). It was also reported that the treatment efficiency is significantly decreased in the case of delayed injection up to several days (3 to 7 days) after noise-exposure (Zhou et al., 2009). In most of the studies described previously, the treatment is administered few hours following the acoustic trauma, and in some cases, several days before the trauma. Obviously, such approaches are not realistic from a clinical point of view. In the clinical practice, patients generally consult few days after they were exposed to noise, once they have clearly realized the hearing loss and were thus treated late after the acute noise exposure.

It is worth noting that despite the widespread use of corticoids to treat hearing disorders, the molecular mechanisms underlying this treatment are not well characterized and poorly understood. Corticoids have multiple mechanisms of action including anti-inflammatory action, membrane stabilization, increased perfusion and ion transport regulation (Czock et al., 2005, Sendowski et al., 2006, Meltser and Canlon, 2011). Regarding the inner ear, many physiopathological mechanisms could be involved in the protection from noise-induced hearing loss. First, corticoids exert benefit effects against oxidative stress in the cochlea by upregulation of glutathione production (Nagashima et al., 2005, Meltser and Canlon, 2011). Indeed, the production of reactive oxygen species is the prevailing physiopathological mechanisms of noise-induced hearing loss and glutathione is a known protective agent (Puel et al., 1998). Secondly, glucocorticoids contribute to reduce the inflammatory reaction. Recent studies have shown that inflammatory responses occur in the inner ear under noise overstimulation and pro-inflammatory cytokines (IL6, IL-1 $\beta$ , TNF- $\alpha$ ) are produced locally in the cochlea. These cytokines are targets for corticosteroids that can inhibit their production (Hirose et al., 2005, Dinh et al., 2008). Finally, corticosteroids could be involved in the apoptosis cascade. Antiapoptotic effects for glucocorticoids have been previously reported (Yildirim et al., 2006) but this mechanism related to noise-exposure needs to be further investigated.

In Chapter III, we demonstrated that the injection of encapsulated DexP (HA-DexP-Lip) resulted in a 5 to 25-fold higher corticoid concentration in perilymph compared to free DexP (HA-DexP) and sustained the release of the corticoid over 30 days. Surprisingly, in this study, the injection HA-DexP resulted in a slightly better efficacy than the injection of HA-DexP-Lip. The threshold toxicity of dexamethasone in the inner ear is not documented. However,

the concentrations obtained for HA-DexP-Lip were in the range 100-800 ng/mL, which are more likely to be therapeutic concentrations than toxic ones (Kim et al., 2009).

Finally, further experiments are needed to elucidate and to confirm the results obtained in the present study. The number of animals per group should be increased to have the statistical power required to detect significant differences between groups. Furthermore, another control group (surgical procedure without gel injection) is necessary to specifically assess the own effect of the surgical procedure without the added effect of the treatment. A higher hearing loss is expected in the control group after middle ear surgery. Thus, a beneficial effect of the local treatment should possibly reach statistical significance.

#### **4. Conclusions**

This work provided preliminary data on the efficacy of hyaluronic acid gels containing a corticoid, encapsulated into liposomes or not, in a guinea pig model of noise-induced hearing loss. The acoustic trauma resulted in a permanent hearing loss in the control group at 8 and 16 kHz. Complete hearing recovery was obtained with the free corticoid solubilized in HA gel, whereas HA gel alone or containing the corticoid loaded into liposomes resulted in hearing recovery at all frequencies except 8 kHz. Further experiments are required to confirm these results and to elucidate the effect of hyaluronic acid *per se* as well as the mechanisms underlying the effect of the corticoid related to its pharmacokinetic profile in the inner ear.

#### **Acknowledgments**

This work was supported by a PhD grant (Naila El Kechai) from the French Ministry of National Education and Research and from Neurelec France /Oticon Medical (Victor Adenis). Authors wish to thank the “Fondation pour la Recherche Médicale”.

## References

- Bao, J., Hungerford, M., Luxmore, R., Ding, D., Qiu, Z., Lei, D., Yang, A., Liang, R., Ohlemiller, K.K., 2013. Prophylactic and therapeutic functions of drug combinations against noise-induced hearing loss. *Hearing Research.* 304, 33-40.
- Chan, E., Suneson, A., Ulfendahl, M., 1998. Acoustic trauma causes reversible stiffness changes in auditory sensory cells. *Neuroscience.* 83, 961-968.
- Chen, L., Dean, C., Gandolfi, M., Nahm, E., Mattiace, L., Kim, A.H., 2014. Dexamethasone's Effect in the Retrocochlear Auditory Centers of a Noise-Induced Hearing Loss Mouse Model. *Otolaryngology -- Head and Neck Surgery.* 151, 667-674.
- Coleman, J.K.M., Littlesunday, C., Jackson, R., Meyer, T., 2007. AM-111 protects against permanent hearing loss from impulse noise trauma. *Hearing Research.* 226, 70-78.
- Czock, D., Keller, F., Rasche, F.M., Häussler, U., 2005. Pharmacokinetics and pharmacodynamics of systemically administered glucocorticoids. *Clinical pharmacokinetics.* 44, 61-98.
- Darrat, I., Ahmad, N., Seidman, K., Seidman, M.D., 2007. Auditory research involving antioxidants. *Current opinion in otolaryngology & head and neck surgery.* 15, 358-363.
- Dinh, C., Haake, S., Chen, S., Hoang, K., Nong, E., Eshraghi, A., Balkany, T., Van De Water, T., 2008. Dexamethasone protects organ of corti explants against tumor necrosis factor-alpha-induced loss of auditory hair cells and alters the expression levels of apoptosis-related genes. *Neuroscience.* 157, 405-413.
- El Kechai, N., Bochot, A., Huang, N., Nguyen, Y., Ferrary, E., Agnely, F., 2015. Effect of liposomes on rheological and syringeability properties of hyaluronic acid hydrogels intended for local injection of drugs. *Int J Pharm.* 487, 187-196.
- Hirose, K., Discolo, C.M., Keasler, J.R., Ransohoff, R., 2005. Mononuclear phagocytes migrate into the murine cochlea after acoustic trauma. *Journal of Comparative Neurology.* 489, 180-194.
- Kim, S.H., Kim, K.X., Raveendran, N.N., Wu, T., Pondugula, S.R., Marcus, D.C., 2009. Regulation of ENaC-mediated sodium transport by glucocorticoids in Reissner's membrane epithelium. *Am J Physiol Cell Physiol.* 296, C544-557.
- Kopke, R., Allen, K.A., Henderson, D., Hoffer, M., Frenz, D., van de Water, T., 1999. A radical demise: toxins and trauma share common pathways in hair cell death. *Annals of the New York Academy of Sciences.* 884, 171-191.
- Lajavardi, L., Camelo, S., Agnely, F., Luo, W., Goldenberg, B., Naud, M.C., Behar-Cohen, F., de Kozak, Y., Bochot, A., 2009. New formulation of vasoactive intestinal peptide using liposomes in hyaluronic acid gel for uveitis. *J Control Release.* 139, 22-30.
- Lasak, J.M., Allen, P., McVay, T., Lewis, D., 2014. Hearing Loss: Diagnosis and Management. *Primary Care: Clinics in Office Practice.* 41, 19-31.
- Le Prell, C.G., Yamashita, D., Minami, S.B., Yamasoba, T., Miller, J.M., 2007. Mechanisms of noise-induced hearing loss indicate multiple methods of prevention. *Hearing Research.* 226, 22-43.
- Lym, H.S., Suh, Y., Park, C.K., 2004. Effects of hyaluronic acid on the polymorphonuclear leukocyte (PMN) release of active oxygen and protection of bovine corneal endothelial cells from activated PMNs. *Korean Journal of Ophthalmology.* 18, 23-28.

- Meltser, I., Canlon, B., 2011. Protecting the auditory system with glucocorticoids. *Hearing Research.* 281, 47-55.
- Mukherjea, D., Rybak, L.P., Sheehan, K.E., Kaur, T., Ramkumar, V., Jajoo, S., Sheth, S., 2011. The design and screening of drugs to prevent acquired sensorineural hearing loss. *Expert opinion on drug discovery.* 6, 491-505.
- Nagashima, R., Sugiyama, C., Yoneyama, M., Ogita, K., 2005. Transcriptional factors in the cochlea within the inner ear. *Journal of pharmacological sciences.* 99, 301-306.
- Olusanya, B.O., Neumann, K.J., Saunders, J.E., 2014. The global burden of disabling hearing impairment: a call to action. *Bulletin of the World Health Organization.* 92, 367-373.
- Ozdogan, F., Ensari, S., Cakir, O., Ozcan, K.M., Koseoglu, S., Ozdas, T., Gurgen, S.G., Dere, H., 2012. Investigation of the cochlear effects of intratympanic steroids administered following acoustic trauma. *The Laryngoscope.* 122, 877-882.
- Plontke, S., Zenner, H.-P., 2004. Current aspects of hearing loss from occupational and leisure noise. *GMS current topics in otorhinolaryngology, head and neck surgery.* 3,
- Puel, J.-L., Ruel, J., d'Aldin, C.G., Pujol, R., 1998. Excitotoxicity and repair of cochlear synapses after noise-trauma induced hearing loss. *Neuroreport.* 9, 2109-2114.
- Schwertfeger, K., Cowman, M., Telmer, P., Turley, E., McCarthy, J., 2015. Hyaluronan, Inflammation and Breast Cancer Progression. *Name: Frontiers in Immunology.* 6, 236.
- Sendowski, I., Abaamrane, L., Raffin, F., Cros, A., Clarençon, D., 2006. Therapeutic efficacy of intra-cochlear administration of methylprednisolone after acoustic trauma caused by gunshot noise in guinea pigs. *Hearing Research.* 221, 119-127.
- Takemura, K., Komeda, M., Yagi, M., Himeno, C., Izumikawa, M., Doi, T., Kuriyama, H., Miller, J.M., Yamashita, T., 2004. Direct inner ear infusion of dexamethasone attenuates noise-induced trauma in guinea pig. *Hearing Research.* 196, 58-68.
- Termeer, C., Sleeman, J.P., Simon, J.C., 2003. Hyaluronan—magic glue for the regulation of the immune response? *Trends in immunology.* 24, 112-114.
- Wang, J., Ruel, J., Ladrech, S., Bonny, C., Van De Water, T.R., Puel, J.-L., 2007. Inhibition of the c-Jun N-terminal kinase-mediated mitochondrial cell death pathway restores auditory function in sound-exposed animals. *Molecular pharmacology.* 71, 654-666.
- Wang, Y., Hirose, K., Liberman, M.C., 2002. Dynamics of noise-induced cellular injury and repair in the mouse cochlea. *Journal of the Association for Research in Otolaryngology.* 3, 248-268.
- Yang, W.P., Henderson, D., Hu, B.H., Nicotera, T.M., 2004. Quantitative analysis of apoptotic and necrotic outer hair cells after exposure to different levels of continuous noise. *Hearing Research.* 196, 69-76.
- Yildirim, E., Ozisik, K., Ozisik, P., Emir, M., Yildirim, E., Misirlioglu, M., Tuncer, S., Kilinc, K., 2006. Apoptosis-related gene bcl-2 in lung tissue after experimental traumatic brain injury in rats. *Heart, Lung and Circulation.* 15, 124-129.
- Zhou, Y., Zheng, H., Shen, X., Zhang, Q., Yang, M., 2009. Intratympanic administration of methylprednisolone reduces impact of experimental intensive impulse noise trauma on hearing. *Acta oto-laryngologica.* 129, 602-607.

## **Chapitre V**

**Étude de l'efficacité thérapeutique du gel de  
liposomes contenant un corticoïde pour la  
préservation de l'audition résiduelle durant  
l'implantation cochléaire manuelle ou robot-assistée**

## Chapitre V

### **Etude de l'efficacité thérapeutique du gel de liposomes contenant un corticoïde pour la préservation de l'audition résiduelle durant l'implantation cochléaire manuelle ou robot-assistée**

#### **Introduction - résumé**

Les indications de l'implant cochléaire découlent de son mode de fonctionnement qui remplace l'oreille externe, l'oreille moyenne et l'organe sensoriel cochléaire. Par le passé, l'implantation cochléaire était réservée aux cas de surdités sévères à profondes bilatérales lorsqu'un gain auditif par audioprothèse était insuffisant. Cependant, ses indications se sont progressivement élargies aux patients ayant une audition résiduelle. Bien que la survie des cellules ganglionnaires semble être essentielle pour la préservation de l'audition résiduelle lors de l'implantation de l'électrode dans la cochlée (**Fig. 0**), la technique a connu une évolution assez lente au cours des vingt dernières années. Aujourd'hui, une insertion non traumatique est l'objectif principal lors de la chirurgie d'implantation cochléaire et ce, afin de préserver l'audition résiduelle des patients. Cependant, la relation entre la qualité de l'insertion, les dommages cochléaires engendrés et l'audition post-opératoire n'est pas encore clairement établie. En outre, des traitements locaux qui pourraient limiter les dommages cochléaires lors de l'implantation se développent de plus en plus en recherche pré-clinique et clinique et semblent très prometteurs.



**Fig. 0.** Représentation schématique de l'électrode dans la cochlée (Krezlin et al. Journal of Controlled Release, 2012)

Le but de ce chapitre est d'abord d'évaluer l'intérêt d'une nouvelle technique d'insertion d'électrodes en utilisant un outil motorisé. D'autre part, un gel de liposomes contenant un corticoïde (dexamethasone phosphate) a été testé sur la préservation de l'audition chez le cobaye. Les cobayes ont été implantés avec une électrode recouverte de silicium de 4 mm de longueur en utilisant soit une technique manuelle ou un outil d'insertion motorisé. A la fin de la procédure d'implantation, le gel d'acide hyaluronique contenant des liposomes encapsulant ou non la dexamethasone phosphate a été injecté dans l'oreille moyenne. Les seuils auditifs ont été enregistrés en pré-opératoire ( $J_0$ ) et 7 jours après l'implantation cochléaire ( $J_7$ ).

Les animaux implantés à l'aide de l'outil d'insertion motorisé ont présenté une meilleure audition résiduelle à  $J_7$  comparés à ceux implantés manuellement. De plus, la préservation de l'audition a été améliorée lorsque le gel de liposomes contenant le corticoïde a été administré localement après insertion manuelle. Cette étude a permis de valider un nouvel outil d'insertion d'électrodes qui permet d'améliorer l'audition post-opératoire après l'implantation cochléaire chez le cobaye. En outre, l'intérêt de la formulation pour la préservation de l'audition résiduelle a été démontré lors de l'insertion manuelle.

Une version ultérieure de ce chapitre sera soumise à publication.

## Projet de publication

### **Enhanced hearing preservation in an animal model of cochlear implantation with motorized insertion and dexamethasone-loaded liposomes dispersed within a hyaluronic acid gel**

*Elisabeth Mamelle<sup>a,b,c</sup>, Naila El Kechai<sup>d</sup>, Amélie Bochot<sup>d</sup>, Florence Agnely<sup>d</sup>, Olivier Sterkers<sup>a,b,c</sup>, Evelyne Ferrary<sup>a,b,c</sup> and Yann Nguyen<sup>a,b,c</sup>*

<sup>a</sup> AP-HP, Pitié-Salpêtrière Hospital, Otolaryngology Department, Unit of Otology, Auditory Implants and Skull Base Surgery, Paris, France.

<sup>b</sup> Sorbonne University, UPMC Univ. Paris 06, Paris, France.

<sup>c</sup> Inserm, Paris 6 UMPC University, UMR S-1159, “Minimally Invasive Robot-based Hearing Rehabilitation”, Paris France.

<sup>d</sup> Institut Galien Paris-Sud, Université Paris-Sud, CNRS UMR 8612, Université Paris-Saclay, 92290 Châtenay-Malabry, France.

#### **Corresponding author**

Elisabeth Mamelle, M.D

ENT Department, Pitié Salpêtrière Hospital, AP-HP,  
47-83 boulevard de l'Hôpital, 75651 Paris cedex 13, France.

E-mail address: [elisabeth.mamelle@gmail.com](mailto:elisabeth.mamelle@gmail.com)

Tel: +331 42 16 31 06

Fax: +331 42 16 26 05

## Abstract

Whereas the survival of ganglion cells seems to be crucial for the preservation of residual hearing during cochlear implantation, this technique showed a slow evolution during the past two decades. Nowadays, a non-traumatic insertion for hearing preservation is the primary goal during cochlear implantation surgery. However, the relationship between the quality of the array insertion, the cochlear damages and the postoperative hearing has not been clearly established. Furthermore, local therapies that could limit these cochlear damages have emerged during the past decade in research. The aim of this study was to evaluate in guinea pigs, the impact on postoperative hearing of a new electrode insertion technique, using a motorized tool on one hand, and, on the other hand, of the local administration of a formulation based on a hyaluronic acid gel containing corticoid-loaded liposomes. Guinea pigs were implanted with a silicon 4-mm length electrode array using either a manual technique, or an in house motorized tool. At the end of the procedure, hyaluronic acid (2.28% w/v) gel containing unloaded liposomes (80 mM), or dexamethasone phosphate loaded ones (15 mg/ml) was injected. Hearing thresholds were recorded before cochlear implantation ( $D_0$ ) and 7 days after ( $D_7$ ). The animals implanted with the motorized insertion tool had better hearing thresholds at  $D_7$  compared to the ones implanted manually. Hearing preservation was improved when dexamethasone phosphate contained in the liposomal gel was administrated locally. This study validated a new array insertion tool that allowed enhancing postoperative hearing after cochlear implantation in an animal model. In addition, the benefit of the original gel formulation containing dexamethasone loaded into liposomes was shown to prevent the postoperative threshold shifts during manual insertion.

## Key words

Cochlear implant, dexamethasone phosphate, hyaluronic acid gel, inner ear, liposomes, residual hearing.

## Abbreviations

ABR: auditory brainstem response, CI: cochlear implantation, Chol: cholesterol, DexP: dexamethasone phosphate, DSPE-PEG2000: 1,2-distearoyl-sn-glycero-3-phosphoethanolamin e-N-[methoxy-poly-(ethyleneglycol)-2000], EPC: Egg phosphatidylcholine, HA: hyaluronic acid, Lip: liposomes, MIT: motorized insertion tool.

## 1. Introduction

Cochlear implant appears to be a mandatory device to treat patients with profound or severe hearing loss with poor or no speech perception. Soft surgery was the first step to modify surgical procedures dedicated to auditory rehabilitation in patients with persistent low frequency hearing (Lehnhardt, et al., 1993). Several techniques have been developed to limit the hearing loss due to damages following the cochlea opening and the electrode insertion. For instance, a slow electrode array insertion (Rajan, et al., 2013), a cochleostomy or round window clogging with soft tissue (Santa Maria, et al., 2014) have been proposed to limit those damages. The final position of the electrode array nearby the neural cells located in the spiral ganglion could also be an issue (Briggs, et al., 2005). Moreover, array design modification, stylet guided insertion and the use of insertion tools have been developed to enhance the manual electrode insertion in order to reduce the potential damages to the basilar membrane and lateral spiral ligament. Minimally invasive robot-based surgery has been developed as well, but its usefulness in the field of cochlear implantation (CI) has not been clinically validated so far (Majdani, et al., 2010; Bell, et al., 2012; Nguyen, et al., 2012). Furthermore, no clear relationship between the estimated quality of the array insertion, the putative cochlear damages and the postoperative hearing performances have been established. It is reasonable to assume that an electrode insertion without mechanical trauma, no tremor and nor fits-and-starts during its progression would limit the putative damages to the cochlear structures.

Additionally, recent studies focused on the development of local drug delivery systems to enhance residual hearing. They had already demonstrated that corticosteroids could minimize the development of fibrotic tissue around the electrode array after cochlear implantation (Leary Swan, et al., 2008; Bas, et al. 2012; Honeder, et al., 2015). The fibrosis circling the array could be an issue to explain the variability of postoperative performances. Due to the petrous location of the inner ear combined to the presence of the blood-perilymph barrier, systemic drug administration delivers only low concentrations of drug to the cochlea and induces side effects. Nevertheless, few specific local therapies for the inner ear are available to prevent hearing loss after surgery whereas their benefit has already been proved in clinical studies when applied through the round window niche (Rajan, et al. 2012; Ramos, et al., 2015).

As demonstrated in Chapter I, HA liposomal gel appears to be a promising and versatile formulation platform for a wide range of applications in local drug delivery when an injection is required. In Chapter III, the liposomal hyaluronic acid gel loaded with dexamethasone

phosphate (DexP) and injected in the middle ear of guinea pigs resulted in a therapeutic drug concentration in perilymph as well as a sustained release of the corticoid until 30 days. Applied to cochlear implantation, the liposomal HA gel loaded with the corticoid could be relevant to minimize the inflammatory response associated with the surgery. In this formulation, HA may allow a long residence time into the middle ear thanks to its mucoadhesive properties and viscoelasticity (Masuda, et al., 2001; Girish and Kemparaju, 2007) while liposomes could act as a reservoir for a sustained release of the corticoid.

The aim of this study was thus to assess the potential benefit of a motorized tool for the cochlear implant insertion, combined with a liposomal HA gel containing DexP locally applied in the middle ear of normal hearing guinea pigs, to improve the residual hearing preservation after implantation.

## 2. Materials and Methods

### 2.1. Materials

Dexamethasone sodium phosphate (DexP, Mw 516.4 Da, purity 98%) was obtained from Fagron (Amsterdam, The Netherlands). Egg phosphatidylcholine (EPC, purity 96%) was provided by Lipoid GmbH (Ludwigshafen, Germany). Cholesterol (Chol) was purchased from Sigma-Aldrich Co. (St. Louis, USA). 1,2-distearoyl-sn-glycero-3-phosphoethanolamine-N-[methoxy-poly-(ethyleneglycol)-2000] (DSPE-PEG2000, purity > 99%) was obtained from Avanti Polar Lipids, inc. (Alabaster, USA). Sodium hyaluronate (HA, Mw 1.5 MDa, purity 95%) was provided by Acros Organics (New Jersey, USA). All other chemicals were of analytical grade.

### 2.2. Preparation of HA gels containing or not liposomes

First, liposomes were prepared as follows. Briefly, lipid films composed of EPC:Chol:DSPE-PEG2000 (60:35:5 mole %) were prepared using rotary evaporation. The lipid film was then hydrated with either 50 mg/mL DexP solution in milliQ water (DexP-Lip) or HEPES/NaCl buffer, 10/115 mM, pH 7.4 (Lip). The liposome suspensions were subsequently extruded through 0.2 µm polycarbonate membranes. The final lipid concentration was evaluated by a colorimetric enzymatic assay (El Kechai, et al., 2015). The concentration of DexP after liposome purification, determined by UV-HPLC, was of  $15 \pm 2$  mg/ml. The mean hydrodynamic diameter and the zeta potential measured using a

Zetasizer Nano ZS (Malvern, Worcestershire, UK) were  $145 \pm 50$  nm and  $-27 \pm 8$  mV respectively for DexP-Lip and  $145 \pm 50$  and  $-25 \pm 7$  respectively for Lip. Then, to prepare the gels, HA powder (2.28% w/v) was dissolved under magnetic stirring either into liposome suspensions at 80 mM final lipid concentration (HA-DexP-Lip and HA-Lip) or in HEPES/NaCl buffer (10/115 mM, pH 7.4). The gels were then homogenized by means of vortex for 5 min, maintained at room temperature for 1 h and then stored at 4°C for at least 12 h prior to *in vivo* injection.

### 2.3. Animals

Cochlear implantation (CI) was performed in 33 male Hartley albinos guinea pigs (Charles River, L'Arbresles, France) with normal hearing, and weighing between 290 and 350 g. Animal care and experimental procedures were conducted in accordance with the European legislation and were approved by the local ethical committee (CEEA n° 26) of Paris-Sud University (permission n° 2013-100).

### 2.4. Study design

A cochleostomy was performed in 6 animals (control group). Cochlear implantation through a cochleostomy was performed in 27 animals: a group of 12 guinea pigs with a manual insertion of the cochlear device and another one of 15 animals with the motorized insertion tool (**Table 1**). In each group, the bulla was filled with a liposomal gel without dexamethasone phosphate (HA-Lip) (control: n = 3; manual: n = 6; motorized tool: n = 6), or with a liposomal gel containing dexamethasone phosphate (HA-DexP-Lip) (control: n = 3; manual: n = 6; motorized tool: n = 9). Normal preoperative hearing was assessed with auditory brainstem response thresholds (ABR) before surgery (D<sub>0</sub>). After the surgical procedure, ABR thresholds were recorded at D<sub>7</sub>. n corresponds to the number of ears.

**Table 1**

Experimental protocol. The control group had a cochleostomy followed by HA-Lip (n = 3) or HA-DexP-Lip (n = 3) injection in the bulla in contact with the round window. A manual cochlear array insertion was performed through a cochleostomy in the second group, followed by the application of HA-Lip or HA-DexP-Lip to fill the bulla (n = 6 in each group). The third group had a cochlear implantation through a cochleostomy with the motorized insertion tool followed by injection of HA-Lip (n = 6) or HA-DexP-Lip (n = 9).

<b>Surgery</b>	<b>Gel injected in the middle ear</b>	<b>Number of ears</b>
<b>Cochleostomy</b>	HA-Lip	3
	HA-DexP-Lip	3
<b>Manual insertion</b>	HA-Lip	6
	HA-DexP-Lip	6
<b>Motorized insertion</b>	HA-Lip	6
	HA-DexP-Lip	9

### *2.5. Surgical procedure*

Cochlear implantation was performed under general anesthesia (xylazine: 4 mg/kg, ketamine: 60 mg/kg, intra-muscular injection). Lidocaine hydrochloride 1% (0.5 ml, Astra Zeneca, London, United Kingdom) was injected in the retroauricular subcutaneous tissues of both ears to complete general anesthesia. The surgical procedure never required further general anesthesia. Spontaneous ventilation was achieved and body temperature was maintained with a heating table. The back of the head was shaved and then cleaned with a cutaneous antisepsis (Betadine, Meda Pharma, Solna, Switzerland). After a retroauricular incision, the bulla was carefully exposed with a 2-mm diamond bur to drill the bone (NSK, Nakashima, Japan). The basal turn of the cochlea was then exposed to perform a cochleostomy of 0.6 mm under the round window using a 0.5 mm micro perforator (Karl Storz, Tuttlingen, Germany). Hyaluronic acid gel without liposomes (HA 2.28% w/v) was placed in front of the cochleostomy to prevent perilymph leakage.

The electrode array was inserted either manually using a micro forceps or using the motorized insertion tool. These insertions were performed by an experienced otologist surgeon familiar with CI technique in human. Electrode arrays were of 7 mm length for a 0.4 mm outer diameter (Oticon Medical, Vallauris, France). They were composed of 6 platinum-

iridium electrodes included in a medical grade silicon array. The insertion depth was similar in all the insertion procedures and stopped when the fifth electrode was next to the cochleostomy corresponding to a 4-mm insertion length. The cochleostomy site was not sealed with muscle in opposition to routine “soft surgery” techniques in humans. At the end of the procedure, the bulla was completely filled with ~ 150 µL of HA-Lip or HA-DexP-Lip, corresponding to 2.25 mg DexP, injected through a 1 mL marked syringe equipped with a 29G needle (diameter = 0.16 mm; length = 88 mm, B.Braun). The skin was then sutured with 3.0 Vicryl suture (Ethicon, Cincinnati, OH). The non-implanted contralateral ear had the same surgical procedure with a larger cochleostomy (1 mm) followed by the introduction of small muscle fragments in the cochlea to obtain a total hearing loss. The contralateral ear was surgically altered to avoid osseous transcranial sound conduction during ABR measurements. Thus, ABR thresholds were specifically assessed for the implanted ear. After CI, guinea pigs received an intramuscular injection of antibiotic prophylaxis (Enrofloxacin Bayer, Leverkusen, Germany) as already described by Quesnel et al. (2011).

In this study, the motorized insertion tool developed in the lab for human implantation (Miroir, et al., 2012) was modified to perform CI in guinea pigs. First, the insertion tube was elongated to guide the array under a binocular microscope to keep a correct visibility due to the small operative fields. Secondly, the diameter of the tube was adapted to the diameter of the electrode array and was reduced to 0.5 mm. The tool was held steady by a flexible arm and the speed was controlled with an input voltage in order to set the array insertion speed at  $0.25 \text{ mm.s}^{-1}$ . Finally, this tool was designed to achieve a linear movement to push the electrode array.

## 2.6. Hearing assessment with Auditory Brainstem Response (ABR)

Implanted ears were tested under gas general anesthesia (isoflurane) before surgery ( $D_0$ ) and at postoperative  $D_7$ . Click bursts of 100 µs were delivered at 2, 4, 8, 16 and 32 kHz, with a high frequency transducer connected to an external ear canal probe (HIS, Miami, FL). Needle electrodes (Medtronic Xomed, Jacksonville, Florida) were placed subcutaneously in the leg (ground electrode), the vertex (active electrode) and the retroauricular side of the analyzed ear (reference electrode). Hearing thresholds were visually determined with 5 dB decreasing increments and the threshold corresponded to the minimal intensity for which one or several ABR waves were clearly recognized. The accuracy of ABR threshold measurements was  $\pm 5 \text{ dB}$ .

## 2.7. Statistical analysis

Results are expressed as mean  $\pm$  SEM. All statistical analysis was performed with Prism version 6.00.283 (GraphPad software, 2014, Inc., La Jolla, USA). Non-parametric tests were conducted. Statistical analysis of the hearing thresholds was performed using two-way analysis of variance (Anova), with a Bonferroni post-test. A p value  $< 0.05$  was considered as significant.

## 3. Results and discussion

### 3.1. Effect of the cochleostomy on post-operative hearing thresholds

Before surgery, all the animals had a normal hearing with no statistical difference between the six groups (two-way Anova, ns). When a cochleostomy was performed, hearing thresholds were not significantly increased at D<sub>7</sub> except at 16 kHz for the cochleostomy group with HA-DexP-Lip injection (**Fig. 1B**). At 2, 4, 8 and 32 kHz, no significant hearing loss was observed at D<sub>7</sub> compared to preoperative in both groups (**Fig. 1A and 1B**, two-way Anova, ns).

It is important to highlight that in this study, the cochleostomy was not sealed with muscle after cochlear implantation. This should allow the diffusion of DexP and/or DexP-Lip through both the round window and the cochleostomy leading to a pharmacokinetic profile that is probably different from the one obtained in Chapter III where the cochlea was not opened. Indeed, the concentration of the corticoid in the cochlea may be significantly higher in the present study because of the cochleostomy (diameter around 0.6 mm). The toxicity of dexamethasone in the inner ear is not well documented. However, it is not excluded that a high DexP concentration in perilymph could generate toxicity especially near the basal turn of the cochlea where ABR thresholds were surprisingly greater in the HA-DexP-Lip control group (16 kHz). In fact, according to the cochlear tonotopy, the cochleostomy was performed near these high frequencies at the basal turn (16 and 32 kHz) of the cochlea. Thus, the iatrogenic consequences of the cochleostomy combined with DexP cannot be excluded.

### 3.2. Benefit of the motorized insertion tool on hearing preservation

When a cochlear implantation was performed either manually or using the MIT, the ABR thresholds were increased in all groups at D<sub>7</sub> and for each frequency compared to the control groups (two-way Anova,  $p < 0.001$ ) and to the preoperative ABR thresholds (two-way Anova,

$p < 0.001$ ) (**Fig. 1**). In HA-Lip groups, the insertion with the motorized tool resulted in lower hearing thresholds at D<sub>7</sub> at all the frequencies compared to the manual insertion technique (two-way Anova,  $p < 0.0001$ , **Fig. 1 C** compared to **E**). Thus, the MIT provided a better hearing preservation at D<sub>7</sub> compared to the classical manual insertion technique.

In order to ensure hearing preservation during Electric-Acoustic Stimulation implantation procedure (EAS), technical refinement and otoprotection strategies have been proposed over the past two decades (Vivero, et al., 2008; Rajan, et al 2012; Santa Maria, et al., 2014). Whereas many animal models have been used to test otoprotection during cochlear implantation, only few studies have focused on the insertion technique itself. In the present study, the benefit of the motorized insertion tool was demonstrated in a guinea pig model of cochlear implantation. In a previous study, this tool was able to provide lower intracochlear friction forces during the array insertion compared to the manual technique in human microdissected cochlea (Nguyen, et al., 2012; 2014). Nevertheless, it is not clearly established that an intact basilar membrane and low friction forces can positively influence postoperative hearing loss (Roland, et al., 2006; Choudhury, et al., 2014; Honeder, et al., 2015). Furthermore, fluid pressure waves occurring during the electrode array insertion could contribute by itself to hearing loss and hair cell damages (Todt, et al., 2014; Choudhury, et al., 2014; Vivero, et al., 2008). However, based on the present study, it seems interesting to develop and to further investigate atraumatic cochlear insertion techniques, able to perform slow insertions, in accordance with the “soft surgery” philosophy (Lehnhardt, 1993; Kontorinis, et al., 2011; Rajan, et al., 2013).

### *3.3. Benefit of HA-DexP-Lip on postoperative hearing thresholds after manual insertion*

A significant hearing preservation was obtained at D<sub>7</sub> in the manual insertion group with HA-DexP-Lip injection compared to HA-Lip injection (two-way Anova,  $p < 0.0001$ , **Fig. 1 D** compared to **C**).

HA-DexP-Lip gel was designed with the hypothesis that hyaluronic acid would allow a prolonged residence time in the middle ear and that liposomes could act as a reservoir for a sustained release of the encapsulated drug. Indeed, the rheological properties of HA combined with its mucoadhesiveness (Chapter I) avoid rapid flow through the Eustachian tube and thus enable a longer persistence in the middle ear in contact with the round window (Chapter III). In addition, hyaluronic acid gel applied in the middle ear of guinea pigs showed no ototoxicity on inner ear hair cells (Saber, et al. 2009).

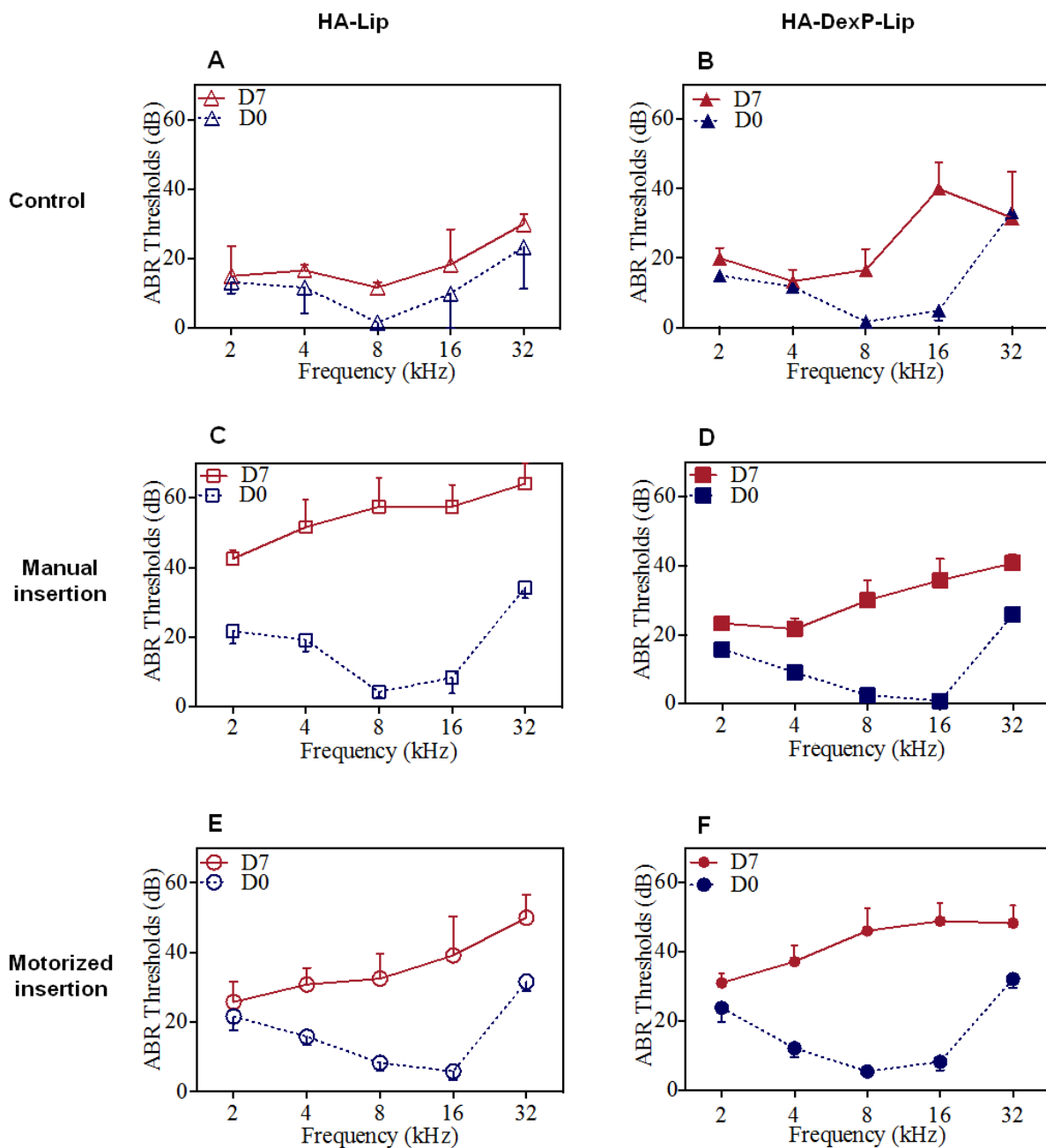


**Fig. 1.** Preoperative ( $D_0$ ) and ( $D_7$ ) postoperative ABR thresholds at 2, 4, 8, 16, and 32 kHz for guinea pigs in control groups (cochleostomy) with HA-Lip (A,  $n = 3$ ) or HA-DexP-Lip (B,  $n = 3$ ) injection, in manual insertion groups with HA-Lip (C,  $n = 6$ ) or HA-DexP-Lip (D,  $n = 6$ ) injection and in motorized insertion groups with HA-Lip (E,  $n = 6$ ) or HA-DexP-Lip (F,  $n = 9$ ) injection. The electrode array insertion with the motorized tool was less traumatic than the manual insertion technique (C compared to E, two-way Anova,  $p < 0.0001$ ). DexP had a benefic effect on hearing loss in the manual insertion group (C compared to D, two-way Anova,  $p < 0.0001$ ) whereas no significant effect was observed in the motorized insertion group (E compared to F, two-way Anova, ns). Values are means  $\pm$  SEM.

In Chapter III, we also demonstrated that the injection of HA-DexP-Lip in the middle ear resulted in a reservoir effect of liposomes in the round window allowing a sustained release of the corticoid until 30 days, whereas only a small fraction of intact liposomes diffused until the inner ear. The present study suggests that the application of HA-DexP-Lip after the surgical trauma can enhance hearing preservation during manual insertion and can be used as an immediate rescue treatment. This local drug delivery system should be preferred to a systemic drug administration during cochlear implantation (Quesnel, et al., 2011; Honeder, et al., 2015; Ramos, et al., 2015). Indeed, it is well known that systemic administration of high doses of corticoids can lead to serious side effects (Liu, et al., 2013). Thus, local administration in the middle ear allows to reduce the dose of corticoid while maximizing its local concentration in the inner and avoiding systemic exposure.

Although electrode array length and diameter are crucial to limit intracochlear damages, it was not possible to reproduce, in guinea pig cochlea, the similar insertion as in the human cochlea (**Fig. 2**). Guinea pig was chosen because the basal turn of its cochlea is easily exposed and large enough to perform a cochleostomy but the scala tympani fastly narrows nearby the second turn.

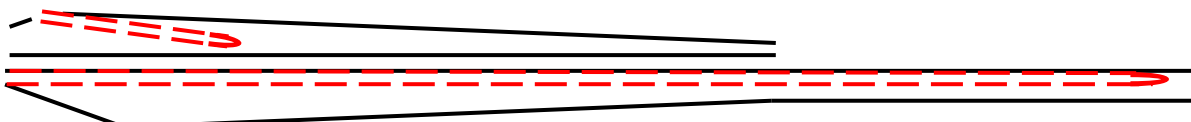


**Fig. 2.** Schema of the guinea pig *scala tympani* (up) and the human *scala tympani* (down) after electrode array insertion. In the guinea pig model, the array (0.4 diameter ; 4 mm length) is inserted through a cochleostomy of 0.6 mm diameter. The length of the *scala tympani* is 16 mm long and fully represented. The human *scala tympani* is 28 mm in length and only 25 mm are represented on the schema. The insertion is performed through the round window with a 24 mm electrode array of 0.4 mm distal diameter and 0.6 mm proximal diameter.

However, in this study, we observed a hearing preservation, even at low frequencies with the manual insertion technique combined with HA-DexP-Lip injection. Interestingly, these frequencies were not supposed to be altered because of the too short insertion length in the basal turn of the cochlea in guinea pigs, which could not theoretically alter the basilar

membrane physically. This global effect on hearing preservation at D<sub>7</sub> suggests other mechanisms than basilar membrane trauma that could occur at the cellular level and need to be further investigated. For instance, vascular injuries may contribute to hearing loss after cochlear implantation (Wright, et al., 2013; Tanaka, et al., 2014). In the study of Tanaka and co-workers, the *stria vascularis* was altered nearby the array region and was correlated to elevated ABR thresholds (Tanaka, et al., 2014). On the other hand, hearing loss was correlated with an increased tissue response surrounding the array one month after cochlear implantation (O’Leary, et al., 2013).

### 3.4. Cumulative effect of HA-DexP-Lip and motorized insertion

In the MIT groups, the injection of HA-DexP-Lip did not improve ABR thresholds at D<sub>7</sub> compared to HA-Lip injection (two-way Anova, ns, **Fig. 1 F** compared to **E**). Furthermore, when HA-DexP-Lip was injected in the bulla, there were no significant differences in hearing thresholds between the manual insertion and the MIT groups (two-way Anova, ns, **Fig. 1 D** compared to **F**). These data suggest that there is no cumulative effect of the local corticoid treatment and the MIT. This could be explained by a minimized inflammatory response with the MIT that reduced the interest of using an anti-inflammatory drug. Indeed, the motorized insertion without corticoid resulted in the same hearing preservation than the manual insertion with corticoid.

In previous studies, we demonstrated a relative stability of ABR threshold shifts between one week and one month after cochlear implantation (Quesnel, et al., 2011). However, it should be interesting to further investigate the effect of HA-DexP-Lip for hearing preservation by recording ABR thresholds after one month. Indeed, the liposomal gel sustained the delivery of the corticoid in the inner ear until 30 days (Chapter III). At day 30, the corticoid could for example avoid the development of fibrosis around the array that was not yet formed at D<sub>7</sub> in the present study. Thus, the therapeutic efficacy of HA-DexP-Lip gel may be underestimated at D<sub>7</sub> and could result in a better hearing preservation if assessed at a longer period.

## **5. Conclusions**

In this study, we showed that an array insertion with a motorized tool could reduce postoperative hearing loss at D<sub>7</sub> compared to the manual conventional cochlear implantation technique. Furthermore, the administration of dexamethasone phosphate contained in a HA liposomal gel also enhanced hearing preservation at D<sub>7</sub> during manual insertion. Thus, research and evaluation of otoprotective drugs during cochlear implantation should use motorized insertion technique to reduce bias introduced by hand-guided insertions.

## **Acknowledgments**

Authors wish to thank Neurelec France /Oticon Medical that designed and provided the electrode arrays adapted for cochlear implantation in guinea pigs. Authors are also grateful to the “Fondation pour la Recherche Médicale” and the French Ministry of National Education and Research.

## References

- Bangham A.D., Standish M.M., Watkins J.C., 1965. Diffusion of univalent ions across the lamellae of swollen phospholipids. *J. Mol. Biol.* 13, 238-252.
- Bas. E., Dinh. C.T., Garnham. C., Polak. M., Van de Water. T.R., 2012. Conservation of hearing and protection of hair cells in cochlear implant patients' with residual hearing. *Anat. Rec.* 295 (11), 1909-27.
- Bell B., Stieger C., Gerber N., Arnold A., Nauer C., Hamacher V., Kompis M., Nolte L., Caversaccio M., Weber S., et al., 2012. A self developed and constructed robot for minimally invasive cochlear implantation. *Acta. Otolaryngol.* 132 (4), 355-60.
- Briggs. R.J., Tykocinski. M., Stidham. K., Roberson. J.B., 2005. Cochleostomy site: implications for electrode placement and hearing preservation. *Acta. Otolaryngol.* 125 (8), 870-6.
- Choudhury. B., Adunka. O.F., Awan. O., Pike. J.M., Buchman. C.A., Fitzpatrick. D.C., 2014. Electrophysiologic consequences of flexible electrode insertions in gerbils with noise-induced hearing loss. *Otol. Neurotol.* 35 (3), 519-25.
- El Kechai N., Bochot A., Huang N., Nguyen Y., Ferrary E., Agnely F., 2015. Effects of liposomes on rheological and syringeability properties of hyaluronic acid hydrogels intended for local injection of drugs. *Int. J. Pharm.* 487, 187-196.
- Falcone. S.J., Palmeri. D.M., Berg. R.A., 2006. Rheological and cohesive properties of hyaluronic acid. *J. Biomed. Mater. Res. A.* 76 (4), 721-8.
- Friedland. D.R., Runge-Samuelson. C., 2009. Soft cochlear implantation: rationale for the surgical approach. *Trends Amplif.* 13 (2), 124-38.
- Girish. K.S., Kemparaju. K., 2007. The magic glue hyaluronan and its eraser hyaluronidase: a biological overview. *Life Sci.* 80 (21), 1921-43.
- Honeder. C., Landegger. L.D., Engleider. E., Gabor. F., Plasenzotti. R., Plenk. H., et al., 2015. Effects of intraoperatively applied glucocorticoid hydrogels on residual hearing and foreign body reaction in a guinea pig model of cochlear implantation. *Acta. Otolaryngol.* 135 (4), 313-9.
- Kontorinis. G., Lenarz. T., Stöver. T., Paasche. G. 2011. Impact of the insertion speed of cochlear implant electrodes on the insertion forces. *Otol. Neurotol.* 32 (4), 565-70.
- Lajavardi. L., Camelo. S., Agnely. F., Luo. W., Goldenberg. B., Naud. M.C., et al., 2009. New formulation of vasoactive intestinal peptide using liposomes in hyaluronic acid gel for uveitis. *J Control Release.* 139 (1), 22-30.
- Lehnhardt. E., 1993. Intracochlear placement of cochlear implant electrodes in soft surgery technique. *HNO.* 1993. 41 (7), 356-9.
- Liao. Y.H., Jones. S.A., Forbes. B., Martin. G.P., Brown. M.B., 2005. Hyaluronan: pharmaceutical characterization and drug delivery. *Drug. Deliv.* 12 (6), 327-42.
- Liu, H., Hao, J., Li, K.S., 2013. Current strategies for drug delivery to the inner ear. *Acta Pharmaceutica Sinica B.* 3, 86-96.
- Majdani. O., Schurzig. D., Hussong. A., Rau. T., Wittkopf. J., Lenarz. T., et al., 2010. Force measurement of insertion of cochlear implant electrode arrays in vitro: comparison of surgeon to automated insertion tool. *Acta. Otolaryngol.* 130 (1), 31-37.

- Masuda, A., Ushida, K., Koshino, H., Yamashita, K., Kluge, T., 2001. Novel Distance Dependence of Diffusion Constants in Hyaluronan Aqueous Solution Resulting from Its Characteristic Nano-Microstructure. *Journal of the American Chemical Society.* 123, 11468-11471.
- Mayol. L., Quaglia. F., Borzacchiello. A., Ambrosio. L., La. Rotonda. M.I., 2008. A novel poloxamers/hyaluronic acid in situ forming hydrogel for drug delivery: rheological, mucoadhesive and in vitro release properties. *Eur. J. Pharm. Biopharm.* 70 (1), 199-206.
- Miroir. M., Nguyen. Y., Kazmitcheff. G., Ferrary. E., Sterkers. O., Grayeli. A.B., 2012. Friction force measurement during cochlear implant insertion: application to a force-controlled insertion tool design. *Otol. Neurotol.* 33 (6), 1092-100.
- Nguyen. Y., Miroir. M., Kazmitcheff. G., Sutter. J., Bensidhoum. M., Ferrary. E., et al., 2012. Cochlear implant insertion forces in microdissected human cochlea to evaluate a prototype array. *Audiol. Neurotol.* 17 (5), 290-8.
- Nguyen. Y., Mosnier. I., Borel. S., Ambert-Dahan. E., Bouccara. D, Bozorg-Grayeli. A., et al., 2013. Evolution of electrode array diameter for hearing preservation in cochlear implantation. *Acta. Otolaryngol.* 133 (2), 116-22.
- Nguyen. Y., Kazmitcheff. G., De Seta. D., Miroir. M., Ferrary. E., Sterkers. O., 2014. Definition of metrics to evaluate cochlear array insertion forces performed with forceps, insertion tool, or motorized tool in temporal bone specimens. *Biomed. Res. Int.*
- O'Leary. S.J., Monksfield. P., Kel. G., Connolly. T., Souter. M.A., Chang. A., et al., 2013. Relations between cochlear histopathology and hearing loss in experimental cochlear implantation. *Hear. Res.* 298, 27-35.
- Quesnel. S., Nguyen. Y., Elmaleh. M., Grayeli. A.B., Ferrary. E., Sterkers. O., et al., 2011. Effects of systemic administration of methylprednisolone on residual hearing in an animal model of cochlear implantation. *Acta. Otolaryngol.* 131 (6), 579-84.
- Rajan. G.P., Kontorinis. G., Kuthubutheen. J., 2013. The effects of insertion speed on inner ear function during cochlear implantation: a comparison study. *Audiol. Neurotol.* 18 (1), 17-22.
- Rajan. G.P., Kuthubutheen. J., Hedne. N., Krishnaswamy. J., 2012. The role of preoperative, intratympanic glucocorticoids for hearing preservation in cochlear implantation: a prospective clinical study. *Laryngoscope.* 22 (1), 190-5.
- Ramos. B.F., Tsuji. R.K., Bento. R.F., Goffi-Gomez. M.V., Ramos. H.F., Samuel. P.A., et al., 2015. Hearing preservation using topical dexamethasone alone and associated with hyaluronic acid in cochlear implantation. *Acta. Otolaryngol.* 26, 1-5.
- Roland. P.S., Wright. C.G., 2006. Surgical aspects of cochlear implantation: mechanisms of insertional trauma. *Adv. Otorhinolaryngol.* 64, 11-30.
- Saber. A., Laurell. G., Bramer. T., Edsman. K., Engmér. C., Ulfendahl. M., 2009. Middle ear application of a sodium hyaluronate gel loaded with neomycin in a Guinea pig model. *Ear. Hear.* 30 (1), 81-9.
- Santa. Maria. P.L., Gluth. M.B., Yuan. Y., Atlas. M.D., Blevins. N.H., 2014. Hearing preservation surgery for cochlear implantation: a meta-analysis. *Otol Neurotol.* 35 (10), 256-69.
- Swan. E.E., Mescher. M.J., Sewell. W.F., Tao. S.L., Borenstein. J.T., 2008. Inner ear drug delivery for auditory applications. *Adv. Drug. Deliv. Rev.* 60 (15), 1583-99.

- Tanaka. C., Nguyen-Huynh. A., Loera. K., Stark. G., Reiss. L., 2014. Factors associated with hearing loss in a normal-hearing guinea pig model of Hybrid cochlear implants. Hear. Res. 316, 82-93.
- Todt. I., Mittmann. P., Ernst. A., 2014. Intracochlear fluid pressure changes related to the insertional speed of a CI electrode. Biomed. Res. Int. 2014, 507241.
- Vivero. R.J., Joseph. D.E., Angeli. S., He. J., Chen. S., Eshraghi. A.A., et al., 2008. Dexamethasone base conserves hearing from electrode trauma-induced hearing loss. Laryngoscope. 118 (11), 2028-35.
- Wilson. B.S., Dorman MF., 2008. Cochlear implants: a remarkable past and a brilliant future. Hear. Res. 242 (1-2), 3-21.
- Wright. C.G., Roland. P.S., 2013. Vascular trauma during cochlear implantation: a contributor to residual hearing loss? Otol. Neurotol. 34 (3), 402-7.
- Zhang. Y., Zhang. W., Löbler. M., Schmitz. K.P., Saulnier. P., Perrier. T., et al., 2011. Inner ear biocompatibility of lipid nanocapsules after round window membrane application. Int J Pharm. 404 (1-2), 211-9.

# **Discussion générale**

Le but de ce travail de thèse a été de mettre au point, de caractériser et d'évaluer *in vivo* une formulation galénique originale constituée d'un gel d'acide hyaluronique contenant des liposomes. Ce travail a eu deux objectifs principaux. Le premier était d'étudier de façon approfondie les propriétés physicochimiques du système (Première partie) en faisant varier les différents paramètres de formulation tels que : la concentration et la composition des liposomes, leur taille, la concentration en HA. Plusieurs techniques ont été utilisées pour caractériser l'effet de ces différents paramètres sur le système « gel de liposomes » en ce qui concerne les propriétés rhéologiques, la seringabilité, la stabilité, la compatibilité, la microstructure et la diffusion des liposomes. Le but final était de faire du gel de liposomes une plateforme de formulation modulable et injectable qui pourrait servir pour différentes voies d'administration locales dont l'administration intratympanique. Le deuxième objectif a été d'évaluer l'intérêt de ce système *in vivo* pour la libération prolongée d'un corticoïde dans l'oreille interne (Deuxième partie). Le choix de la formulation retenue pour l'étude *in vivo* a été basé sur les résultats obtenus dans la première partie. Ainsi, nous avons choisi d'encapsuler la dexamethasone phosphate dans des liposomes PEGylés dispersés au sein du gel d'HA à 2.28%. Cette formulation a été testée sur le cobaye Hartley Albinos après injection dans l'oreille moyenne. Les expériences ont été menées de façon à répondre aux questions suivantes :

- La formulation a-t-elle un effet sur la fonction auditive du cobaye normo-entendant ? (étude d'innocuité)
- Que deviennent les constituants de la formulation (HA, liposomes, DexP) au cours du temps ? (étude de biodistribution locale)
- Quel est l'intérêt thérapeutique de la formulation pour la récupération de l'audition après un traumatisme sonore et pour la préservation de l'audition durant l'implantation cochléaire (étude d'efficacité thérapeutique)

Les différents chapitres ont fait chacun l'objet d'une discussion propre des résultats obtenus. Dans cette discussion générale, nous discuterons et remettrons en perspective uniquement les points qui ne l'ont pas été précédemment, en considérant l'ensemble des principaux résultats et en s'appuyant sur les données de la littérature.

## 1. Intérêt de l'acide hyaluronique

Dans ce travail, nous avons choisi l'acide hyaluronique pour ces propriétés physicochimiques et biologiques uniques qui en font un véhicule de choix pour l'administration de substances actives dans les domaines pharmaceutique (Jiao et al., 2015) et biomédical (Borzacchiello et al., 2015).

L'HA est un polysaccharide naturellement présent dans de nombreux tissus de l'organisme. C'est le composant principal de la matrice extracellulaire des tissus conjonctifs. Il joue un rôle structurel pour la peau et il est présent en concentration importante dans le liquide synovial des articulations, l'humeur vitrée de l'œil, le cartilage hyalin, les disques intervertébraux et le cordon ombilical (Monheit and Coleman, 2006, Volpi et al., 2009, Borzacchiello et al., 2015). L'HA est biocompatible et biodégradable par l'intermédiaire des hyaluronidases naturellement présentes dans l'organisme (Girish and Kemparaju, 2007). De plus, l'HA de masse molaire élevée (~1 MDa) se lie de manière non covalente au mucus qui recouvre les tissus épithéliaux, ce qui lui confère un pouvoir mucoadhésif (Mayol et al., 2008). D'un point de vue physicochimique, l'HA est un polyélectrolyte chargé négativement à pH neutre grâce aux groupements carboxylates présents sur ses unités disaccharides (Masuda et al., 2001). En outre, c'est un polymère très soluble en milieux aqueux dont les chaînes s'enchevêtrent entrainant la formation d'un réseau temporaire et réversible qui offre des propriétés viscoélastiques intéressantes, même à faible concentration (De Smedt et al., 1993, Masuda et al., 2001). En clinique, l'HA est très utilisé en rhumatologie et en ophtalmologie comme agent de viscosupplémentation (Barbucci et al., 2002), en cosmétologie et dans le domaine de la régénération tissulaire pour son action procicatrisante (Borzacchiello et al., 2015). En médecine esthétique, il y a un intérêt particulier pour les HA réticulés chimiquement dans le comblement des rides (Kablik et al., 2009). En otologie, l'HA est utilisé comme dispositif médical en chirurgie lors de l'implantation cochléaire (Friedland and Runge-Samuelson, 2009).

Dans ce travail, les propriétés physicochimiques, en particulier rhéologiques, de l'HA ont été caractérisées et ont mis en évidence l'intérêt d'utiliser ce polymère pour l'injection locale de substances actives. En effet, son caractère rhéofluidifiant lui permet d'être facilement injectable même au travers d'aiguilles fines et longues (Chapitre I). Par ailleurs, nous avons mis en évidence une contrainte seuil pour l'écoulement de l'HA qui est largement inférieure à la contrainte appliquée lors de l'injection (Chapitre III). Son caractère non-thixotrope lui permet de retrouver sa structure et donc sa viscosité initiale juste après injection. Enfin, sa

viscosité élevée au repos couplée à son élasticité assurent un temps de résidence prolongé au site d'injection (Chapitres I et III).

Ainsi, l'HA présente de nombreux avantages : il possède des propriétés rhéologiques pertinentes au regard des propriétés d'usage pour l'injection locale de substances actives (**Fig. 1**). Ces propriétés sont modulables par sa concentration et sa masse molaire (Krause et al., 2001). Sa structure chimique et sa conformation permettent des interactions physicochimiques avec de nombreux composés (Scott et al., 1991, De Smedt et al., 1994). En outre, sa biocompatibilité et sa biodégradabilité le rendent quasiment invisible pour le système immunitaire. Ces propriétés en font un polymère de choix pouvant être utilisé pour diverses voies d'administration locales notamment lorsqu'une injection est requise (injection transtympanique en otologie, injection intra-vitréenne en ophtalmologie, injection intra-articulaire en rhumatologie) mais aussi par exemple pour une application topique sur la peau.

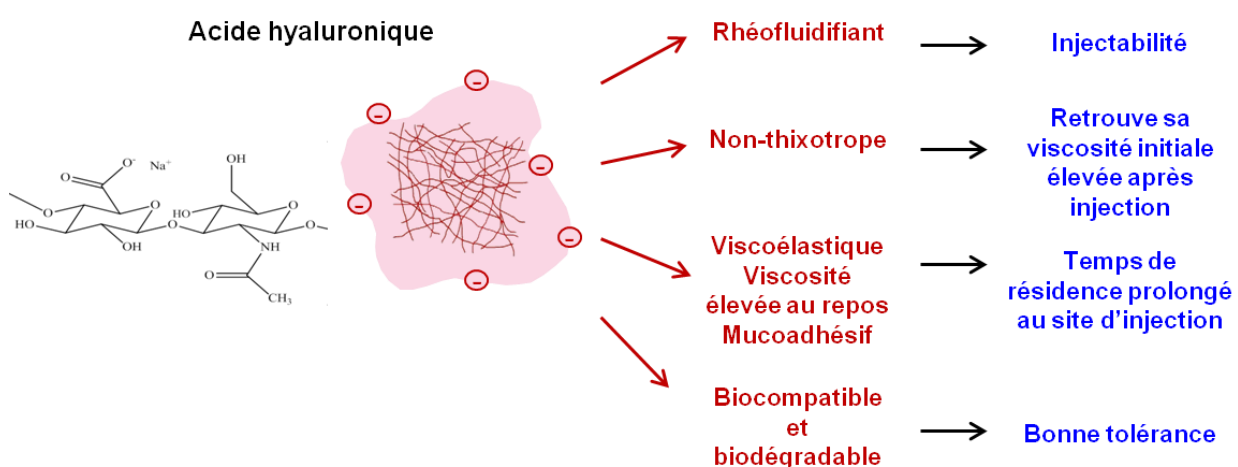


**Fig. 1.** Résumé des propriétés rhéologiques de l'acide hyaluronique à 2.28% (m/v) et leur impact sur les propriétés d'usage pour l'injection locale de substances actives.

La masse molaire et la concentration de l'HA choisies dans le chapitre I et pour l'évaluation *in vivo* ( $M = 1.5 \text{ MDa}$ , 2.28% m/v) sont celles que Laure Lajavardi a adaptées, au cours de sa thèse (Lajavardi, 2008), pour l'HA d'origine animale (Acros organics) afin d'obtenir les mêmes propriétés rhéologiques que le produit commercial (Provisc<sup>®</sup>) utilisé en chirurgie ophtalmologique. Il paraissait judicieux de garder cette concentration relativement élevée qui offre une viscosité intéressante tout en restant facilement injectable. Nous avons choisi de préparer le gel d'HA dans un tampon HEPES/NaCl dont le pH et la concentration en

NaCl peuvent être facilement ajustés de manière à obtenir un pH et une osmolalité physiologiques (pH 7.4 et 300 mOsm/kg).

Par ailleurs, il est important de noter que dans ce manuscrit, nous appelons l'HA à une concentration de 2.28% en solution aqueuse « gel » ou « gel de liposomes » quand celui-ci contient des liposomes. Un gel se caractérise par la formation d'un réseau réticulé physiquement ou chimiquement qui lui confère un comportement rhéologique élastique dominant sans croisement des deux modules visqueux et élastique. L'HA, avec ou sans liposomes, présente un comportement viscoélastique évident (Chapitre I). Ainsi, d'un point de vue physicochimique, l'HA n'est pas un gel, au sens strict du terme, mais une solution de polymère enchevêtré. Cela dit, nous avons utilisé la dénomination « gel » car celle-ci est très couramment utilisée dans le domaine pharmaceutique pour qualifier ce type de systèmes viscoélastiques (Barbucci et al., 2002, Borden et al., 2011, Borzacchiello et al., 2015). La **Figure 1** résume les propriétés rhéologiques de l'acide hyaluronique à 2.28% (m/v) et leur impact sur les propriétés d'usage pour l'injection locale de substances actives.

## 2. Le « gel de liposomes » : une plateforme de formulation modulable et injectable pour administrer localement des substances actives

Le gel d'HA contenant des liposomes peut être considéré comme une plateforme de formulation polyvalente et ce, pour plusieurs raisons. D'abord, l'HA présente un intérêt dans de nombreuses applications pharmaceutiques et biomédicales qui ont fait l'objet du paragraphe précédent. Ensuite les liposomes sont des nanovecteurs versatiles pouvant encapsuler des molécules hydrophiles (dans le cœur aqueux) ou hydrophobes (dans la bicouche phospholipidique) (Torchilin and Weissig, 2003). Dans ce système, plusieurs paramètres de formulation peuvent être adaptés selon les spécifications de l'application finale. Pour l'HA, ces paramètres sont représentés par sa concentration et sa masse molaire qui ont un impact direct sur ses propriétés rhéologiques (Lapčík et al., 1998). En ce qui concerne les liposomes, leur composition, et en particulier leurs propriétés de surface, leur taille et leur concentration peuvent être adaptées en fonction de la molécule à encapsuler, de la cinétique de libération souhaitée et des interactions avec l'HA voulues.

Dans la première partie des travaux expérimentaux, nous avons mis en évidence des interactions de natures différentes entre les liposomes et l'acide hyaluronique qui se sont traduites, selon les propriétés de surface des liposomes (surface hydrophile ou hydrophobe, chargée positivement, négativement ou neutre) et leur concentration (10 à 80 mM), par des

propriétés physicochimiques macroscopiques et microscopiques plus ou moins différentes (Chapitres I et II). Les interactions entre l'HA et les liposomes et leur influence sur les propriétés rhéologiques et de seringabilité des gels de liposomes, la stabilité macroscopique et la diffusion des liposomes sont résumées dans la **Figure 2** et le **Tableau 1** :

- **Les liposomes neutres** pourraient interagir par des liaisons de Van der Walls avec les régions hydrophobes de l'HA (Taglienti et al., 2006) ou former des ponts hydrogène avec ses régions hydrophiles (Ionov et al., 2004). Ces interactions ont entraîné la plus faible augmentation de viscosité et d'élasticité du système et une très faible diffusion des liposomes dans le gel d'HA à 2.28%.
- **Les liposomes cationiques** entraînent probablement des interactions électrostatiques attractives et une complexation qui se traduisent par une forte immobilisation de ces liposomes dans le gel d'HA même à faible concentration (Chapitre II) et une augmentation de la viscosité et de l'élasticité supérieure à celle des liposomes neutres mais inférieure à celle obtenue avec les liposomes anioniques (Chapitre I). De plus, le système HA 2.28% contenant les liposomes cationiques présente un phénomène de synérèse qui a été observé macroscopiquement et par microscopie confocale (Chapitre II).
- **Les liposomes anioniques** devraient interagir par l'intermédiaire de répulsions électrostatiques avec l'HA chargé négativement. Ces interactions ont entraîné une augmentation importante de la viscosité mais qui reste inférieure à celle obtenue avec les liposomes PEGylés. La mobilité de ces liposomes est quasi-équivalente à celle des liposomes PEGylés sauf lors de l'étude macroscopique où ces liposomes n'ont pas migré au sein du gel d'HA contrairement aux liposomes PEGylés (Chapitre II).
- **Les liposomes PEGylés** semblent interagir avec l'HA par des répulsions stériques qui entraînent l'augmentation la plus importante de la viscosité et de l'élasticité et la mobilité la plus élevée dans le gel d'HA même à forte concentration. L'injectabilité de ce système a été démontrée manuellement (Chapitre III) et par les tests de seringabilité (Chapitre I).

Malgré une viscosité au repos et une élasticité différente suivant la composition et la concentration des liposomes, les gels d'HA contenant ces différents liposomes ont en commun le fait d'être facilement injectables (Chapitre I) même à une forte concentration en lipides (80 mM).

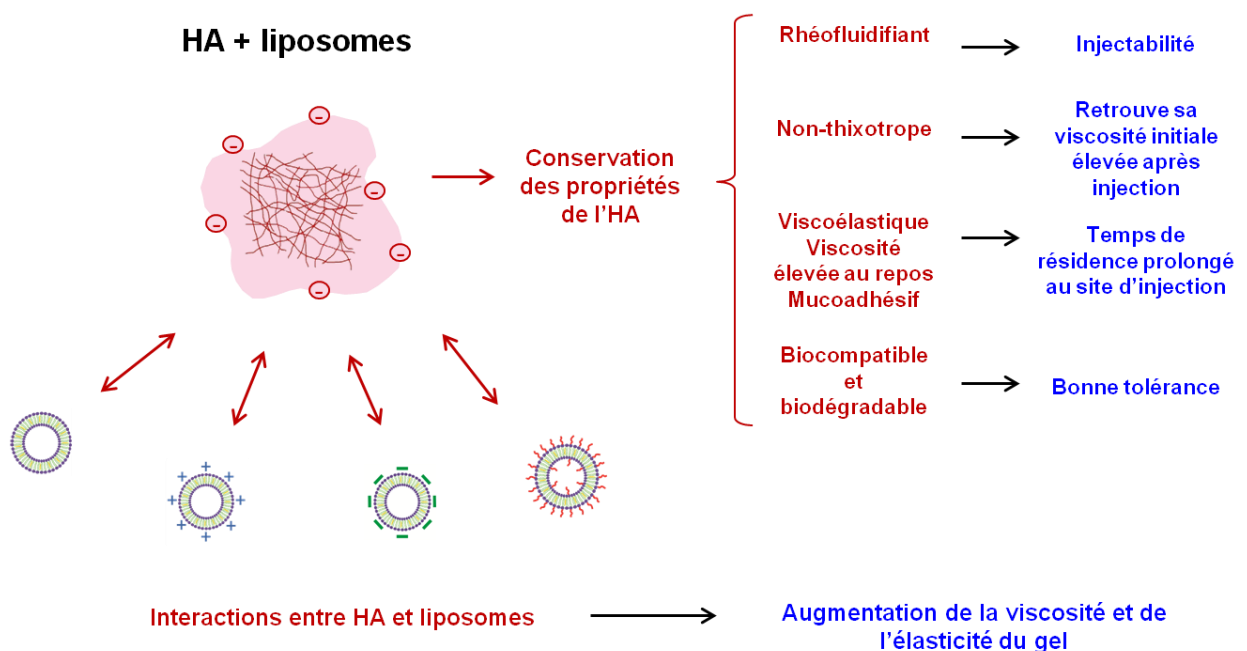


**Fig. 2.** Addition des liposomes dans le gel d'HA et leur impact sur ses propriétés rhéologiques.

**Tableau 1**

Nature des interactions entre l'HA et les différents types de liposomes (neutres, chargés positivement ou négativement, PEGylés) et leur influence sur la viscosité et l'élasticité du gel, sa seringabilité, sa stabilité et la diffusion des liposomes.

Nature des interactions	Interactions de Van der Waals Liaisons hydrogène	Attractions électrostatiques	Répulsions électrostatiques	Répulsions stériques
Viscosité, Elasticité	+	++	+++	++++
Diffusion	+	-	++++	++++
Seringabilité	+++	+++	+++	+++
Stabilité macroscopique	+	+/-	+	+

Initialement, nous avions interprété nos résultats de rhéologie en considérant les liposomes comme des nœuds de réticulation physiques entre les chaînes d'HA, ou comme modifiant leur conformation (étirement des chaînes) (Chapitre I). L'étude structurale (Chapitre II) et en milieu plus dilué nous a permis de mettre en évidence une microséparation de phases. En effet, malgré ces interactions qui pour certaines sont attractives, l'effet de déplétion semble prédominant.

Les liposomes neutres, chargés positivement ou négativement présentent une structure microscopique caractérisée par des agrégats de liposomes dispersés de façon homogène au sein du réseau d'HA (Chapitre II). Les liposomes PEGylés, quant à eux, semblent former un réseau bicontinu d'agrégats de liposomes interpénétré par un réseau d'HA. Cette microstructure a été mise en évidence par des observations en microscopie confocale et par AFM (Chapitre II) mais aussi par la méthode de microscopie électronique après cryofracture dont les résultats à une échelle plus petite ont été présentés dans le chapitre I. A une échelle plus grande, nous avons observé la même ségrégation entre les liposomes PEGylés et l'HA que celle observée avec les deux autres techniques (**Fig. 3**). En effet, l'image de cryofracture (**Fig. 3A**) montre des zones granuleuses (liposomes) entourées par de zones lisses (HA). A plus fort grossissement sur les zones granuleuses, nous observons les images présentées dans le chapitre I qui montrent des liposomes intacts mais fortement concentrés.

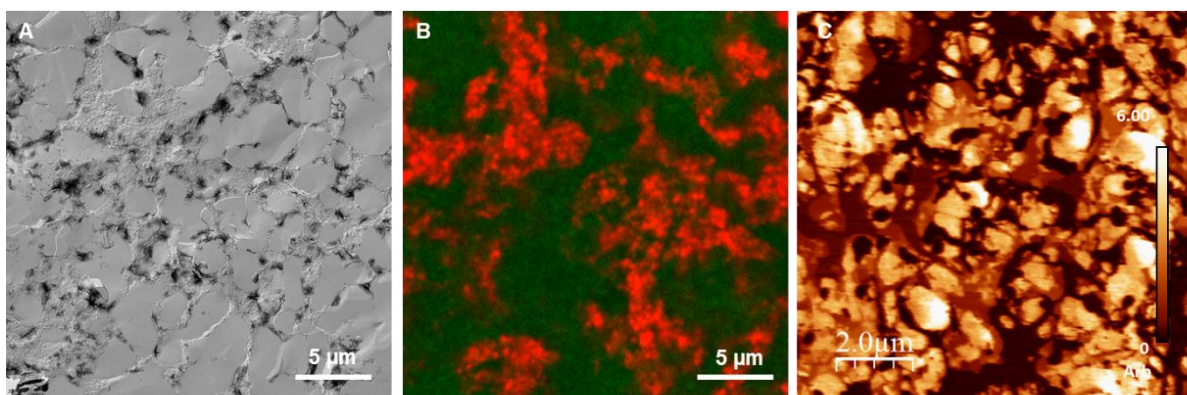


**Fig. 3.** Microstructure du gel d'acide hyaluronique contenant 80 mM de liposomes PEGylés (EPC:Chol:DSPE-PEG 2000 60:35:5). A: observation par microscopie électronique à transmission après cryofracture (Cf. matériel et méthodes chapitre I, les taches sombres sur l'image sont des résidus de gel de liposomes sur la réplique qu'il a été difficile d'éliminer). B: observation par microscopie confocale et C: observation en AFM en mode dissipation (Cf. matériel et méthodes Chapitre II).

La microstructure formée par les liposomes et l'HA semble figée dans un état métastable grâce à la viscosité élevée du gel au repos. Cependant, la configuration de cette microstructure pourrait être influencée par la méthode de préparation du gel de liposomes. Dans ce travail, nous avons choisi une méthode de préparation « douce » qui repose sur une homogénéisation au vortex et une phase de repos d'au moins 12 h, ce qui permet de préserver l'intégrité des liposomes et celle des chaînes d'HA. Avec cette méthode, les mesures de rhéologie ont été très reproductibles entre les différents lots préparés.

D'autres études ont déjà été conduites sur des mélanges de vésicules lipidiques et de polymères. Elles ont été réalisées dans le régime de concentration dilué du polymère et ont montré que ce dernier pouvait avoir un effet sur la microstructure des vésicules lipidiques (Antunes et al., 2009). Les polymères greffés de chaînes hydrophobes et/ou chargés peuvent induire différents changements dans la forme des vésicules et la fluidité de la bicoche lipidique (Antunes et al., 2007). Ils peuvent entraîner une modification de la température de transition de phase des lipides (Laroche et al., 1989), une modification de la forme sphérique en forme polygonale (Dubois et al., 2004), une fusion des vésicules entre elles pour former des vésicules géantes (Marques et al., 1999) ou encore une rupture de la bicoche lipidique (Diederich et al., 1998).

La microstructure de notre système, et notamment l'influence du polymère sur la structure des liposomes, pourrait être étudiée de façon plus approfondie en milieu dilué par diffusion des rayons X (SAXS) ou par microscopie électronique à transmission (Cryo-TEM).

Enfin, il est à noter que l'étude de la mobilité des liposomes au sein du gel d'HA que nous avons menée est importante pour notre système de délivrance de substances actives mais elle peut également être considérée comme un modèle *in vitro* pour prédire la mobilité des différents liposomes dans des milieux biologiques contenant une concentration importante en HA tels que le vitré (œil) ou le liquide synovial (articulations).

En conclusion, le système gel de liposomes peut s'adapter à différentes problématiques de formulation en modulant sa composition (concentration et masse molaire de l'HA, composition et concentration en liposomes). Par exemple, pour un système à libération prolongée, l'utilisation de liposomes neutres ou cationiques semble judicieuse car, en plus de la rétention de la molécule dans les liposomes, ces derniers seront immobiles dans le gel et joueront ainsi un rôle de réservoir. Si au contraire, il est préférable que les liposomes puissent diffuser au sein du gel (pour la protection d'une molécule fragile et/ou pour permettre un

passage à travers une membrane), l'utilisation de liposomes PEGylés ou anioniques semble plus adaptée. Par ailleurs, si la substance active a un taux d'encapsulation faible et qu'il est nécessaire d'augmenter la concentration en lipides dans le gel pour atteindre la dose nécessaire, la concentration en HA ou sa masse molaire pourra aussi être adaptée pour obtenir une viscosité optimale du système. De plus, l'ajustement du pourcentage de cholestérol dans les liposomes ainsi que l'utilisation de phospholipides à haute température de transition de phase pourraient être envisagés dans le but de ralentir la libération de la substance active ou de la contrôler par la température (Torchilin and Weissig, 2003). Par ailleurs, les liposomes pourraient être fonctionnalisés par des ligands spécifiques pour un ciblage actif (Wang et al., 2012). Enfin, ce système possède l'avantage d'être facile à préparer et ne requiert pas l'utilisation de solvants organiques ou de forces mécaniques importantes qui pourraient être délétères pour la substance active ou les liposomes.

### **3. Le gel de liposomes comme système d'administration locale en otologie**

Nous nous sommes intéressés à l'application de ce système en otologie car plusieurs études ont mis en évidence l'intérêt d'utiliser des gels pour prolonger et augmenter la libération de substances actives dans l'oreille interne. Dans ce contexte, une collaboration entre notre laboratoire (Institut Galien Paris-Sud) et le laboratoire de chirurgie otologique mini-invasive robotisé (Hôpital Bichat) a été initiée en 2010. Avant de s'intéresser au gel de liposomes, des gels de poloxamer 407 avaient été étudiés dans le cadre de cette collaboration.

Lors de l'étude *in vivo* du gel de liposomes sur le cobaye, nous avons choisi d'encapsuler la dexamethasone phosphate dans les liposomes PEGylés. Nous avons voulu répondre aux questions suivantes dans le but d'évaluer l'intérêt de ce système pour l'administration de corticoïdes dans l'oreille interne :

- La présence du gel dans l'oreille moyenne affecte-t-elle la fonction auditive des cobayes normo-entendants ?
- Quel est le temps de persistance de la formulation dans l'oreille moyenne et sur la fenêtre ronde ?
- Les liposomes PEGylés sont-ils capable de traverser la fenêtre ronde en préservant leur intégrité ? Par quel(s) mécanisme(s) traversent-ils cette membrane ?
- Cette formulation permet-elle d'atteindre une dose thérapeutique en corticoïde au niveau de l'oreille interne ?

- Les liposomes ont-ils un intérêt pour augmenter et/ou prolonger la libération du corticoïde dans l'oreille interne ?

Dans le chapitre III, nous avons donné les réponses à ces questions et nous avons démontré que la formulation choisie (HA 2.28%, Liposomes PEGylés 80 mM, DexP 10 mg/mL) répondait au cahier des charges défini pour l'administration intratympanique (Cf. Travaux antérieurs). En effet, cette formulation est facilement injectable au travers d'aiguilles adaptées à l'injection transtympanique chez le cobaye (29G, 88mm) grâce au comportement rhéofluidifiant de l'HA. Ce gel devrait être encore plus facile à injecter chez l'homme puisque les aiguilles utilisées pour l'injection transtympanique peuvent être plus grosses (25G ou 27G) que celles employées chez l'animal. Au repos, la viscosité élevée du gel de liposomes utilisé (~ 800 Pa.s) couplée aux propriétés mucoadhésives, non-thixotropes et viscoélastiques de l'HA entraînent un temps de résidence prolongé du gel dans l'oreille moyenne et au contact de la fenêtre ronde, sans aucun effet négatif sur la fonction auditive des cobayes. Le gel de liposomes permet de délivrer une concentration thérapeutique du corticoïde dans la périlymphe. De plus, les liposomes semblent jouer un rôle de réservoir dans la fenêtre ronde offrant une libération prolongée du corticoïde jusqu'à 30 jours.

Le devenir des différents composants de la formulation (HA, liposomes, DexP) après dépôt dans l'oreille moyenne a été évoqué brièvement dans le chapitre III. Dans cette discussion, nous nous intéresserons plus en détails à ces aspects de biodistribution en nous appuyant sur les données de la littérature pour formuler des hypothèses quant au devenir de ces composés.

### *3.1. Devenir de l'HA*

Typiquement, les liquides injectés dans l'oreille moyenne sont rapidement éliminés par la trompe d'Eustache lors de la déglutition. Grâce à sa viscosité relativement élevée au repos et à son caractère non-thixotrope, le gel d'HA ne s'écoule pas facilement à travers la trompe d'Eustache et persiste ainsi plus longtemps dans l'oreille moyenne. Cependant, les parois de l'oreille moyenne sont tapissées d'une fine muqueuse sécrétoire qui permet de maintenir une certaine humidité dans la cavité tympanique (Pracy et al., 1998, Hoskison et al., 2013). Ainsi, une dilution du gel au cours du temps par les sécrétions de l'oreille moyenne pourrait être à l'origine d'un gonflement du gel par absorption d'eau et, par conséquent, d'une diminution de sa viscosité qui entraînerait un écoulement d'une partie du gel et une élimination par la trompe d'Eustache. Les produits éliminés par la trompe d'Eustache se retrouvent au niveau du rhino-pharynx lors de la déglutition et rejoignent la voie digestive. Ainsi, une partie du gel, et

par conséquent une partie de la dose de corticoïde administrée dans l'oreille moyenne pourrait être absorbée par voie orale entraînant une exposition systémique. La molécule active pourrait également rejoindre la circulation générale par le biais des vaisseaux sanguins et lymphatiques présents dans l'oreille moyenne (Pracy et al., 1998). Dans ce travail, nous n'avons pas évalué la concentration plasmatique du corticoïde après administration locale. Cependant, d'autres études ont démontré une exposition systémique assez faible après une administration similaire de corticoïdes sous forme liquide ou gélifiée dans l'oreille moyenne (Paulson et al., 2008, Wang et al., 2009, Honeder et al., 2014). De ce fait, l'exposition systémique à la suite de l'absorption d'une partie de la dose par voie orale ou par le biais de la vascularisation locale semble être négligeable comparée à une administration systémique.

Même si la majeure partie du gel n'est plus observé dans la cavité tympanique après 7 jours (Chapitre III), il n'est pas exclu que le gel puisse persister sous forme d'une fine pellicule qui n'a pas pu être observée sous binoculaire lors de notre étude. En effet, la muqueuse tapissant la cavité du tympan (Pracy et al., 1998, Hoskison et al., 2013) pourrait permettre à l'HA de se lier de manière non-covalente à certains composés grâce à ces propriétés mucoadhésives (Nilsson et al., 1992, Girish and Kempuraju, 2007, Mayol et al., 2008). De plus, le gel pourrait sécher et persister sous forme d'un film tapissant la cavité tympanique.

Enfin, une dégradation enzymatique de l'HA pourrait être envisagée. La dégradation enzymatique de l'HA est assurée par l'activité coordonnée de trois enzymes distinctes, à savoir une hyaluronidase, une endoglycosidase et deux autres exoglycosidases qui éliminent les sucres terminaux, une  $\beta$ -glucuronidase et  $\beta$ -N-acétyl hexosaminadase. La dégradation initiale accomplie par la première enzyme, la hyaluronidase, génère des oligosaccharides de différentes longueurs de chaînes et ceux-ci sont des substrats pour les deux exoglycosidases (Stern and Jedrzejas, 2006). Les hyaluronidases sont retrouvées sous plusieurs isoformes dans différents tissus de l'organisme chez l'homme et chez le rongeur (Girish and Kempuraju, 2007). Cependant, la présence de ces enzymes dans l'oreille moyenne n'a pas été prouvée à notre connaissance.

Malgré sa masse molaire élevée, la diffusion de l'HA dans l'oreille interne n'est pas complètement exclue. Dans ce travail, nous n'avons pas été en mesure de mettre en évidence un quelconque passage de l'HA dans l'oreille interne même si le gel d'HA seul a montré un effet bénéfique sur l'audition (Chapitre IV). Etant donné le degré d'enchevêtrement des

chaines d'HA à une concentration de 2.28%, cette hypothèse semble peu probable mais mériterait d'être étudiée de façon plus approfondie.

### 3.2. Devenir des liposomes et de la DexP

Pour atteindre l'oreille interne, la DexP peut diffuser à travers la fenêtre ronde sous forme libre ou encapsulée dans les liposomes. Aussi, dans la périlymphe, la DexP peut se retrouver sous forme libre ou associée aux liposomes. Ainsi, trois possibilités peuvent être envisagées pour le passage de la DexP et/ou des liposomes à travers la fenêtre ronde. Elles sont résumées dans la **Figure 4**.

- Les liposomes encapsulant la DexP peuvent diffuser à travers la fenêtre ronde en préservant leur intégrité et se retrouver dans la périlymphe.
- Les liposomes, mobiles dans le gel, diffusent jusqu'à la fenêtre ronde mais sont retenus dans cette membrane entraînant le passage de la DexP libérée vers la périlymphe.
- Les liposomes peuvent aussi libérer une partie de la DexP dans le gel dans l'oreille moyenne. La DexP va alors diffuser à travers la fenêtre ronde sous forme libre.

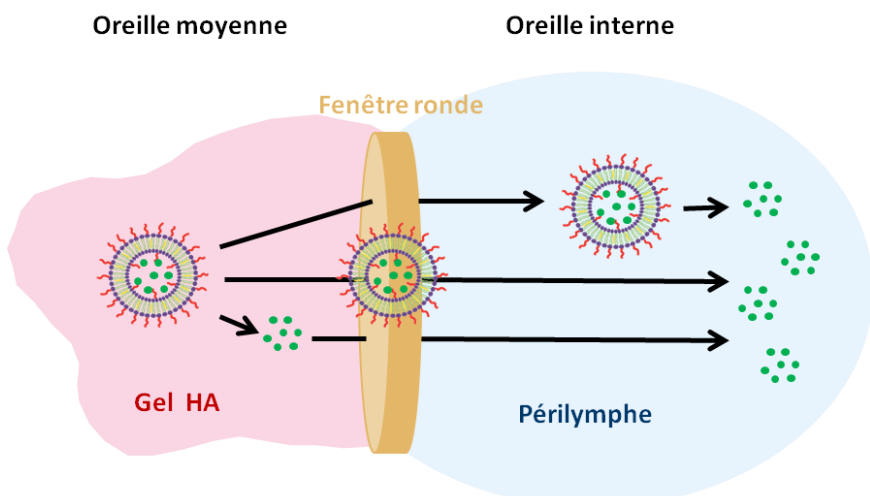


**Fig.4.** Passage des liposomes et/ou de la DexP à travers la fenêtre ronde.

Les résultats obtenus dans le chapitre III montrent que les liposomes semblent promouvoir la conversion de la prodrogue encapsulée (DexP) en sa forme active (Dex). Cette conversion peut avoir lieu lors du passage à travers la fenêtre ronde ou au niveau de la périlymphe. Une faible quantité de liposomes intacts a été visualisée dans la périlymphe alors que la majeure

partie des liposomes semble plutôt retenue dans la fenêtre ronde. En tenant compte de ces résultats et de la structure de la fenêtre ronde, les hypothèses concernant les mécanismes de passage de la DexP et/ou des liposomes à travers la fenêtre ronde peuvent être affinées. Plusieurs possibilités peuvent être envisagées et sont représentées dans la **Figure 5** :

- **Hypothèse 1 : internalisation des liposomes**

Les liposomes encapsulant la DexP (DexP-Lip) sont endocytés par les cellules épithéliales au niveau de la couche externe de la fenêtre ronde. Les liposomes sont alors déstabilisés et relarguent leur contenu (DexP) qui est métabolisé en Dex dans la cellule. La Dex diffuse alors à travers le tissu conjonctif et la couche épithéliale interne pour se retrouver dans la périlymphe.

- **Hypothèse 2 : passage paracellulaire des liposomes**

DexP-Lip passent à travers les espaces intercellulaires de l'épithélium externe de la fenêtre ronde et diffusent à travers son tissu conjonctif. Si les liposomes sont endocytés par des cellules présentes dans le tissu conjonctif (eg. Fibrocytes), leur devenir rejoint l'hypothèse 1. Sinon, les liposomes peuvent traverser le deuxième épithélium à travers les pores et préserver ainsi leur intégrité dans la périlymphe. Ce mécanisme de passage est également décrit dans la littérature pour le passage de nanocapsules lipidiques à travers la fenêtre ronde (Zou et al., 2008). La DexP encapsulée peut être libérée à partir des liposomes présents dans la périlymphe. Cette DexP libre peut alors être métabolisée en Dex dans la périlymphe.

- **Hypothèse 3 : rétention des liposomes dans la fenêtre ronde**

Après passage des DexP-Lip à travers les espaces intercellulaires de l'épithélium externe de la fenêtre ronde, les liposomes sont retenus dans le tissu conjonctif sans être endocytés mais ne passent pas le deuxième épithélium. Ces liposomes servent de réservoir dans la fenêtre ronde où ils libèrent la DexP qui sera métabolisée ou non avant de passer dans la périlymphe.

- **Hypothèse 4 : passage de la DexP libre**

Une partie de la DexP encapsulée dans les liposomes peut être libérée dans le gel dans l'oreille moyenne. La DexP libre peut alors diffuser à travers les différentes couches de la fenêtre ronde pour se retrouver dans la périlymphe. La DexP libre peut aussi être

métabolisée en Dex lors du passage à travers la fenêtre ronde ou une fois dans la périlymphe. Cependant, selon les résultats obtenus dans le chapitre III avec le gel d'HA contenant la DexP libre, cette dernière semble majoritairement diffuser sous forme DexP et la conversion en Dex est relativement faible dans ce cas-là.

Selon nos résultats (Chapitre III), ces quatre voies de passage peuvent avoir lieu simultanément. Cependant, étant donné la concentration relativement élevée de Dex dans la périlymphe ainsi que la très faible proportion de liposomes intacts dans la périlymphe observée et quantifiée par microscopie confocale, la rétention des liposomes dans la fenêtre ronde (hypothèse 3) ainsi que l'internalisation des liposomes dans cette membrane (hypothèse 1) semblent prépondérantes en ce qui concerne le passage des liposomes et de la DexP. Suite à l'application du gel HA-DexP-Lip dans l'oreille moyenne, nous retrouvons à la fois des liposomes, de la DexP et de la Dex dans la périlymphe. Ces trois composés peuvent alors atteindre les cibles thérapeutiques représentées par les cellules neurosensorielles contenues dans l'organe de Corti qui baigne dans la périlymphe (Ghanem et al., 2008). Plusieurs études ont démontré l'internalisation de nanovecteurs, y compris des liposomes, au niveau des cellules ciliées et des neurones des ganglions spiraux dans la cochlée suite à une administration dans l'oreille moyenne (Zou et al., 2008, Zou et al., 2010, Zhang et al., 2011, Buckiova et al., 2012).

Une étude récente a démontré qu'environ 15% des protéines contenues dans la périlymphe (~ 1g/L) sont des enzymes telles que la prostaglandine synthase, la carboxylestérase, la créatine kinase, la phosphodiesterase (Swan et al., 2009). La phosphodiesterase pourrait être à l'origine de la métabolisation de la DexP en Dex dans la périlymphe. De plus, cette étude a également confirmé la présence d'albumine, d'apolipoprotéines et de glycoprotéines dans la périlymphe qui pourraient se lier au corticoïde et jouer un rôle de réservoir.

Par ailleurs, la concentration de lipides dans la périlymphe estimée entre 0.18 et 1.8  $\mu\text{M}$  (Chapitre III), suite à l'administration du gel HA-Lip dans l'oreille moyenne, ne devrait pas entraîner d'effets cytotoxiques au niveau de la cochlée puisque cette concentration est largement inférieure à la concentration de lipides à partir de laquelle des effets cytotoxiques (~ 1mM) sont observés *in vitro* sur différentes lignées cellulaires (Layton et al., 1980). De plus, dans la littérature, l'administration de nanovecteurs dans l'oreille moyenne ou interne n'a montré aucun effet cytotoxique sur la cochlée (Scheper et al., 2009, Zhang et al., 2011, Zou et al., 2014).

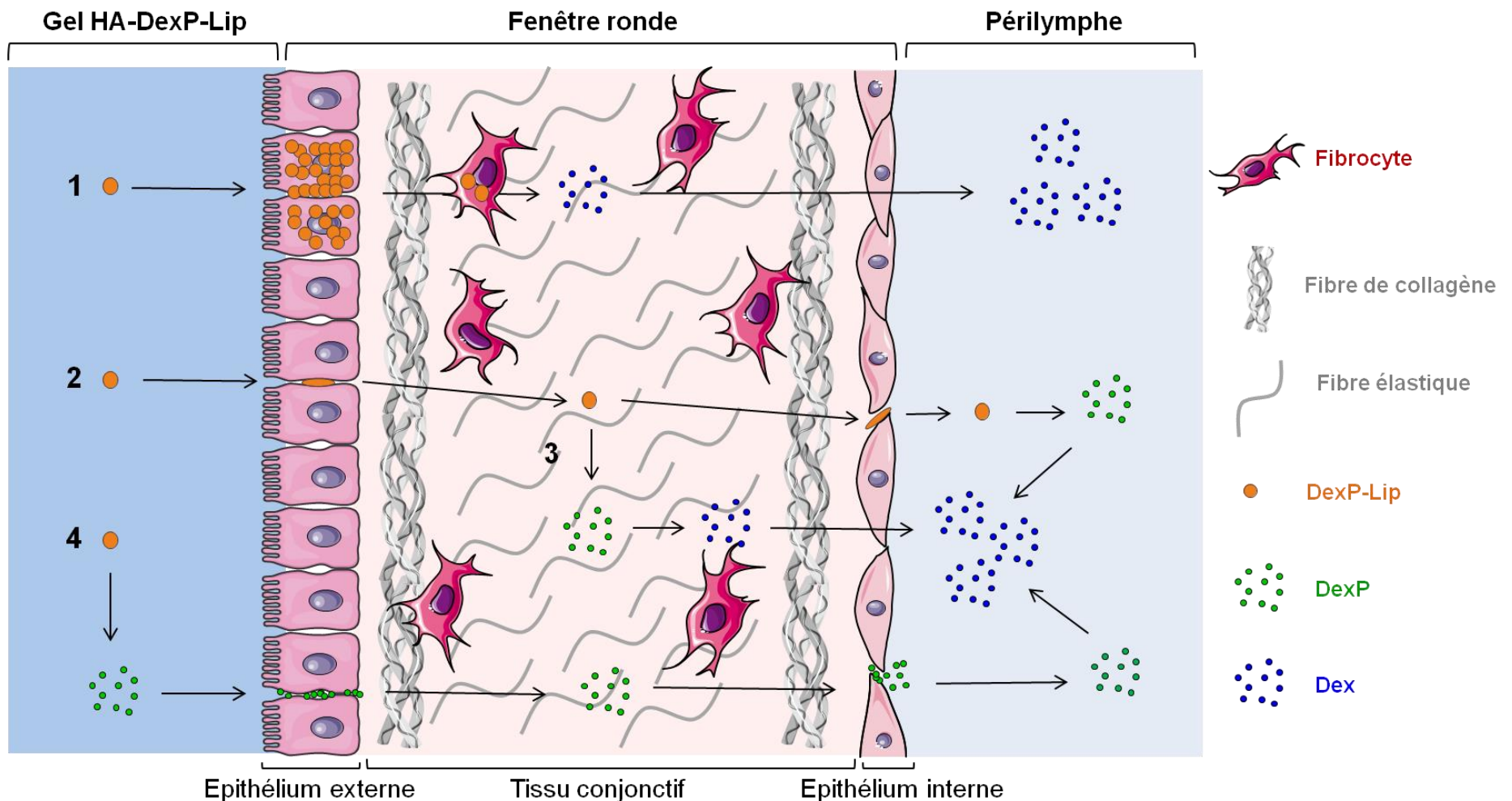


**Fig.5.** Mécanismes de passage des liposomes et/ou de la dexamethasone phosphate (DexP) à travers la fenêtre ronde et sa conversion en dexamethasone (Dex). Hypothèse 1 : internalisation des liposomes et conversion de la DexP en Dex. Hypothèse 2 : passage para-cellulaire des liposomes intacts. Hypothèse 3 : rétention des liposomes dans la fenêtre ronde et effet réservoir. Hypothèse 4 : passage de la DexP sous forme libre.

### 3.3. Gels HA-DexP-Lip et HA-DexP comparés aux autres gels pour la libération prolongée de la dexamethasone dans la périlymphe

Comparé au gel de poloxamer 407 (Wang et al., 2009, Salt et al., 2011, Wang et al., 2011) ou de chitosan (Paulson et al., 2008) (**Tableau 2**), le gel HA-DexP-Lip présente l'avantage de ne pas entraîner de surdité de transmission. La surdité de transmission peut être expliquée par une réduction de la mobilité de la chaîne ossiculaire due à la présence physique du gel dans la cavité tympanique (Salt et al., 2011). La vibration des osselets pourrait alors être altérée par les propriétés mécaniques du gel. Le module élastique ( $G'$ ) du gel utilisé dans notre étude (HA-DexP-Lip) à 37 °C à une fréquence de 1 Hz est d'environ 330 Pa (Chapitres I et III). Celui d'un gel de poloxamer 407 à 17 % (m/m) (préparé lors des expériences décrites dans le chapitre I) est d'environ 10000 Pa (37°C à 1 Hz), soit une élasticité du poloxamer 407 25 fois supérieure à celle de notre gel à 37 °C. Cette différence de module élastique pourrait expliquer le fait que notre formulation HA-DexP-Lip n'entraîne pas de surdité de transmission contrairement au gel de poloxamer 407.

Sur le modèle de traumatisme sonore (Chapitre IV), contrairement au groupe contrôle (pas de chirurgie, pas d'injection de gel), une élévation -non significative- des seuils auditifs a été observée à J<sub>7</sub> dans les groupes ayant subi la chirurgie rétro-auriculaire et l'injection de gel (HA, HA-DexP ou HA-DexP-Lip). Etant donnée l'absence de témoin ayant subi uniquement la chirurgie dans notre protocole expérimental, il est difficile de conclure sur l'origine de cette augmentation des seuils. En effet, l'élévation des seuils peut être attribuée soit à la chirurgie, soit à la présence du gel dans la cavité tympanique (surdité de transmission). Bien que sur le cobaye normo-entendant, aucun de ces deux paramètres n'a entraîné de surdité de transmission (Chapitre III), l'impact de la chirurgie ou du gel présent dans l'oreille moyenne pourrait être différent sur un cobaye ayant subi un traumatisme sonore. Comme évoqué dans le chapitre IV, pour vérifier cela, il est nécessaire d'évaluer l'effet propre de la chirurgie en ajoutant un groupe témoin qui subit l'abord chirurgical sans injection de gel.

Le **tableau 2** met en évidence qu'une injection unique de nos deux gels (avec et sans liposomes) conduit à un temps de persistance du corticoïde dans la périlymphe (30 jours pour HA-DexP-Lip et 15 jours pour HA-DexP) supérieur à celui décrit dans les autres études (maximum de 10 jours avec le poloxamer 407 (Wang et al., 2009)). Les concentrations en corticoïde dans la périlymphe après injection du gel de liposomes (HA-DexP-Lip) sont globalement inférieures à celles rapportées dans la littérature pour des gels d'HA, de

poloxamer 407 ou de chitosan (Paulson et al., 2008, Wang et al., 2009, Salt et al., 2011, Wang et al., 2011). Contrairement aux autres systèmes, le gel de liposomes constitue une forme à libération prolongée qui permet d'obtenir des concentrations en corticoïde plus faibles dans la périlymphe mais pour une durée plus importante. Toutefois, étant donné les différences de protocoles d'administration entre les études présentées dans le **tableau 2** (bulle remplie ou dépôt sur la fenêtre ronde), les différences de volume ainsi que la méthode de prélèvement des échantillons de périlymphe, la comparaison des différents systèmes entre eux doit être effectuée avec prudence.

Notre étude a également montré une variabilité importante des concentrations de Dex et de DexP dans la périlymphe au sein d'un même groupe d'animaux (Chapitre III). En plus de la variabilité interindividuelle décrite précédemment, la différence entre les animaux peut être due à une variabilité de la qualité du prélèvement de périlymphe. En effet, il a été démontré précédemment que 1  $\mu\text{L}$  de périlymphe prélevée au niveau du tour basal de la cochlée contenait environ 20% de liquide céphalorachidien (Salt et al., 2003), ce qui entraîne une dilution de l'échantillon de périlymphe et une sous-estimation de la concentration réelle en corticoïde. Dans notre étude, le volume moyen des prélèvements de périlymphe était de 2  $\mu\text{L}$  mais celui-ci variait entre 1.5 et 3.5  $\mu\text{L}$  (volume mesuré de façon précise pour chaque échantillon prélevé) en raison de la difficulté à aspirer avec précision un volume exact de 2  $\mu\text{L}$  lors du prélèvement (Chapitre III, matériel et méthodes).

**Tableau 2.**

Comparaison du gel de liposomes encapsulant la DexP (HA-DexP-Lip) et du gel contenant la DexP libre (HA-DexP) avec les autres gels décrits dans la littérature pour l'administration de dexamethasone (Dex) et de dexamethasone phosphate (DexP) dans l'oreille interne.

	<b>HA-DexP-Lip</b> (Chapitre III)	<b>HA-DexP</b> (Chapitre III)	<b>HA</b> (Borden et al., 2011)	<b>Chitosan</b> (Paulson et al., 2008)	<b>Poloxamer 407</b> (Wang et al., 2011)	<b>Poloxamer 407</b> (Salt et al., 2011)	<b>Poloxamer 407</b> (Wang et al., 2009)
Composition du gel	[HA] = 2.28% (m/v) [Lipides] = 80 mM [DexP] = 10 mg/mL (encapsulée dans les liposomes)	[HA] = 2.28% (m/v) [DexP] = 10 mg/mL (en solution)	thiol-HA/gelatin 90/10	Chitosan-glycerophosphate 3.4% (m/m)	Poloxamer 407 17% (m/m) Dex 15 mg/mL (suspension) ou DexP 20 mg/mL (en solution)	Poloxamer 407 17% (m/m) [Dex] = 45 mg/mL (en suspension)	Poloxamer 407 17 ou 15.5% (m/m) Dex 15 ou 45 mg/mL (en suspension)
Modèle animal	Cobaye	Cobaye	Cobaye	Souris	Cobaye	Cobaye	Cobaye
Volume injecté	150 µL	150 µL	~ 200 µL	/	50 µL	50 µL	50 µL
Dose injectée	1.5 mg	1.5 mg	2 mg	0.35 mg	0.75 ou 1 mg	2.25 mg	0.75 ou 2.25 mg
Prélèvement de périlymph	Basal 2 µL	Basal 2 µL	Basal 10 µL	/	Basal 0.25 µL	Apical 5 µL	Basal 8 x 1 µL
Concentration du corticoïde dans la périlymph	DexP : <b>50 (J<sub>15</sub>) à 135 (J<sub>30</sub>) ng/mL</b> Dex : <b>0 (J<sub>30</sub>) à 833 (J<sub>15</sub>) ng/mL</b>	DexP : <b>45 (J<sub>15</sub>) à 152 (J<sub>7</sub>) ng/mL</b> Dex : <b>0 (J<sub>15</sub>) à 40 (J<sub>2</sub>) ng/mL</b>	DexP : <b>100 (J<sub>3</sub>) à 2000 ng/mL (J<sub>1</sub>)</b>	Dex : <b>1300 (J<sub>5</sub>) à 3200 (J<sub>1</sub>) ng/mL</b>	Dex (15 mg/mL) : <b>70 (J<sub>10</sub>) à 970 (J<sub>1</sub>) ng/mL</b> DexP (20 mg/mL) : <b>100 (J<sub>1</sub>) à 2500 (6h) ng/mL</b>	Dex : <b>100 à 1000 ng/mL à J<sub>1</sub></b> DexP (20 mg/mL) : <b>100 (J<sub>1</sub>) à 2500 (6h) ng/mL</b>	Dex (15 mg/mL) : <b>73 (J<sub>10</sub>) à 974 (J<sub>1</sub>) ng/mL</b> Dex (45 mg/mL) : <b>1000 (J<sub>1</sub>) à 2000 (J<sub>10</sub>) ng/mL</b>
Temps de persistance du corticoïde dans la périlymph	<b>30 jours</b>	<b>15 jours</b>	<b>3 jours</b>	<b>5 jours</b>	<b>10 jours pour Dex 24 h pour DexP</b>	<b>24 h</b>	<b>Au moins 10 jours ( Dex 45 mg/mL)</b>
Surdité de transmission	<b>non</b>	<b>ND</b>	<b>ND</b>	<b>oui</b>	<b>ND</b>	<b>oui</b>	<b>oui</b>

#### 4. L'utilisation des corticoïdes pour le traitement des pathologies de l'oreille interne : efficacité et limites

Au niveau cellulaire, et dans de nombreux tissus, la dexamethasone agit à des concentrations allant de 1 à 30 ng/mL (Czock et al., 2005). Dans l'oreille interne, la dexamethasone peut moduler l'activité des canaux sodiques épithéliaux à des concentrations d'environ 40 ng/mL (Pondugula et al., 2006, Kim et al., 2009), ce qui est du même ordre de grandeur que dans les autres tissus. Ces résultats soutiennent l'hypothèse que les effets thérapeutiques bénéfiques de la dexamethasone dans l'oreille interne peuvent se produire à des concentrations d'environ 30-40 ng/mL (Wang et al., 2011). Dans le chapitre III, les concentrations périlymphatiques de la Dex et de la DexP obtenues varient entre 45 et 152 ng/mL pour le gel HA-DexP et entre 50 et 833 ng/mL pour le gel HA-DexP-Lip. Ces concentrations peuvent être considérées comme des concentrations thérapeutiques. Nous avons vérifié cela *in vivo* sur deux modèles (implantation cochléaire et traumatisme sonore). L'administration du gel de liposomes contenant la DexP a entraîné un effet thérapeutique sur ces deux modèles. D'une part, le gel de liposomes contenant la DexP a permis de préserver l'audition résiduelle des cobayes implantés manuellement (Chapitre V). En effet, les seuils auditifs dans le groupe traité avec HA-DexP-Lip étaient significativement plus faibles que ceux du groupe traité avec HA-Lip lors de l'implantation manuelle. D'autre part, l'administration du gel HA-DexP-Lip après un traumatisme sonore a permis une récupération de l'audition sur la fréquence 16 kHz alors qu'une perte auditive d'environ 15 dB persistait sur cette fréquence dans le groupe témoin (Chapitre IV). Néanmoins, sur le modèle de traumatisme sonore, le gel contenant la DexP libre (HA-DexP) a conduit à une efficacité thérapeutique supérieure à celle du groupe HA-DexP-Lip (Chapitre IV). Ce résultat est surprenant au vu des concentrations en Dex et DexP obtenues dans la périlymphe. En effet, le gel HA-DexP-Lip permet d'atteindre une concentration totale en corticoïde (Dex + DexP) 4 à 25 fois supérieure à celle obtenue avec le gel HA-DexP, une libération prolongée jusqu'à 30 jours (avec HA-DexP-Lip) contre seulement 15 jours pour HA-DexP et une conversion de la DexP en sa forme active dès J<sub>2</sub> (Chapitre III). Une des explications possibles serait que, suite au traumatisme sonore, la modification de certains paramètres biologiques ait pu altérer la diffusion des liposomes et/ou de la DexP dans l'oreille interne chez ces animaux conduisant un profil pharmacocinétique différent de celui des animaux normo-entendants sur lesquels l'étude de biodistribution a été conduite. Une autre explication serait que la concentration

optimale en dexamethasone pour une action bénéfique sur les mécanismes physiopathologiques induits par le traumatisme sonore se situe à des concentrations faibles, de l'ordre de 40 à 150 ng/mL. Des expériences complémentaires sont nécessaires pour élucider ce résultat. Il serait intéressant de doser à nouveau le corticoïde dans périlymphe à J<sub>30</sub> chez les animaux ayant subi un traumatisme sonore et qui ont été traités avec les gels HA-DexP et HA-DexP-Lip.

En pratique clinique, les corticoïdes et en particulier la dexamethasone et la méthylprednisolone sont très utilisées dans le traitement des pathologies de l'oreille interne telles que la maladie de Ménière, la surdité neurosensorielle aiguë, la surdité neurosensorielle induite par le bruit et pour la protection contre des agents ototoxiques (Cf. travaux antérieurs). Bien que l'administration de fortes doses de corticoïde dans l'oreille interne par voie locale ou systémique soit associée à des effets bénéfiques sur la récupération de l'audition chez les patients (Meltser and Canlon, 2011), les protocoles de traitement sont très hétérogènes et souvent empiriques (Alles et al., 2006, Pai and Lee, 2013). De plus, la dose optimale de corticoïde à administrer n'est pas clairement établie. Par ailleurs, les mécanismes d'action des corticoïdes dans l'oreille interne pour la récupération de l'audition ne sont pas complètement élucidés. Ces molécules semblent avoir davantage un effet global dans l'oreille interne plutôt que ciblé (Staecker and Rodgers, 2013). Plusieurs mécanismes sont décrits dans la littérature et pourraient entrer en jeu tels que l'action anti-inflammatoire, la régulation du transport ionique, l'augmentation de la perfusion sanguine ou encore la réduction du stress oxydant conduisant à l'apoptose (Chapitre IV). Le fait de ne pas connaître le mécanisme exact par lequel la dexamethasone agit dans l'oreille interne rend l'interprétation de nos résultats difficile en particulier concernant l'efficacité thérapeutique sur le modèle de traumatisme sonore (Chapitre IV) et celui de l'implantation cochléaire (Chapitre V). Cependant, dans ce travail, la dexamethasone a servi de molécule modèle afin d'établir une preuve de concept pour la libération prolongée du corticoïde grâce aux liposomes dans le gel d'HA. De plus, nous avons démontré que l'addition des liposomes permet d'obtenir une concentration plus importante du corticoïde dans l'oreille interne pouvant être considérée comme une concentration thérapeutique.

## Références

- Alles, M.J., der Gaag, M.A., Stokroos, R.J., 2006. Intratympanic steroid therapy for inner ear diseases, a review of the literature. *Eur Arch Otorhinolaryngol.* 263, 791-797.
- Antunes, F.E., Brito, R.O., Marques, E.F., Lindman, B., Miguel, M., 2007. Mechanisms behind the faceting of catanionic vesicles by polycations: chain crystallization and segregation. *The Journal of Physical Chemistry B.* 111, 116-123.
- Antunes, F.E., Marques, E.F., Miguel, M.G., Lindman, B., 2009. Polymer–vesicle association. *Advances in Colloid and Interface Science.* 147, 18-35.
- Barbucci, R., Lamponi, S., Borzacchiello, A., Ambrosio, L., Fini, M., Torricelli, P., Giardino, R., 2002. Hyaluronic acid hydrogel in the treatment of osteoarthritis. *Biomaterials.* 23, 4503-4513.
- Borden, R.C., Saunders, J.E., Berryhill, W.E., Krempl, G.A., Thompson, D.M., Queimado, L., 2011. Hyaluronic acid hydrogel sustains the delivery of dexamethasone across the round window membrane. *Audiol Neurotol.* 16, 1-11.
- Borzacchiello, A., Russo, L., Malle, B.M., Schwach-Abdellaoui, K., Ambrosio, L., 2015. Hyaluronic Acid Based Hydrogels for Regenerative Medicine Applications. *BioMed Research International.* 2015,
- Buckiova, D., Ranjan, S., Newman, T.A., Johnston, A.H., Sood, R., Kinnunen, P.K., Popelar, J., Chumak, T., Syka, J., 2012. Minimally invasive drug delivery to the cochlea through application of nanoparticles to the round window membrane. *Nanomedicine (Lond).* 7, 1339-1354.
- Czock, D., Keller, F., Rasche, F.M., Häussler, U., 2005. Pharmacokinetics and pharmacodynamics of systemically administered glucocorticoids. *Clinical pharmacokinetics.* 44, 61-98.
- De Smedt, S.C., Dekeyser, P., Ribitsch, V., Lauwers, A., Demeester, J., 1993. Viscoelastic and transient network properties of hyaluronic acid as a function of the concentration. *Biorheology.* 30, 31-41.
- De Smedt, S.C., Lauwers, A., Demeester, J., Engelborghs, Y., De Mey, G., Du, M., 1994. Structural information on hyaluronic acid solutions as studied by probe diffusion experiments. *Macromolecules.* 27, 141-146.
- Diederich, A., Bähr, G., Winterhalter, M., 1998. Influence of polylysine on the rupture of negatively charged membranes. *Langmuir.* 14, 4597-4605.
- Dubois, M., Lizunov, V., Meister, A., Gulik-Krzywicki, T., Verbavatz, J.M., Perez, E., Zimmerberg, J., Zemb, T., 2004. Shape control through molecular segregation in giant surfactant aggregates. *Proceedings of the National Academy of Sciences of the United States of America.* 101, 15082-15087.
- Friedland, D.R., Runge-Samuelson, C., 2009. Soft cochlear implantation: rationale for the surgical approach. *Trends Amplif.* 13, 124-138.
- Ghanem, T.A., Breneman, K.D., Rabbitt, R.D., Brown, H.M., 2008. Ionic composition of endolymph and perilymph in the inner ear of the oyster toadfish, *Opsanus tau*. *Biol Bull.* 214, 83-90.
- Girish, K.S., Kemparaju, K., 2007. The magic glue hyaluronan and its eraser hyaluronidase: a biological overview. *Life Sci.* 80, 1921-1943.

- Honeder, C., Engleider, E., Schopper, H., Gabor, F., Reznicek, G., Wagenblast, J., Gstoeftner, W., Arnoldner, C., 2014. Sustained release of triamcinolone acetonide from an intratympanically applied hydrogel designed for the delivery of high glucocorticoid doses. *Audiol Neurotol.* 19, 193-202.
- Hoskison, E., Daniel, M., Al-Zahid, S., Shakesheff, K.M., Bayston, R., Birchall, J.P., 2013. Drug delivery to the ear. *Ther Deliv.* 4, 115-124.
- Ionov, R., El-Abed, A., Goldmann, M., Peretti, P., 2004. Interactions of lipid monolayers with the natural biopolymer hyaluronic acid. *Biochim Biophys Acta.* 1667, 200-207.
- Jiao, Y., Pang, X., Zhai, G., 2015. Advances in hyaluronic acid-based drug delivery systems. *Current drug targets.*
- Kablik, J., Monheit, G.D., Yu, L., Chang, G., Gershkovich, J., 2009. Comparative physical properties of hyaluronic acid dermal fillers. *Dermatol Surg.* 35 Suppl 1, 302-312.
- Kim, S.H., Kim, K.X., Raveendran, N.N., Wu, T., Pondugula, S.R., Marcus, D.C., 2009. Regulation of ENaC-mediated sodium transport by glucocorticoids in Reissner's membrane epithelium. *American Journal of Physiology-Cell Physiology.* 296, C544-C557.
- Krause, W.E., Bellomo, E.G., Colby, R.H., 2001. Rheology of Sodium Hyaluronate under Physiological Conditions. *Biomacromolecules.* 2, 65-69.
- Lajavardi, L. (2008). Nouvelle stratégie thérapeutique des uvéites par l'administration intraoculaire d'un peptide immunomodulateur, le vasoactive intestinal peptide, dans des liposomes, Paris 11.
- Lapčík, L., Lapčík, L., De Smedt, S., Demeester, J., Chabreček, P., 1998. Hyaluronan: Preparation, Structure, Properties, and Applications. *Chem Rev.* 98, 2663-2684.
- Laroche, G., Pezolet, M., Dufourcq, J., Dufourc, E. (1989). Modifications of the structure and dynamics of dimyristoylphosphatidic acid model membranes by calcium ions and poly-L-lysines. A Raman and deuterium NMR study. *Trends in Colloid and Interface Science III*, Springer: 38-42.
- Layton, D., Luckenbach, G.A., Andreesen, R., Munder, P.G., 1980. The interaction of liposomes with cells: The relation of cell specific toxicity to lipid composition. *European Journal of Cancer (1965).* 16, 1529-1538.
- Marques, E.F., Regev, O., Khan, A., Miguel, M.d.G., Lindman, B., 1999. Interactions between catanionic vesicles and oppositely charged polyelectrolytes phase behavior and phase structure. *Macromolecules.* 32, 6626-6637.
- Masuda, A., Ushida, K., Koshino, H., Yamashita, K., Kluge, T., 2001. Novel Distance Dependence of Diffusion Constants in Hyaluronan Aqueous Solution Resulting from Its Characteristic Nano-Microstructure. *Journal of the American Chemical Society.* 123, 11468-11471.
- Mayol, L., Quaglia, F., Borzacchiello, A., Ambrosio, L., La Rotonda, M.I., 2008. A novel poloxamers/hyaluronic acid in situ forming hydrogel for drug delivery: rheological, mucoadhesive and in vitro release properties. *Eur J Pharm Biopharm.* 70, 199-206.
- Meltser, I., Canlon, B., 2011. Protecting the auditory system with glucocorticoids. *Hear Res.* 281, 47-55.
- Monheit, G.D., Coleman, K.M., 2006. Hyaluronic acid fillers. *Dermatologic therapy.* 19, 141-150.

- Nilsson, M., Hellström, S., Hedlund, U., 1992. The use of hyaluronidase and glucosidase to remove mucus from the rat middle ear cavities for SEM studies. *The Histochemical Journal*. 24, 166-169.
- Pai, Y.-C., Lee, C.-F., 2013. Intratympanic steroid injection for inner ear disease. *Tzu Chi Medical Journal*. 25, 146-149.
- Paulson, D.P., Abuzeid, W., Jiang, H., Oe, T., O'Malley, B.W., Li, D., 2008. A novel controlled local drug delivery system for inner ear disease. *Laryngoscope*. 118, 706-711.
- Pondugula, S.R., Raveendran, N.N., Ergonul, Z., Deng, Y., Chen, J., Sanneman, J.D., Palmer, L.G., Marcus, D.C., 2006. Glucocorticoid regulation of genes in the amiloride-sensitive sodium transport pathway by semicircular canal duct epithelium of neonatal rat. *Physiological genomics*. 24, 114-123.
- Pracy, J., White, A., Mustafa, Y., Smith, D., Perry, M., 1998. The comparative anatomy of the pig middle ear cavity: a model for middle ear inflammation in the human? *Journal of anatomy*. 192, 359-368.
- Salt, A.N., Hartsock, J., Plontke, S., LeBel, C., Piu, F., 2011. Distribution of dexamethasone and preservation of inner ear function following intratympanic delivery of a gel-based formulation. *Audiol Neurotol*. 16, 323-335.
- Salt, A.N., Kellner, C., Hale, S., 2003. Contamination of perilymph sampled from the basal cochlear turn with cerebrospinal fluid. *Hear Res*. 182, 24-33.
- Scheper, V., Wolf, M., Scholl, M., Kadlecova, Z., Perrier, T., Klok, H.A., Saulnier, P., Lenarz, T., Stover, T., 2009. Potential novel drug carriers for inner ear treatment: hyperbranched polylysine and lipid nanocapsules. *Nanomedicine (Lond)*. 4, 623-635.
- Scott, J.E., Cummings, C., Brass, A., Chen, Y., 1991. Secondary and tertiary structures of hyaluronan in aqueous solution, investigated by rotary shadowing-electron microscopy and computer simulation. Hyaluronan is a very efficient network-forming polymer. *Biochem J*. 274 ( Pt 3), 699-705.
- Staecker, H., Rodgers, B., 2013. Developments in delivery of medications for inner ear disease. *Expert Opin Drug Deliv*. 10, 639-650.
- Stern, R., Jedrzejas, M.J., 2006. Hyaluronidases: their genomics, structures, and mechanisms of action. *Chem Rev*. 106, 818-839.
- Swan, E.E., Peppi, M., Chen, Z., Green, K.M., Evans, J.E., McKenna, M.J., Mescher, M.J., Kujawa, S.G., Sewell, W.F., 2009. Proteomics analysis of perilymph and cerebrospinal fluid in mouse. *Laryngoscope*. 119, 953-958.
- Taglienti, A., Cellesi, F., Crescenzi, V., Sequi, P., Valentini, M., Tirelli, N., 2006. Investigating the interactions of hyaluronan derivatives with biomolecules. The use of diffusional NMR techniques. *Macromol Biosci*. 6, 611-622.
- Torchilin, V., Weissig, V. 2003. Liposomes: a practical approach. Oxford University Press.
- Volpi, N., Schiller, J., Stern, R., Soltes, L., 2009. Role, Metabolism, Chemical Modifications and Applications of Hyaluronan. *Current Medicinal Chemistry*. 16, 1718-1745.
- Wang, A.Z., Langer, R., Farokhzad, O.C., 2012. Nanoparticle delivery of cancer drugs. *Annu Rev Med*. 63, 185-198.
- Wang, X., Dellamary, L., Fernandez, R., Harrop, A., Keithley, E.M., Harris, J.P., Ye, Q., Lichter, J., LeBel, C., Piu, F., 2009. Dose-dependent sustained release of

- dexamethasone in inner ear cochlear fluids using a novel local delivery approach. *Audiol Neurotol.* 14, 393-401.
- Wang, X., Dellamary, L., Fernandez, R., Ye, Q., LeBel, C., Piu, F., 2011. Principles of inner ear sustained release following intratympanic administration. *Laryngoscope.* 121, 385-391.
- Zhang, Y., Zhang, W., Johnston, A.H., Newman, T.A., Pyykk, I., Zou, J., 2011. Comparison of the distribution pattern of PEG-b-PCL polymersomes delivered into the rat inner ear via different methods. *Acta Otolaryngol.* 131, 1249-1256.
- Zhang, Y., Zhang, W., Lobler, M., Schmitz, K.P., Saulnier, P., Perrier, T., Pyykko, I., Zou, J., 2011. Inner ear biocompatibility of lipid nanocapsules after round window membrane application. *Int J Pharm.* 404, 211-219.
- Zou, J., Saulnier, P., Perrier, T., Zhang, Y., Manninen, T., Toppila, E., Pyykko, I., 2008. Distribution of lipid nanocapsules in different cochlear cell populations after round window membrane permeation. *J Biomed Mater Res B Appl Biomater.* 87, 10-18.
- Zou, J., Sood, R., Ranjan, S., Poe, D., Ramadan, U.A., Kinnunen, P.K., Pyykko, I., 2010. Manufacturing and in vivo inner ear visualization of MRI traceable liposome nanoparticles encapsulating gadolinium. *J Nanobiotechnology.* 8, 32.
- Zou, J., Sood, R., Zhang, Y., Kinnunen, P.K., Pyykko, I., 2014. Pathway and morphological transformation of liposome nanocarriers after release from a novel sustained inner-ear delivery system. *Nanomedicine (Lond).* 9, 2143-2155.

## **Conclusion et perspectives**

Les travaux réalisés au cours de cette thèse ont apporté des éléments significatifs permettant de conclure sur l'intérêt du gel de liposomes pour l'administration de substances actives par voie locale. En effet, le gel de liposomes constitue une plateforme de formulation modulable et prometteuse qui pourrait servir pour différentes applications dans l'administration locale de substances actives, lorsqu'une injection est requise, comme c'est le cas pour les injections transtympaniques.

Les paramètres clés qui impactent les propriétés du système ont été identifiés grâce à une étude physicochimique approfondie. Les résultats montrent que les liposomes interagissent avec l'acide hyaluronique entraînant un renforcement du réseau formé par les chaînes de polymère qui se traduit par une augmentation de la viscosité et de l'élasticité du gel. La nature et les effets résultants de ces interactions dépendent à la fois des propriétés de surface, de la concentration des liposomes mais aussi de leur surface d'échange avec le polymère. A une concentration de 2.28% en acide hyaluronique, la microstructure du gel de liposomes est caractérisée par une micro-séparation de phases entre HA et liposomes qui est probablement induite par un effet de déplétion du polymère vis-à-vis des liposomes. La diffusion des liposomes au sein du gel dépend à la fois de la concentration en HA, des propriétés de surface et de la concentration en liposomes. Les liposomes PEGylés ont montré l'aptitude à la diffusion la plus élevée au sein du gel d'HA aux échelles macro- et microscopique. Ces liposomes sont également ceux qui permettent d'obtenir des systèmes dont la viscosité et l'élasticité sont les plus élevées, tout en ayant une formulation facilement injectable. Enfin, la dispersion de liposomes PEGylés au sein du gel d'HA se distingue des autres formulations de liposomes par une microstructure formant un réseau bicontinu d'HA et de liposomes.

Lors de l'évaluation *in vivo*, nous avons démontré que le gel de liposomes PEGylés répondait au cahier des charges défini pour la voie transtympanique. En effet, le gel est facilement injectable grâce au comportement rhéofluidifiant de l'HA. Il a montré une parfaite innocuité vis-à-vis de la fonction auditive des cobayes. Il a également permis une persistance prolongée de la formulation dans l'oreille moyenne et sur la fenêtre ronde grâce à sa viscosité élevée couplée à ses propriétés viscoélastique et non-thixotrope. La présence de liposomes dans la formulation a abouti à une libération prolongée du corticoïde dans le périlymphe jusqu'à 30 jours. En outre, les liposomes semblent promouvoir la conversion de la prodrogue encapsulée (DexP) en sa forme active (Dex). Enfin, une faible quantité de liposomes intacts a été visualisée dans le périlymphe. La majeure partie des liposomes semble plutôt retenue dans

la fenêtre ronde qui jouerait ainsi un rôle de réservoir pour une libération prolongée du corticoïde dans l'oreille interne. Enfin, la concentration en corticoïde retrouvée dans la périlymphe est compatible avec une efficacité thérapeutique. En effet, nous avons obtenu des résultats préliminaires encourageants sur deux modèles différents pour le traitement de la surdité induite par un traumatisme sonore et pour la préservation de l'audition durant l'implantation cochléaire.

De nombreuses perspectives de recherche peuvent être proposées à la suite de cette thèse. En effet, plusieurs études complémentaires permettant d'étayer et d'affiner certaines hypothèses et d'approfondir certains aspects peuvent être envisagées.

D'abord, afin de compléter l'étude physicochimique, il serait intéressant d'évaluer l'influence de la masse molaire de l'HA sur les propriétés du gel de liposomes en testant un ou plusieurs grades d'HA de masse molaire plus faible (eg. 500 kDa). Il paraît également important d'évaluer l'influence des liposomes sur les propriétés adhésives de l'HA. La mesure des forces d'adhésion peut être réalisée par AFM mais cela nécessite une optimisation des paramètres de mesure et du protocole expérimental. Nous n'avons pas été en mesure de quantifier ce paramètre lors de nos essais d'AFM. La mucoadhésion des formulations pourrait être mesurée indirectement en mélangeant le gel de liposomes avec de la mucine et en évaluant l'impact du mélange sur les propriétés rhéologiques du système. Ceci pourrait mettre en évidence une synergie plus ou moins importante avec la mucine selon les formulations. Par ailleurs, la microstructure du gel de liposomes, notamment l'effet du polymère sur la structure des liposomes, pourrait être caractérisée de façon plus approfondie par des méthodes telles que la diffusion des neutrons aux petits angles (SANS) ou la diffusion des rayons X aux petits angles (SAXS). Enfin, il pourrait être intéressant de vérifier si la microstructure obtenue est influencée par la méthode de préparation des gels et dans quelle mesure les propriétés rhéologiques obtenues en dépendent.

Afin de mieux comprendre le comportement du gel de liposomes *in vivo* dans l'oreille moyenne, il serait intéressant de mettre en place des modèles d'évaluation *in vitro*. D'une part, cela permettrait d'étudier le gonflement et éventuellement le séchage du gel de liposomes dans un milieu reproduisant les conditions d'humidité et de température de la cavité tympanique. D'autre part, une étude de la libération de la substance active pourrait être mise en place en utilisant des Transwell®. Similaires au principe des cellules de diffusion de Franz, ces dispositifs de culture cellulaire possèdent un compartiment donneur et un

compartiment receveur séparés par une membrane polymère de surface et de porosité variable. Ce modèle est souvent décrit dans la littérature pour évaluer la cinétique de libération de substances actives à partir de formulations destinées à l'administration intratympanique. Même si les dimensions du Transwell®, en particulier celles de la membrane, ne sont pas représentatives de l'anatomie de l'oreille moyenne, ce modèle devrait permettre d'évaluer la cinétique de libération intrinsèque de la formulation et ainsi de comparer différentes formulations entre elles en termes de profil de libération *in vitro*.

Pour étayer les hypothèses concernant les mécanismes de passage des liposomes à travers la fenêtre ronde, il est indispensable d'améliorer la méthode de prélèvement de la fenêtre ronde afin de pouvoir visualiser la localisation des liposomes dans les différentes couches de cette membrane par microscopie confocale. De plus, afin d'évaluer plus précisément le temps de persistance du gel de liposomes dans l'oreille moyenne et éventuellement dans l'oreille interne, la technique d'imagerie *in vivo* (IVIS, Lumina®) semble pertinente mais nécessite le couplage de l'HA ou des liposomes à un fluorophore permettant de s'affranchir de l'autofluorescence des tissus vivants et en particulier celle de la bulle tympanique. Dans une étude préliminaire, nous avons essayé de suivre, *ex vivo* en prélevant la bulle tympanique des cobayes, la fluorescence de l'HA marqué à la fluorescéine et celle des liposomes marqués à la rhodamine. Cependant, en raison des longueurs d'ondes d'émission de ces deux fluorophores (500 à 650 nm) qui étaient trop proches de celle de la bulle tympanique vide, nous n'avons pas été en mesure de quantifier de façon précise la fluorescence émise par le gel lorsque la bulle était remplie. Pour pouvoir quantifier la fluorescence dans le temps, l'HA et/ou les liposomes devraient être couplés à un fluorophore émettant à des longueurs d'ondes élevées (695 à 770 nm) comme c'est le cas de la Cyanine 7. L'évaluation de l'efficacité thérapeutique, quant à elle, va nécessiter des expériences supplémentaires sur le cobaye comme l'addition d'un groupe témoin permettant de vérifier l'impact de la chirurgie retro-auriculaire sur l'audition après le traumatisme sonore. Si la chirurgie a un effet négatif sur l'audition, il serait plus pertinent de passer à une injection transtympanique directe sur ce modèle.

A plus long terme, une étude de la biodistribution des liposomes dans la cochlée (organe de Corti, *scala tympani*, *scala vestibuli*) pourrait être envisagée par histologie ou par microscopie confocale. Les aspects biopharmaceutiques pourraient être à nouveau évalués *in vivo* en utilisant un autre type de liposomes tels que les liposomes neutres qui diffusent très peu dans le gel et qui servirait alors de réservoir dans l'oreille moyenne. Enfin, il serait intéressant d'encapsuler une autre substance active ayant une action spécifique sur un mécanisme

physiopathologique impliqué dans la perte auditive, par exemple, un inhibiteur de l'apoptose ou une neurotrophine. L'utilisation des liposomes serait par ailleurs très pertinente pour la thérapie génique (ADN, siRNA) qui est un domaine émergeant et très prometteur en otologie.

## **Gels d'acide hyaluronique contenant des liposomes pour la libération prolongée d'un corticoïde dans l'oreille interne**

### **Résumé**

Les traitements des pathologies de l'oreille interne par voie locale se développent en alternative aux traitements par voie générale peu efficaces et responsables de nombreux effets secondaires. Dans ce travail, nous avons développé une formulation originale constituée de liposomes dispersés au sein d'un gel d'acide hyaluronique pour la libération prolongée d'un corticoïde dans l'oreille interne après administration locale dans l'oreille moyenne. D'abord, une étude physicochimique approfondie a permis d'identifier les paramètres clés de formulation qui ont un impact sur les propriétés du gel de liposomes en termes de caractéristiques rhéologiques, de seringabilité, de stabilité, de microstructure et enfin de diffusion des liposomes dans le gel. Ensuite, le gel de liposomes contenant la dexamethasone phosphate a été évalué *in vivo* chez le cobaye. L'administration locale du gel de liposomes a abouti à une libération prolongée du corticoïde dans l'oreille interne, sans aucun effet négatif sur la fonction auditive. L'évaluation de l'efficacité thérapeutique de la formulation pour le traitement de la surdité secondaire à un traumatisme sonore et pour la préservation de l'audition durant l'implantation cochléaire a montré des résultats préliminaires très prometteurs.

**Mots clés :** acide hyaluronique, administration locale, dexamethasone phosphate, gel, liposomes, oreille interne.

## **Hyaluronic acid liposomal gels for the sustained delivery of a corticoid to the inner ear**

### **Abstract**

Local, rather than systemic drug delivery is being developed to treat inner ear diseases. In this work, we developed an original drug delivery system based on liposomes dispersed within a hyaluronic acid gel for the sustained delivery of a corticoid to the inner ear after local administration in the middle ear. First, a thorough physicochemical study allowed to identify the key formulation parameters that impact the liposomal gel properties in terms of rheological behavior, syringeability, stability, microstructure and diffusion of liposomes within the gel. Then, the liposomal gel containing dexamethasone phosphate was evaluated *in vivo* in guinea pig. The local administration of the liposomal gel in the middle ear resulted in a sustained release of the corticoid in the inner ear without any negative effect on the hearing function. Promising preliminary data were obtained regarding the therapeutic efficacy of the formulation for hearing recovery after acoustic trauma and for hearing preservation during cochlear implantation.

**Keywords :** dexamethasone phosphate, gel, hyaluronic acid, inner ear, liposomes, local drug delivery.

### **Laboratoire de rattachement :**

Institut Galien Paris-Sud, UMR CNRS 8612  
Université Paris-Sud, UFR de pharmacie  
5 Rue Jean Baptiste Clément  
92290 Châtenay-Malabry

